COPPE
Instituto Alberto Luiz Coimbra de Pós-Graduação e Pesquisa de Engenharia
UFRJ

MONITORING STRATEGIES IN ADAPTIVE SLIDING MODE CONTROL AND EVENT-TRIGGERED EXTREMUM SEEKING

Victor Hugo Pereira Rodrigues

Tese de Doutorado apresentada ao Programa de Pós-graduação em Engenharia Elétrica, COPPE, da Universidade Federal do Rio de Janeiro, como parte dos requisitos necessários à obtenção do título de Doutor em Engenharia Elétrica.

Orientadores: Liu Hsu
Tiago Roux de Oliveira

Rio de Janeiro
Junho de 2022

MONITORING STRATEGIES IN ADAPTIVE SLIDING MODE CONTROL AND EVENT-TRIGGERED EXTREMUM SEEKING

Victor Hugo Pereira Rodrigues

TESE SUBMETIDA AO CORPO DOCENTE DO INSTITUTO ALBERTO LUIZ COIMBRA DE PÓS-GRADUAÇÃO E PESQUISA DE ENGENHARIA DA UNIVERSIDADE FEDERAL DO RIO DE JANEIRO COMO PARTE DOS REQUISITOS NECESSÁRIOS PARA A OBTENÇÃO DO GRAU DE DOUTOR EM CIÊNCIAS EM ENGENHARIA ELÉTRICA.

Orientadores: Liu Hsu
Tiago Roux de Oliveira

Aprovada por: Prof. Liu Hsu
Prof. Tiago Roux de Oliveira
Prof. Amit Bhaya
Prof. Marcelo Carvalho Minhoto Teixeira
Prof. Reinaldo Martínez Palhares

RIO DE JANEIRO, RJ – BRASIL
JUNHO DE 2022

Rodrigues, Victor Hugo Pereira

Monitoring strategies in adaptive sliding mode control and event-triggered extremum seeking/Victor Hugo Pereira Rodrigues. – Rio de Janeiro: UFRJ/COPPE, 2022.

XIV, 144 p.: il.; 29, 7cm.

Orientadores: Liu Hsu

Tiago Roux de Oliveira

Tese (doutorado) – UFRJ/COPPE/Programa de Engenharia Elétrica, 2022.

Referências Bibliográficas: p. 129 – 139.

1. Sliding Mode Control. 2. Unit Vector Control. 3. Extremum Seeking. 4. Event-Triggered Control. I. Hsu, Liu *et al.* II. Universidade Federal do Rio de Janeiro, COPPE, Programa de Engenharia Elétrica. III. Título.

To my parents, brothers,
relatives, friends, advisors and
professors, for teaching me every
thing which I know and
supporting my every choice.

Acknowledgments

This study was financed in part by the Coordenação de Aperfeiçoamento de Pessoal de Nível Superior – Brasil (CAPES) – Finance Code 001. The authors also acknowledge the Brazilian Funding Agencies Conselho Nacional de Desenvolvimento Científico e Tecnológico (CNPq) and Fundação de Amparo à Pesquisa do Estado do Rio de Janeiro (FAPERJ).

Resumo da Tese apresentada à COPPE/UFRJ como parte dos requisitos necessários para a obtenção do grau de Doutor em Ciências (D.Sc.)

MONITORING STRATEGIES IN ADAPTIVE SLIDING MODE CONTROL AND EVENT-TRIGGERED EXTREMUM SEEKING

Victor Hugo Pereira Rodrigues

Junho/2022

Orientadores: Liu Hsu
Tiago Roux de Oliveira

Programa: Engenharia Elétrica

Esta tese propõe estratégias de monitoração para o controle por modo deslizante adaptativoe a busca extremal acionada por eventos.

Os novos controladores por modos deslizantes (SMC) e por vetor unitário (UVC) utilizam realimentação de saída para uma classe de sistemas não-lineares e podem lidar com incertezas paramétricas e perturbações (des)casadas com majorantes desconhecidos. A convergência em tempo finito do erro de rastreamento para uma vizinhança predefinida da origem do sistema em malha fechada é provada com garantia de desempenho transitório e em regime permanente. A novidade do resultado está na combinação de duas eficientes ferramentas de adaptação: funções de monitoração e de barreira. Resultados de simulação incluindo a aplicação em um sistema de frenagem antibloqueio (ABS) e um guindaste ponte rolante ilustram as vantagens das estratégias adaptativas propostas.

Finalmente, considerando mapas estáticos, esta tese propõe esquemas acionados por eventos para busca extremal escalar e multivariável. Enquanto a busca de extremal permite que a saída de um mapa não-linear seja mantida dentro de uma vizinhança de seu extremo, a estratégia de acionamento por eventos é responsável por executar aperiodicamente a lei de controle através de um mecanismo de monitoração. Condições para o acionamento estático e dinâmico são desenvolvidas. Integrando a teoria de estabilidade de Lyapunov com o método da média para sistemas descontínuos, um procedimento sistemático de projeto e análise de estabilidade é desenvolvido. Os benefícios das novas estratégias de controle são apresentados através de resultados de simulação consistentes, que comparam as abordagens de acionamento estático e dinâmico.

Abstract of Thesis presented to COPPE/UFRJ as a partial fulfillment of the requirements for the degree of Doctor of Science (D.Sc.)

MONITORING STRATEGIES IN ADAPTIVE SLIDING MODE CONTROL AND EVENT-TRIGGERED EXTREMUM SEEKING

Victor Hugo Pereira Rodrigues

June/2022

Advisors: Liu Hsu
Tiago Roux de Oliveira

Department: Electrical Engineering

This thesis proposes monitoring strategies for adaptive sliding mode controllers and event-triggered extremum seeking.

The new adaptive sliding mode and unit vector controllers use output feedback for a class of nonlinear systems and can deal with parametric uncertainties and (un)matched disturbances with unknown upper bounds. Finite-time convergence of the tracking error to a predefined neighborhood of the origin of the closed-loop system is proved with guaranteed transient and steady-state performance. The novelty of our result lies on two important adaptation tools: monitoring and barrier functions. Simulation results including the application to Anti-lock Braking System and Overhead-crane to illustrate the advantages of the proposed adaptive control strategies.

Finally, based on static maps, this thesis proposes event-triggered schemes for both scalar and multivariable extremum seeking. While the extremum seeking allows the output of a nonlinear map to be held within a vicinity of its extremum, the event-triggered strategy is responsible to execute the control task aperiodically by using a monitoring mechanism. Static and dynamic triggering condition are developed. Integrating Lyapunov and averaging theories for discontinuous systems, a systematic design procedure and stability analysis are developed. Illustration of the benefits of the new control method are presented using consistent simulation results, which compare the static and the dynamic triggering approaches.

Contents

List of Figures

List of Tables

List of Acronyms

ABS	Anti-lock Braking System
B-MRAC	Binary Model Reference Adaptive Control
ESC	Extremum Seeking Control
ETC	Event-Triggered Control
FOAF	First Order Approximation Filter
ISS	Input-to-State Stability
MBF	Monitoring and Barrier Functions
MIMO	Multiple-Input Multiple-Output
MRAC	Model Reference Adaptive Control
PBF	Positive definite Barrier Function
PDEs	Partial Differential Equations
PSBF	Positive Semi-definite Barrier Function
SISO	Single-Input Single-Output
SMC	Sliding Mode Control
UVC	Unit Vector Control
ZOH	Zero-Order Hold

Chapter 1

Introduction

In this thesis, the term "monitoring" means checking "something" to observe how it develops, so that an "appropriate decision" can be taken. Such informal but direct definition unifies the different contributions proposed throughout this thesis. In our context, the aforementioned word "something" should be read as an output signal of a plant or an error signal. While the term "appropriate decision" can mean the increase, decrease or stagnation of an adaptation gain or the update action of a control signal. Basically, contributions can be divided into three fields: sliding mode-based controllers, a binary model reference adaptive control strategy and event-triggered extremum seeking approaches. In sliding mode-based controllers, the output signals are monitored to adapt the controller gains for stabilization and tracking scenarios. In the binary model reference adaptive control, the monitoring process of the error between the plant and the reference model outputs is used for unknown parameters estimation. In event-triggered extremum seeking approaches, the execution control task is orchestrated by a monitoring mechanism that invokes control updates when the difference between the current state value and the last transmitted state value satisfy the designed triggered condition.

1.1 Sliding Mode and Unit Vector Controllers

The disturbance rejection task for uncertain systems is a longstanding issue in control theory. The most common way to solve this problem is using control strategies based on sliding mode [3–9]. In closed-loop, theoretically, the sliding mode control strategies are able to provide insensitivity to these disturbances while ensuring the finite-time convergence of the sliding variable [10]. In practice, the implementation of the standard sliding mode controllers are based on overestimated disturbance's upper bounds leading to energetic control efforts and revealing the main drawback of such strategies: the so-called chattering effect, *i.e.*, dangerous high-frequency vibrations of the controlled system [11]. On the other hand, this upper bound in

general is non constant and frequently unknown [12].

If the upper bound of the disturbance exists but it is unknown, adaptive sliding mode controllers [12–15] were proposed. In references [13, 14] the control gain increases until the closed-loop reaches the ideal sliding mode and then the gain is kept fixed. If the disturbance grows, the loss of the sliding mode occurs but the gain increases to compensate it again. Since the gain cannot decrease, the control becomes overestimated when the disturbance decreases. Notice that, the disturbance rejection problem with perturbations of unknown upper bounds has not been restricted to the first-order sliding mode scenario. For instance, reference [16] proposes an adaptive super-twisting sliding mode controller with disturbances bounded by unknown upper-bounds. In reference [17], the main focus was to mitigate the super-twisting control effort by using equivalent control. In reference [18], the constant gains of the classic super-twisting controller are replaced by adaptive gains also based on equivalent control estimates, to increase or decrease such gains when necessary.

To avoid the overestimation, consequently, to alleviate the chattering, and to guarantee prescribed transient and steady-state performance, this thesis proposes new adaptive sliding mode control strategies based on monitoring [15] and barrier functions [12].

Originally, the monitoring function was designed for variable-structure model reference adaptive controllers [19] to deal with plants without the prior knowledge of the high-frequency gain sign [20], [21] and [22]. The monitoring function supervises the tracking error time-response changing the control sign every time they meet. Then, after a finite number of sign switchings, the true control direction is eventually found and thereafter the tracking error goes to zero at least exponentially. Several researches have been conducted in order to extend such results for unit vector control [22], binary robust adaptive control [23], extremum seeking control via monitoring function [24], and adaptation of the gains of higher-order sliding mode-based exact differentiators [25].

In [26], an adaptive first-order sliding mode approach based on monitoring functions is proposed to reject disturbances with unknown bounds. The global tracking problem is successfully addressed ensuring the convergence of the error signal to a residual set even considering uncertain plants with non-smooth disturbances. Nevertheless, the residual set could not be rigorously characterized. This issue was overcome in reference [15], where a new switching scheme was able to guarantee a prespecified transient time, maximum overshoot, and steady-state error for multivariable uncertain plants. Unfortunately, such objectives could be guaranteed using a discontinuous control signal so that control chattering could not be precluded.

On the other hand, the barrier function has successfully been applied to adaptive

sliding-mode based schemes to achieve the convergence of the output error to a predefined ϵ-vicinity of zero, with a control signal that is not overestimated and without using any information about the upper bound of the disturbance [12]. For instance, in [12, 27] such a strategy is applied to a class of first-order sliding mode controllers (first-order and integral); in [28, 29], to the case of second-order sliding mode controllers (twisting and variable-gain super twisting) and in [30, 31], to algorithms for adaptation of the Levant's differentiator gains [32]. In all above mentioned papers, only uncertain single-input/single-output plants were considered without ensuring the specification of the transient phase (prespecified fixed-time convergence to the residual set and overshoot constraint).

In order to mitigate the indicated issues, the proposed adaptive schemes in this thesis are divided in two phases: the reaching and the residual phases. In the reaching phase, the idea is to design an adaptive modulation function to ensure the convergence of the system outputs of the multivariable plant to the interior of an ϵ-vicinity of the origin by applying a monitoring function which also guarantees a prespecified transient time and a maximum overshoot with a finite number of switchings. In the residual phase, inside the ϵ-vicinity, the barrier function maintain the output error within such neighborhood of zero, independently of the unknown upper bound of the disturbances and without overestimating the control signal. Since the method combines **m**onitoring with **b**arrier **f**unctions, it will be referred as MBF (controller/method).

The main advantages of the monitoring and barrier functions (MBF) adaptive controllers are:

- Unlike reference [12], a prespecified transient time and maximum overshoot in the reaching phase is guaranteed.
- Differently from [15], the barrier function in the proposed approach can be chosen to avoid chattering during the residual phase.
- The control signal overestimation is ultimately avoided.
- The proposed scheme does not require known bounds for the matched and/or unmatched disturbances.

On the application side, research on modern vehicle engineering has focused on the design of energy storage devices in electric and hybrid vehicles [33, 34]. Also, anti-lock braking system (ABS) can be designed taking advantage of the sensors embedded in the new cars [35] with robust and adaptive control strategies [36–38]. In this context, our adaptive sliding mode controller scheme seems appropriate to be applied to an ABS ensuring that the slip coefficient corresponding to the maximum

coefficient of friction between the tire and road is quickly achieved during the braking process of the car. On the other hand, overhead cranes are widely used to move the large/heavy objects horizontally for either manufacturing or maintenance practices in many industrial environments, such as ocean engineering, nuclear industries, and airports [39]. Indeed, it is not an easy task to control a crane system since naturally the crane acceleration, required for motion, always induces undesirable load swing. The acceleration and the deceleration of the overhead crane lead to swings of the payload; these swings can be dangerous and may cause damage and/or accidents [40]. The crane control consists of a crane motion and load hoisting control as well as a payload swing suppression [41]. In the literature, several attempts have been made to control the load swing [39, 40, 42–44]. In this context, our adaptive unit vector controller scheme seems appropriate to be applied to an overhead crane system ensuring the closed-loop properties of fixed-time convergence and prescribed-performance via monitoring and barrier functions.

1.2 Event-Triggered Extremum Seeking

The final part of this thesis proposes monitoring mechanisms of execution, *i.e*, event-triggered schemes, for both scalar and multivariable extremum seeking.

In spite of the fact that the concept of extremum seeking control (ESC) was introduced 100 years ago by the French Engineer Maurice Leblanc already in 1922 [45], a rigorous demonstration of stability under feedback control only appeared about 20 years ago [46]. ESC based on the perturbation method [47] adds a periodic dither signal of small amplitude to the input of the nonlinear map and estimates its gradient in real time by using a suitable demodulation process. Extremum Seeking is a control and optimization strategy that allows the output of a nonlinear map to be held within a vicinity of its extremum. When the parameters of the nonlinear map are available, it is possible to obtain exactly the gradient of the nonlinearity and the control objective can be defined as its stabilization. However, because of parametric uncertainties, the gradient is not always known and the control task is not always straightforward. Despite the several ESC strategies found in the literature, the methods based on perturbations (dither signals) are the oldest and, even remain nowadays quite popular.

After the consolidation of ESC stability results for static and general nonlinear dynamic continuous-time systems [46], discrete-time systems [48], stochastic systems [49, 50], multivariable systems [51], and non-cooperative games [52], the theoretical advances of ESC overcome the border of finite-dimension systems to arrive in the world of Partial Differential Equations (PDEs). For such infinite-dimensional systems, boundary feedback controllers are designed to ensure convergence of the ESC

in the closed-loop form by compensating the input and/or output under propagation through transport PDEs (delays) [53, 54], diffusion PDEs [55, 56], wave PDEs [57], Lighthill–Whitham–Richards nonlinear PDEs [58], parabolic PDEs [59], and PDE-PDE cascades [57].

In the current technological age of network science, researchers are focusing on decreasing wiring costs by designing fast and reliable communication schemes where the plant and controller might not be physically connected, or might even be in different geographical locations. These networked control systems offer advantages in the financial cost of installation and maintenance [60]. However, one of their major disadvantages is the resulting high-traffic congestion, which can lead to transmission delays and packet dropouts, *i.e.*, data may be lost while in transit through the network [61]. These issues are highly related to the limited resource or available communication channels' bandwidth. To alleviate or mitigate this problem, Event-Triggered Controllers (ETC) can be used.

ETC executes the control task, non-periodically, in response to a triggering condition designed as a function of the plant's state [62]. Besides the asymptotic stability properties [63], this strategy reduces control effort since the control update and data communication only occur when the error between the current state and the equilibrium set exceeds a value that might induce instability [64]. Pioneering works towards the development of resource-aware control design includes the construction of digital computer design [65], the event-based PID design [66] and the event-based controller for stochastic systems [67]. Works dedicated to the extension of event-based control for networked control systems with a high level of complexity exist for both linear [68–70] and nonlinear [63, 71, 72] systems. Among others, results on event-based control deal with the robustness against the effect of possible perturbations [73, 74] or parametric uncertainties [75]. In [76], ETC is designed to satisfy a cyclic-small-gain condition such that the stabilization of a class of nonlinear time-delay systems is guaranteed. As well, the authors in [77] proposed distributed event-triggered leaderless and leader-follower consensus control laws for general linear multi-agent networks. An event-triggered output-feedback design [78] has been employed aiming to stabilize a class of nonlinear systems by combining techniques from event-triggered and time-triggered control. Recently, substantial works have been carried out to conceive event-based approaches for infinite dimensional systems [79–83]. We emphasize that among existing results [84, 85] are focused on infinite-dimensional observer-based event-triggered control for reaction-diffusion PDEs.

To the best of our knowledge, this thesis is the first contribution on event-triggered ESC based on perturbation method. For static maps, we consider the design and analysis of the scalar and multivariable ESC within both static and dynamic event-triggered control frameworks. As opposed to hybrid systems design [86],

the stability analysis are carried out using Lyapunov criterion as well as averaging theory for discontinuous systems to characterize the properties of the closed-loop systems.

1.3 Organization and Notation

The thesis is organized as follows. Chapters 2 and 3 show the effectiveness of the new adaptive sliding mode (scalar) and unit vector (multivariable) control approaches, respectively. Chapter 4 presents the scalar ESC within static event-triggered mechanism. The scalar dynamic event-triggered ESC is presented in Chapter 5. The multivariable ESC generalization within both static and dynamic event-triggered control frameworks are developed in Chapter 6. The concluding remarks of this thesis are given in Chapter 7.

Notation: Throughout the manuscript, the 2-norm (Euclidean) of vectors and induced norm of matrices are denoted by double bars $\|\cdot\|$ while absolute value of scalar variables are denoted by single bars $|\cdot|$. The terms $\lambda_{\min}(\cdot)$ and $\lambda_{\max}(\cdot)$ denote the minimum and maximum eigenvalues of a matrix, respectively. Consider $\varepsilon \in [-\varepsilon_0\,, \varepsilon_0] \subset \mathbb{R}$ and the mappings $\delta_1(\varepsilon)$ and $\delta_2(\varepsilon)$, where $\delta_1 : [-\varepsilon_0\,, \varepsilon_0] \to \mathbb{R}$ and $\delta_2 : [-\varepsilon_0\,, \varepsilon_0] \to \mathbb{R}$. One states that $\delta_1(\varepsilon)$ has magnitude order of $\delta_2(\varepsilon)$, *i.e.*, $\delta_1(\varepsilon) = \mathcal{O}(\delta_2(\varepsilon))$, if there exist positive constants k and c such that $|\delta_1(\varepsilon)| \leq k|\delta_2(\varepsilon)|$, for all $|\varepsilon| < c$.

Chapter 2

Adaptive Sliding Mode Control with Guaranteed Performance based on Monitoring and Barrier Functions

This chapter proposes a new adaptive sliding mode control approach via output feedback for a class of nonlinear systems. The sliding-mode based controller can deal with parametric uncertainties and (un)matched disturbances with unknown upper bounds. Finite-time convergence of the tracking error of the closed-loop system to a predefined neighborhood of the origin is proved with guaranteed transient and steady-state performance. Basically, the novelty of our result lies on combining two important adaptation tools: monitoring and barrier functions (MBF). The adaptation process is divided into two stages, where an appropriate monitoring function allows for the specification of performance criteria during the transient phase, while the barrier function ultimately confines the tracking error within a small residual set in steady-state. Simulation results including an application to Anti-lock Braking System illustrate the advantages of the proposed adaptive control strategy.

2.1 Problem Formulation

Consider the uncertain SISO nonlinear plant in regular form

$$\dot{\eta}(t) = A_{11}\eta(t) + A_{12}\sigma(t) + d_1(\eta(t)\,,\sigma(t)\,,t)\,, \tag{2.1}$$

$$\dot{\sigma}(t) = A_{21}\eta(t) + A_{22}\sigma(t) + d_2(\eta(t)\,,\sigma(t)\,,t) + K_p u\,, \tag{2.2}$$

where the state vector is defined as $x^T(t) := [\eta^T(t)\,,\sigma(t)] \in \mathbb{R}^n$, $\eta(t) \in \mathbb{R}^{n-1}$ denotes the unmeasured part, $\sigma(t) \in \mathbb{R}$ is the output, $u \in \mathbb{R}$ is the control input, while the mapping $d_1 : \mathbb{R}^{n-1} \times \mathbb{R} \times \mathbb{R}^+ \mapsto \mathbb{R}^{n-1}$ and $d_2 : \mathbb{R}^{n-1} \times \mathbb{R} \times \mathbb{R}^+ \mapsto \mathbb{R}$ represent the unmatched and matched disturbances, respectively.

Throughout the thesis, the 2-norm (Euclidean) of vectors and induced norm of a matrices are denoted by double bars $\|\cdot\|$. The stability margin of a real Hurwitz matrix A is here defined as $\lambda_0 := \min_j \{-\mathrm{Re}(\lambda_j)\}$ where $\{\lambda_j\}$'s are the eigenvalues of A. Moreover, the following assumptions are made throughout the thesis:

(A1) Matrices $A_{11} \in \mathbb{R}^{(n-1)\times(n-1)}$, $A_{12} \in \mathbb{R}^{(n-1)\times 1}$, $A_{21} \in \mathbb{R}^{1\times(n-1)}$, and $A_{22} \in \mathbb{R}^{1\times 1}$ are all uncertain.

(A2) It is assumed that A_{11} is Hurwitz, *i.e.*, the plant (2.1)–(2.2) is minimum phase from u to σ. This assumption is extremely important since it allows the design of a stable upper bound for the absolute value of the unmeasured state variable $\eta(t)$.

(A3) The induced norm of the matrix A_{12} is majorized by a known positive constant $c_{\eta\sigma}$.

(A4) The disturbances $d_1(x(t)\,,t)$ and $d_2(x(t)\,,t)$ are Lipschitz in x, piece-wise continuous in t and uniformly bounded by unknown constants $\bar{d}_1$ and $\bar{d}_2$, *i.e.*,

$$||d_1(x,t)|| \leq \bar{d}_1 \quad \text{and} \quad |d_2(x,t)| \leq \bar{d}_2\,, \quad \forall x \text{ and } \forall t \geq 0\,.$$

(A5) Without loss of generality, the high-frequency gain is $K_p := 1$.

(A6) Only the output $\sigma(t)$ is available for control design.

The control objective is the ultimate confinement of $\sigma(t)$ to an ϵ-vicinity of the origin in the global sense, *i.e.*, for all initial conditions and for all time instant t greater than a finite time t_s ($|\sigma(t)| \leq \epsilon$, $\forall t \geq t_s$), by using only output feedback. To achieve this goal without knowing the upper bounds $\bar{d}_1$ and $\bar{d}_2$, some adaptation strategy is necessary.

2.2 Basic Techniques

In this section, basic techniques for the proposed control strategy are introduced.

2.2.1 State-Norm Observer

The first step to start the control design is to obtain an instantaneous norm bound for the unmeasured state vector. The norm observer, also called first order

approximation filter (FOAF), is an important tool that allows to reach it by using only output information [87]. From [88, Lemma 2], the solution of

$$\dot{\bar{\eta}}(t) = -\gamma_1 \bar{\eta}(t) + k_1 |\sigma(t)| + k_2 \bar{d}_1 \,, \tag{2.3}$$

where $\bar{\eta} \in \mathcal{R}^1$, with the scalar $\gamma_1 > 0$ being a lower bound for the stability margin of A_{11} and appropriate positive constants k_1 and k_2, is an upper bound for $\|\eta(t)\|$, modulo some exponentially decaying term, i.e.

$$\|\eta(t)\| \leq |\bar{\eta}(t)| + \pi_\eta(t) \,, \quad \forall t \geq 0 \,, \tag{2.4}$$

where $\pi_\eta(t)$ is an exponentially decaying term depending on the initial conditions $\eta(0)$ and $\bar{\eta}(0)$, with $\eta(t)$ provided in (2.1).

Note that, although $\bar{\eta}(t)$ is an upper bound for the unmeasured state $\eta(t)$, it cannot be used yet since, from assumption (A5), $\bar{d}_1$ is unknown. The next section introduces the monitoring function, an important tool which allows the implementation of an upper bound for $\eta(t)$ by means of a hybrid state-norm estimation using switching adaptation.

2.2.2 Monitoring Function - Reaching Phase

The monitoring function is an appropriate switching-based scheme originally designed to compensate the lack of knowledge about the system such as: the control direction information [21], unknown bounds of disturbances [26] or disturbances with unknown and arbitrary growth rate [25]. Here, a more recent version of [21] is presented in [15] whereby the performance specifications of the closed-loop system can be achieved, according to the following definition.

Definition 1. *The stabilization/tracking error $\sigma(t)$ is said to satisfy the reaching and residual phase specifications, if*

- $|\sigma(t)| \leq |\sigma(0)| + \Delta$, $\forall t \in [0\,, T)$,
- $|\sigma(t)| \leq \epsilon \,, \quad \forall t \geq T \,,$

where $\Delta > 0$ is the maximum allowed overshoot, $T > 0$ is the maximum transient time, $\epsilon \in (0\,, \Delta]$ is the allowed maximum steady-state error, all of which can be arbitrarily specified by the user/designer.

The monitoring switching scheme is such that the next switching instant is de-

fined as [15]

$$t_{k+1} := \min \begin{cases} \\ t > t_k : \\ \\ \end{cases} \begin{array}{c} |\sigma(t)| = |\sigma(0)| + \Delta\left(1 - \frac{1}{R_1^k}\right) \\ \text{or} \\ t = T\left(1 - \frac{1}{R_1^k}\right) \quad \text{and} \quad |\sigma(t)| > \epsilon/R_2 \end{array} , \quad k = 1, 2, \ldots \tag{2.5}$$

where $R_1 > 1$ and $R_2 > 1$ are design constants. If, for some time instant $\bar{t} \leq T$, the condition $|\sigma(\bar{t})| = \epsilon/R_2$ is reached, then the Residual Phase (Section 2.2.3) is started.

Moreover, the switching index k, is employed in the design of positive monotonically increasing unbounded sequences $\hat{d}_1(k)$ and $\hat{d}_2(k)$ to counteract the absence of the constants $\bar{d}_1$ and $\bar{d}_2$ in (A4),

$$\hat{d}_1(k) = c_1 b_1^k \,, \tag{2.6}$$

$$\hat{d}_2(k) = c_2 b_2^k \,, \tag{2.7}$$

where $c_1\,, c_2 > 0$, and $b_1\,, b_2 > \max\{R_1\,, R_2\}$ are arbitrarily constants. Then, a hybrid state-norm estimation scheme is introduced, based on (2.3)–(2.4), such that

$$\dot{\hat{\eta}}(t) = -\gamma_1 \hat{\eta}(t) + k_1 |\sigma(t)| + k_2 \hat{d}_1(k) \,, \tag{2.8}$$

and

$$\|\eta(t)\| \leq |\hat{\eta}(t)| + \pi_\eta(t) \,. \quad \forall t \geq 0 \,, \tag{2.9}$$

The norm observer $\hat{\eta}(t)$ flows through a continuous state space but also moves through different discrete switching modes, as defined by [89].

An important property of the switching rule is that, if k grows and becomes sufficiently large, then $\sigma(t)$ satisfies its predefined specifications on the reaching phase through the switching law (2.5). In the reaching phase, the switching makes $\hat{d}_1(k)$ and $\hat{d}_2(k)$ to grow unboundedly as $k \to \infty$. As a result, during the reaching phase, the monitoring function forces $|\sigma(t)| \leq \epsilon/R_2$ before the time instant T while ensuring no violation of the overshoot specification.

2.2.3 Barrier Function - Residual Phase

The Barrier Function, for a given and fixed $\epsilon > 0$, is defined as an even continuous function $\rho_B : \chi \in (-\epsilon\,, \epsilon) \to \rho_B(\chi) \in [\, b\,, \infty\,)$ strictly increasing on $[\, 0\,, \epsilon\,)$ such that $\lim_{|\chi| \to \epsilon} \rho_B(\chi) = +\infty$, $\rho_B(\chi)$ has a unique minimum at zero and $\rho_B(0) = b \geq 0$.

just requires them to be bounded, but there is no need to know what the bounds

In the residual phase, the introduction of a barrier function imposes a hard bound on the sliding variable by restricting it within a prescribed ϵ-vicinity. The important features of the controllers based on barrier functions just requires the disturbances to be bounded, but there is no need to know what the bounds are and the assurance of avoiding overestimated control gains. Basically, as shown in Figure 2.1, in the sliding mode control framework, there are two kinds of barrier functions:

- Positive definite Barrier Function (PBF):

$$\rho_{PB}(\chi) := \frac{\epsilon \bar{F}}{\epsilon - |\chi|}\,, \quad i.e.\,, \quad \rho_{PB}(0) = \bar{F} > 0\,. \tag{2.10}$$

- Positive Semi-definite Barrier Function (PSBF):

$$\rho_{PSB}(\chi) := \frac{|\chi|}{\epsilon - |\chi|}\,, \quad i.e.\,, \quad \rho_{PSB}(0) = 0\,. \tag{2.11}$$

For more details, please see [12].

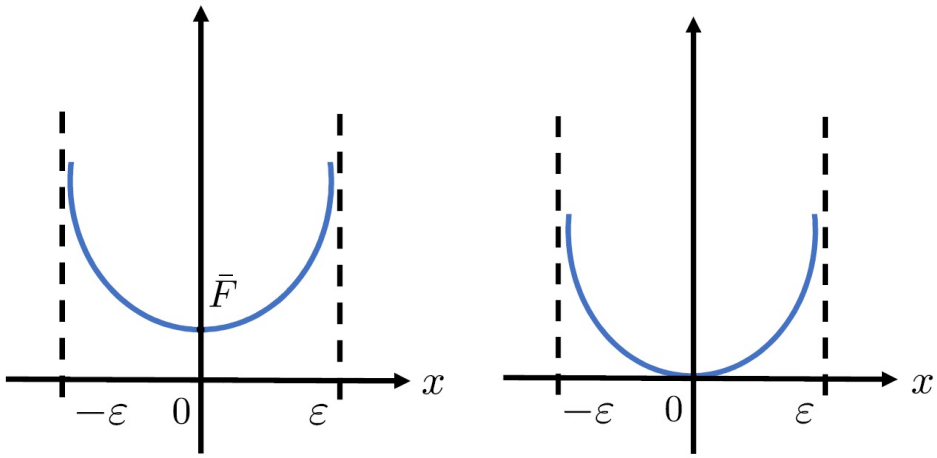

(a) Positive definite Barrier Function.

(b) Positive Semi-definite Barrier Function.

Figure 2.1: Positive definite and Positive Semi-definite Barrier Functions.

The next section shows how the Barrier Functions can be employed as an adaptive strategy avoiding overestimated gains for sliding mode schemes.

2.3 MBF Adaptive Sliding Mode Control

The Monitoring and Barrier Function (MBF) adaptive sliding mode control law is given by

$$u = -\rho(t)\text{sgn}(\sigma(t))\,, \tag{2.12}$$

where $\rho(t)$ is the *modulation function* such that

$$\rho(t) = \begin{cases} \rho_M(t)\,, & \text{if} \quad t < \bar{t} \\ \rho_B(t)\,, & \text{if} \quad t \geq \bar{t} \end{cases} \quad . \tag{2.13}$$

While the closed-loop system is in the reaching phase, it is under the monitoring function action and, using the hybrid state-norm observer (2.8) and the disturbance estimate (2.7) with the modulation function designed as

$$\rho_M(t) = c_\sigma|\sigma(t)| + c_{d_\sigma}\hat{d}_2(k) + c_\eta\hat{\eta}(t) + \delta\,, \tag{2.14}$$

with appropriate positive constants c_σ, c_{d_2}, c_η, and δ. On the other hand, in the residual phase, the modulation function is driven by barrier function such that $\rho_B(t)$ is defined by (2.10) or (2.11).

2.3.1 Stability Analysis

Theorem 1 stated below summarizes the main results of the stability properties of the MBF closed-loop system.

Theorem 1. *Consider the plant (2.1)-(2.2), the monitoring scheme with switching times (2.5), switching-based disturbance estimates (2.6) and (2.7), hybrid state-norm observer (2.8), and the output-feedback sliding mode control law (2.12) with modulation function (2.13). Assume that (A1)–(A6) hold. Then, all prespecified transient and steady-state behaviors (maximum overshoot Δ, maximum transient time T and residual absolute error $|\sigma(t)|$ less than ϵ) are guaranteed. Furthermore, there exists an unknown upper bound d_{max} for the equivalent disturbance in equation (2.2) and the practical stabilization/tracking is achieved, with the output error $\sigma(t)$ ultimately converging to the interior of an ϵ-neighborhood of the origin so that:*

- *If the barrier function is the positive definite in (2.10), $|\sigma(t)| \leq \epsilon_1$ such that $|\sigma(t)| \leq \epsilon_1 < \epsilon$ where $\epsilon_1 = \epsilon(1 - \overline{F}/d_{max})$ if $\overline{F} < d_{max}$ and $\epsilon_1 = 0$ if $\overline{F} \geq d_{max}$.*
- *If the barrier function is the positive semi-definite in (2.11), $|\sigma(t)| \leq \epsilon_2 < \epsilon$ where $\epsilon_2 = \epsilon d_{max}/(d_{max} + 1)$.*

Proof. The first step of the proof is to demonstrate that when using the control law (2.12) with modulation function (2.14), the sliding variable reaches the region $|\sigma| \leq \epsilon/R_2$ with the guarantee that the specifications of the settling time and maximum *overshoot* are not violated.

Consider the following Lyapunov-like candidate function for (2.2)

$$V(\sigma) = \frac{1}{2}\sigma^2, \tag{2.15}$$

whose time-derivative satisfies

$$\begin{aligned}\dot{V} &= \sigma\dot{\sigma} \\ &= \sigma\left[A_{21}\eta + A_{22}\sigma + d_2 + u\right] \\ &\leq |\sigma|\left[\|A_{21}\|\|\eta\| + |A_{22}||\sigma| + |d_2|\right] + \sigma(t)u\,. \end{aligned} \tag{2.16}$$

By using the control law (2.12) and taking into account assumption (A4),

$$\dot{V} \leq |\sigma|\left[\|A_{21}\|\|\eta\| + |A_{22}||\sigma| + \bar{d}_2 - \rho\right]. \tag{2.17}$$

Then, employing the inequality (2.9) and defining the constants $c_\eta > \|A_{21}\|$, $c_\sigma > |A_{22}|$ and $c_{d_\sigma} > \max\{1\,, \|A_{21}\|\}$, one has

$$\begin{aligned}\dot{V} &\leq |\sigma|\left[c_\eta\hat{\eta} + c_\sigma|\sigma| + c_{d_\sigma}d_\sigma - \rho\right] \\ &= \sqrt{V}\left[c_\eta\hat{\eta} + c_\sigma\sqrt{V} + c_{d_\sigma}d_\sigma - \rho\right],\end{aligned}$$

where $d_\sigma(t) := \bar{d}_2 + \pi_\eta(t)$. Notice that d_σ can be upper bounded by a constant $\bar{d}_\sigma$ such that $\bar{d}_\sigma \geq \bar{d}_2 + \pi_\eta(0)$. Nevertheless, $\bar{d}_\sigma$ depends on the unavailable information $\bar{d}_2$ and $\eta(0)$.

Thus, by using modulation function $\rho(t) = \rho_M(t)$, as in (2.14),

$$\begin{aligned}\dot{V} &\leq -\delta\sqrt{V} + c_{d_\sigma}\left(d_\sigma - \hat{d}_2\right)\sqrt{V} \\ &\leq c_{d_\sigma}\left(\bar{d}_\sigma - \hat{d}_2\right)\sqrt{V}\,.\end{aligned} \tag{2.18}$$

First, it is proved by contradiction that, if one starts in the Reaching Phase ($|\sigma| > \epsilon$), then after at most finite number of switchings, the Residual Phase ($|\sigma| \leq \epsilon$) will start. Indeed, suppose that the system never enters in Residual Phase. Then, from (2.5), $\hat{d}_1(k)$ and $\hat{d}_2(k)$ will switch without stopping either due to $|\sigma(t)| \to |\sigma(0)| + \Delta$ or to $t \to T$. Therefore, from the σ-equation and taking (2.6) and (2.7) into consideration, it follows that, no matter how large $\bar{d}_\sigma$ is, after at most finite

switchings, one has

$$\hat{d}_2(k) > \bar{d}_\sigma\,, \quad \forall t \in [t_k\,, t_{k+1})\ . \tag{2.19}$$

Once condition (2.19) is satisfied, the disturbance estimate $\hat{d}_2$ will completely dominate the right-hand side of inequality (2.18) and guarantees that there exist a positive integer $\tilde{k} > 0$, such that, $\forall k \geq \tilde{k}$,

$$\dot{V} < 0\,, \quad \forall t \in [t_k\,, t_{k+1})\ . \tag{2.20}$$

The inequality (2.20) implies that any new switching is only due to $t = T(1-1/R_1^k)$ because, from (2.5), $|\sigma(t)| = |\sigma(0)| + \Delta(1-1/R_1^k)$ implies that $|\sigma|$ would be increasing, contradicting (2.20). As a result, the time interval between two switchings is

$$t_{k+1} - t_k = T(1-1/R_1^k) - T(1-1/R_1^{k-1}) = T(R_1-1)/R_1^k\,. \tag{2.21}$$

Then, through rigorous analysis, it is proven in [15, Theorem 1]that the second stage starts and it is characterized in what follows.

Now, the dynamic behavior of (2.1)–(2.2) is briefly analyzed under the residual regime. Since $\|d_1(x,t)\| \leq \bar{d}_1$ and $|\sigma(t)| \leq \epsilon$, from the solution the of (2.3) it is easy to verify that

$$\|\eta(t)\| \leq \frac{\gamma_1\|\eta(0)\| + k_1\epsilon + k_2\bar{d}_1}{\gamma_1}\,. \tag{2.22}$$

Therefore, using the control law (2.12) with modulation function $\rho(t) = \rho_B(t)$, given by (2.10) or (2.11), equation (2.2) can be rewritten as

$$\dot{\sigma}(t) = [d(x,t) - \rho_B(\sigma(t))\mathrm{sgn}(\sigma(t))]\ , \tag{2.23}$$

$$d(x,t) = A_{21}\eta(t) + A_{22}\sigma(t) + d_2(x,t)\,, \tag{2.24}$$

such that the disturbance $d(t)$ verifies the following inequality

$$\begin{aligned} |d(x,t)| &\leq \|A_{21}\|\|\eta(t)\| + |A_{22}||\sigma(t)| + |d_2(x,t)| \\ &\leq \|A_{21}\|\frac{\left(\gamma_1\|\eta(0)\| + k_1\epsilon + k_2\bar{d}_1\right)}{\gamma_1} + |A_{22}|\epsilon + \bar{d}_2\,, \\ &= d_{\max} \end{aligned} \tag{2.25}$$

i.e., in the residual phase, the disturbance $d(x,t)$ is bounded by an unknown constant.

Now, consider the following Lyapunov-like function

$$V(\sigma) = \frac{1}{2}\sigma^2 + \frac{1}{2}(\rho_B(\sigma) - \rho_B(0))^2 \,. \tag{2.26}$$

whose time derivative, along (2.23) and (2.25), is

$$\begin{aligned} \dot{V} &= \sigma\dot{\sigma} + (\rho_B(\sigma) - \rho_B(0))\dot{\rho}_B \\ &\leq -(-d_{\max} + \rho_B)|\sigma| + (\rho_B(\sigma) - \rho_B(0))\dot{\rho}_B \,. \end{aligned} \tag{2.27}$$

At this point we have two options:

- Adaptation with Positive definite Barrier Function:

  With $\rho_B = \rho_{PB}$ in (2.10), the inequality (2.27) is rewritten as

  $$\begin{aligned} \dot{V} &\leq -(-d_{\max} + \rho_{PB})|\sigma| - (\rho_{PB} - \bar{F})\frac{\epsilon\bar{F}}{(\epsilon - |\sigma|)^2}\,(-d_{\max} + \rho_{PB}) \\ &= -\beta_{\sigma 1}|\sigma| - \zeta_1\beta_{\sigma 1}|\rho_{PB} - \bar{F}|\,, \end{aligned} \tag{2.28}$$

  where $\beta_{\sigma 1} = -d_{\max} + \rho_{PB}$, $\zeta_1 = \frac{\epsilon\bar{F}}{(\epsilon-|\sigma|)^2}$. Then, from [12, Lemma 5], one can conclude that (2.28) satisfies

  $$\dot{V} \leq -\beta_1 V^{1/2}, \quad \text{with} \quad \beta_1 = \beta_{\sigma 1}\sqrt{2}\min\{1, \zeta_1\}\,, \tag{2.29}$$

  that results a finite time convergence of the output variable to the region $|\sigma(t)| \leq \epsilon_1$ such that $|\sigma(t)| \leq \epsilon_1 < \epsilon$ where $\epsilon_1 = \epsilon(1 - \overline{F}/d_{\max})$ if $\overline{F} < d_{\max}$ and $\epsilon_1 = 0$ if $\overline{F} \geq d_{\max}$.

- Adaptation with Positive Semi-definite Barrier Function:

  With $\rho_B = \rho_{PSB}$ in (2.11), the inequality (2.27) is rewritten as

  $$\begin{aligned} \dot{V} &\leq -(-d_{\max} + \rho_{PSB})|\sigma| - \rho_{PSB}\frac{\epsilon}{(\epsilon - |\sigma|)^2}\,(-d_{\max} + \rho_{PSB}) \\ &= -\beta_{\sigma 2}|\sigma| - \zeta_2\beta_{\sigma 2}|\rho_{PSB}|\,, \end{aligned} \tag{2.30}$$

  where $\beta_{\sigma 2} = -d_{\max} + \rho_{PSB}$, $\zeta_2 = \frac{\epsilon}{(\epsilon-|\sigma|)^2}$. Then, from [12, Lemma 6], one can conclude that (2.30) satisfies

  $$\dot{V} \leq -\beta_2 V^{1/2}, \quad \text{with} \quad \beta_2 = \beta_{\sigma 2}\sqrt{2}\min\{1, \zeta_2\}\,, \tag{2.31}$$

that results in a finite time convergence of the output variable to the region $|\sigma(t)| \leq \epsilon_2$ such that $|\sigma(t)| \leq \epsilon_2 < \epsilon$ where $\epsilon_2 = \epsilon d_{\max}/(d_{\max}+1)$.

Thus, the proof is completed. □

It is clear from the proof of the Theorem 1 that, independently of the barrier strategy (positive definite or semi-definite) used in the residual phase, the proposed MBF adaptive scheme is simple and advantageous, since the monitoring function is able to ensure the convergence of the closed-loop system in a fixed time while the positive semi-definite barrier function allows the elimination of the chattering in the residual phase. For the positive definite barrier function case, a residual sliding mode remains in steady state but has the advantage of zeroing the output error if the persistent disturbance is ultimately small enough.

2.4 Numerical Examples

In this section two simulation results are presented, an academic example and application to anti-lock braking system, to illustrate the advantages of the MBF strategy.

2.4.1 Academic Example

In order to validate the MBF control strategy, this section considers an academic example of output-feedback stabilization for a nonlinear unstable system (2.1)–(2.2) such that $x^T = [\eta^T, \sigma]$, $A_{11} = \begin{bmatrix} -2 & 1 \\ 1 & -2 \end{bmatrix}$, $A_{12} = \begin{bmatrix} 0 \\ 1 \end{bmatrix}$, $A_{21} = \begin{bmatrix} 1 & 1 \end{bmatrix}$, $A_{22} = 1.75$, $K_p = 1$,

$$d_1(x,t) = \begin{bmatrix} \sin(10t)\mathrm{sgn}(\eta_1\eta_2) \\ \arctan(\eta_1+\eta_2+\sigma) + \cos(2t) + \exp(-\sigma^2/2) \end{bmatrix} [\mathbb{1}(t) - \mathbb{1}(t-25)]$$
$$d_2(x,t) = \left[0.25(1-\exp(-|\eta_2|)) - \exp(-\sigma^2/2)\right] [\mathbb{1}(t) - \mathbb{1}(t-25)] \ ,$$

where $\mathbb{1}(\cdot)$ is the unit step function and the initial conditions are $\eta^T(0) = [3, -2]$ and $\sigma(0) = 1$.

In the numerical tests, a maximum overshoot $\Delta = 0.5$, maximum transient time $T = 1$ [sec] and maximum residual value $\epsilon = 0.1$ was chosen as performance criteria. Then, the switching adaptation based on monitoring function follows (2.5) with parameters $R_1 = 1.01$ and $R_2 = 1.1$. Estimates for the disturbances bounds $\bar{d}_1$ and $\bar{d}_2$ are found according to (2.6) and (2.7), respectively, by setting $b_1 = b_2 = 1.21$,

$c_1 = 0.05$ and $c_2 = 0.1$. The hybrid state-norm observer (2.8) parameters are $\lambda_1 = -0.8$, $k_1 = 1.1$ and $k_2 = 1$. The constants of the sliding mode controller (2.12) are $c_\sigma = 0.003$, $c_{d\sigma} = 0.4$, $c_\eta = 0.5$ (see below (2.17)) and $\delta = 0.0001$. The results obtained for the proposed sliding mode controller combining monitoring and barrier functions are shown in Figs. 2.2 and 2.3.

The adaptation based on monitoring function guarantees the convergence of $\sigma(t)$ into the ϵ-neighborhood of the origin in fixed time $\bar{t} = 0.9582$ and 34 switchings, blue see Figures 2.2(b), 2.2(d), 2.3(b) and 2.3(d). In addition, the maximum allowed *overshoot* specification is satisfied, Figures 2.2(b) and 2.3(b). Since in the sliding mode reaching phase the monitoring functions were configured identically, there is an identical behavior of the closed loop system during time interval $0 \leq t \leq \bar{t}$.

During the residual phase, if the barrier function is positive definite, depending on the value of the constant $\overline{F}$, different behaviors can be observed. Note that, the upper bound $d_{\max}$ for the absolute value of the equivalent disturbance $d(x,t)$ in equation (2.24) is an unknown constant. Therefore, if $\overline{F}$ is chosen large enough such that $\overline{F} > d_{max}$, the ideal sliding mode occurs with $\sigma(t) \equiv 0 \ \forall t > \bar{t}$ and the control signal switches at infinite frequency with amplitude $\overline{F} = 2$. This situation is illustrated by the blue curves in Figures 2.2(b) and 2.2(c). On the other hand, if $\overline{F} < |d(x,t)|$, the control objective is achieved with the practical sliding mode and continuous control signal until $\overline{F} > |d(x,t)|$ where the ideal sliding mode begins, these situations are illustrated in red and yellow in Figures 2.2(b) and 2.2(c) with $\overline{F} = 1$ and $\overline{F} = 0.5$, respectively. While $\overline{F} < |d(x,t)|$, the control signals behave as estimates of the equivalent control. When $\overline{F} > |d(x,t)|$, the control signals switch in infinite frequency and amplitude $\overline{F}$.

If the barrier function is positive semi-definite, it is easy to verify that the control signal u attempts to cancel the equivalent disturbance $d(x,t)$ in (2.23), mathematically, $u \approx -d(x,t)$, see Figure 2.3(c). In other words, the control signal is always an estimate of the equivalent control. In a nutshell, the practical stabilization (convergence to a predefined neighborhood of the origin) is reached with a continuous control signal, see Figure 2.3.

When comparing the numerical results, it is noted that both approaches are able to ensure the control objective with guaranteed transient and steady-state performance for the output signal, see Figures 2.2(a), 2.2(b) and 2.3(a), 2.3(b).

2.4.2 Application Example

In sudden braking processes, the car's wheel may lock up, leading the driver to loose the vehicle control. In general, this behavior results in accidents with material damage and often involves fatal victims. To attenuate those effects, an important

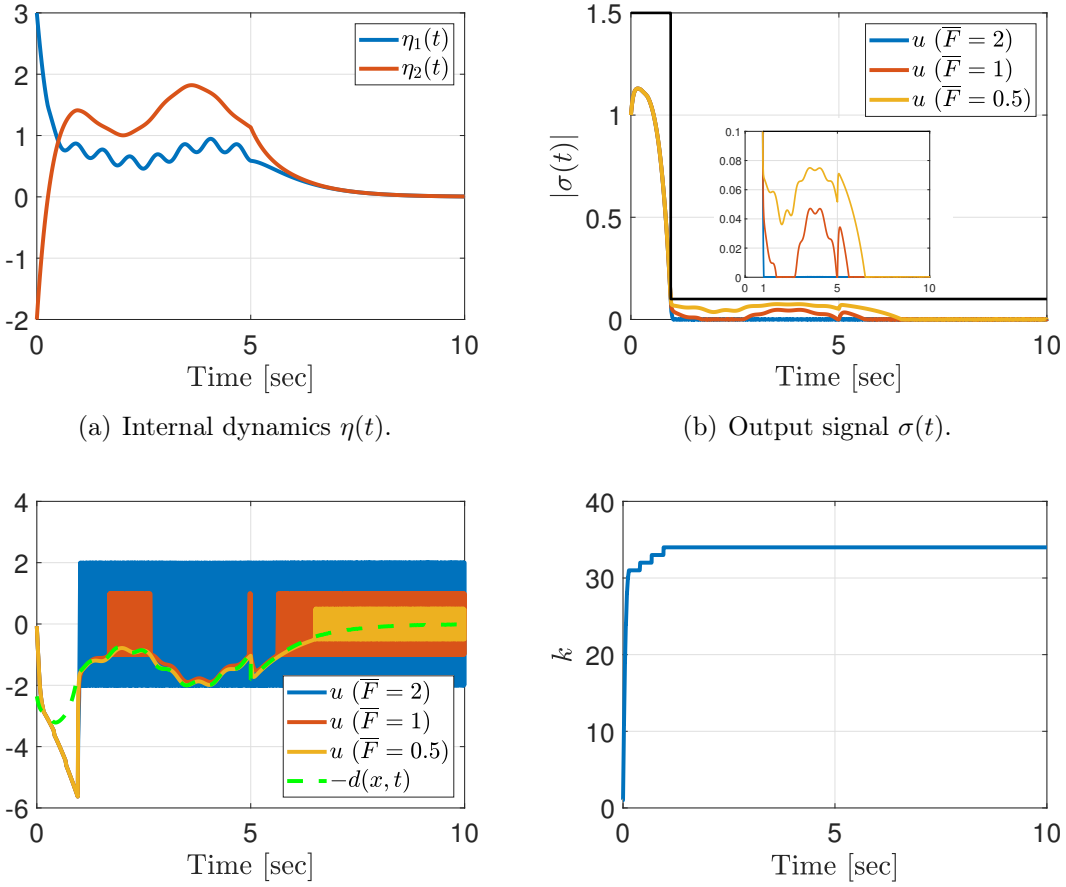

(a) Internal dynamics $\eta(t)$.

(b) Output signal $\sigma(t)$.

(c) Control signal u.

(d) Index of monitoring function switching k.

Figure 2.2: Simulation results - MBF control with positive definite barrier.

electromechanical device was designed, the Anti-lock Braking System (ABS). The ABS is able to detect the locking up of one or more wheels, and selectively reduce the braking pressure by means of the torque to be applied. Such procedure ensures to the driver that, even in a total braking situation, the vehicle will stop safely and quickly.

In this section, a simplified mathematical model based on INTECO laboratory anti-lock braking system [1] is developed. Consider the free body diagram in Figure 2.4, the lower wheel represents the car motion while the upper one represents the car's wheel motion and all parameters are given in Table 2.1. The upper wheel is equipped with the disk brake system connected to the brake lever which during deceleration is responsible for increasing the intensity of contact between the wheels generating a large friction force and causing the wheel speed reduction. From Figure 2.4, it is easy to see that the torque on the upper wheel is given by the friction torque between the wheels $F_N r_1 \mu(\lambda)$, by the friction torque in upper bearing M_{10}, and the input braking torque M_1. On the other hand, two friction torques appear on the lower wheel: between the wheels $F_N r_2 \mu(\lambda)$ and in the lower bearing M_{20}.

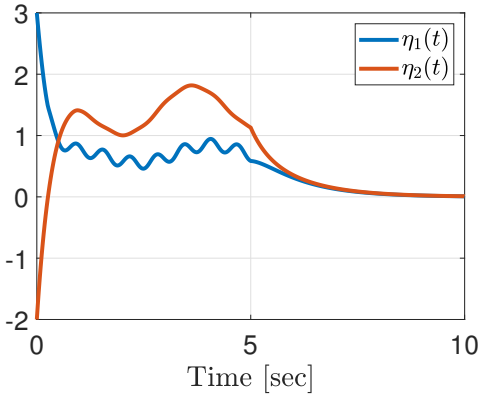

(a) Internal dynamics $\eta(t)$.

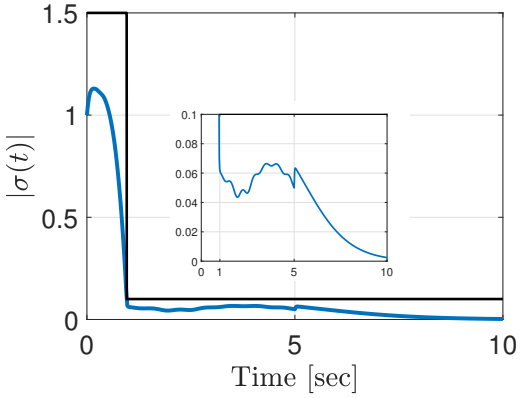

(b) Output signal $\sigma(t)$.

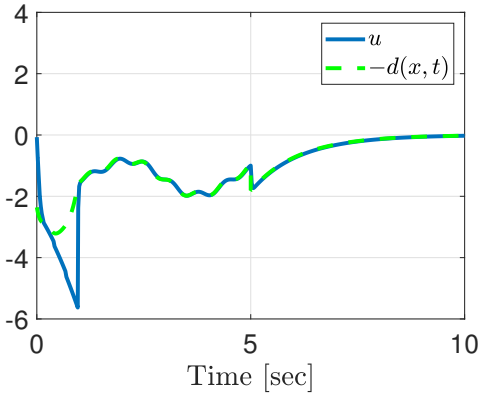

(c) Control signal u.

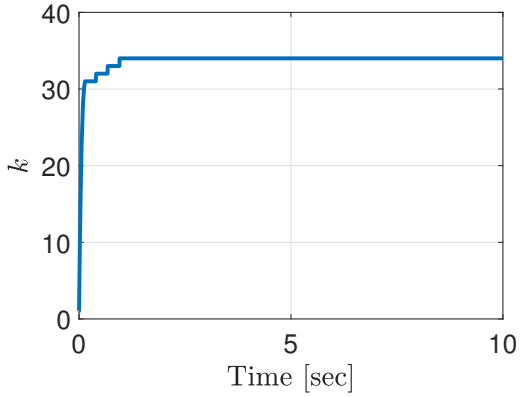

(d) Index of monitoring function switching k.

Figure 2.3: Simulation results - MBF control with semi-positive definite barrier.

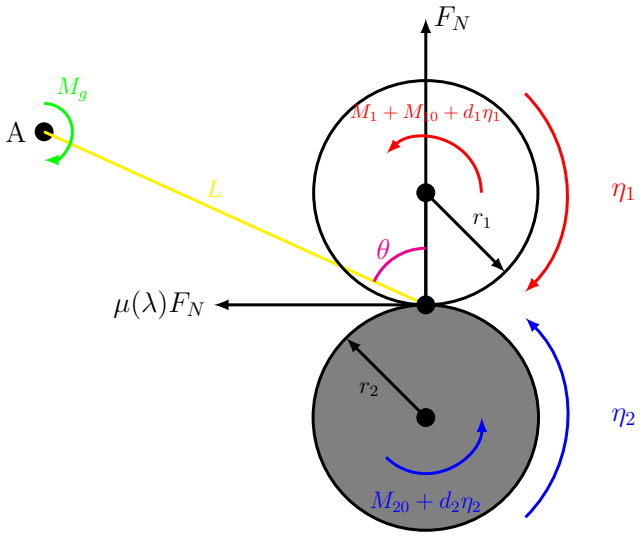

Figure 2.4: Free body diagram of ABS [1].

Besides these, we have two forces acting on the lower wheel: the gravity force of the upper wheel and the pressing force of the shock absorber. Moreover, the constant

M_g represents the gravitational and shock absorber torques acting on the balance lever.

Table 2.1: Parameters of INTECO ABS.

Parameter	**Description**	**Unit**	**Value**
r_1	radius of upper wheel	m	0.0990
r_2	radius of lower wheel	m	0.0995
L	balance lever length	m	0.370
θ	angle between the normal and the line L	$^\circ$	65.61
J_1	moment of inertia of upper wheel	kgm^2	7.53×10^{-3}
J_2	moment of inertia of lower wheel	kgm^2	25.60×10^{-3}
d_1	viscous friction coefficient of the upper wheel	kgm^2/s	1.1874×10^{-4}
d_2	viscous friction coefficient of the lower wheel	kgm^2/s	2.1468×10^{-4}
M_{10}	static friction of the upper wheel	Nm	0.0032
M_{20}	static friction of the lower wheel	Nm	0.0925
M_g	gravitational and shock absorber torques	Nm	19.62

By defining $\eta_1(t)$ as the angular velocity of the upper wheel of radius r_1 and $\eta_2(t)$ as the angular velocity of the lower wheel of radius r_2, the relative difference of the wheels velocities $\lambda(t)$ is given by

$$\lambda(t) := \begin{cases} \dfrac{r_2\eta_2(t) - r_1\eta_1(t)}{r_2\eta_2(t)}\,, & r_2\eta_2(t) > r_1\eta_1(t)\,, \quad \eta_1(t) > 0\,, \eta_2(t) > 0 \\ \dfrac{r_1\eta_1(t) - r_2\eta_2(t)}{r_1\eta_1(t)}\,, & r_1\eta_1(t) > r_2\eta_2(t)\,, \quad \eta_1(t) > 0\,, \eta_2(t) > 0 \\ 1\,, \qquad \eta_1(t) \leq 0 \text{ and } \eta_2(t) > 0 \quad \text{or} \quad \eta_1(t) > 0 \text{ and } \eta_2(t) \leq 0 \end{cases} . \tag{2.32}$$

Since the friction force is obtained as the product of the normal pressing force $F_N(t)$ with the proportionality coefficient

$$\mu(\lambda(t)) = \frac{c_4\lambda^p(t)}{a + \lambda^p(t)} + c_3\lambda^3(t) + c_2\lambda^2(t) + c_1\lambda(t)\,, \tag{2.33}$$

the Newton's second law for rotatory motion leads to

$$\dot{\eta}_1(t) = \frac{1}{J_1}F_N(t)r_1 s\mu(\lambda) - \frac{d_1}{J_1}\eta_1(t) - s_1\frac{M_{10}}{J_1} - \frac{1}{J_1}s_1 M_1(t)\,, \tag{2.34}$$

$$\dot{\eta}_2(t) = -\frac{1}{J_2}F_N(t)r_2 s\mu(\lambda) - \frac{d_2}{J_2}\eta_2(t) - s_2\frac{M_{20}}{J_2}\,, \tag{2.35}$$

with auxiliary variables

$$s = \operatorname{sgn}(r_2\eta_2(t) - r_1\eta_1(t))\,, \tag{2.36}$$

$$s_1 = \operatorname{sgn}(\eta_1(t))\,, \tag{2.37}$$

$$s_2 = \operatorname{sgn}(\eta_2(t))\,. \tag{2.38}$$

Notice that, from the sum of torques with respect to the point A in Figure 2.4, the normal force is given by

$$F_N(t) = \frac{M_g + s_1 M_1(t) + s_1 M_{10} + d_1 \eta_1(t)}{L(\sin(\theta) - s\mu(\lambda(t))\cos(\theta))} \,. \tag{2.39}$$

Therefore, from (2.32)–(2.39), the dynamics of the slip rate $\lambda(t)$ is given by

$$\frac{d\lambda(t)}{dt} = f(\eta, t) + g(\eta, t) M_1(t) \,, \tag{2.40}$$

satisfying

$$|f(\eta, t)| \leq \overline{f} \quad \text{and} \quad 0 < \underline{g} \leq |g(\eta, t)| \,, \tag{2.41}$$

where $\overline{f}$ and $\underline{g}$ are unknown constants, see Appendix.

In this chapter, the braking torque applied to the upper wheel, M_1 [Nm], is defined as the input signal, the state vector is defined as $\eta(t) = [\eta_1(t) \,, \eta_2(t)]^T \in \mathbb{R}^2$ and $\lambda(t)$ is an output of unitary relative degree. Besides that, $r_1\eta_1$ represents the vehicle wheel longitudinal velocity, while $r_2\eta_2$ represents the car velocity.

The role of the ABS is to control the wheel slip to maximize the coefficient of friction between the tire and road for any given road surface while the car is controllable. In this sense, the control objective is defined as the regulation of the slip coefficient in λ_{ref} such that $\mu(\lambda)$ reaches its maximum value $\overline{\mu}$ [90–92]. Figure 2.5 shows in blue the longitudinal friction μ-λ curve generated from (2.33) with parameters of Table 2.2 and in red color the optimum ABS operation point is denoted, where $\lambda_{\text{ref}} = 0.1875$ and $\overline{\mu} = \mu(\lambda_{\text{ref}}) = 0.3954$.

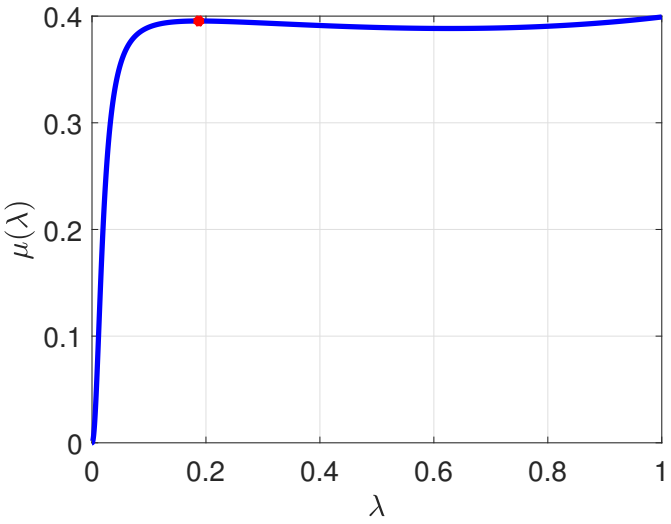

Figure 2.5: Longitudinal friction μ-λ curve.

Table 2.2: Parameters of the friction coefficient equation (2.33).

Parameter	Value
a	0.00025724985785
c_1	-0.04240011450454
c_2	0.00000000029375
c_3	0.03508217905067
c_4	0.40662691102315
p	2.09945271667129

The output error is defined as

$$\sigma(t) := \lambda(t) - \lambda_{\text{ref}}\,, \tag{2.42}$$

such that, from (2.32), its dynamics is governed by

$$\dot{\sigma}(t) = f(\eta, t) + g(\eta, t)M_1\,, \tag{2.43}$$

where it is assumed the torque M_1 as an input signal. Of course (2.34), (2.35) and (2.43) differ structurally from (2.1) and (2.2), nevertheless, by using the control law (2.12) as

$$M_1 = -s\rho(t)\text{sgn}(\sigma(t))\,, \tag{2.44}$$

where s is given by (2.36), the positive constant $\underline{g}$ satisfies (A.10), and modulation function $\rho(t)$ in (2.13), all properties and results provided from Theorem 1 are ensured to the closed-loop system. In order to illustrate it, consider the following energy function

$$V_\sigma = \frac{1}{2}\sigma^2\,, \tag{2.45}$$

whose time derivative, along with (2.43) and (2.44), is

$$\begin{aligned}
\dot{V}_\sigma &= \sigma\dot{\sigma} \\
&= \sigma\left[f(\eta, t) + g(\eta, t)M_1\right] = \sigma g(\eta, t)\left[g^{-1}(\eta, t)f(\eta, t) + M_1\right] \\
&= \sigma s|g(\eta, t)|\left[s|g^{-1}(\eta, t)|f(\eta, t) - s\rho(t)\text{sgn}(\sigma)\right] \\
&= \sigma|g(\eta, t)|\left[d(\eta, t) - \rho(t)\text{sgn}(\sigma)\right]\,, \quad d(\eta, t) = |g^{-1}(\eta, t)|f(\eta, t)\,.
\end{aligned} \tag{2.46}$$

From (A.9) and (A.10), it is possible to find an upper bound for equation (2.46) such as

$$\dot{V}_\sigma \leq |g(\eta, t)|\left[|d(\eta, t)| - \rho(t)\right]|\sigma|\,. \tag{2.47}$$

Thus, during the reaching phase, by using $\rho(t) = \rho_M(t)$ in (2.14) with $c_\sigma = c_\eta = 0$, $c_{d_\sigma} = 1$, $\hat{d}_2(k) = \hat{d}(k)$, the inequality (2.47) is rewritten as

$$\dot{V}_\sigma \leq -|g(\eta,t)|(\hat{d}(k) - \overline{d})|\sigma| - \delta|g(\eta,t)||\sigma|\,. \tag{2.48}$$

From Theorem 1, no matter how large $\overline{d}$ is, there exist a finite switching number $\bar{k}$ such that $\hat{d}(k) > \overline{d}$ for all $k \geq \bar{k}$ and, therefore, the sliding mode condition,

$$\sigma\dot{\sigma} \leq -\delta\underline{g}|\sigma|\,, \tag{2.49}$$

is verified until the residual phase begins, where the barrier function ultimately confines the output variable into a residual set of $\mathcal{O}(\epsilon)$. Therefore, the ABS remains active at its optimal operating point, leading to the quickly reaching of the threshold velocities $\underline{\eta}_1$ and $\underline{\eta}_2$.

In the simulation, the initial conditions are $\eta_1(0) = \eta_2(0) = 180$ [rad/s], the monitoring function parameters are $\epsilon = 0.001$, $R_1 = 1.01$, $R_2 = 2.5$, $\Delta = 0.001$ while $T \in \{0.25, 0.50, 0.75, 1\}$ and the positive barrier function is $\overline{F} = 4.5$.

Figures 2.6 and 2.7 show the performance of the proposed adaptive sliding mode controller (2.44) with monitoring and barrier functions in an ABS for distinct values of maximum transient time T. As mentioned earlier, the ABS is turned on only for a short period of time. Figures 2.6(d) and 2.7(d) show that the system is activated for approximately 1.5 seconds and less than 1.6 seconds is needed to completely stop the car which had an initial velocity of 64 km/h, see Figures 2.6(g), 2.6(h) and Figures 2.7(g), 2.7(h) with traveled distances given in Figures 2.6(i), 2.6(j) and Figures 2.7(i), 2.7(j). With a finite number of commutations, the control objective is reached, see Figures 2.6(a), 2.6(b) and Figures 2.7(a), 2.7(b), and the braking process is carried out with the optimum efficient friction coefficient, Figure 2.6(c)–2.6(f) and Figure 2.7(c)–2.7(f).

Notice that, no matter which barrier function was chosen, positive definite or positive semi-definite, the proposed strategy based on monitoring function ensures the design of adaptation gains which can increase in an event-driven fashion during the reaching phase to respect the maximum allowed transient time T and overshooting Δ, see Figures 2.6 and 2.7. There are differences between the proposed approaches and they are clear in the residual phase. Of course, from an application point of view, the chattering phenomenon can cause unacceptable loading and energy consumption of the actuators and, therefore, it should be avoided. Although the positive barrier is effective to guarantee the control objectives, the positive semi-definite one is also efficient since it avoids chattering, as can be seen from Figures 2.6(d)–2.6(f) and 2.7(d)–2.7(f), respectively. In the ABS problem, this residual error does not have any significant effect.

In order to establish a comparison with another existing method , consider the adaptive sliding mode control law [2],

$$M_1 = -sK(t)\ \mathrm{sgn}(\sigma(t))\,, \tag{2.50}$$

$$\dot{K}(t) = \bar{K}|\sigma(t)|\,, \tag{2.51}$$

where the constants are $\bar{K} > 0$ and $K(0) \geq 0$. In Figure 2.8, the initial condition is $K(0) = 0$ while $\bar{K} \in \{25, 50, 75, 100\}$. This approach does not require the knowledge of an upper bound for the disturbance but can lead to its overestimation leading to chattering, see Figures 2.8(d)–2.8(f). Furthermore, this methodology cannot ensures the transient pre-specification and consequently, the traveled distance may be higher than achieved with the MBF strategy proposed here, see Figure 2.8(a)–2.8(c) and Figures2.8(g)–2.8(j).

The sliding modes control law M_1 in Figure 2.6 switches in infinite frequency and, therefore, its slow rate component, the equivalent control $M_1^{\mathrm{eq}}(t)$, acts in order to cancel the disturbance $d(\eta, t)$ in (2.46). In other words, on the manifold $\sigma(t) = 0$, $M_1^{\mathrm{eq}}(t)$ is the continuous control effort that yields $\dot{\sigma}(t) \equiv 0$, *i.e.*, $M_1^{\mathrm{eq}}(t) = -d(\eta, t)$. Although $M_1^{\mathrm{eq}}(t)$ cannot be obtained physically, a realizable estimate is found by averaging the discontinuous control with a first-order filter [93]

$$\tau \dot{M}_1^{\mathrm{av}}(t) = -M_1^{\mathrm{av}}(t) + M_1\,, \quad M_1^{\mathrm{av}}(0) = 0\,, \tag{2.52}$$

satisfying, almost everywhere,

$$|M_1^{\mathrm{av}}(t) - M_1^{\mathrm{eq}}(t)| \leq \mathcal{O}(\tau)\,, \quad \lim_{\tau \to 0} \mathcal{O}(\tau) = 0\,. \tag{2.53}$$

In practice, the time constant $0 < \tau << 1$ should be small enough as compared to the slow frequency components and large enough to filter out the high frequency components [10].

Now, there is one more detail to be explored between the MBF method with positive definite (MPBF) or semi-definite barrier function (MPSBF). The control gain generated by the positive semi-definite barrier leads to a slightly inferior perturbation compensation. This is not significant since a precise compensation is not needed. Note that the chattering does not occur at the price of a residual nonzero error in $\sigma(t)$. On the other hand, in the positive definite barrier case, high frequency chattering appears (only) when the bias $\bar{F}$ in (2.10) exceeds the disturbance upper bound $\bar{d}$. Then, the equivalent control $M_1^{\mathrm{eq}}(t)$ exactly compensates the perturbation, see Figure 2.9.

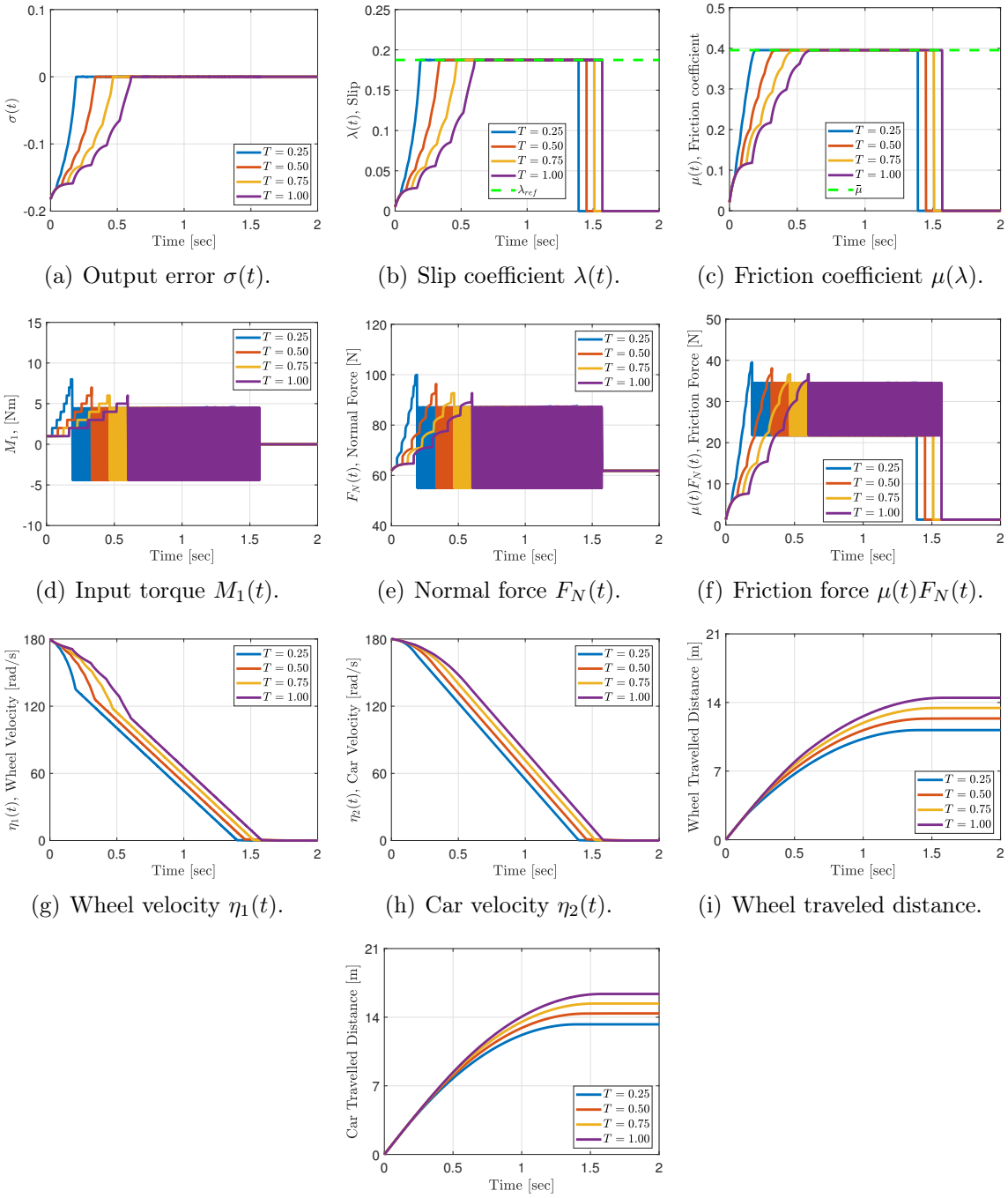

(a) Output error $\sigma(t)$. (b) Slip coefficient $\lambda(t)$. (c) Friction coefficient $\mu(\lambda)$.

(d) Input torque $M_1(t)$. (e) Normal force $F_N(t)$. (f) Friction force $\mu(t)F_N(t)$.

(g) Wheel velocity $\eta_1(t)$. (h) Car velocity $\eta_2(t)$. (i) Wheel traveled distance.

(j) Car traveled distance.

Figure 2.6: ABS with MBF control and positive definite barrier.

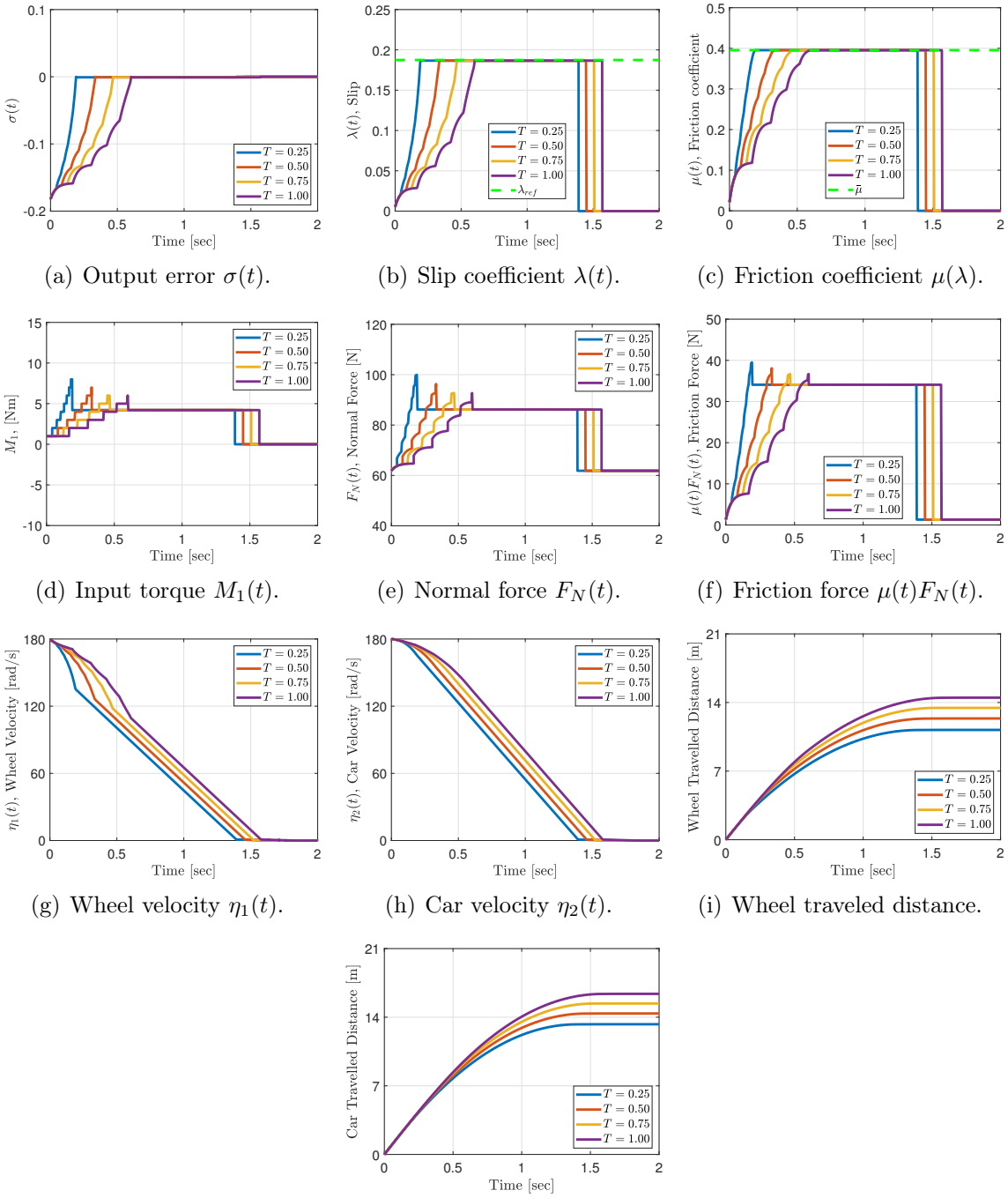

(a) Output error $\sigma(t)$. (b) Slip coefficient $\lambda(t)$. (c) Friction coefficient $\mu(\lambda)$.

(d) Input torque $M_1(t)$. (e) Normal force $F_N(t)$. (f) Friction force $\mu(t)F_N(t)$.

(g) Wheel velocity $\eta_1(t)$. (h) Car velocity $\eta_2(t)$. (i) Wheel traveled distance.

(j) Car traveled distance.

Figure 2.7: ABS with MBF control and semi-positive definite barrier.

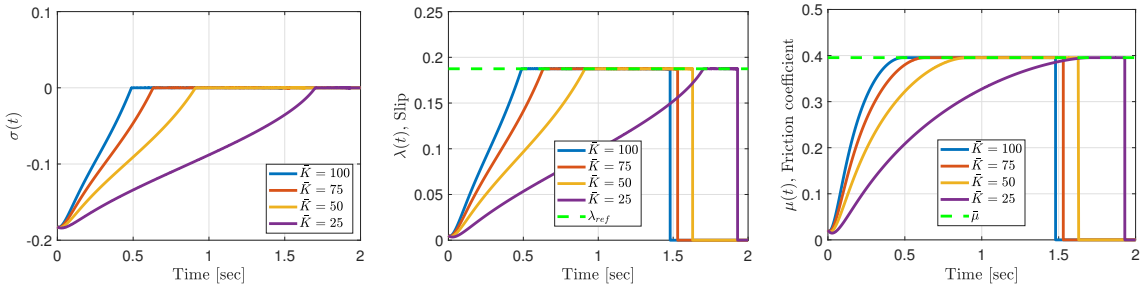

(a) Output error $\sigma(t)$. (b) Slip coefficient $\lambda(t)$. (c) Friction coefficient $\mu(\lambda)$.

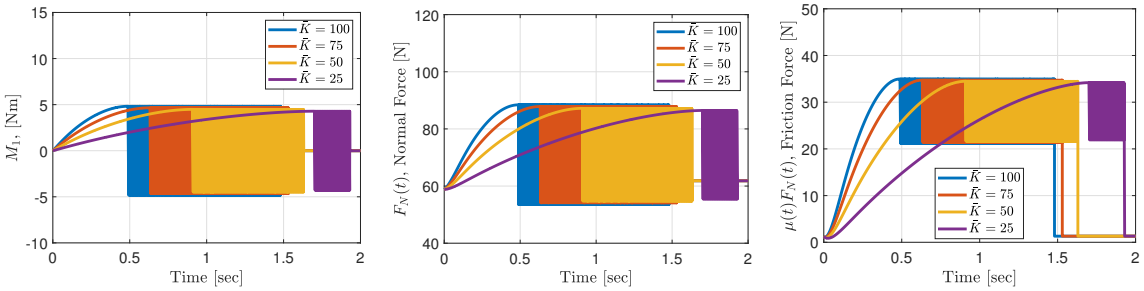

(d) Input torque $M_1(t)$. (e) Normal force $F_N(t)$. (f) Friction force $\mu(t)F_N(t)$.

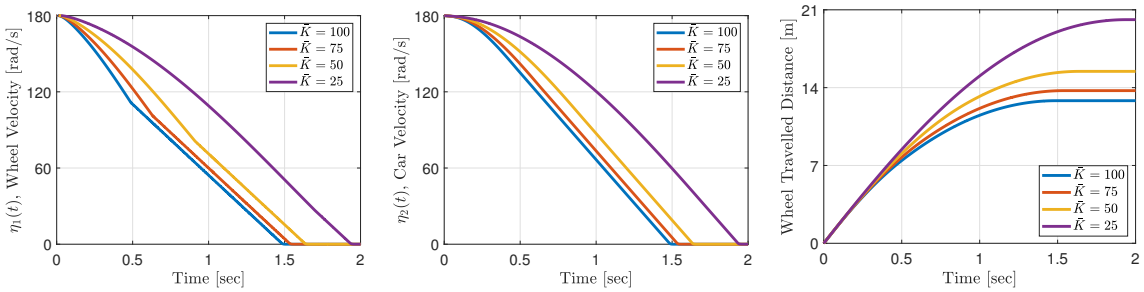

(g) Wheel velocity $\eta_1(t)$. (h) Car velocity $\eta_2(t)$. (i) Wheel traveled distance.

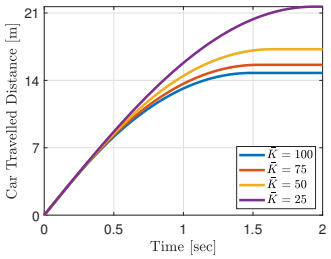

(j) Car traveled distance.

Figure 2.8: ABS with adaptive SMC [2].

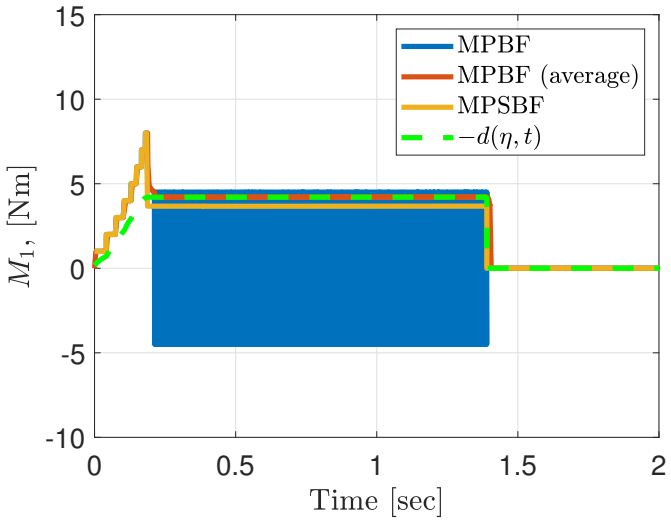

Figure 2.9: Comparison between the control efforts.

Chapter 3

Multivariable Unit Vector Control with Prescribed Performance via Monitoring and Barrier Functions

This chapter proposes an adaptive unit vector control approach via output feedback for a class of multivariable nonlinear systems. The sliding-mode based controller can deal with parametric uncertainties and (un)matched disturbances with unknown upper bounds. Fixed-time convergence of the output to a predefined neighborhood of the origin of the closed-loop system is proved with guaranteed transient performance. The novelty of our result lies on combining two important adaptation tools: monitoring and barrier functions. The adaptation process is divided into two stages, where an appropriate monitoring function allows for the specification of performance criteria during the transient phase, while the barrier function ultimately confines the output within a small residual set in steady-state. Simulation results including an application to Overhead Crane System illustrate the advantages of the proposed adaptive control strategy.

3.1 Problem Formulation

Consider the uncertain MIMO nonlinear plant in regular form

$$\dot{\eta}(t) = A_{11}\eta(t) + A_{12}\sigma(t) + d_1(\eta(t)\,,\sigma(t)\,,t)\,, \tag{3.1}$$

$$\dot{\sigma}(t) = A_{21}\eta(t) + A_{22}\sigma(t) + d_2(\eta(t)\,,\sigma(t)\,,t) + B_2 u\,, \tag{3.2}$$

where the state is defined as $x^T(t) := [\eta^T(t)\,,\sigma^T(t)] \in \mathbb{R}^n$, $\eta(t) \in \mathbb{R}^{n-m}$ its unmeasured part, $\sigma(t) \in \mathbb{R}^m$ is the output, $u \in \mathbb{R}^m$ is the input control vector while the mapping $d_1 : \mathbb{R}^{n-m} \times \mathbb{R}^m \times \mathbb{R}^+ \mapsto \mathbb{R}^{n-m}$ and $d_2 : \mathbb{R}^{n-m} \times \mathbb{R}^m \times \mathbb{R}^+ \mapsto \mathbb{R}^m$ represent the disturbances. Moreover, the following assumptions are considered throughout

the chapter:

(A1) The matrix $A_{11} \in R^{(n-m)\times(n-m)}$, $A_{12} \in R^{(n-m)\times m}$, $A_{21} \in R^{m\times(n-m)}$, $A_{22} \in R^{m\times m}$ and $B_2 \in \mathbb{R}^{m\times m}$ are constant and uncertain.

(A2) It is known that A_{11} is Hurwitz, *i.e.*, the plant (3.1)–(3.2) has minimum phase. This assumption is extremely important since it allows the design of a stable upper bound for the norm of the unmeasured state variable $\eta(t)$.

(A3) The norm of matrix A_{12} is majored by a known constant $c_{\eta\sigma}$.

(A4) The disturbances $d_1(x(t)\,,t)$ and $d_2(x(t)\,,t)$ are Lipschitz in x, piece wise continuous in t and uniformly bounded by unknown constants $\bar{d}_1$ and $\bar{d}_2$:

$$||d_1(x,t)|| \leq \bar{d}_1 \quad \text{and} \quad ||d_2(x,t)|| \leq \bar{d}_2\,, \quad \forall t \geq 0\,.$$

(A5) There exists a matrix S_p such that the high-frequency gain matrix is defined by

$$K_p := B_2 S_p$$

and $-K_p$ is Hurwitz.

(A6) Only the output $\sigma(t)$ is available to the feedback design.

The control objective is the ultimate confinement of $\sigma(t)$ to an ϵ-vicinity of the origin in the global sense for all instant t greater than a finite time t_s ($||\sigma(t)|| \leq \epsilon$, $\forall t \geq t_s$), by using only output feedback. To reach it, with the constraint of unknowing the upper bounds $\bar{d}_1$ and $\bar{d}_2$, some adaptation strategy is necessary.

3.2 Basic Techniques

In this section, basic techniques for the proposed control strategy are introduced.

3.2.1 Norm Observer

The first step to start the control design is to overcome the unmeasured state problem. The norm observer, also called first order approximation filter (FOAF), is an important tool that allows to reach it by using only output information, for more details see [87]. Lemma 1 shows how the solution of the dynamics

$$\dot{\bar{\eta}}(t) = -k_1\bar{\eta}(t) + k_2(||\sigma(t)|| + \bar{d}_1)\,, \tag{3.3}$$

is an upper bound for the norm of $\eta(t)$ in (3.1) where, from (A4), $\bar{d}_1$ is a positive constant. Furthermore, $\eta(t)$ and $\bar{\eta}(t)$ satisfy the inequality

$$\|\eta(t)\| \leq k_3|\bar{\eta}(t)| + \pi_\eta(t)\,, \quad \forall t \geq 0\,, \tag{3.4}$$

with constants $k_1, k_2, k_3 > 0$ while $\pi_\eta(t)$ is a exponentially decreasing term and depend on the initial conditions $\eta(0)$ and $\bar{\eta}(0)$.

Lemma 1. *Consider the η-dynamics in (3.1) and suppose that the assumptions (A1)-(A3) are satisfied. Then, $\bar{\eta}(t)$ in (3.3) is a norm observer of $\eta(t)$ satisfying (3.4).*

Proof. Consider the following candidate Lyapunov function

$$V_\eta(t) = \eta(t)^T P_\eta \eta(t)\,, \quad P_\eta = P_\eta^T > 0\,, \tag{3.5}$$

P_η being the solution of the Lyapunov equation

$$A_{11}^T P_\eta + P_\eta A_{11} = -Q_\eta, \quad Q_\eta = Q_\eta^T > 0\,, \tag{3.6}$$

and the Rayleigh-Ritz inequality,

$$\lambda_{\min}\{P_\eta\}\|\eta(t)\|^2 \leq V_\eta \leq \lambda_{\max}\{P_\eta\}\|\eta(t)\|^2\,, \tag{3.7}$$

where $\lambda_{\min}\{\cdot\}$ and $\lambda_{\max}\{\cdot\}$ denote, respectively, the minimum and maximum eigenvalue of a given matrix.

By taking the time derivative of (3.5) with (3.1) and (3.6), one arrives at

$$\begin{aligned}
\dot{V}_\eta(t) &= \dot{\eta}^T(t)P_\eta\eta(t) + \eta(t)^T P_\eta\dot{\eta}(t) \\
&= \eta^T(t)(A_{11}^T P_\eta + P_\eta A_{11})\eta(t) + 2\sigma^T(t)A_{12}^T P_\eta\eta(t) + 2d_1^T(x,t)A_{12}^T P_\eta\eta(t) \\
&= -\eta^T(t)Q_\eta\eta(t) + 2\sigma^T(t)A_{12}^T P_\eta\eta(t) + 2d_1^T(x,t)A_{12}^T P_\eta\eta(t)\,.
\end{aligned} \tag{3.8}$$

Then, equation (3.8) is upper bounded by

$$\begin{aligned}
\dot{V}_\eta(t) &\leq -\lambda_{\min}\{Q_\eta\}\|\eta(t)\|^2 + 2\|A_{12}\|\|P_\eta\|(\|\sigma(t)\| + \|d_1(x,t)\|)\|\eta(t)\| \\
&= -\lambda_{\min}\{Q_\eta\}\|\eta(t)\|^2 + 2\|A_{12}\|\lambda_{\max}\{P_\eta\}(\|\sigma(t)\| + \|d_1(x,t)\|)\|\eta(t)\|\,,
\end{aligned} \tag{3.9}$$

by using the inequality (3.39) and (A4),

$$\begin{aligned}
\dot{V}_\eta(t) &\leq -\frac{\lambda_{\min}\{Q_\eta\}}{\lambda_{\max}\{P_\eta\}}V_\eta + \frac{2\|A_{12}\|\lambda_{\max}\{P_\eta\}}{\lambda_{\min}\{P_\eta\}}(\|\sigma(t)\| + \|d_1(x,t)\|)\sqrt{V_\eta} \\
&\leq -\frac{\lambda_{\min}\{Q_\eta\}}{\lambda_{\max}\{P_\eta\}}V_\eta + \frac{2\|A_{12}\|\lambda_{\max}\{P_\eta\}}{\lambda_{\min}\{P_\eta\}}(\|\sigma(t)\| + \bar{d}_1)\sqrt{V_\eta}\,.
\end{aligned} \tag{3.10}$$

Now, defining $\tilde{\eta} := \sqrt{V_\eta}$ whose time derivative is $\dot{\tilde{\eta}} = \dfrac{\dot{V}_\eta}{2\sqrt{V_\eta}}$, is possible to upper bound it as

$$\dot{\tilde{\eta}}(t) \leq -\frac{\lambda_{\min}\{Q_\eta\}}{2\lambda_{\min}\{P_\eta\}}\tilde{\eta}(t) + \frac{\|A_{12}\|\lambda_{\max}\{P_\eta\}}{\lambda_{\min}\{P_\eta\}}(\|\sigma(t)\| + \bar{d}_1)\,. \tag{3.11}$$

Now, it is defined the constants $0 < k_1 < \frac{\lambda_{\min}\{Q_\eta\}}{2\lambda_{\min}\{P_\eta\}}$ and $k_2 > \frac{\|A_{12}\|\lambda_{\max}\{P_\eta\}}{\lambda_{\min}\{P_\eta\}}$, and upper bound for (3.11) is given by

$$\dot{\tilde{\eta}}(t) \leq -k_1\tilde{\eta}(t) + k_2(\|\sigma(t)\| + \bar{d}_1)\,. \tag{3.12}$$

Then, invoking the Comparison Lemma [94, p. 102], the solution $\bar{\eta}(t)$ of (3.3) is an upper bound for $\tilde{\eta}(t)$ such that

$$\tilde{\eta}(t) \leq \bar{\eta}(t) + \exp(-k_1 t)(\tilde{\eta}(0) - \bar{\eta}(0))\,, \tag{3.13}$$

consequently,

$$\tilde{\eta}(t) \leq |\bar{\eta}(t)| + \exp(-k_1 t)(|\tilde{\eta}(0)| + |\bar{\eta}(0)|)\,, \tag{3.14}$$

and, by using the Rayleigh-Ritz inequality (3.39),

$$\|\eta(t)\| \leq \frac{1}{\sqrt{\lambda_{\min}\{P_\eta\}}}|\bar{\eta}(t)| + \exp(-k_1 t)\frac{(|\tilde{\eta}(0)| + |\bar{\eta}(0)|)}{\sqrt{\lambda_{\min}\{P_\eta\}}}\,, \tag{3.15}$$

therefore the inequality (3.4) is satisfied for any

$$k_3 > \frac{1}{\sqrt{\lambda_{\min}\{P_\eta\}}} \quad \text{and} \quad \pi_\eta(t) > \exp(-k_1 t)\frac{(|\tilde{\eta}(0)| + |\bar{\eta}(0)|)}{\sqrt{\lambda_{\min}\{P_\eta\}}}. \tag{3.16}$$

□

Note that although $\bar{\eta}(t)$ is a upper bound for the unmeasured part of the state $\eta(t)$, it cannot be implemented since, by assumption (A5), $\bar{d}_1$ is unknown. The next section introduces the monitoring function, an important tool that finally allows the implementation of an upper bound for $\eta(t)$ by means of a hybrid state-norm estimation [25].

3.2.2 Monitoring Function - Reaching Phase

The monitoring function is an appropriate switching scheme designed to compensate the absence of information such as unknown control direction [21], unknown bounds of disturbances [26] or disturbances with unknown and arbitrary growth rate [95].

Here a more recent version [15] is presented in which performance specifications of the closed-loop system could be achieved.

Definition 2. *The stabilization of $\sigma(t)$ is said to satisfy the reaching and residual phase specifications, if*

- $\|\sigma(t)\| \leq \|\sigma(0)\| + \Delta$, $\forall t \in [0\,, T)$,
- $\|\sigma(t)\| \leq \epsilon\,, \quad \forall t \geq T\,,$

where $\Delta > 0$ is the allowed maximum overshoot, $T > 0$ is the maximum transient time, $\varepsilon > 0$ is the allowed maximum steady-state error, which can be freely specified.

In the reaching phase the monitoring function should force $\|\sigma(t)\| \leq \varepsilon/R_2$ before a fixed time T ensuring non-infringement of the overshoot specification. The monitoring switching scheme is such that for every k for which $\|\sigma(t_k)\| > \varepsilon/R_2$, the next switching instant is defined as

$$t_{k+1} := \min \left\{ t > t_k : \begin{array}{c} \|\sigma(t)\| = \|\sigma(0)\| + \Delta\left(1 - \frac{1}{R_1^k}\right) \\ \text{or} \\ t = T\left(1 - \frac{1}{R_1^k}\right) \quad \text{and} \quad \|\sigma(t)\| > \epsilon/R_2 \end{array} \right. , \quad k = 1, 2, \ldots \tag{3.17}$$

where $R_1 > 1$ and $R_2 > 1$ are design constants. If, for some time interval $\bar{t} < T$, the condition $\|\sigma(\bar{t})\| = \varepsilon/R_2$ is reached, then the Residual Phase (Section 3.2.3) is started.

Moreover, the switching index k is employed in the design of positive monotonically increasing unbounded sequences $\hat{d}_1(k)$ and $\hat{d}_2(k)$ to counteract the absence of constants $\bar{d}_1$ and $\bar{d}_2$, respectively, *i.e.*,

$$\hat{d}_1(k) = c_1 b_1^k\,, \tag{3.18}$$

$$\hat{d}_2(k) = c_2 b_2^k\,, \tag{3.19}$$

where $c_1\,, c_2 > 0$, and $b_1\,, b_2 > \max\{R_1\,, R_2\}$ are arbitrarily chosen constants. Then, it is introduced a hybrid state-norm estimation scheme, based on (3.3)–(3.4),

$$\dot{\hat{\eta}}(t) = -k_1\hat{\eta}(t) + k_2(||\sigma(t)|| + \hat{d}_1(k))\,, \tag{3.20}$$

such that

$$\|\eta(t)\| \leq k_3|\hat{\eta}(t)| + \pi_\eta(t)\,, \quad \forall t \geq 0\,. \tag{3.21}$$

The norm observer $\hat{\eta}(t)$ flows through a continuous state space but also moves through different discrete switching modes, as defined by [89].

An important property of the switching rule is that, if k grows and becomes sufficiently large, then $\sigma(t)$ satisfies its predefined specifications on the reaching phase through the switching law (3.17). In the reaching phase, the switching makes $\hat{d}_1(k)$ and $\hat{d}_2(k)$ to grow unboundedly as $k \to \infty$. As a result, during the reaching phase, the monitoring function forces $\|\sigma(t)\| \leq \epsilon/R_2$ before the fixed time instant T while ensuring no violation of the overshoot specification.

3.2.3 Barrier Function - Residual Phase

The Barrier Function, for a given and fixed $\varepsilon > 0$, is defined as an even continuous function $\rho_B : \chi \in (-\varepsilon\,, \varepsilon) \to \rho_B(\chi) \in [\, b\,, \infty\,)$ strictly increasing on $[\, 0\,, \varepsilon\,)$ such that $\lim_{|\chi|\to\varepsilon} \rho_B(\chi) = +\infty$, $\rho_B(\chi)$ has a unique minimum at zero and $\rho_B(0) = b \geq 0$.

In the residual phase, the introduction of a barrier function imposes a hard bound on the sliding variable by trapping it within a prescribed ϵ-vicinity. The important features of the controllers based on barrier functions just requires the disturbances to be bounded, but there is no need to know what the bounds are and the assurance of avoiding overestimated control gains. Basically as shown in Figure 2.1, in sliding mode control framework, there are two kinds of barrier functions:

- Positive definite Barrier Function (PBF)

$$\rho_{pb}(\chi) := \frac{\varepsilon \bar{F}}{\varepsilon - |\chi|} \quad i.e., \quad \rho_{PB}(0) = \bar{F} > 0\,. \tag{3.22}$$

- Positive Semi-definite Barrier Function (PSBF)

$$\rho_{psb}(\chi) := \frac{|\chi|}{\varepsilon - |\chi|} \quad i.e. \quad \rho_{PSB}(0) = 0\,. \tag{3.23}$$

For more details, please see [12].

The next section shows how the Barrier Functions can be employed as an adaptive strategy for not overestimated Unit Vector Control schemes.

3.2.4 Adaptive Unit Vector Control

The Monitoring and Barrier Function (MBF) adaptive unit vector control law is given by

$$u = -\rho(t) S_p \frac{\sigma(t)}{\|\sigma(t)\|}\,, \tag{3.24}$$

where the matrix S_p is chosen to verify assumption **(A2)** and $\rho(t)$ is the *modulation function* such that

$$\rho(t) = \begin{cases} \rho_M(t)\,, & \text{if} \quad t < \bar{t} \\ \rho_B(t)\,, & \text{if} \quad t \geq \bar{t} \end{cases} \quad . \tag{3.25}$$

While the closed-loop system is in the reaching phase, it is under monitoring function action and, using the hybrid norm observer (3.20) and disturbance estimate (3.19) with the modulation function designed as

$$\rho_M(t) = c_\sigma \|\sigma(t)\| + c_{d_\sigma} \hat{d}_2(k) + c_\eta \hat{\eta}(t) + \delta\,, \tag{3.26}$$

with appropriate positive constants c_σ, c_{d_2}, c_η, and δ. On the other hand, when in the residual phase, the modulation function is driven by barrier function such that $\rho_B(t)$ is (3.22) or (3.23).

Notice, the switching law given by (3.17) means that k increases aggressively if the output $\sigma(t)$ tends to its prespecified transient T and steady-state values Δ. This behavior makes the sequences $\hat{d}_1(k)$ and $\hat{d}_2(k)$ in (3.20) and (3.21) to behave as exponentially increasing functions, $\forall t \leq \bar{t}$, so that the modulation function $\rho(t)$ in (3.26) is increased to force the convergence of $\sigma(t)$ to a residual set of order $\mathcal{O}(\epsilon)$. When the condition $\|\sigma(t)\| \leq \epsilon/R_2$ is reached, the residual phase is stared and the increment of the sequence k ceases forever such that the adaptive scheme is driven by the barrier functions (3.22) or (3.23).

3.3 Stability Analysis

Theorem 2 summarizes the main results of the closed-loop system stability. Notice, inspired by [96], in our MIMO control strategy, the only required a priori information about the matrix B_2 of the plant is the knowledge of a matrix S_p such that $K_p = B_2 S_p$ and $-K_p$ is a Hurwitz matrix. This relaxes the positive definiteness property and allows the application of our unit vector control.

Theorem 2. *Consider the multivariable system (3.1)-(3.2), the monitoring scheme with switching times (3.17), switching-based disturbance estimates (3.18) and (3.19), hybrid norm observer (3.20), barrier function (3.22) or (3.23), and the output-feedback unit vector control law (3.24) with modulation function (3.25). Assume that (A1)–(A6) hold. Then, all prespecified transient and steady-state behaviors (maximum overshoot Δ, maximum transient time T and residual absolute error $\|\sigma(t)\|$ less than ϵ) are guaranteed. Furthermore, there exists an unknown upper bound d_{max} for the equivalent disturbance in equation (3.2) and the practical stabilization*

is achieved, with the output error $\sigma(t)$ ultimately converging to the interior of an ϵ-neighborhood of the origin so that:

- *If the barrier function is the positive definite in (3.22), $\|\sigma(t)\| \leq \epsilon_1$ such that $\|\sigma(t)\| \leq \epsilon_1 < \epsilon$ where $\epsilon_1 = \epsilon(1 - \overline{F}/d_{max})$ if $\overline{F} < d_{max}$ and $\epsilon_1 = 0$ if $\overline{F} \geq d_{max}$.*
- *If the barrier function is the positive semi-definite in (3.23), $\|\sigma(t)\| \leq \epsilon_2 < \epsilon$ where $\epsilon_2 = \epsilon d_{max}/(d_{max} + 1)$.*

Then, practical stabilization is achieved, with the output signal converging ultimately close to an ε-neighborhood of the origin. Moreover, all the closed-loop signals are uniformly bounded and all prespecified reaching and residual phase behavior are guaranteed as well.

Proof. Consider the following Lyapunov candidate

$$V(\sigma) = \sigma^T P \sigma \,, \tag{3.27}$$

where $P = P^T$ is the solution of the Lyapunov Equation $PK_p + K_p^T P = I$. Then, its time derivative satisfies

$$\begin{aligned} \dot{V} &= \sigma^T P \dot{\sigma} + \dot{\sigma}^T P \sigma \\ &= \sigma^T \left(P A_{22} + A_{22}^T P \right) \sigma + 2\eta^T A_{21}^T P \sigma + 2 d_2^T P \sigma + \sigma^T P B_2 u + u^T B_2^T P \sigma \,. \end{aligned} \tag{3.28}$$

By using the control law (3.24) and (A4),

$$\begin{aligned} \dot{V} &= \sigma^T \left(P A_{22} + A_{22}^T P \right) \sigma + 2\eta^T A_{21}^T P \sigma + 2 d_2^T P \sigma - \frac{\rho}{\|\sigma\|} \sigma^T (P K_p + K_p^T P) \sigma \\ &= \sigma^T \left(P A_{22} + A_{22}^T P \right) \sigma + 2\eta^T A_{21}^T P \sigma + 2 d_2^T P \sigma - \rho \|\sigma\| \\ &\leq \left[\lambda_{\max} \left(P A_{22} + A_{22}^T P \right) \|\sigma\| + 2\lambda_{\max}(P) \|A_{21}\| \|\eta\| + 2\lambda_{\max}(P) \|d_2\| - \rho \right] \|\sigma\| \,. \end{aligned}$$

Then, employing the inequality (3.21) and defining $c_\sigma > \lambda_{\max}\left(PA_{22} + A_{22}^T P\right)$, $c_{d_\sigma} > \max(2\lambda_{\max}(P)\|A_{21}\|, 2\lambda_{\max}(P))$, and $c_\eta > 2\lambda_{\max}(P)\|A_{21}\|$, one has

$$\begin{aligned} \dot{V} &\leq \left[c_\sigma \|\sigma\| + c_\eta \hat{\eta} + c_{d_\sigma} d_\sigma - \rho \right] \|\sigma\| \\ &= \left[c_\sigma \sqrt{V} + c_\eta \hat{\eta} + c_{d_\sigma} d_\sigma - \rho \right] \sqrt{V} \,, \end{aligned}$$

where $d_\sigma(t) := \|d_2(t)\| + \pi_\eta(t)$. Thus, by using modulation function $\rho(t) = \rho_M(t)$, as in (3.26),

$$\begin{aligned} \dot{V} &\leq -\delta \sqrt{V} + c_{d_\sigma} \left(d_\sigma - \hat{d}_2 \right) \sqrt{V} \\ &\leq c_{d_\sigma} \left(d_\sigma - \hat{d}_2 \right) \sqrt{V} \,, \end{aligned}$$

Now, defining $\bar{V} := \sqrt{V} = \|\sigma\|$ whose time derivative is $\dot{\bar{V}} = \frac{\dot{V}}{2\sqrt{V}}$ and upper bounded by

$$\dot{\bar{V}} \leq \frac{c_{d_\sigma}}{2}\left(d_\sigma - \hat{d}_2\right) . \tag{3.29}$$

Notice that d_σ can be upper bounded by a constant $\bar{d}_\sigma$,

$$d_\sigma \leq \bar{d}_\sigma \, , \tag{3.30}$$

such that $\bar{d}_\sigma \geq \bar{d}_2 + \pi_\eta(0)$. Nevertheless, by assumption $\bar{d}_\sigma$ depends on the unavailable information $\bar{d}_2$ and $\eta(0)$.

First, it is proved by contradiction that, if one starts in the Reaching Phase ($\|\sigma\| > \epsilon$), then after at most finite number of switchings, the Residual Phase ($\|\sigma\| \leq \epsilon$) will start. Indeed, suppose that the system never enters in Residual Phase. Then, from (3.17), $\hat{d}_1(k)$ and $\hat{d}_2(k)$ will switch without stopping either due to $\|\sigma(t)\| \to \|\sigma(0)\| + \Delta$ or to $t \to T$. Therefore, from the σ-equation and taking (3.18), (3.19) and (3.30) into consideration, it follows that, no matter how large $\bar{d}_\sigma$ is, after at most finite switchings, one has

$$\hat{d}_2(k) > \bar{d}_\sigma \, , \quad \forall t \in [t_k \, , t_{k+1}) \, . \tag{3.31}$$

Once condition (3.31) is satisfied, the disturbance estimate $\hat{d}_2$ will completely dominate the right-hand side of inequality (3.29) and guarantees that there exist a positive integer $\tilde{k} > 0$, such that, $\forall k \geq \tilde{k}$,

$$\dot{\bar{V}} < 0 \, , \quad \forall t \in [t_k \, , t_{k+1}) \, . \tag{3.32}$$

The inequality (3.32) implies that any new switching is only due to $t = T(1 - 1/R_1^k)$ because, from (3.17), $\|\sigma(t)\| = \|\sigma\| + \Delta(1 - R_1^k)$ implies that $\|\sigma\|$ is increasing. As a result, the time interval between two switchings is

$$t_{k+1} - t_k = T(1 - 1/R_1^k) - T(1 - 1/R_1^{k-1}) = T(R_1 - 1)/R_1^k \, . \tag{3.33}$$

Then, through rigorous analysis, it is proven in [15, Theorem 1] that the second stage starts and it is characterized in what follows.

Now, the dynamic behavior of (3.1)–(3.2) is briefly analyzed under the residual regime. Since $\|d_1(x,t)\| \leq \bar{d}_1$ and $|\sigma(t)| \leq \epsilon$, from (3.3) and (3.4), it is easy to verify that

$$\|\eta(t)\| \leq \frac{k_2 k_3}{k_1}(\epsilon + \bar{d}_1) + \pi_\eta(\bar{t}) \, . \tag{3.34}$$

Therefore, by using control law (3.24) with modulation function based on barrier (3.26), the equation (3.2) can be rewritten as

$$\dot{\sigma}(t) = K_p \left[d(x,t) - \rho_B(\sigma(t)) \frac{\sigma(t)}{\|\sigma(t)\|} \right] , \tag{3.35}$$

$$d(x,t) = K_p^{-1} A_{21} \eta(t) + K_p^{-1} A_{22} \sigma(t) + K_p^{-1} d_2(x,t) , \tag{3.36}$$

with equivalent disturbance $d(x,t)$ satisfying

$$\begin{aligned} \|d(x,t)\| &\leq \|K_p^{-1}\|\|A_{21}\|\|\eta(t)\| + \|K_p^{-1}\|\|A_{22}\|\|\sigma(t)\| + \|K_p^{-1}\|\|d_2(x,t)\| \\ &\leq \|K_p^{-1}\| \left\{ \|A_{21}\| \left[\frac{k_2 k_3}{k_1}(\epsilon + \bar{d}_1) + \pi_\eta(\bar{t}) \right] + \|A_{22}\|\varepsilon + \bar{d}_2 \right\} \\ &= d_{\max} , \end{aligned} \tag{3.37}$$

in other words, in residual phase, the disturbance $d(x,t)$ is upper bounded by unknown constant $d_{\max}$.

Now, consider the following candidate Lyapunov function

$$V = \frac{1}{2}\sigma^T P \sigma + \frac{1}{2}(\rho_B - \rho_B(0))^2 , \quad P = P^T > 0 , \tag{3.38}$$

and the Rayleigh-Ritz inequality,

$$\lambda_{\min}(P)\|\sigma\|^2 \leq \sigma^T P \sigma \leq \lambda_{\max}(P)\|\sigma\|^2 . \tag{3.39}$$

The time derivative V, along (3.37) and (3.35), satisfies

$$\begin{aligned} \dot{V} &= \frac{1}{2}\sigma^T P \dot{\sigma} + \frac{1}{2}\dot{\sigma} P \sigma + (\rho_B - \rho_B(0))\dot{\rho}_B \\ &= d^T K_p^T P \sigma - \frac{1}{2}\frac{\rho_B}{\|\sigma(t)\|}\sigma^T (P K_p + K_p^T P)\sigma + (\rho_B - \rho_B(0))\dot{\rho}_B \\ &= d^T K_p^T P \sigma - \frac{1}{2}\rho_B \|\sigma\| + (\rho_B - \rho_B(0))\dot{\rho}_B \\ &\leq -\frac{(-2\|K_p\|\lambda_{\max}(P)\|d\| + \rho_B)}{2}\|\sigma\| + (\rho_B - \rho_B(0))\dot{\rho}_B \\ &\leq -\frac{(-2\|K_p\|\lambda_{\max}(P) d_{\max} + \rho_B)}{2}\|\sigma\| + (\rho_B - \rho_B(0))\dot{\rho}_B . \end{aligned} \tag{3.40}$$

At this point we have two options:

- Adaptation with Positive definite Barrier Function

  With $\rho_B = \rho_{PB}$ in (3.22), the inequality (3.40) is rewritten as

$$\begin{aligned}
\dot{V} &\leq -\frac{(-2\|K_p\|\lambda_{\max}(P)d_{\max}+\rho_{PB})}{2}\|\sigma\| + (\rho_{PB}-\bar{F})\dot{\rho}_{PB} \\
&= -\frac{(-2\|K_p\|\lambda_{\max}(P)\|d_{\max}+\rho_{PB})}{2}\|\sigma\| + \\
&\quad + (\rho_{PB}-\bar{F})\frac{\epsilon\bar{F}}{(\epsilon-\|\sigma\|)^2}\frac{1}{\|\sigma\|}\left(\sigma^T K_p d - \rho_{PB}\frac{\sigma^T K_p \sigma}{\|\sigma\|}\right) \\
&\leq -\frac{(-2\|K_p\|\lambda_{\max}(P)\|d_{\max}+\rho_{PB})}{2}\|\sigma\| + \\
&\quad + (\rho_{PB}-\bar{F})\frac{\epsilon\bar{F}\lambda_{\min}(K_p)}{(\epsilon-\|\sigma\|)^2}\left(\frac{\|K_p\|}{\lambda_{\min}(K_p)}d_{\max}-\rho_{PB}\right)\|\sigma\| \\
&\leq -\frac{(-\bar{d}_{\max}+\rho_{PB})}{2}\|\sigma\| - (\rho_{PB}-\bar{F})\frac{\epsilon\bar{F}\lambda_{\min}(K_p)}{(\epsilon-\|\sigma\|)^2}\left(-\bar{d}_{\max}+\rho_{PB}\right) \\
&\leq -\frac{(-\bar{d}_{\max}+\rho_{PB})}{2}\|\sigma\| - (\rho_{PB}-\bar{F})\frac{\epsilon\bar{F}\lambda_{\min}(K_p)}{(\epsilon-\|\sigma\|)^2}\frac{\left(-\bar{d}_{\max}+\rho_{PB}\right)}{2} \\
&= -\beta_{\sigma 1}\frac{\|\sigma\|}{\sqrt{2}} - \zeta_1\beta_{\sigma 1}\frac{|\rho_{PB}-\bar{F}|}{\sqrt{2}}\,, \qquad (3.41)
\end{aligned}$$

  where $\beta_{\sigma 1} = \frac{-\bar{d}_{\max}+\rho_{PB}}{\sqrt{2}}$, $\zeta_1 = \frac{\epsilon\bar{F}\lambda_{\min}(K_p)}{(\epsilon-\|\sigma\|)^2}$, and by using (3.37), the unknown constant

$$\bar{d}_{\max} = \max\left\{2\lambda_{\max}(P), \frac{1}{\lambda_{\min}(K_p)}\right\}\|K_p\|d_{\max}\,. \qquad (3.42)$$

  Then, from [12, Lemma 5], one can conclude that (3.41) satisfies

$$\begin{aligned}
\dot{V} &\leq -\frac{1}{\sqrt{\lambda_{\min}\{P\}}}\beta_{\sigma 1}\sqrt{\lambda_{\min}\{P\}}\frac{\|\sigma\|}{\sqrt{2}} - \zeta_1\beta_{\sigma 1}\frac{|\rho_{PB}-\bar{F}|}{\sqrt{2}} \\
&\leq \quad -\beta_1\left(\frac{\sqrt{\lambda_{\min}\{P\}}}{\sqrt{2}}\|\sigma\| + \frac{1}{\sqrt{2}}|\rho_{PB}-\bar{F}|\right) \\
&\leq \quad -\beta_1 V^{1/2}\,, \quad \text{with} \quad \beta_1 = \beta_{\sigma 1}\sqrt{2}\min\left\{\frac{1}{\sqrt{\lambda_{\min}\{P\}}}, \zeta_1\right\}\,, \qquad (3.43)
\end{aligned}$$

  that results a finite time convergence of the output variable to the region $|\sigma(t)| \leq \epsilon_1$ such that $|\sigma(t)| \leq \epsilon_1 < \epsilon$ where $\epsilon_1 = \epsilon(1-\overline{F}/d_{\max})$ if $\overline{F} < d_{\max}$ and $\epsilon_1 = 0$ if $\overline{F} \geq d_{\max}$.

- Adaptation with Positive Semi-definite Barrier Function

With $\rho_B = \rho_{PSB}$ in (3.23), the inequality (3.40) is rewritten as

$$\begin{aligned}
\dot{V} \leq & -\frac{(-2\|K_p\|\lambda_{\max}(P)d_{max}+\rho_{PSB})}{2}\|\sigma\| + \rho_{PSB}\dot{\rho}_{PSB} \\
= & -\frac{(-2\|K_p\|\lambda_{\max}(P)d_{max}+\rho_{PSB})}{2}\|\sigma\| + \\
& + \rho_{PSB}\frac{\epsilon}{(\epsilon-\|\sigma\|)^2}\frac{1}{\|\sigma\|}\left(\sigma^T K_p d - \rho_{PSB}\frac{\sigma^T K_p \sigma}{\|\sigma\|}\right) \\
\leq & -\frac{(-2\|K_p\|\lambda_{\max}(P)d_{max}+\rho_{PSB})}{2}\|\sigma\| + \\
& + \rho_{PSB}\frac{\epsilon\lambda_{\min}(K_p)}{(\epsilon-\|\sigma\|)^2}\left(\frac{\|K_p\|}{\lambda_{\min}(K_p)}\|d\| - \rho_{psb}\right) \\
\leq & -\frac{(-2\|K_p\|\lambda_{\max}(P)d_{max}+\rho_{PSB})}{2}\|\sigma\| + \\
& + \rho_{PSB}\frac{\epsilon\lambda_{\min}(K_p)}{(\epsilon-\|\sigma\|)^2}\left(\frac{\|K_p\|}{\lambda_{\min}(K_p)}d_{\max} - \rho_{PSB}\right) \\
\leq & -\frac{(-\bar{d}_{\max}+\rho_{PSB})}{2}\|\sigma\| - \rho_{PSB}\frac{\epsilon\lambda_{\min}(K_p)}{(\epsilon-\|\sigma\|)^2}\left(-\bar{d}_{\max}+\rho_{PSB}\right) \\
\leq & -\frac{(-\bar{d}_{\max}+\rho_{PSB})}{2}\|\sigma\| - \rho_{PSB}\frac{\epsilon\lambda_{\min}(K_p)}{(\epsilon-\|\sigma\|)^2}\frac{(-\bar{d}_{\max}+\rho_{PSB})}{2} \\
= & -\beta_{\sigma 2}\frac{\|\sigma\|}{\sqrt{2}} - \zeta_2\beta_{\sigma 2}\frac{|\rho_{PSB}|}{\sqrt{2}}\,, \qquad (3.44)
\end{aligned}$$

where $\beta_{\sigma 2} = \frac{-\bar{d}_{\max}+\rho_{PSB}}{\sqrt{2}}$, $\zeta_2 = \frac{\epsilon\lambda_{\min}(K_p)}{(\epsilon-\|\sigma\|)^2}$, and by using (3.37), the unknown constant $\bar{d}_{max}$ given by (3.42).

Then, from [12, Lemma 6], one can conclude that (3.44) satisfies

$$\begin{aligned}
\dot{V} \leq & -\frac{1}{\sqrt{\lambda_{\min}\{P\}}}\beta_{\sigma 2}\sqrt{\lambda_{\min}\{P\}}\frac{\|\sigma\|}{\sqrt{2}} - \zeta_2\beta_{\sigma 2}\frac{|\rho_{PSB}|}{\sqrt{2}} \\
\leq & \quad -\beta_2\left(\frac{\sqrt{\lambda_{\min}\{P\}}}{\sqrt{2}}\|\sigma\| + \frac{1}{\sqrt{2}}|\rho_{PSB}|\right) \\
\leq & -\beta_2 V^{1/2}\,, \quad \text{with} \quad \beta_2 = \beta_{\sigma 2}\sqrt{2}\min\left\{\frac{1}{\sqrt{\lambda_{\min}\{P\}}}, \zeta_2\right\}\,, \qquad (3.45)
\end{aligned}$$

that results in a finite time convergence of the output variable to the region $\|\sigma(t)\| \leq \epsilon_2$ such that $\|\sigma(t)\| \leq \epsilon_2 < \epsilon$ where $\epsilon_2 = \epsilon d_{\max}/(d_{\max}+1)$.

Thus, the proof is completed. □

In this chapter, we consider a perturbed and uncertain system with state separated by their internal and external dynamics whose solutions are $\eta(t)$ and $\sigma(t)$,

respectively. Two strategies are employed. In both cases, the monitoring function, without any knowledge of the disturbances' upper bounds, is able to drive the sliding variable $\sigma(t)$ to inside of a prespecified ϵ-neighborhood of the origin ensuring that there are no violation of the desired overshoot and settling time. It is worth to mention that the residual width ϵ in (3.22) and (3.23) is an arbitrary parameter completely chosen by the designer, *i.e.*, different from [18] where an estimate of the equivalent control based on filtering is employed, our strategy does not depend on any upper bounds of the disturbance or its derivative, see inequality (21) of [18].

Initially, the monitoring function adapts the gain of the unit vector controller by using a monotonically increasing sequence k, given by (3.17), able to increase without bound until the controller's gain (3.26) achieves its appropriated value to lead $\sigma(t)$ to the residual phase. In the first scenario, the adaptive scheme is given by a combination of the positive definite barrier and the monitoring functions, (3.22) and (3.26). In this case, already inside of the residual set ϵ, if the bias F is sufficient larger than the norm of the equivalent disturbance, the control signal is discontinuous and the positive barrier is able to guarantee ideal sliding mode ($\sigma \equiv 0$) and, if F is insufficient to overcome the norm of the equivalent disturbance, the control signal is smooth and the practical sliding mode ($\|\sigma\| \leq \epsilon$) is achieved. In the second case, by using the semi-positive definite barrier function (3.23), the control signal is continuous and only the practical sliding mode can be indeed reached.

On the other hand, the unmeasured part of the state, the variable $\eta(t)$, will converge to a domain around the origin dependent on the unknown but bounded the amplitude of the perturbation.

3.4 Numerical Examples

In this section two simulation results are presented, an academic example and application to an overhead crane system, to illustrate the advantages of the MBF strategy.

3.4.1 Academic Example

In order to validate the proposed control strategy, this section considers an academic example of output-feedback stabilization for a MIMO nonlinear unstable system (3.1)–(3.2) such that $A_{11} = \begin{bmatrix} -2 & 1 \\ 1 & -2 \end{bmatrix}$, $A_{12} = \begin{bmatrix} 0 & 1 \\ 1 & 0 \end{bmatrix}$, $A_{21} = \begin{bmatrix} 1 & 1 \\ 1 & 1 \end{bmatrix}$,

$$A_{22} = \begin{bmatrix} 1 & 1 \\ 0.4 & 0.5 \end{bmatrix}, \; B_2 = \begin{bmatrix} 1 & 0 \\ 0 & 1 \end{bmatrix},$$

$$d_1(x,t) = \begin{bmatrix} \sin(10t)\mathrm{sgn}(\eta_1\eta_2) \\ \arctan(\eta_1+\eta_2+\sigma_1+\sigma_2) + \cos(2t) + \exp(-\sigma_2^2/2) \end{bmatrix} [\mathbb{1}(t) - \mathbb{1}(t-25)]$$

$$d_2(x,t) = \begin{bmatrix} 0.25(1-\exp(-|\eta_2|)) - \exp(-\sigma_2^2/2) \\ \exp(-\sigma_1^2/2) + \cos(t) \end{bmatrix} [\mathbb{1}(t) - \mathbb{1}(t-25)]$$

where $\mathbb{1}(t)$ is the step function and initial conditions $\eta^T(0) = [3\,, -2]$ and $\sigma^T(0) = [2\,, -1]$.

It was chosen as performance criteria a maximum overshoot $\Delta = 0.5$, maximum transient time $T = 5$ [sec] and maximum residual $\epsilon = 0.01$. Then, the switching law based on monitoring function follows (3.17) with parameters $R_1 = 2$ and $R_2 = 1.2$. Estimates for disturbances bounds $\bar{d}_1$ and $\bar{d}_2$ are found from (3.18) and (3.19), respectively, setting $b_1 = 1.5$, $b_2 = 1.2$, $c_1 = 0.05$ and $c_2 = 0.1$. The hybrid norm observer (3.20) parameters are $\lambda_1 = -0.8$ and $c_{\eta\sigma} = 1.1$. The positive barrier (3.22) has parameter $\bar{F} = 20$ and the unit vector controller (3.24) parameters are $c_\sigma = 3$, $c_{d\sigma} = 4$, $c_\eta = 5$, and $S_p = \begin{bmatrix} 1 & 0 \\ 0 & 1 \end{bmatrix}$.

The results obtained for the proposed unit vector controller combining monitoring, positive and semi-positive barrier functions are shown, respctively, in Figs. 3.1 and 3.2. From the control objective point of view, both approaches are able to ensure the practical stabilization (convergence to a predefined neighbor of the origin) with guaranteed transient and steady-state behavior, compares Figures 3.1(a) and 3.1(b) with Figures 3.2(a) and 3.2(b). For both strategies, there is an equivalent behavior of the closed loop system in the reach phase since the monitoring functions were configured identically. The monitoring function is allows the specification of the transition instant to the barrier function avoiding an abrupt discontinuity in the control, see Figures 3.1(c) and 3.2(c). Moreover, the control effort required by using the semi-positive barrier is considerably reduced. On the other hand, the residue when using the positive barrier is lower, Figures 3.1(d) and 3.2(d). Notice that for $t \geq 25$ there is no perturbations therefore the semi-definite barrier goes to zero.

3.4.2 Application Example

Overhead cranes are well known machines used to dislocate heavy, large or even hazardous materials from an origin to a target localization. This procedure is held by lifting and lowering a given payload to avoid obstacles in the path. Cranes can be easily found in harbors, nuclear industries, building sites, factories and airports [39, 40, 42–44].

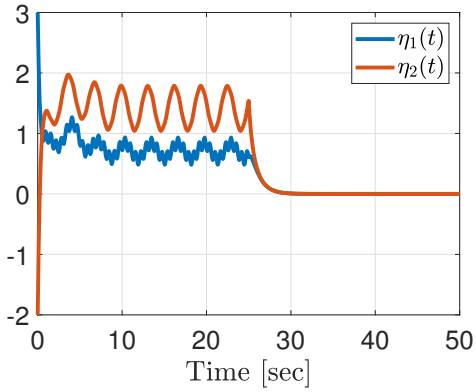

(a) Internal dynamics $\eta(t)$.

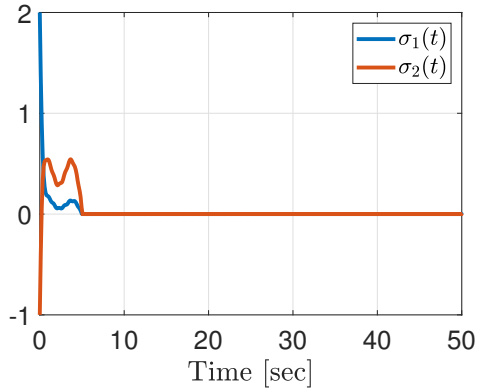

(b) Output vector $\sigma(t)$.

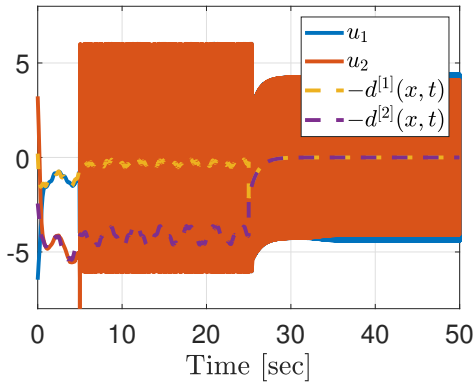

(c) Control vector u.

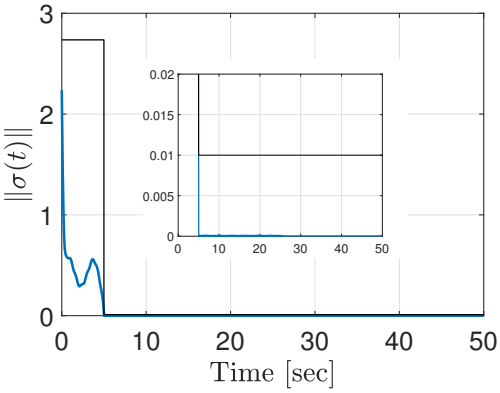

(d) Norm of output variable $\sigma(t)$ and performance criteria.

Figure 3.1: Simulation results - unit vector control with monitoring and positive barrier.

A overhead crane is composed by the hoisting and support mechanisms, respectively, hoisting line and a trolley-girder. Unfortunately, the hoisting and trolley-girder accelerations always induce undesirable load swing. This unavoidable load swing frequently causes efficiency drop, load damages, and even accidents [32]. Moreover, most crane systems are handled by humans which demands a long training to avoid accidents and to increase the work efficiency.

In this section, to develop a safety and efficient autonomous crane system, the MBF Adaptive UVC is applied to the INTECO overhead crane system [97]. Consider the free body diagram in Figure 3.3(b), $x_c(t)$, $y_c(t)$ and $z_c(t)$ are the coordinates of the payload, $x_w(t)$ denotes the distance of the rail with the cart from the center of the construction of the crane, $y_w(t)$ denotes the distance of the cart from the center of the rail, $R(t)$ denotes the length of the lift-line, $\alpha(t)$ denotes the angle between the Y axis and the lift-line, $\beta(t)$ denotes the angle between the negative direction on the Z axis and the projection of the lift-line onto the XZ plane, m_c is the mass

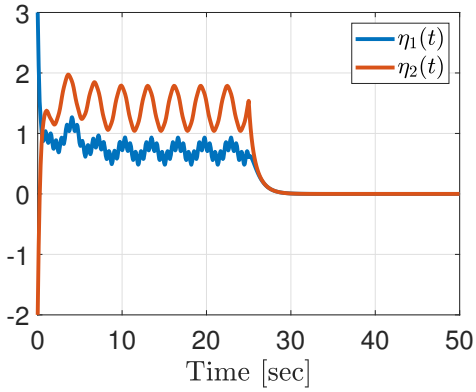

(a) Internal dynamics $\eta(t)$.

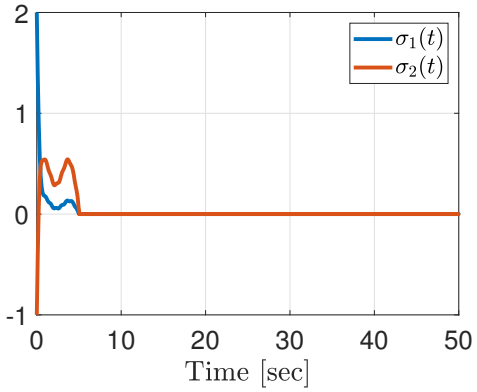

(b) Output vector $\sigma(t)$.

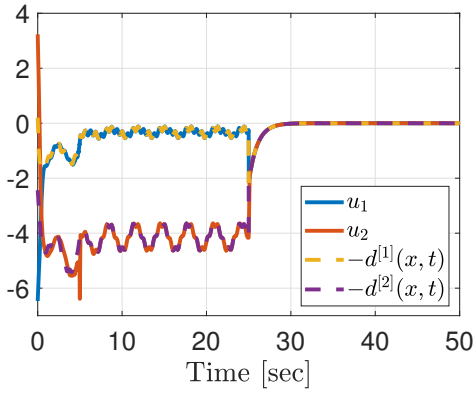

(c) Control vector u.

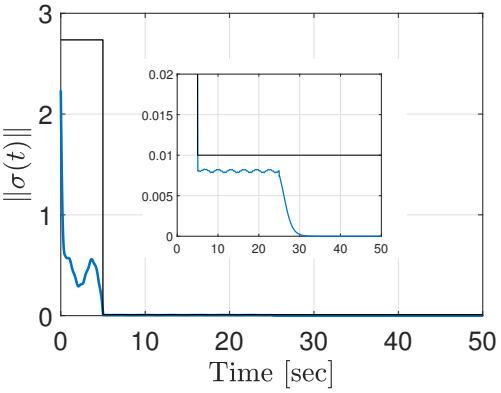

(d) Norm of output variable $\sigma(t)$ and performance criteria.

Figure 3.2: Simulation results - unit vector control with monitoring and positive barrier.

of the payload, m_w is the mass of the cart and m_s is the mass of the moving rail.

The spherical system has been adopted such that the coordinates of the moving rail (body of mass m_s) are

$$x_s(t) = X(t)\,, \tag{3.46}$$
$$y_s(t) = 0\,, \tag{3.47}$$
$$z_s(t) = H\,, \tag{3.48}$$

of the cart (body of mass m_w) are

$$x_w(t) = X(t)\,, \tag{3.49}$$
$$y_w(t) = Y(t)\,, \tag{3.50}$$
$$z_w(t) = H\,, \tag{3.51}$$

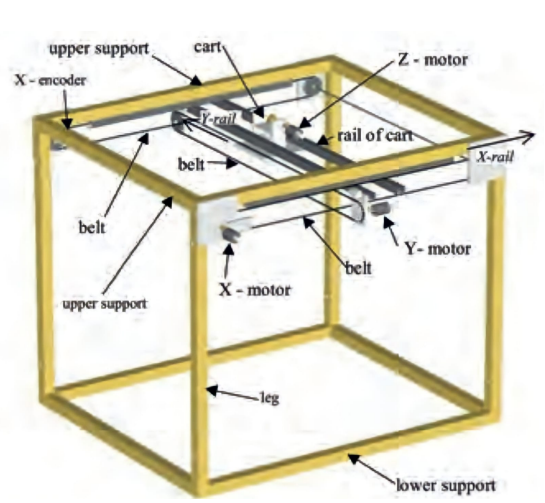

(a) View of INTECO 3D crane. Figure adapted from [98].

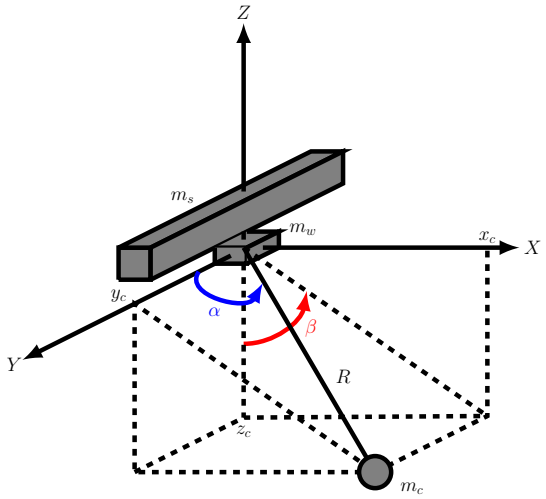

(b) Free body diagram of INTECO overhead crane [97].

Figure 3.3: INTECO overhead crane - view and free body diagram.

and, of the payload (body of mass m_c) are

$$x_c(t) = X(t) + R(t)\text{sen}(\alpha(t))\text{sen}(\beta(t))\,, \tag{3.52}$$

$$y_c(t) = Y(t) + R(t)\cos(\alpha(t))\,, \tag{3.53}$$

$$z_c(t) = H - R(t)\text{sen}(\alpha(t))\cos(\beta(t))\,. \tag{3.54}$$

The equations of motion are provided from Lagrange's equation by considering the payload as a point mass and neglecting the mass and stiffness of the rope. The kinetic energy is

$$K = \frac{m_s}{2}\left(\dot{x}_s^2 + \dot{y}_s^2 + \dot{z}_s^2\right) + \frac{m_w}{2}\left(\dot{x}_w^2 + \dot{y}_w^2 + \dot{z}_w^2\right) + \frac{m_c}{2}\left(\dot{x}_c^2 + \dot{y}_c^2 + \dot{z}_c^2\right) \tag{3.55}$$

$$\begin{aligned} = \quad & \frac{m_s}{2}\dot{X}^2 + \frac{m_w}{2}(\dot{X}^2 + \dot{Y}^2) + \frac{m_c}{2}\Big(\dot{X}^2 + \dot{Y}^2 + 2\sin(\beta)\cos(\alpha)R\dot{\alpha}\dot{X} \\ & - \cos^2(\alpha)R^2\dot{\beta}^2 + \cos(\alpha)\dot{R}\dot{Y} + R^2\dot{\alpha}^2 + R^2\dot{\beta}^2 - \sin(\alpha)R\dot{\alpha}\dot{Y} \\ & + 2\cos(\beta)\sin(\alpha)R\dot{\beta}\dot{X} + \dot{R}^2 + 2\sin(\alpha)\sin(\beta)\dot{R}\dot{X}\Big)\,, \end{aligned} \tag{3.56}$$

and the potential energy is given by

$$U = (m_s + m_w)gH + m_c g(H - \cos(\beta)\sin(\alpha)R)\,. \tag{3.57}$$

Therefore, the Lagrangian is

$$
\begin{aligned}
L &= K - U \qquad (3.58)\\
&= \frac{m_s}{2}\dot{X}^2 + \frac{m_w}{2}(\dot{X}^2+\dot{Y}^2) + \frac{m_c}{2}\Big(\dot{X}^2+\dot{Y}^2+2\sin(\beta)\cos(\alpha)R\dot{\alpha}\dot{X}\\
&\quad -\cos^2(\alpha)R^2\dot{\beta}^2+\cos(\alpha)\dot{R}\dot{Y}+R^2\dot{\alpha}^2+R^2\dot{\beta}^2-\sin(\alpha)R\dot{\alpha}\dot{Y}\\
&\quad +2\cos(\beta)\sin(\alpha)R\dot{\beta}\dot{X}+\dot{R}^2+2\sin(\alpha)\sin(\beta)\dot{R}\dot{X}\Big)\\
&\quad -(m_s+m_w)gH - m_c g(H-\cos(\beta)\sin(\alpha)R)\,. \qquad (3.59)
\end{aligned}
$$

The equations of motion are obtained by calculating

$$
\frac{\partial}{\partial t}\left(\frac{\partial L}{\partial \dot{q}_i}\right) - \frac{\partial L}{\partial q_i} = F_{q_i} - k_{q_i}\dot{q}_i\,, \qquad (3.60)
$$

for each generalized coordinate q_i such that $q = [X(t)\,, Y(t)\,, R(t)\,, \alpha(t)\,, \beta(t)]^T$, leading us to

$$
\begin{aligned}
&(m_s+m_w+m_c)\ddot{X} + m_c\sin(\alpha)\sin(\beta)\ddot{R} + m_c\cos(\alpha)\sin(\beta)R\ddot{\alpha} + m_c\cos(\beta)\sin(\alpha)R\ddot{\beta}\\
&= m_c\sin(\alpha)\sin(\beta)R\dot{\alpha}^2 + m_c\sin(\alpha)\sin(\beta)R\dot{\beta}^2 - 2m_c\cos(\alpha)\sin(\beta)\dot{\alpha}\dot{R}+\\
&- 2m_c\cos(\beta)\sin(\alpha)\dot{\beta}\dot{R} - 2m_c\cos(\alpha)\cos(\beta)R\dot{\alpha}\dot{\beta} + F_X - k_X\dot{X}\,, \qquad (3.61)\\
&(m_c+m_w)\ddot{Y} + m_c\cos(\alpha)\ddot{R} - m_c\sin(\alpha)R\ddot{\alpha} = m_c\cos(\alpha)R\dot{\alpha}^2 + 2m_c\sin(\alpha)\dot{\alpha}\dot{R}+\\
&+ F_Y - k_Y\dot{Y}\,, \qquad (3.62)\\
&m_c\sin(\alpha)\sin(\beta)\ddot{X} + m_c\cos(\alpha)\ddot{Y} + m_c\ddot{R} = m_cR\dot{\alpha}^2 + m_cR\dot{\beta}^2 - m_c\cos^2(\alpha)R\dot{\beta}^2+\\
&+ m_cg\cos(\beta)\sin(\alpha) + F_R - k_R\dot{R}\,, \qquad (3.63)\\
&m_c\cos(\alpha)\sin(\beta)R\ddot{X} - m_c\sin(\alpha)R\ddot{Y} + m_cR^2\ddot{\alpha} = -2m_c\dot{\alpha}R\dot{R}+\\
&+ m_cg\cos(\alpha)\cos(\beta)R + m_c\cos(\alpha)\sin(\alpha)R^2\dot{\beta}^2\,, \qquad (3.64)\\
&m_c\cos(\beta)\sin(\alpha)R\ddot{X} + m_c\sin^2(\alpha)R^2\ddot{\beta} = -2m_c\dot{\beta}R\dot{R} - m_cg\sin(\alpha)\sin(\beta)R+\\
&+ 2m_c\cos^2(\alpha)\dot{\beta}R\dot{R} - 2m_c\cos(\alpha)\sin(\alpha)R^2\dot{\alpha}\dot{\beta}\,. \qquad (3.65)
\end{aligned}
$$

By the assumption of small swing angles and small accelerations as presented in [32], one has: $|\ddot{X}|\,, |\ddot{Y}|\,, |\ddot{R}| \ll g$, $|\dot{R}| \ll |R|$, leading to $|R\ddot{\alpha}|\,, |R\ddot{\beta}| \ll g$, and$|\dot{\alpha}|\,, |\dot{\beta}| \ll 1$. Therefore, for the overhead crane, $\sin(\alpha) \approx 1$, $\cos(\alpha) \approx 0$, $\sin(\beta) \approx \beta$, $\cos(\beta) \approx 1$ and neglecting higher-order terms, the nonlinear system (3.61)–(3.65) is simplified

to

$$(m_s + m_w + m_c)\ddot{X} + m_c\beta\ddot{R} + m_cR\ddot{\beta} = F_X - k_X\dot{X}\,, \tag{3.66}$$

$$(m_c + m_w)\ddot{Y} - m_cR\ddot{\alpha} = F_Y - k_Y\dot{Y}\,, \tag{3.67}$$

$$m_c\beta\ddot{X} + m_c\ddot{R} = m_cg + F_R - k_R\dot{R}\,, \tag{3.68}$$

$$-\ddot{Y} + R\ddot{\alpha} = 0\,, \tag{3.69}$$

$$\ddot{X} + R\ddot{\beta} = -g\beta\,. \tag{3.70}$$

Consequently,

$$\ddot{X} = -\frac{k_X}{m_s + m_w}\dot{X} + \frac{1}{m_s + m_w}F_X + \frac{1}{m_s + m_w}\beta F_R\,, \tag{3.71}$$

$$\ddot{Y} = -\frac{k_Y}{m_w}\dot{Y} + \frac{1}{m_w}F_Y\,, \tag{3.72}$$

$$\ddot{R} = -\frac{k_R}{m_c}\dot{R} + \frac{k_X}{m_s + m_w}\beta\dot{X} - \frac{1}{m_s + m_w}\beta F_X + \left(\frac{1}{m_c} - \frac{1}{m_s + m_w}\beta^2\right)F_R + g\,, \tag{3.73}$$

$$\ddot{\alpha} = -\frac{k_Y}{m_w}\frac{1}{R}\dot{Y} + \frac{k_Y}{m_w}\frac{1}{R}F_Y\,, \tag{3.74}$$

$$\ddot{\beta} = -g\frac{1}{R}\beta + \frac{k_X}{m_s + m_w}\frac{1}{R}\dot{X} - \frac{1}{m_s + m_w}\frac{1}{R}F_X - \frac{1}{m_s + m_w}\frac{1}{R}\beta F_R\,. \tag{3.75}$$

By design, the control signal are $u_X = F_X$, $u_Y = F_Y$ and $u_R = F_R + m_cg$. Then, the nonlinear system (3.75)–(3.75) is rewritten as

$$\ddot{X} = -\frac{k_X}{m_s + m_w}\dot{X} - \frac{m_cg}{m_s + m_w}\beta + \frac{1}{m_s + m_w}u_X + \frac{1}{m_s + m_w}\beta u_R\,, \tag{3.76}$$

$$\ddot{Y} = -\frac{k_Y}{m_w}\dot{Y} + \frac{1}{m_w}u_Y\,, \tag{3.77}$$

$$\ddot{R} = -\frac{k_R}{m_c}\dot{R} + \frac{k_X}{m_s + m_w}\beta\dot{X} + \frac{m_cg}{m_s + m_w}\beta^2 - \frac{1}{m_s + m_w}\beta u_X + \left(\frac{1}{m_c} - \frac{1}{m_s + m_w}\beta^2\right)u_R\,, \tag{3.78}$$

$$\ddot{\alpha} = -\frac{k_Y}{m_w}\frac{1}{R}\dot{Y} + \frac{k_Y}{m_w}\frac{1}{R}u_Y\,, \tag{3.79}$$

$$\ddot{\beta} = -\left(1 - \frac{m_c}{m_s + m_w}\right)g\frac{1}{R}\beta + \frac{k_X}{m_s + m_w}\frac{1}{R}\dot{X} - \frac{1}{m_s + m_w}\frac{1}{R}u_X - \frac{m_c}{m_s + m_w}\frac{1}{R}\beta u_R\,. \tag{3.80}$$

Finally, neglecting quadratic and weakly interacting terms, one arrives to the

nonlinear system

$$\ddot{X} = -\frac{k_X}{m_s + m_w}\dot{X} - \frac{m_c g}{m_s + m_w}\beta + \frac{1}{m_s + m_w}u_X\,, \tag{3.81}$$

$$\ddot{Y} = -\frac{k_Y}{m_w}\dot{Y} + \frac{1}{m_w}u_Y\,, \tag{3.82}$$

$$\ddot{R} = -\frac{k_R}{m_c}\dot{R} + \frac{1}{m_c}u_R\,, \tag{3.83}$$

$$\ddot{\alpha} = -\frac{k_Y}{m_w}\frac{1}{R}\dot{Y} + \frac{k_Y}{m_w}\frac{1}{R}u_Y\,, \tag{3.84}$$

$$\ddot{\beta} = -\left(1 - \frac{m_c}{m_s + m_w}\right) g\frac{1}{R}\beta + \frac{k_X}{m_s + m_w}\frac{1}{R}\dot{X} - \frac{1}{m_s + m_w}\frac{1}{R}u_X\,. \tag{3.85}$$

In our application example, for the sake of simplicity, the state is available for feedback and there is no displacement in Y axis such that $Y = Y(0)$ and $\ddot{Y} = \dot{Y} = 0$, then $u_Y = 0$ and, consequently, $\alpha = \alpha(0) = \pi/2$ and $\ddot{\alpha} = \dot{\alpha} = 0$, for all $t > 0$. Inspired by [99], the sliding vector σ to efficient payload transportation and the swing suppression is designed as

$$\sigma_1 = \dot{X} - \dot{X}_d + c_1(X - X_d) - c_2\beta\,, \tag{3.86}$$

$$\sigma_2 = \dot{R} - \dot{R}_d + c_3(R - R_d)\,, \tag{3.87}$$

where the constants $c_1, c_2, c_3 > 0$ and the variables X_d and R_d are the desired cart position and the desired length of the lift-line, respectively. The time derivative of (3.86) and (3.87) are given by

$$\begin{aligned}\dot{\sigma}_1 &= \ddot{X} - \ddot{X}_d + c_1(\dot{X} - \dot{X}_d) - c_2\dot{\beta} \\ &= \left(c_1 - \frac{k_X}{m_s + m_w}\right)\dot{X} - \frac{m_c g}{m_s + m_w}\beta - c_2\dot{\beta} + \frac{1}{m_s + m_w}u_X - (\ddot{X}_d + c_1 + \dot{X}_d)\,,\end{aligned} \tag{3.88}$$

$$\begin{aligned}\dot{\sigma}_2 &= \ddot{R} - \ddot{R}_d + c_3(\dot{R} - \dot{R}_d) \\ &= \left(c_3 - \frac{k_R}{m_c}\right)\dot{R} + \frac{1}{m_c}u_R - (\ddot{R}_d + c_3\dot{R}_d)\,.\end{aligned} \tag{3.89}$$

Now, inspired by [100], we introduce the feedback law

$$u_X = (m_s + m_w)\left[-\left(c_1 - \frac{k_X}{m_s + m_w}\right)\dot{X} + \frac{m_c g}{m_s + m_w}\beta + c_2\dot{\beta} + U_1\right]\,, \tag{3.90}$$

$$u_R = m_c\left[-\left(c_3 - \frac{k_R}{m_c}\right)\dot{R} + U_2\right]\,, \tag{3.91}$$

where U_1 and U_2 represent the discontinuous control law, and define the exogenous

disturbances

$$d_1 = -(\ddot{X}_d + c_1\dot{X}_d)\,, \tag{3.92}$$

$$d_2 = -(\ddot{R}_d + c_3\dot{R}_d)\,. \tag{3.93}$$

By plugging (3.90)–(3.93) in (3.88) and (3.89), the sliding variable dynamics can be rewritten in a compact form as

$$\dot{\sigma}(t) = d(t) + U\,, \tag{3.94}$$

with state $\sigma(t) = [\sigma_1(t), \sigma_2(t)]^T$, Lipschitz disturbance $d(t) = [d_1(t), d_2(t)]^T$ and discontinuous control vector $U = [U_1, U_2]^T$.

In the simulation results, the payload must be lifted and lowered while the crane is in motion and the swing of the payload should be kept as small as possible. The desired trajectory is given by a parabolic shape such as

$$X_d(t) = \begin{cases} t - X_M\,, & 0 \le t \le 2X_M \\ 0, & t > 2X_M \end{cases}\,, \quad X_M > 0\,, \tag{3.95}$$

$$R_d(t) = R_m + R_M \frac{(X_M + X_d(t))(X_M - X_d(t))}{X_M^2}\,. \quad Rm\,,\ R_M > 0. \tag{3.96}$$

The crane parameters are: $m_c = 1$kg, $m_w = 0.6$kg, $m_s = 1$kg, $k_X = 4.1$kg/s, $k_Y = 3.1$kg/s and $k_R = 4.1$kg/s. The minimum lift length is $R_m = 0.1$m, the lift length must vary of $R_M = 0.6$m, while the cart travel from $-X_M$ to X_M with $X_m = 30$m. It was chosen as the performance criteria a maximum overshoot of $\Delta = 0.4$, maximum transient time $T = 1$ [sec] and maximum residual $\epsilon = 0.2$. Then, the switching law based on monitoring function follows (3.17) with parameters $R_1 = 2$ and $R_2 = 10$. Moreover, during the residual phase, the disturbance $d(t)$ in (3.94) is estimated by the monitoring function such that the modulation ρ_M in (3.25) is simply

$$\rho_M = \hat{d} = cb^k\,, \tag{3.97}$$

where $c = 0.2$ and $b = 1.01$. The positive barrier function (3.22) has the parameter $\bar{F} = 5$ and the unit vector controller (3.24) employs $S_p = \begin{bmatrix} 1 & 0 \\ 0 & 1 \end{bmatrix}$. As presented in [100], an initial payload swing is considered with initial conditions $X(0) = -29$m, $Y(0) = 0$m, $R(0) = 0.1$m, $\dot{X}(0) = \dot{Y}(0) = \dot{R} = 0$m/s, $\alpha(0) = 90^o$, $\beta(0) = 6^o$ and $\dot{\alpha}(0) = 0^o$/s and $\dot{\beta}(0) = 11.4^o$/s.

First, the performance of the Adaptive UVC is evaluated with monitoring and

positive barrier functions (Figures 3.4–3.10). In closed-loop, while the reference is given by a parabolic trajectory, the control law is able to successfully ensure the tracking on the actuated state variables $X(t)$, $\dot{X}(t)$, $Y(t)$, $\dot{Y}(t)$, $R(t)$ and $\dot{R}(t)$, see Figures 3.4–3.6, as well as the antiswing and antiskew behavior on the underactuated state variables $\alpha(t)$, $\dot{\alpha}(t)$, $\beta(t)$ and $\dot{\beta}(t)$, see Figures 3.7 and 3.8. It takes less than 10 seconds to suppress the payload oscillations, see Figure 3.8(a). From the point of view of the prescribed tracking performance, during the reaching phase, the monitoring function is able to guarantee an exponential increase of the modulation function such that the sliding condition is verified in the fixed-time $T = 1$ (see Figure 3.9), where the dashed lines represent the frontiers of allowable excursion of the sliding vector. Indeed, beyond the fixed-time convergence, the monitoring function ensures that there is no overshoot violation, as specified in Definition 1. In the residual phase, with the positive barrier function, the adaptive UVC is discontinuous (Figures 3.10(a) and 3.10(b)), and leads to an exact sliding motion, *i.e.*, $\sigma \equiv 0$ for all $t > T$, see Figures 3.9(e) and 3.9(f).

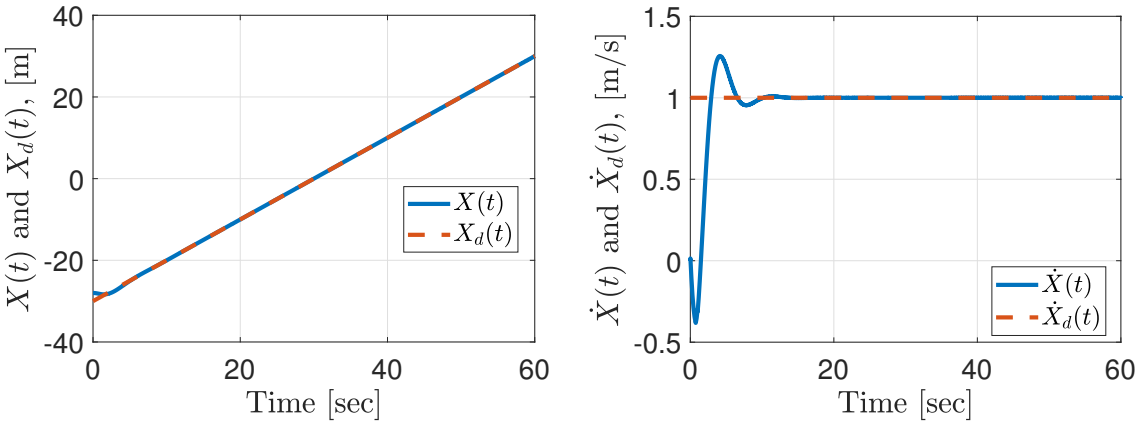

(a) State variable $X(t)$.

(b) State variable $\dot{X}(t)$.

Figure 3.4: 3D Crane - MBF UVC with positive barrier, $X(t)$ and $\dot{X}(t)$.

Now, the performance of the Adaptive UVC is evaluated with monitoring and semi-positive barrier functions (Figures 3.11–3.17). In closed-loop, as in the case the adaptive strategy with positive barrier function, while the reference is given by a parabolic trajectory, the control law is able to successfully ensure the tracking on the actuated state variables $X(t)$, $\dot{X}(t)$, $Y(t)$, $\dot{Y}(t)$, $R(t)$ and $\dot{R}(t)$, see Figures 3.11–3.13, as well as the antiswing and antiskew behavior on the underactuated state variables $\alpha(t)$, $\dot{\alpha}(t)$, $\beta(t)$ and $\dot{\beta}(t)$, see Figures 3.14 and 3.15. It takes less than 10 seconds to suppress the payload oscillations, see Figure 3.15(a). From the point of view of the prescribed tracking performance, during the reaching phase, the monitoring function is able to guarantee an exponential increase of the modulation function such that the sliding condition is verified in the fixed-time $T = 1$ (Figure 3.16),

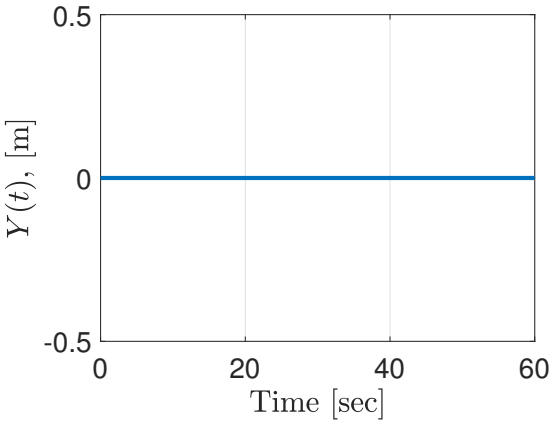

(a) State variable $Y(t)$.

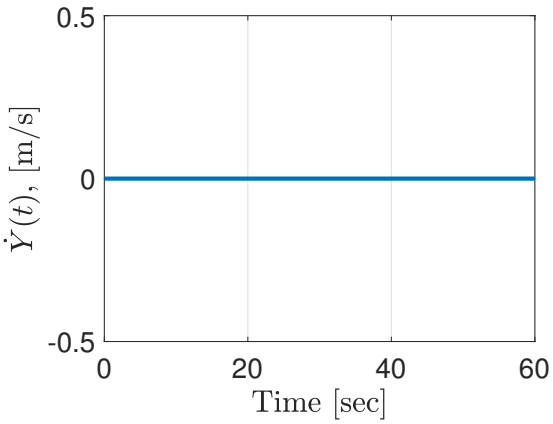

(b) State variable $\dot{Y}(t)$.

Figure 3.5: 3D Crane - MBF UVC with positive barrier, $Y(t)$ and $\dot{Y}(t)$.

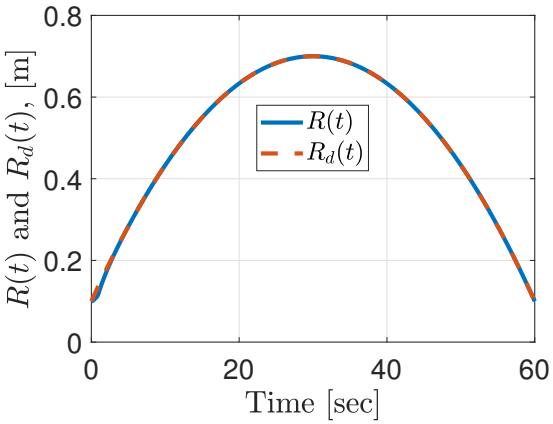

(a) State variable $R(t)$.

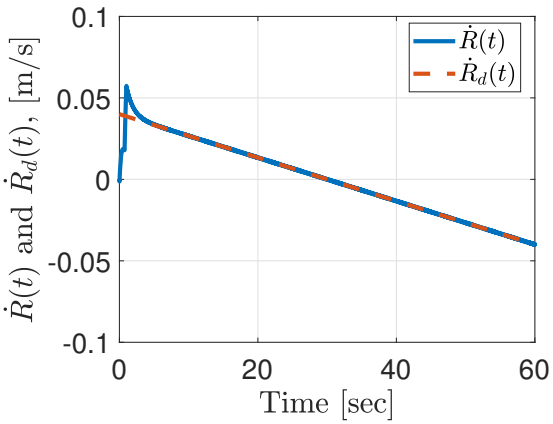

(b) State variable $\dot{R}(t)$.

Figure 3.6: 3D Crane - MBF UVC with positive barrier, $R(t)$ and $\dot{R}(t)$.

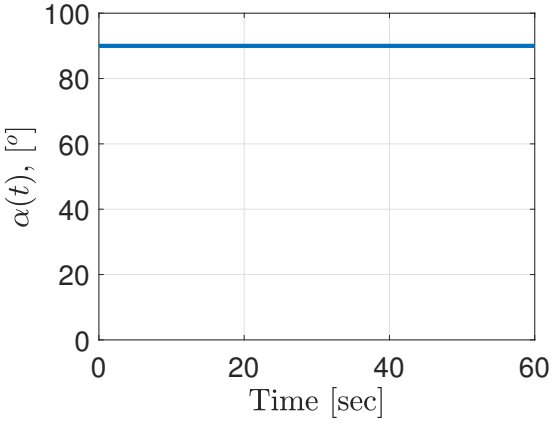

(a) State variable $\alpha(t)$.

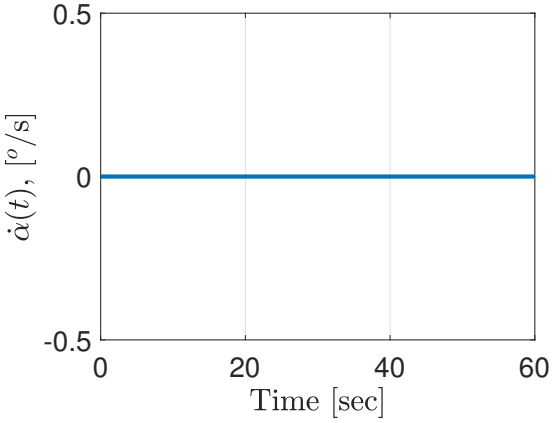

(b) State variable $\dot{\alpha}(t)$.

Figure 3.7: 3D Crane - MBF UVC with positive barrier, $\alpha(t)$ and $\dot{\alpha}(t)$.

where the dashed lines represent the frontiers of allowable excursion of the sliding vector. Indeed, beyond the fixed-time convergence, the monitoring function ensures

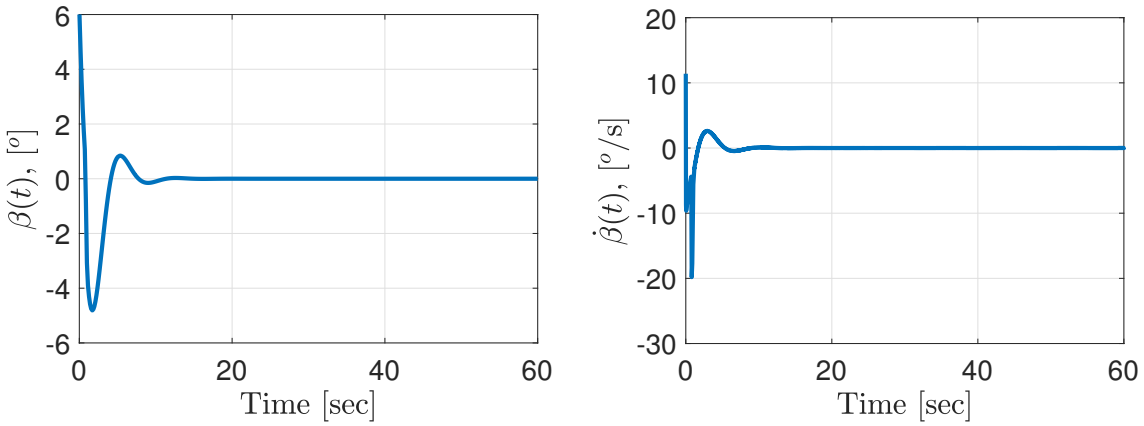

(a) State variable $\beta(t)$.

(b) State variable $\dot{\beta}(t)$.

Figure 3.8: 3D Crane - MBF UVC with positive barrier, $\beta(t)$ and $\dot{\beta}(t)$.

that there is no overshoot violation, as specified in Definition 1. In the residual phase, with the semi-positive barrier function, different from the adaptive strategy with positive barrier function, the adaptive UVC is continuous (Figures 3.17(a) and 3.17(b)), and leads to a pratical sliding motion, *i.e.*, $\|\sigma\| \leq \epsilon$ for all $t > T$, see Figures 3.16(e) and 3.16(f).

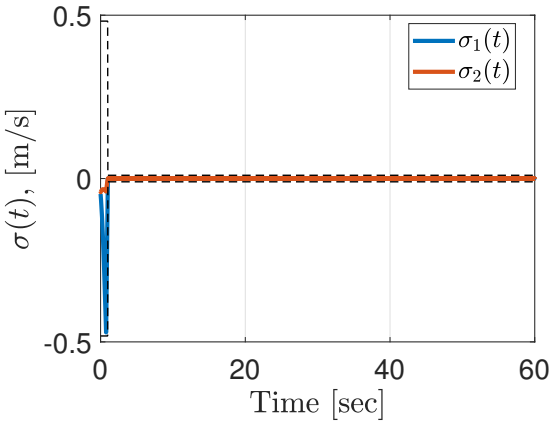

(a) Sliding vector, $\sigma(t)$.

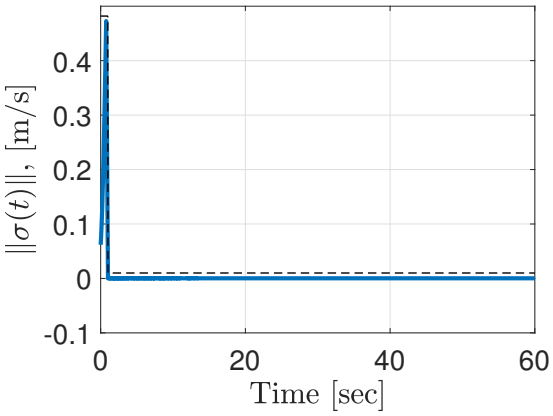

(b) Norm of the sliding vector, $\|\sigma(t)\|$.

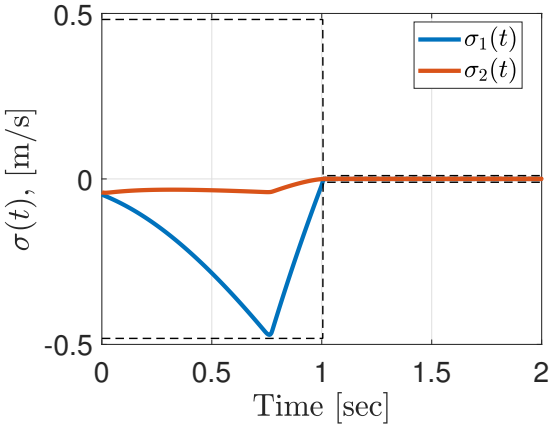

(c) Sliding vector, $\sigma(t)$.

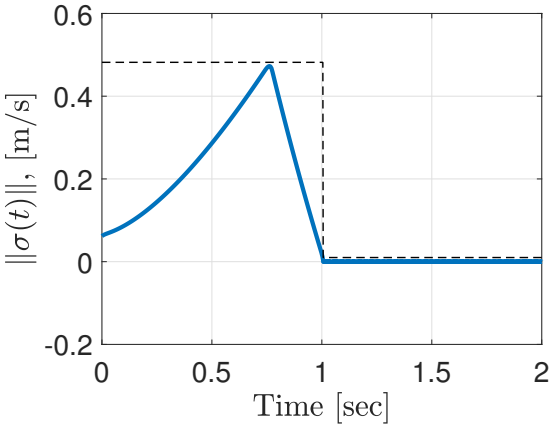

(d) Norm of the sliding vector, $\|\sigma(t)\|$.

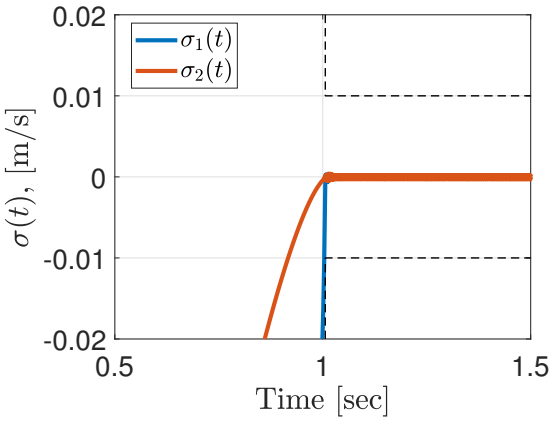

(e) Sliding vector, $\sigma(t)$.

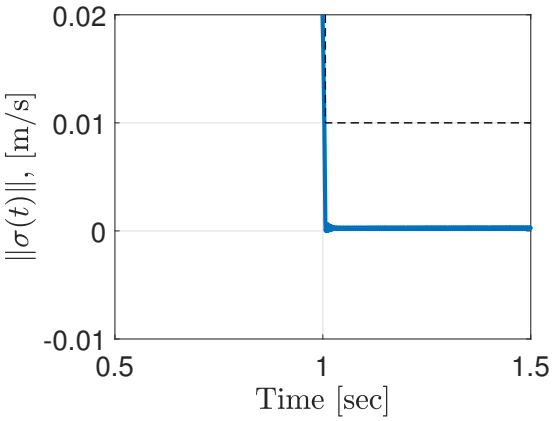

(f) Norm of the sliding vector, $\|\sigma(t)\|$.

Figure 3.9: 3D Crane - MBF UVC with positive barrier, $\sigma(t)$ and $\|\sigma(t)\|$.

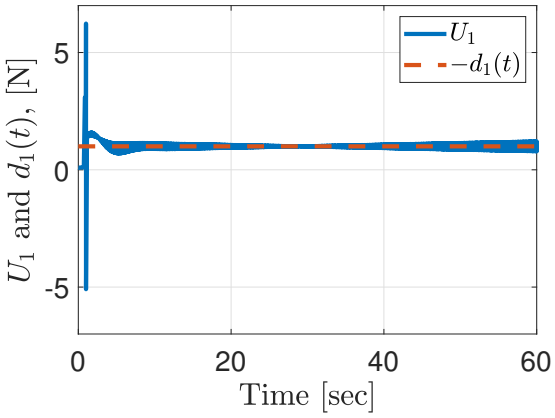

(a) Control and disturbance components, U_1 and $d_1(t)$.

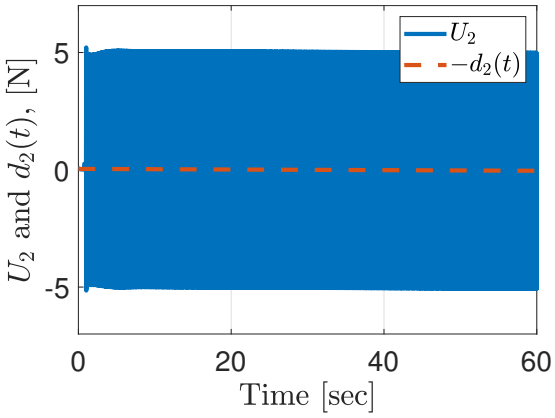

(b) Control and disturbance components, U_2 and $d_2(t)$.

Figure 3.10: 3D Crane - MBF UVC with positive barrier, U and $d(t)$.

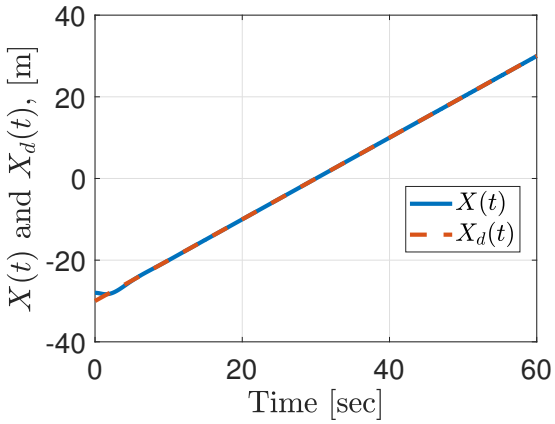

(a) State variable $X(t)$.

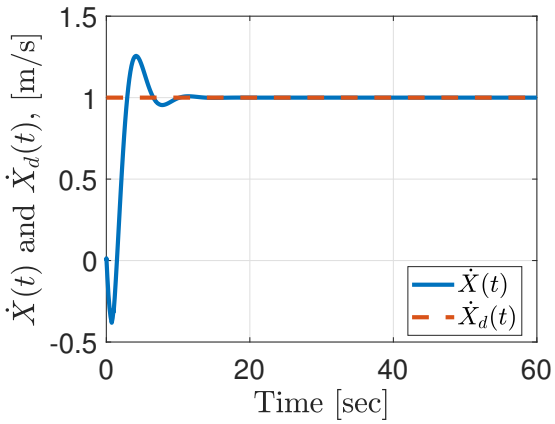

(b) State variable $\dot{X}(t)$.

Figure 3.11: 3D Crane - MBF UVC with semi-positive barrier, $X(t)$ and $\dot{X}(t)$.

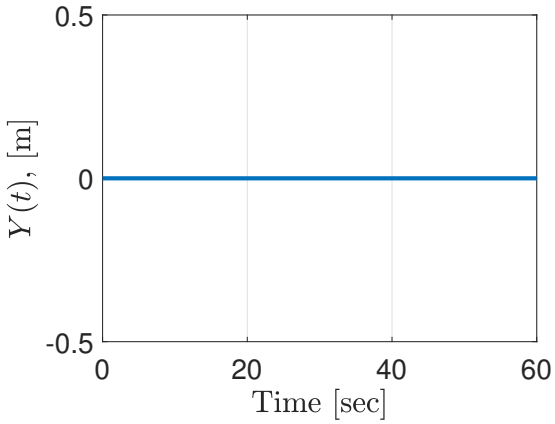

(a) State variable $Y(t)$.

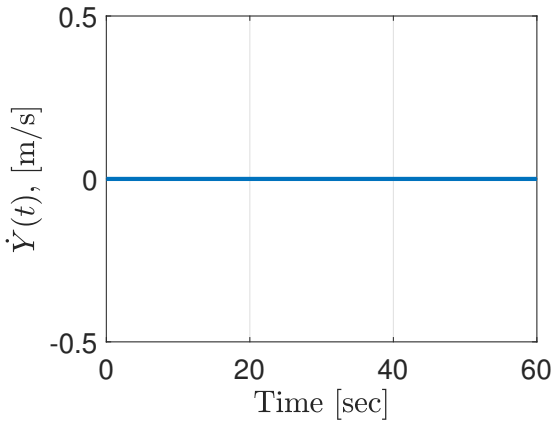

(b) State variable $\dot{Y}(t)$.

Figure 3.12: 3D Crane - MBF UVC with semi-positive barrier, $Y(t)$ and $\dot{Y}(t)$.

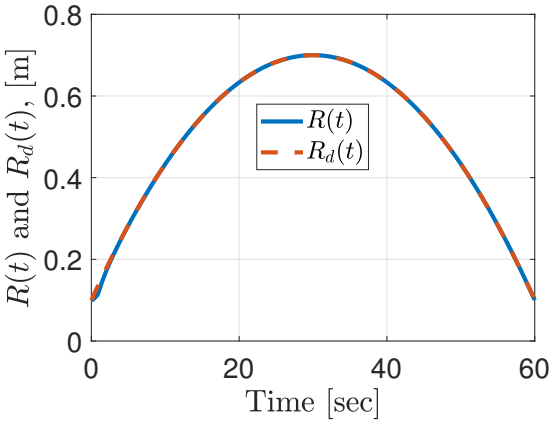

(a) State variable $R(t)$.

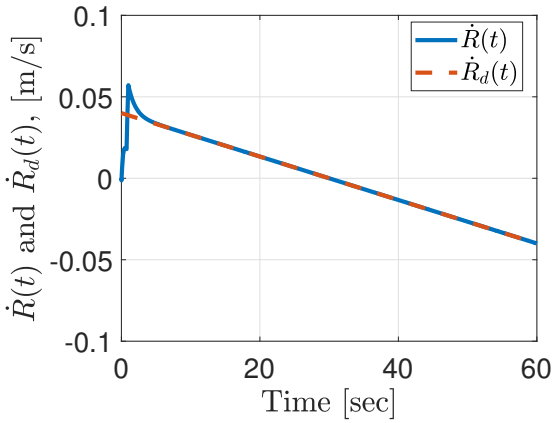

(b) State variable $\dot{R}(t)$.

Figure 3.13: 3D Crane - MBF UVC with semi-positive barrier, $R(t)$ and $\dot{R}(t)$.

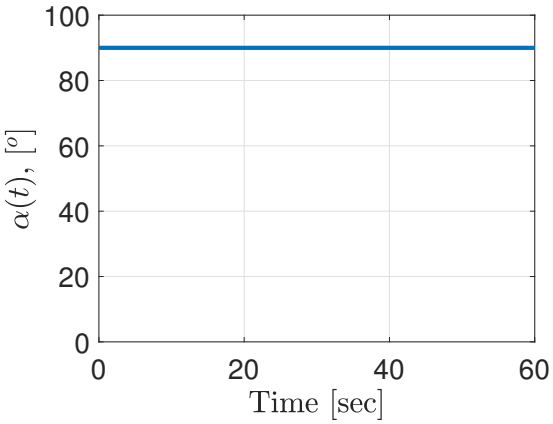

(a) State variable $\alpha(t)$.

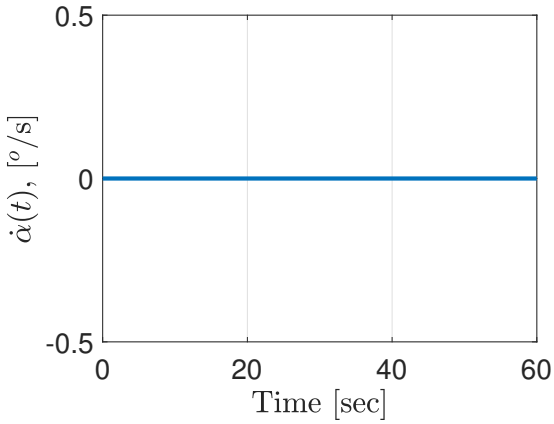

(b) State variable $\dot{\alpha}(t)$.

Figure 3.14: 3D Crane - MBF UVC with semi-positive barrier, $\alpha(t)$ and $\dot{\alpha}(t)$.

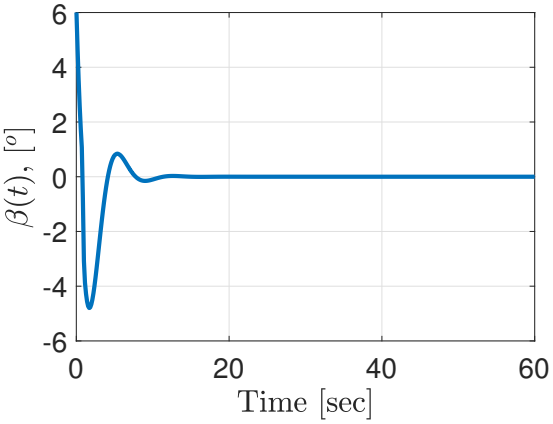

(a) State variable $\beta(t)$.

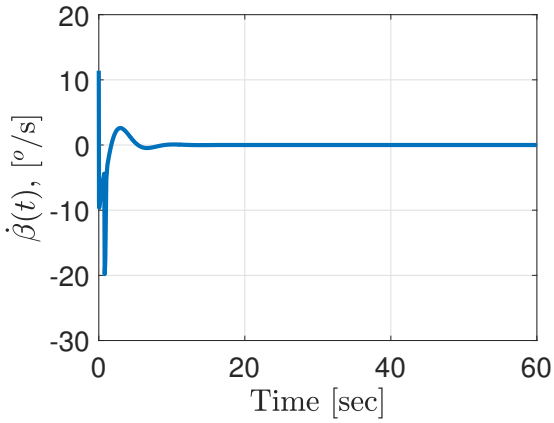

(b) State variable $\dot{\beta}(t)$.

Figure 3.15: 3D Crane - MBF UVC with semi-positive barrier, $\beta(t)$ and $\dot{\beta}(t)$.

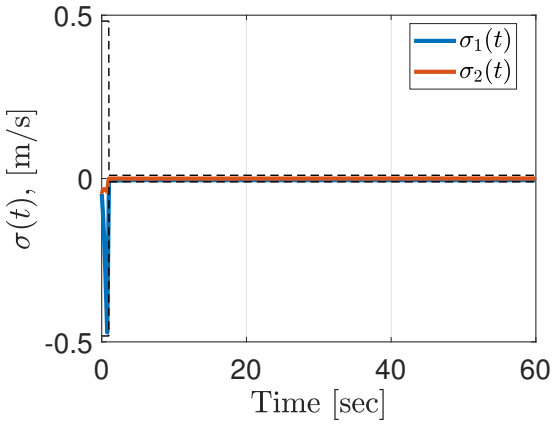

(a) Sliding vector, $\sigma(t)$.

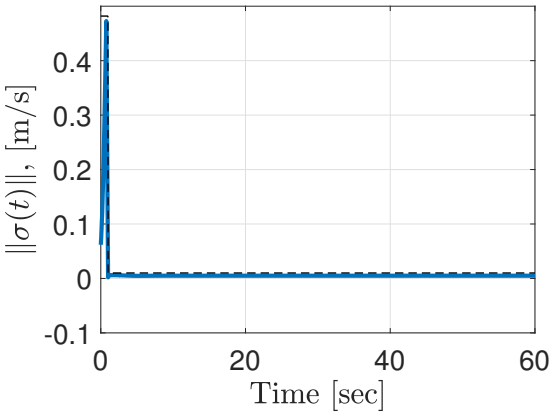

(b) Norm of the sliding vector, $\|\sigma(t)\|$.

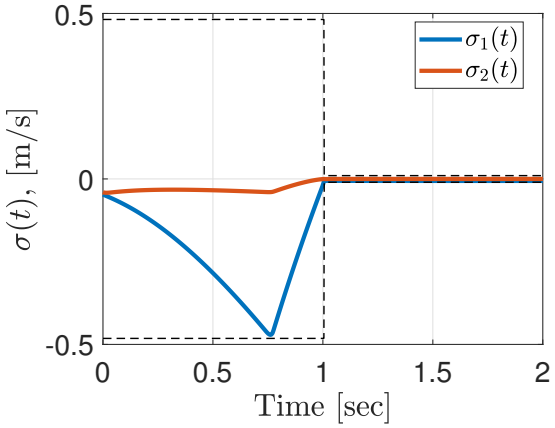

(c) Sliding vector, $\sigma(t)$.

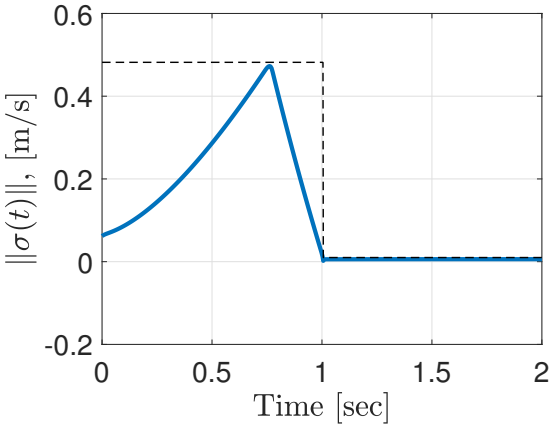

(d) Norm of the sliding vector, $\|\sigma(t)\|$.

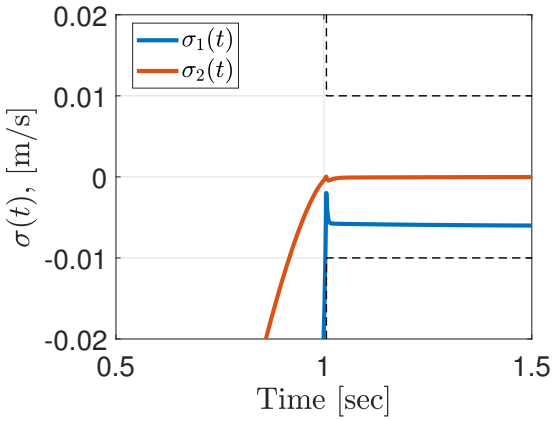

(e) Sliding vector, $\sigma(t)$.

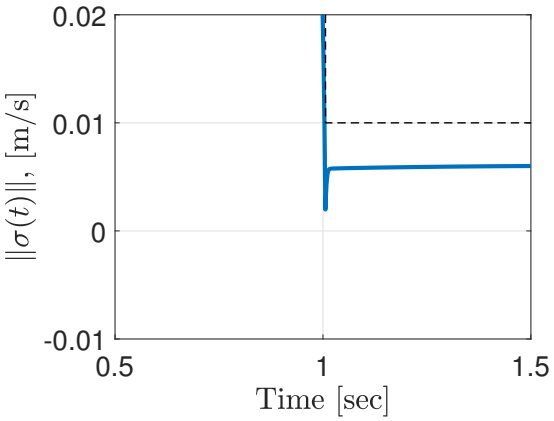

(f) Norm of the sliding vector, $\|\sigma(t)\|$.

Figure 3.16: 3D Crane - MBF UVC with semi-positive barrier, $\sigma(t)$ and $\|\sigma(t)\|$.

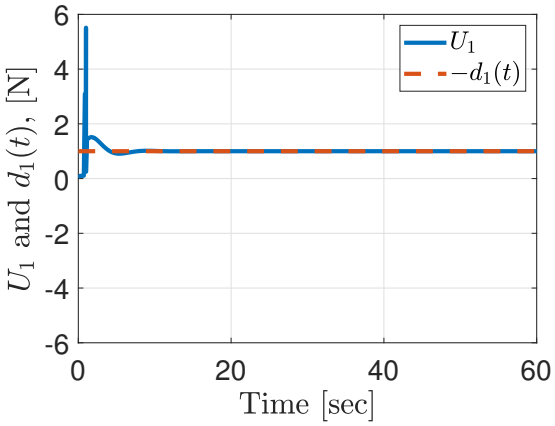

(a) Control and disturbance components, U_1 and $d_1(t)$.

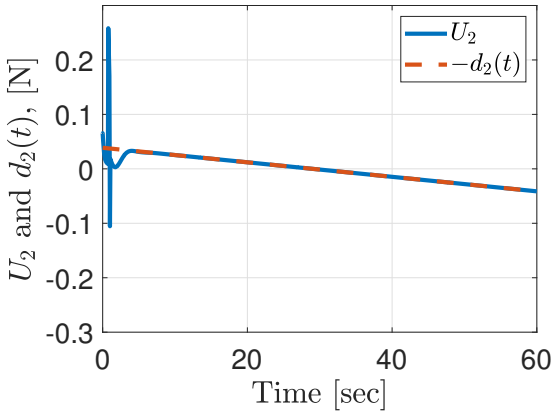

(b) Control and disturbance components, U_2 and $d_2(t)$.

Figure 3.17: 3D Crane - MBF UVC with semi-positive barrier, U and $d(t)$.

Chapter 4

Static Event-Triggered Extremum Seeking Control

Considering static maps, this chapter proposes a static event-triggered [63] scheme for scalar extremum seeking control. While the extremum seeking allows the output of a nonlinear map to be held within a vicinity of its extremum, the event-triggered strategy is responsible to execute the control task aperiodically by using a monitoring mechanism. The event-triggered strategy ensures asymptotic stability properties to the closed-loop system and reduces control effort since the control update and data communication only occur when a designed triggered-condition is satisfied. Integrating Lyapunov stability theory and averaging method generalized for discontinuous systems, a systematic design procedure and stability analysis is developed. Ultimately, the resulting closed-loop dynamics exhibits the advantages of integrating both approaches, event-triggered and extremum seeking. The Zeno behavior is precluded and the local exponential stability of the closed-loop system is guaranteed. An illustration of the benefits of the new control method is presented using consistent simulation results.

4.1 Problem Formulation

We consider the following nonlinear static map

$$Q(\theta(t)) = Q^* + \frac{H^*}{2}(\theta(t) - \theta^*)^2\,, \tag{4.1}$$

where $H^* \in \mathbb{R} - \{0\}$ is the Hessian, $\theta^* \in \mathbb{R}$ is the unknown optimizer, and the input of the map $\theta(t) \in \mathbb{R}$ is designed as the real-time estimate $\hat{\theta}(t) \in \mathbb{R}$ of θ^* additively perturbed by the sinusoid $a\sin(\omega t)$, *i.e.*,

$$\theta(t) = \hat{\theta}(t) + a\sin(\omega t)\,. \tag{4.2}$$

Figure 4.1 shows the structure of the event-triggered-based extremum seeking control system to be designed.

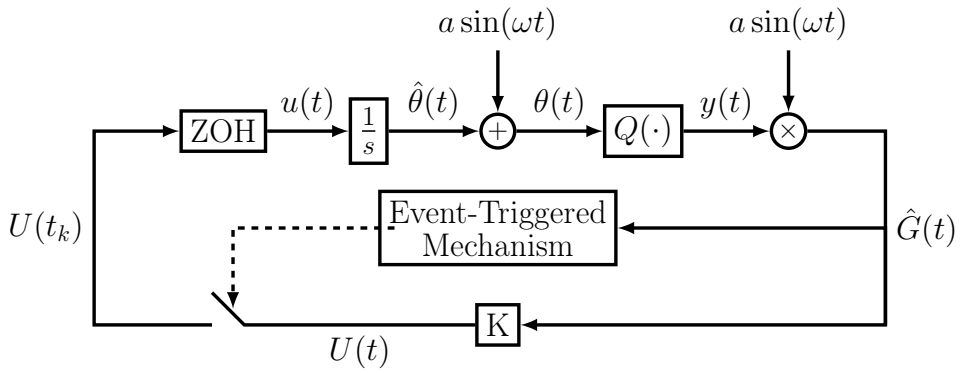

Figure 4.1: Event-triggered based on extremum seeking scheme.

From Figure 4.1, the output of the nonlinear map (4.1) can be written as

$$y(t) = Q(\theta(t)) = Q^* + \frac{H^*}{2}(\theta(t) - \theta^*)^2 \,. \tag{4.3}$$

4.1.1 Continuous-Time Extremum Seeking

Let us define the estimation error

$$\tilde{\theta}(t) = \hat{\theta}(t) - \theta^* \,, \tag{4.4}$$

and the Gradient estimate

$$\hat{G}(t) = a\sin(\omega t)\; y(t) \,, \tag{4.5}$$

by the demodulation signal, $a\sin(\omega t)$, which has nonzero amplitudes a and frequency ω [51, 101].

From (4.2) and (4.4), we can write

$$\theta(t) = \tilde{\theta}(t) + a\sin(\omega t) + \theta^* \,, \tag{4.6}$$

and, therefore, by plugging (4.6) into (4.3), $y(t)$ can also be written as

$$y(t) = Q^* + \frac{H^* a^2}{4} + \frac{H^*}{2}\tilde{\theta}^2(t) + a\sin(\omega t)H^*\tilde{\theta}(t) - \frac{H^* a^2}{4}\cos(2\omega t) \,. \tag{4.7}$$

Thus, from (4.5) and (4.7), the gradient estimate [55], is given by

$$\hat{G}(t) = \frac{a^2 H^*}{2}\left(1-\cos\left(2\omega t\right)\right)\tilde{\theta}(t) + \frac{aH^*}{2}\sin\left(\omega t\right)\tilde{\theta}^2(t) + \\ + \left(aQ^* + \frac{3a^3H^*}{8}\right)\sin\left(\omega t\right) - \frac{a^3H^*}{8}\sin\left(3\omega t\right)\,. \tag{4.8}$$

Notice the term quadratic in $\tilde{\theta}(t)$ in (4.8) may be neglected in a local analysis [102]. Thus, hereafter the gradient estimate is given by

$$\hat{G}(t) = \frac{a^2 H^*}{2}\left(1-\cos\left(2\omega t\right)\right)\tilde{\theta}(t) + \left(aQ^* + \frac{3a^3H^*}{8}\right)\sin\left(\omega t\right) - \frac{a^3H^*}{8}\sin\left(3\omega t\right)\,. \tag{4.9}$$

On the other hand, from the time-derivative of (4.4) and the ESC scheme of Figure 4.1, the dynamics that governs $\hat{\theta}(t)$, as well as $\tilde{\theta}(t)$, is given by

$$\dot{\tilde{\theta}}(t) = \dot{\hat{\theta}}(t) = u(t)\,, \tag{4.10}$$

where u is the ESC law to be designed as

$$u(t) = K\hat{G}(t)\,, \quad \forall t \geq 0\,. \tag{4.11}$$

By taking the time-derivative of (4.9) and the equation (4.10), one gets

$$\dot{\hat{G}}(t) = \frac{a^2 H^*}{2}\left(1-\cos\left(2\omega t\right)\right)u(t) + a^2\omega H^*\sin\left(2\omega t\right)\tilde{\theta}(t) \\ + \left(a\omega Q^* + \frac{3a^2\omega H^*}{8}\right)\cos\left(\omega t\right) - \frac{3a^2\omega H^*}{8}\cos\left(3\omega t\right)\,. \tag{4.12}$$

4.1.2 Event-Triggered Control Emulation of the Extremum Seeking Design

Let t_k denote the unbounded monotonically increasing sequence of time instants, *i.e.*,

$$0 = t_0 < t_1 < \ldots < t_k < \ldots\,, \quad k \in \mathbb{N}\,, \lim_{k\to\infty} t_k = \infty\,, \tag{4.13}$$

with the aperiodic sampling intervals $\tau_k = t_{k+1} - t_k > 0$.

We consider continuous measurement of the system output while actuating the system using an event-based approach. The actuator transforms the discrete-time control input $U(t_k)$ to a continuous control input $u(t)$ as in sampled data systems with zero-order hold. By assuming that there is no delay in the Sensor-to-Controller

and Controller-to-Actuator branches, one has

$$u(t) = U_k = U(t_k)\,, \quad t \in [t_k\,, t_{k+1})\,, \quad k \in \mathbb{N}\,. \tag{4.14}$$

Thus, define the control input for all $t \in [t_k\,, t_{k+1})$, $k \in \mathbb{N}$,

$$u_k = K\hat{G}(t_k)\,, \tag{4.15}$$

and we introduce the error vector

$$e(t) := \hat{G}(t_k) - \hat{G}(t)\,, \quad \forall t \in [t_k\,, t_{k+1})\,, \quad k \in \mathbb{N}\,. \tag{4.16}$$

Therefore, by using the event-triggered control law (4.15), adding and subtracting the term $\frac{a^2H^*K}{2}\left(1-\cos\left(2\omega t\right)\right)\hat{G}(t)$ into (4.12) and adding and subtracting the term $K\hat{G}(t)$ into (4.10), one arrives at the Input-to-State Stable (ISS) representation of the dynamics of $\hat{G}(t)$ and $\tilde{\theta}$ with respect to the error vector $e(t)$ in equation (4.16):

$$\begin{aligned}\dot{\hat{G}}(t)=&\frac{a^2H^*K}{2}\left(1-\cos\left(2\omega t\right)\right)\hat{G}(t)+\frac{a^2H^*K}{2}\left(1-\cos\left(2\omega t\right)\right)e(t)-\frac{3a^2\omega H^*}{8}\cos\left(3\omega t\right)\\&+a^2\omega H^*\sin\left(2\omega t\right)\tilde{\theta}(t)+\left(a\omega Q^*+\frac{3a^2\omega H^*}{8}\right)\cos\left(\omega t\right)\,,\end{aligned} \tag{4.17}$$

$$\begin{aligned}\dot{\tilde{\theta}}(t)=&K\hat{G}(t_k)+K\hat{G}(t)-K\hat{G}(t)=K\hat{G}(t)+K\left[\hat{G}(t_k)-\hat{G}(t)\right]\\=&\frac{a^2H^*K}{2}\left(1-\cos\left(2\omega t\right)\right)\tilde{\theta}(t)+Ke(t)+\left(aQ^*K+\frac{3a^3H^*K}{8}\right)\sin\left(\omega t\right)+\\&-\frac{a^3H^*K}{8}\sin\left(3\omega t\right)\,.\end{aligned} \tag{4.18}$$

In a conventional sampled-data implementation, the transmission times are distributed equidistantly in time, meaning that $t_{k+1} = t_k + h$, for all k , and some interval $h > 0$. In event-triggered control, however, these transmission are orchestrated by a monitoring mechanism that invokes transmissions when the difference between the current value of the output and its previously transmitted value becomes too large in an appropriate sense [69].

4.1.3 Static Event-Triggering Condition

In Definition 3 our triggering strategy is presented.

Definition 3 (Static-Triggering Condition)**.** *Consider the nonlinear mapping* $\Xi : \mathbb{R} \times \mathbb{R} \mapsto \mathbb{R}$ *given by*

$$\Xi(\hat{G}, e) = \sigma\hat{G}^2(t) + \hat{G}(t)e(t)\,, \tag{4.19}$$

and K be the control gain in (4.15). The event-triggered controller with triggering condition consists of two components:

1. *A set of increasing time sequence $I = \{t_0\,, t_1\,, t_2\,, \ldots\}$ with $t_0 = 0$ generated under the following rules:*
   - *If $\left\{t \in \mathbb{R}^+ : t > t_k \ \wedge \ \Xi(\hat{G}, e) < 0 = \emptyset\right\}$, then the set of the times of the events is $I = \{t_0\,, t_1\,, \ldots, t_k\}$.*
   - *If $\left\{t \in \mathbb{R}^+ : t > t_k \ \wedge \ \Xi(\hat{G}, e) < 0 \neq \emptyset\right\}$, the next event time is given by*

$$t_{k+1} = \min\left\{t \in \mathbb{R}^+ : t > t_k \ \wedge \ \Xi(\hat{G}, e) < 0\right\}\,, \tag{4.20}$$

   which is the event-trigger mechanism.

2. *A feedback control action updated at the generated triggering instants given by*

$$u_k = K\hat{G}(t_k)\,, \quad \forall t \in [t_k\,, t_{k+1})\,, \quad k \in \mathbb{N}\,. \tag{4.21}$$

4.1.4 Time-scaling System

By using the transformation $\bar{t} = \omega t$ where

$$\omega := \frac{2\pi}{T}\,, \tag{4.22}$$

it is possible to rewrite the dynamics (4.17)–(4.18) in a different time-scale such that

$$\frac{d\hat{G}(\bar{t})}{d\bar{t}} = \frac{1}{\omega}\hat{\mathcal{G}}\left(\bar{t}, \hat{G}, \tilde{\theta}, \frac{1}{\omega}\right)\,, \tag{4.23}$$

$$\frac{d\tilde{\theta}(\bar{t})}{d\bar{t}} = \frac{1}{\omega}\tilde{\Theta}\left(\bar{t}, \hat{G}, \tilde{\theta}, \frac{1}{\omega}\right)\,, \tag{4.24}$$

with

$$\begin{aligned}\hat{\mathcal{G}}\left(\bar{t}, \hat{G}, \tilde{\theta}, \frac{1}{\omega}\right) = &\frac{a^2H^*K}{2}\left(1-\cos\left(2\omega t\right)\right)\hat{G}(t) + \frac{a^2H^*K}{2}\left(1-\cos\left(2\omega t\right)\right)e(t) + \\ &-\frac{3a^2\omega H^*}{8}\cos\left(3\omega t\right) + a^2\omega H^*\sin\left(2\omega t\right)\tilde{\theta}(t) + \\ &+\left(a\omega Q^* + \frac{3a^2\omega H^*}{8}\right)\cos\left(\omega t\right)\,,\end{aligned} \tag{4.25}$$

$$\begin{aligned}\tilde{\Theta}\left(\bar{t}, \hat{G}, \tilde{\theta}, \frac{1}{\omega}\right) = &\frac{a^2H^*K}{2}\left(1-\cos\left(2\omega t\right)\right)\tilde{\theta}(t) + Ke(t) + \left(aQ^*K + \frac{3a^3H^*K}{8}\right)\sin\left(\omega t\right) + \\ &-\frac{a^3H^*K}{8}\sin\left(3\omega t\right)\,.\end{aligned} \tag{4.26}$$

4.1.5 Averaging System

Now, by defining the augmented state

$$X^T(\bar{t}) := \left[\hat{G}(\bar{t})\,, \tilde{\theta}(\bar{t})\right]\,, \tag{4.27}$$

one arrives at the dynamics

$$\frac{dX(\bar{t})}{d\bar{t}} = \frac{1}{\omega}\mathcal{F}\left(\bar{t}, X, \frac{1}{\omega}\right)\,, \quad \mathcal{F}^T = \left[\hat{\mathcal{G}}\,, \tilde{\Theta}\right]\,. \tag{4.28}$$

Due to the discontinuous nature of the proposed control strategy, throughout the article the averaging theory for discontinuous systems is used as presented by [103, Theorems 1 and 2].

The augmented system (4.28) has a small parameter $1/\omega$ as well as a T-periodic function $\mathcal{F}\left(\bar{t}, X, \frac{1}{\omega}\right)$ in $\bar{t}$, hence it admits the averaging method for stability analysis by averaging $\mathcal{F}\left(\bar{t}, X, \frac{1}{\omega}\right)$ at $\lim_{\omega\to\infty}\frac{1}{\omega} = 0$, as shown in [103], *i.e.*,

$$\frac{dX_{\text{av}}(\bar{t})}{d\bar{t}} = \frac{1}{\omega}\mathcal{F}_{\text{av}}\left(X_{\text{av}}\right)\,, \tag{4.29}$$

$$\mathcal{F}_{\text{av}}\left(X_{\text{av}}\right) = \frac{1}{T}\int_0^T \mathcal{F}\left(\delta, X_{\text{av}}, 0\right)d\delta\,. \tag{4.30}$$

Basically, the problem in the averaging method is to determine in what sense the behavior of the autonomous system (4.29) approximates the behavior of the nonautonomous system (4.28) such that (4.28) can be represented as a perturbation of system (4.29).

Therefore, treating the states $\hat{G}(\bar{t})$, $e(\bar{t})$ and $\tilde{\theta}(\bar{t})$ as constants in (4.17), and by using the averaging values, one gets

$$\frac{d\hat{G}_{\text{av}}(\bar{t})}{d\bar{t}} = \frac{a^2H^*K}{2\omega}\hat{G}_{\text{av}}(\bar{t}) + \frac{a^2H^*K}{2\omega}e_{\text{av}}(\bar{t})\,, \tag{4.31}$$

$$e_{\text{av}}(\bar{t}) = \hat{G}_{\text{av}}(\bar{t}_k) - \hat{G}_{\text{av}}(\bar{t})\,. \tag{4.32}$$

Hence, from (4.31) it is easy to verify the ISS relations of $\hat{G}_{\text{av}}(\bar{t})$ with respect to the averaged measurement error $e_{\text{av}}(\bar{t})$.

Moreover, from (4.9),

$$\hat{G}_{\text{av}}(\bar{t}) = \frac{a^2 H^*}{2}\tilde{\theta}_{\text{av}}(\bar{t})\,, \tag{4.33}$$

and, consequently,

$$\tilde{\theta}_{\text{av}}(\bar{t}) = \frac{2}{a^2 H^*}\hat{G}_{\text{av}}(\bar{t})\,, \tag{4.34}$$

with time-derivative

$$\frac{d\tilde{\theta}_{\text{av}}(\bar{t})}{d\bar{t}} = \frac{a^2 H^* K}{2\omega}\tilde{\theta}_{\text{av}}(\bar{t}) + \frac{1}{\omega}K e_{\text{av}}(\bar{t})\,. \tag{4.35}$$

Therefore, the following average event-triggered detection laws can be introduced for the average system.

Definition 4 (Average Static-Triggering Condition)**.** *Consider the nonlinear mapping* $\Xi : \mathbb{R} \times \mathbb{R} \mapsto \mathbb{R}$ *given by*

$$\Xi(\hat{G}_{\text{av}}, e_{\text{av}}) = \sigma \hat{G}^2_{\text{av}}(\bar{t}) + \hat{G}_{\text{av}}(\bar{t}) e_{\text{av}}(\bar{t})\,, \tag{4.36}$$

and K *be the control gain in (4.15). The event-triggered controller with triggering condition consists of two components:*

1. *A set of increasing sequence of time* $I = \{\bar{t}_0\,, \bar{t}_1\,, \bar{t}_2\,, \ldots\}$ *with* $\bar{t}_0 = 0$ *generated under the following rules:*

   - *If* $\left\{\bar{t} \in \mathbb{R}^+ : \bar{t} > \bar{t}_k \ \wedge\ \Xi(\hat{G}_{\text{av}}, e_{\text{av}}) < 0 = \emptyset\right\}$*, then the set of the times of the events is* $I = \{\bar{t}_0\,, \bar{t}_1\,, \ldots, \bar{t}_k\}$.
   - *If* $\left\{\bar{t} \in \mathbb{R}^+ : \bar{t} > \bar{t}_k \ \wedge\ \Xi(\hat{G}_{\text{av}}, e_{\text{av}}) < 0 \neq \emptyset\right\}$*, next event time is given by*

   $$\bar{t}_{k+1} = \min\left\{\bar{t} \in \mathbb{R}^+ : \bar{t} > \bar{t}_k \ \wedge\ \Xi(\hat{G}_{\text{av}}, e_{\text{av}}) < 0\right\}\,, \tag{4.37}$$

   that is the average event-trigger mechanism.

2. *A feedback control action updated at the the generated triggering instants given as*

   $$u_k = K\hat{G}(\bar{t}_k)\,, \quad \forall \bar{t} \in [\bar{t}_k\,, \bar{t}_{k+1})\,, \quad k \in \mathbb{N}\,. \tag{4.38}$$

4.1.6 Assumptions

The following assumptions are considered throughout the thesis:

(A1) The unique optimizer value $\theta^* \in R$ and the scalar Q^* are unknown parameters of the nonlinear map (4.1).

(A2) The Hessian H^* has known sign, but it is unknown in norm.

(A3) The control gain K satisfies

$$\text{sign}(K) = -\text{sign}(H^*)\,. \tag{4.39}$$

(A4) There is no delays due processing of sensor and actuator as well as transmission in the sensor-to-controller and controller-to-actuator branches.

(A5) Only $\hat{G}(t)$ is available for the event-triggered design.

4.2 Stability Analysis

This section assumes a partial knowledge of the nonlinear map (4.1) such that the Hessian sign is a known parameter. Although this hypothesis appears to simplify the problem, the designer should know if he/she is dealing with an seeking strategy to reach a maximum or minimum extremum. On the other hand, the optimizer value θ^* and parameter Q^* are completely unknown.

Theorem 3. *Consider the closed-loop average dynamics of the gradient estimate (4.31) and the average event-triggered mechanism given by (4.37). Suppose that Assumptions (A1)–(A5) are hold. If $\Xi(\hat{G}_{\text{av}}, e_{\text{av}})$ is given by (4.36) and ω in (4.22) is a constant sufficiently large compared to the parameters of (4.31), the average gradient estimate $\hat{G}_{av}(t)$ system (4.31) is locally exponentially stable and, consequently, $\tilde{\theta}_{av}(t)$ converges exponentially to zero. Therefore, there exist constants $m\,, M_\theta\,, M_y > 0$ such that*

$$|\theta(t) - \theta^*| \leq M_\theta \exp(-mt) + \mathcal{O}\left(a + \frac{1}{\omega}\right)\,, \tag{4.40}$$

$$|y(t) - Q^*| \leq M_y \exp(-mt) + \mathcal{O}\left(a^2 + \frac{1}{\omega^2}\right)\,, \tag{4.41}$$

where $a > 0$, and the constants M_θ and M_y depend on the initial condition $\theta(0)$. Moreover, there exists a lower bound τ^* for the inter-execution interval $t_{k+1} - t_k$ for all $k \in \mathbb{N}$ precluding the Zeno behavior.

Proof. Now, consider the following Lyapunov function candidate

$$V_{\text{av}}(\bar{t}) = \hat{G}^2_{\text{av}}(\bar{t})\,, \tag{4.42}$$

with time-derivative

$$\frac{dV_{\text{av}}(\bar{t})}{d\bar{t}} = -\frac{a^2|H^*||K|}{\omega}\hat{G}^2_{\text{av}}(\bar{t}) - \frac{a^2|H^*||K|}{\omega}\hat{G}_{\text{av}}(\bar{t})e_{\text{av}}(\bar{t})\,. \tag{4.43}$$

From (4.43), if there is no measurement error $e(t)$, *i.e.*, $e(t) \equiv 0\ \forall t > 0$, therefore the classic extremum seeking implementation, according to equation (4.43) becomes $\frac{dV_{\text{av}}}{d\bar{t}} = -\frac{a^2|H^*||K|}{\omega}\hat{G}^2_{\text{av}}(\bar{t})$. On the other hand, the proposed event-triggered approach, with update law (4.37) and $\Xi(\hat{G}_{\text{av}}, e_{\text{av}})$ given by (4.36), ensures in closed-loop an exponential decay of $V_{\text{av}}(\bar{t})$ given by a pre-specified fraction of the ideal decay rate such that

$$\frac{dV_{\text{av}}(\bar{t})}{d\bar{t}} \leq -\frac{(1-\sigma)a^2|H^*||K|}{\omega}\hat{G}^2_{\text{av}}(\bar{t})\,. \tag{4.44}$$

Now, plugging equation (4.43) in the left-hand side of inequality (4.44), one gets

$$-\frac{a^2|H^*||K|}{\omega}\hat{G}^2_{\text{av}}(\bar{t}) - \frac{a^2|H^*||K|}{\omega}\hat{G}_{\text{av}}(\bar{t})e_{\text{av}}(\bar{t}) \leq -\frac{(1-\sigma)a^2|H^*||K|}{\omega}\hat{G}^2_{\text{av}}(\bar{t})\,. \tag{4.45}$$

Then,

$$\sigma\hat{G}^2_{\text{av}}(\bar{t}) + \hat{G}_{\text{av}}(\bar{t})e_{\text{av}}(\bar{t}) \geq 0\,, \tag{4.46}$$

or, equivalently,

$$\Xi(\hat{G}_{\text{av}}, e_{\text{av}}) \geq 0\,. \tag{4.47}$$

The event-triggered mechanism supervises the time derivative of the Lyapunov function given by (4.43) and its pre-specified upper bound in (4.44) to set the instant on which these signals meet. This time-instant is the same to send data over the network and update the actuator, where the condition $\Xi(\hat{G}_{\text{av}}, e_{\text{av}}) < 0$ is verified as in (4.37). This process can takes place for an indefinite number of times, in other words, whenever necessary, and guarantees the exponential stability of $\hat{G}_{\text{av}}(\bar{t})$ in closed-loop.

By using (4.42) and (4.44), for $\bar{t} \in (\bar{t}_k, , \bar{t}_{k+1})$, an upper bound for (4.43) is

$$\frac{dV_{\text{av}}(\bar{t})}{d\bar{t}} \leq -\frac{(1-\sigma)a^2|H^*||K|}{\omega}V_{\text{av}}(\bar{t})\,. \tag{4.48}$$

Then, invoking the Comparison Lemma [94] an upper bound $\bar{V}_{\text{av}}(\bar{t})$ for $V_{\text{av}}(\bar{t})$ is

$$V_{\text{av}}(\bar{t}) \leq \bar{V}_{\text{av}}(\bar{t})\,, \quad \forall \bar{t} \in [\bar{t}_k, \bar{t}_{k+1})\,. \tag{4.49}$$

given by the solution of the following dynamics

$$\frac{d\bar{V}_{\rm av}(\bar{t})}{d\bar{t}} = -\frac{(1-\sigma)a^2|H^*||K|}{\omega}\bar{V}_{\rm av}(\bar{t}), \quad \bar{V}_{\rm av}(\bar{t}_k) = V_{\rm av}(\bar{t}_k)\,, \tag{4.50}$$

In other words, $\forall \bar{t} \in [\bar{t}_k, \bar{t}_{k+1})$,

$$\bar{V}_{\rm av}(\bar{t}) = \exp\left(-\frac{(1-\sigma)a^2|H^*||K|}{\omega}(\bar{t}-\bar{t}_k)\right) V_{\rm av}(\bar{t}_k)\,, \tag{4.51}$$

and the inequality (4.49) is rewritten as

$$V_{\rm av}(\bar{t}) \leq \exp\left(-\frac{(1-\sigma)a^2|H^*||K|}{\omega}(\bar{t}-\bar{t}_k)\right) V_{\rm av}(\bar{t}_k)\,. \tag{4.52}$$

By defining, $\bar{t}_k^+$ and $\bar{t}_k^-$ as the right and left limits of $\bar{t} = \bar{t}_k$, respectively, it easy to verify that $V_{\rm av}(\bar{t}_{k+1}^-) \leq \exp\left(-\frac{(1-\sigma)a^2|H^*||K|}{\omega}(\bar{t}_{k+1}^- - \bar{t}_k^+)\right) V_{\rm av}(\bar{t}_k^+)$. Since $V_{\rm av}(\bar{t})$ is continuous, $V_{\rm av}(\bar{t}_{k+1}^-) = V_{\rm av}(\bar{t}_{k+1})$ and $V_{\rm av}(\bar{t}_k^+) = V_{\rm av}(\bar{t}_k)$, and therefore,

$$V_{\rm av}(\bar{t}_{k+1}) \leq \exp\left(-\frac{(1-\sigma)a^2|H^*||K|}{\omega}(\bar{t}_{k+1}-\bar{t}_k)\right) V_{\rm av}(\bar{t}_k)\,. \tag{4.53}$$

Hence, for any $\bar{t} \geq 0$ in $\bar{t} \in [\bar{t}_k, \bar{t}_{k+1})$, $k \in \mathbb{N}$, one has

$$\begin{aligned}
&V_{\rm av}(\bar{t}) \leq \exp\left(-\frac{(1-\sigma)a^2|H^*||K|}{\omega}(\bar{t}-\bar{t}_k)\right) V_{\rm av}(\bar{t}_k) \\
&\leq \exp\left(-\frac{(1-\sigma)a^2|H^*||K|}{\omega}(\bar{t}-\bar{t}_k)\right) \exp\left(-\frac{(1-\sigma)a^2|H^*||K|}{\omega}(\bar{t}_k-\bar{t}_{k-1})\right) V_{\rm av}(\bar{t}_{k-1}) \\
&\leq \ldots \leq \\
&\leq \exp\left(-\frac{(1-\sigma)a^2|H^*||K|}{\omega}(\bar{t}-\bar{t}_k)\right) \prod_{i=1}^{i=k} \exp\left(-\frac{(1-\sigma)a^2|H^*||K|}{\omega}(\bar{t}_i-\bar{t}_{i-1})\right) V_{\rm av}(\bar{t}_{i-1}) \\
&= \exp\left(-\frac{(1-\sigma)a^2|H^*||K|}{\omega}\bar{t}\right) V_{\rm av}(0)\,.
\end{aligned} \tag{4.54}$$

Now, one obtains

$$|\hat{G}_{\rm av}(\bar{t})|^2 \leq \exp\left(-\frac{(1-\sigma)a^2|H^*||K|}{\omega}\bar{t}\right) |\hat{G}_{\rm av}(0)|^2 \tag{4.55}$$

$$= \left[\exp\left(-\frac{(1-\sigma)a^2|H^*||K|}{2\omega}\bar{t}\right) |\hat{G}_{\rm av}(0)|\right]^2\,. \tag{4.56}$$

Hence,

$$|\hat{G}_{\rm av}(\bar{t})| \leq \exp\left(-\frac{(1-\sigma)a^2|H^*||K|}{2\omega}\bar{t}\right) |\hat{G}_{\rm av}(0)|\,. \tag{4.57}$$

Since (4.17) is T-periodic in t, $1/\omega$ is a positive small parameter, and from inequality (4.57) the origin $\hat{G}_{\text{av}} = 0$ is at least an exponentially stable equilibrium point of the closed-loop event-triggered system. Then, by invoking [103, Theorem 2], there exists an upper bound for (4.9) such that

$$\begin{aligned}|\hat{G}(t)| &\leq |\hat{G}_{\text{av}}(t)| + \mathcal{O}\left(\frac{1}{\omega}\right) \\ &\leq \exp\left(-\frac{(1-\sigma)a^2|H^*||K|}{2\omega}\bar{t}\right)|\hat{G}_{\text{av}}(0)| + \mathcal{O}\left(\frac{1}{\omega}\right).\end{aligned} \tag{4.58}$$

Although the analysis has been focused on the convergence of $\hat{G}_{\text{av}}(\bar{t})$ and, consequently $\hat{G}(t)$, the obtained results through (4.58) can be easily extended to the variable $\tilde{\theta}_{\text{av}}(\bar{t})$ and $\tilde{\theta}(t)$. Notice that, by using (4.33) and the equation (4.42), one has

$$V_{\text{av}} = \left(\frac{a^2 H^*}{2}\tilde{\theta}_{\text{av}}(\bar{t})\right)^2 = \frac{a^4 H^{*2}}{4}\tilde{\theta}^2_{\text{av}}(\bar{t})\,. \tag{4.59}$$

Then, plugging (4.59) into (4.52), we get

$$|\tilde{\theta}_{\text{av}}(\bar{t})|^2 \leq \exp\left(-\frac{(1-\sigma)a^2|H^*||K|}{\omega}\bar{t}\right)|\tilde{\theta}_{\text{av}}(0)|^2\,. \tag{4.60}$$

Therefore, following the same development carried out between equations (4.56) to (4.57), one arrives at

$$|\tilde{\theta}_{\text{av}}(\bar{t})| \leq \exp\left(-\frac{(1-\sigma)a^2|H^*||K|}{2\omega}\bar{t}\right)|\tilde{\theta}_{\text{av}}(0)|\,, \tag{4.61}$$

and

$$\begin{aligned}|\tilde{\theta}(\bar{t})| &\leq |\tilde{\theta}_{\text{av}}(\bar{t})| + \mathcal{O}\left(\frac{1}{\omega}\right) \\ &\leq \exp\left(-\frac{(1-\sigma)a^2|H^*||K|}{2\omega}\bar{t}\right)|\tilde{\theta}_{\text{av}}(0)| + \mathcal{O}\left(\frac{1}{\omega}\right).\end{aligned} \tag{4.62}$$

Now, from (4.6), we have

$$\theta(t) - \theta^* = \tilde{\theta}(t) + a\sin(\omega t)\,, \tag{4.63}$$

whose norm satisfies

$$\begin{aligned}|\theta(t) - \theta^*| &= |\tilde{\theta}(t) + S(t)| \leq |\tilde{\theta}(t)| + |a\sin(\omega t)| \\ &\leq \exp\left(-\frac{(1-\sigma)a^2|H^*||K|}{2\omega}\bar{t}\right)|\theta(0) - \theta^*| + \mathcal{O}\left(a + \frac{1}{\omega}\right).\end{aligned} \tag{4.64}$$

Defining the error variable $\tilde{y}(t)$ as

$$\tilde{y}(t) := y(t) - Q^* \,, \tag{4.65}$$

and using (4.3) as well as the Cauchy-Schwarz Inequality, its absolute value satisfies

$$|\tilde{y}(t)| = |y(t) - Q^*| = |H^*||\theta(t) - \theta^*|^2 \,, \tag{4.66}$$

and its upper bounded with (4.64)is given by

$$\begin{aligned} |y(t)-Q^*| \leq & \exp\left(-\frac{(1-\sigma)a^2|H^*||K|}{2}t\right)|H^*|\left[|\theta(0)-\theta^*| + 2\mathcal{O}\left(a+\frac{1}{\omega}\right)\right]|\theta(0)-\theta^*| \\ & + \mathcal{O}\left(a^2+\frac{1}{\omega^2}\right) . \end{aligned} \tag{4.67}$$

Therefore, by defining the positive constants

$$m = \frac{(1-\sigma)a^2|H^*||K|}{2} \,, \tag{4.68}$$

$$M_\theta = |\theta(0) - \theta^*| \,, \tag{4.69}$$

$$M_y = \left[|\theta(0) - \theta^*| + 2\mathcal{O}\left(a + \frac{1}{\omega}\right)\right]|\theta(0) - \theta^*| \,, \tag{4.70}$$

the inequalities (4.64) and (4.67) satisfy (4.40) and (4.41), respectively.

By invoking [63, Corollary IV.1], the inter-execution instants are lower bounded by interval $\bar{\tau}^*$ spent by the solution of

$$\frac{d\phi(\bar{t})}{d\bar{t}} = \frac{a^2|H^*||K|}{2\omega}(1+\phi(\bar{t}))^2 \,, \quad \phi(0) = 0 \,, \tag{4.71}$$

to reach $\phi(\bar{\tau}^*) = \sigma$. Then, solving the initial value problem (4.71) by using the method of separation of variables[104] and reminding that $\bar{t} = \omega t$ implies in $\bar{\tau}^* = \omega\tau^*$ that

$$\int_{\phi(0)}^{\phi(\bar{\tau}^*)} \frac{1}{(1+\phi(\bar{t}))^2} d\phi(\bar{t}) = \frac{a^2|H^*||K|}{2\omega} \int_0^{\bar{\tau}^*} d\bar{t} \,, \tag{4.72}$$

$$\left[-\frac{1}{1+\phi(\bar{t})}\right]_{\phi(0)}^{\phi(\bar{\tau}^*)} = \frac{a^2|H^*||K|}{2\omega} \left[\bar{t}\right]_0^{\bar{\tau}^*} \,, \tag{4.73}$$

$$\frac{1}{1+\phi(0)} - \frac{1}{1+\phi(\bar{\tau}^*)} = \frac{a^2|H^*||K|}{2\omega}\bar{\tau}^* \,, \tag{4.74}$$

$$\frac{\sigma}{1+\sigma} = \frac{a^2|H^*||K|}{2\omega}\bar{\tau}^* \,. \tag{4.75}$$

Then,

$$\tau^* = \frac{1}{|H^*||K|}\frac{2}{a^2}\left(\frac{\sigma}{1+\sigma}\right), \tag{4.76}$$

and the Zeno behavior is avoided which completes the proof. □

4.3 Simulation results

To highlight the main ideas of the proposed Event-triggered Extremum Seeking strategy the nonlinear map (4.1) has input $\theta(t) \in \mathbb{R}$, output $y(t) \in \mathbb{R}$, and unknown parameters $H = -1$, $Q^* = 7$ and $\theta^* = 5$. The dither signals have parameters $a = 0.1$, $\omega = 3$ [rad/sec], and we selected the event-triggered parameters $\sigma = 0.1$. The control gain matrix $K = 30$ and the initial condition is $\hat{\theta}(0) = 0.4$.

In Figures 4.2(a) and 4.2(b)the Gradient estimate in (4.9) and the error $e(t)$ in (4.16) are presented. In both cases, the event-triggered mechanism ensures their convergence to neighborhood of zero. The Gradient stabilization implies reaching the optimizer θ^*, see Figures 4.2(e) and 4.2(f). Figure 4.2(d) shows the aperiodic behavior of how often the control signal $U(t)$ is updated, see also Figure 4.2(c). During 300 seconds of simulation, there were 29 updates of the control signal, consequently, the average inter-execution interval is equal to 10.7143 seconds. Comparing the proposed strategy with the classic sample-hold implementation, assuming the same initial condition and a constant sampling period of $h = 0.01$ seconds, we would have 30,000 updates of the control signal in 300 seconds of simulation. That is, a number more than 1,000 times higher than the strategy proposed in this chapter.

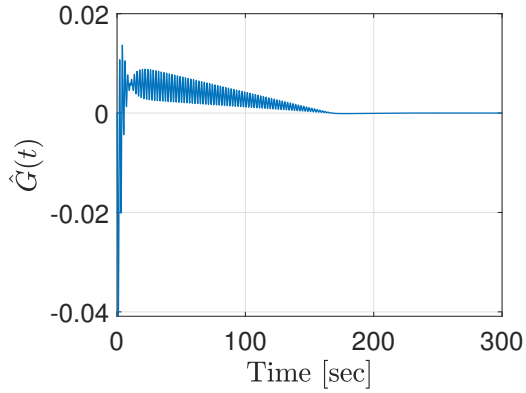

(a) Gradient estimate, $\hat{G}(t)$.

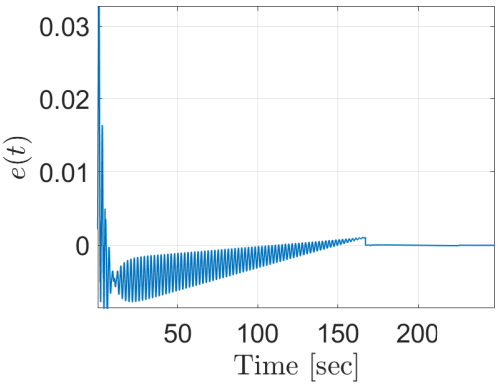

(b) Measurement error, $e(t)$.

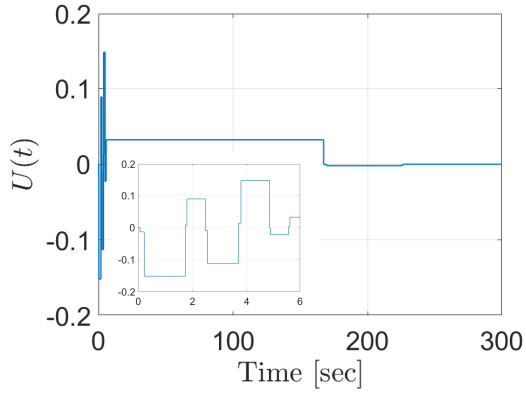

(c) Control input, $U(t)$.

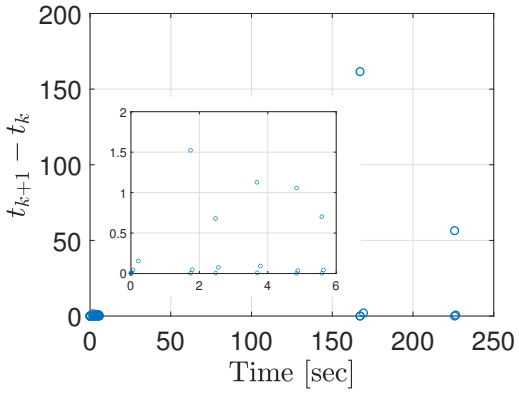

(d) The inter-execution times using the static event-triggered extremum seeking.

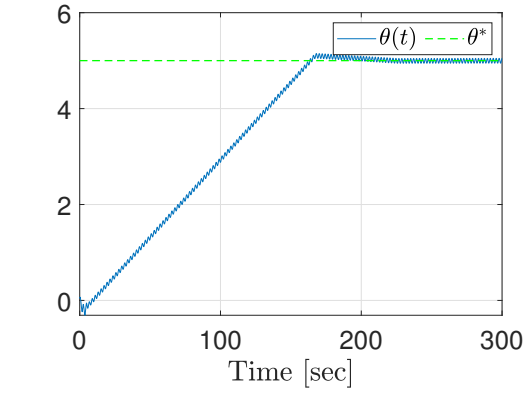

(e) Input of the nonlinear map, $\theta(t)$.

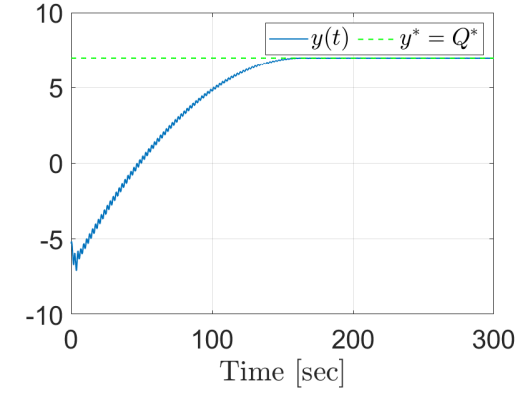

(f) Output of the nonlinear map, $y(t)$.

Figure 4.2: Event-triggered Extremum Seeking Control System.

Chapter 5

Dynamic Event-Triggered Extremum Seeking Feedback

This chapter proposes a dynamic event-triggered scheme for scalar extremum seeking control. While the extremum seeking allows the output of a nonlinear map to be held within a vicinity of its extremum, the event-triggered strategy is responsible to execute the control task aperiodically by using a monitoring mechanism. The event-triggered strategy ensures asymptotic stability properties to the closed-loop system and reduces control effort since the control update and data communication only occur when a designed triggered-condition is satisfied. Integrating Lyapunov and averaging theories for discontinuous systems, a systematic design procedure and stability analysis are developed. Ultimately, the resulting closed-loop dynamics proves the advantages of integrating both approaches, dynamic event-triggered and extremum seeking. The Zeno behavior is precluded and the local exponential stability of the closed-loop system are guaranteed. An illustration of the benefits of the new control method is presented using consistent simulation results.

5.1 Problem Formulation for Event-Triggered Extremum Seeking

We define the following nonlinear static map

$$Q(\theta(t)) = Q^* + \frac{H^*}{2}(\theta(t) - \theta^*)^2\,, \tag{5.1}$$

where $H^* \in \mathbb{R} - \{0\}$ is the Hessian, $\theta^* \in \mathbb{R}$ is the unknown optimizer, and the input of the map $\theta(t) \in \mathbb{R}$ is designed as the real-time estimate $\hat{\theta}(t) \in \mathbb{R}$ of θ^* additively

perturbed by the sinusoid $a\sin(\omega t)$, *i.e.*,

$$\theta(t) = \hat{\theta}(t) + a\sin(\omega t)\,. \tag{5.2}$$

Figure 5.1 shows the structure of the event-triggered-based extremum seeking control system to be designed.

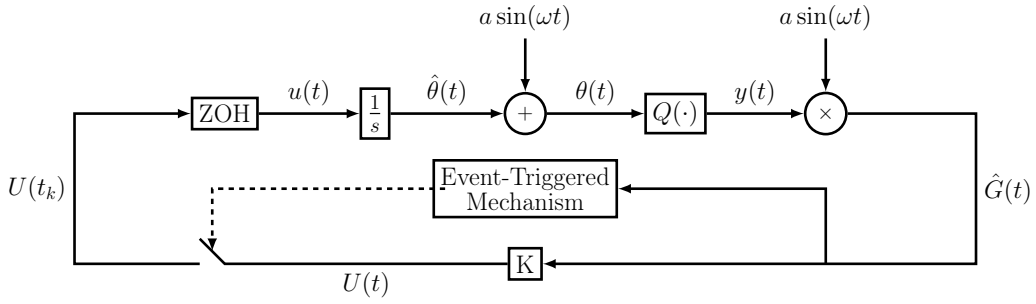

Figure 5.1: Event-triggered based on extremum seeking scheme.

From Figure 5.1, the output of the nonlinear map (5.1) can be written as

$$\begin{aligned} y(t) &= Q(\theta(t)) \\ &= Q^* + \frac{H^*}{2}(\theta(t) - \theta^*)^2\,. \end{aligned} \tag{5.3}$$

5.1.1 Assumptions

The following assumptions are considered throughout the thesis:

(A1) The unique optimizer value $\theta^* \in R$ and the scalar Q^* are unknown parameters of the nonlinear map (5.1).

(A2) The Hessian H^* is a known parameter.

(A3) The control gain K satisfies

$$\text{sign}(K) = -\text{sign}(H^*)\,. \tag{5.4}$$

(A4) There is no delays due processing of sensor and actuator as well as transmission in the sensor-to-controller and controller-to-actuator branches.

(A5) Only $\hat{G}(t)$ is available for the event-triggered design.

5.1.2 Continuous-time Extremum Seeking

Let us define the estimation error

$$\tilde{\theta}(t) = \hat{\theta}(t) - \theta^* \,, \tag{5.5}$$

and the Gradient estimate

$$\hat{G}(t) = a \sin(\omega t)\ y(t) \,, \tag{5.6}$$

by the demodulation signal, $a \sin(\omega t)$, which has nonzero amplitudes a and frequency ω [51, 101].

From (5.2) and (5.5), we can write

$$\theta(t) = \tilde{\theta}(t) + a \sin(\omega t) + \theta^* \,, \tag{5.7}$$

and, therefore, by plugging (5.7) into (5.3), $y(t)$ can also be written as

$$y(t) = Q^* + \frac{H^* a^2}{4} + \frac{H^*}{2}\tilde{\theta}^2(t) + a \sin(\omega t) H^* \tilde{\theta}(t) - \frac{H^* a^2}{4} \cos(2\omega t) \,. \tag{5.8}$$

Thus, from (5.6) and (5.8), the gradient estimate [55], is given by

$$\begin{aligned} \hat{G}(t) = {} & \frac{a^2 H^*}{2} \left(1 - \cos\left(2\omega t\right)\right) \tilde{\theta}(t) + \frac{a H^*}{2} \sin\left(\omega t\right) \tilde{\theta}^2(t) \\ & + \left(a Q^* + \frac{3 a^3 H^*}{8} \right) \sin\left(\omega t\right) - \frac{a^3 H^*}{8} \sin\left(3\omega t\right) \,. \end{aligned} \tag{5.9}$$

Notice the term quadratic in $\tilde{\theta}(t)$ in (5.9) may be neglected in a local analysis [102]. Thus, hereafter the gradient estimate is given by

$$\hat{G}(t) = \frac{a^2 H^*}{2} \left(1 - \cos\left(2\omega t\right)\right) \tilde{\theta}(t) + \left(a Q^* + \frac{3 a^3 H^*}{8} \right) \sin\left(\omega t\right) - \frac{a^3 H^*}{8} \sin\left(3\omega t\right) \,. \tag{5.10}$$

On the other hand, from the time-derivative of (5.5) and the ESC scheme of Figure 5.1, the dynamics that governs $\hat{\theta}(t)$, as well as $\tilde{\theta}(t)$, is given by

$$\dot{\tilde{\theta}}(t) = \dot{\hat{\theta}}(t) = u(t) \,, \tag{5.11}$$

where u is the ESC law to be designed as

$$u(t) = K \hat{G}(t) \,, \quad \forall t \geq 0 \,. \tag{5.12}$$

By taking the time-derivative of (5.10) and the equation (5.11), one gets

$$\dot{\hat{G}}(t) = \frac{a^2 H^*}{2}\left(1-\cos\left(2\omega t\right)\right)u(t) + a^2\omega H^* \sin\left(2\omega t\right)\tilde{\theta}(t) + \left(a\omega Q^* + \frac{3a^2\omega H^*}{8}\right)\cos\left(\omega t\right) - \frac{3a^2\omega H^*}{8}\cos\left(3\omega t\right) . \tag{5.13}$$

5.1.3 Event-Triggered Control Emulation of the Extremum Seeking Design

Let t_k denote the unbounded monotonically increasing sequence of time, *i.e.*,

$$0 = t_0 < t_1 < \ldots < t_k < \ldots , \quad k \in \mathbb{Z}^+ , \lim_{k\to\infty} t_k = \infty , \tag{5.14}$$

with the aperiodic sampling intervals $\tau_k = t_{k+1} - t_k > 0$.

We consider continuous measurement of the system output while actuating the system using an event-based approach. The actuator transforms the discrete-time control input $U(t_k)$ to a continuous control input $u(t)$ as in sampled data systems with zero-order hold. By assuming that there is no delay in the Sensor-to-Controller and Controller-to-Actuator branches, one has

$$u(t) = U_k = U(t_k) , \quad t \in \ [t_k , t_{k+1}[, \quad k \in \mathbb{Z}^+ . \tag{5.15}$$

Thus, define the control input for all $t \in [t_k , t_{k+1}[$, $k \in \mathbb{N}$,

$$u_k = K\hat{G}(t_k) , \tag{5.16}$$

and we introduce the error vector

$$e(t) := \hat{G}(t_k) - \hat{G}(t) , \quad \forall t \in [t_k , t_{k+1}[, \quad k \in \mathbb{N} . \tag{5.17}$$

Therefore, by using the event-triggered control law (5.16), adding and subtracting the term $\frac{a^2 H^* K}{2}\left(1-\cos\left(2\omega t\right)\right)\hat{G}(t)$ into (5.13) and adding and subtracting the term $K\hat{G}(t)$ into (5.11), one arrives at the Input-to-State Stable (ISS) representation of

the dynamics of $\hat{G}(t)$ and $\tilde{\theta}$ with respect to the error vector $e(t)$ in equation (5.17):

$$\begin{aligned}\dot{\hat{G}}(t)=&\frac{a^2H^*K}{2}\left(1-\cos\left(2\omega t\right)\right)\hat{G}(t)+\frac{a^2H^*K}{2}\left(1-\cos\left(2\omega t\right)\right)e(t)+\\&-\frac{3a^2\omega H^*}{8}\cos\left(3\omega t\right)+a^2\omega H^*\sin\left(2\omega t\right)\tilde{\theta}(t)+\left(a\omega Q^*+\frac{3a^2\omega H^*}{8}\right)\cos\left(\omega t\right)\,,\end{aligned} \tag{5.18}$$

$$\begin{aligned}\dot{e}(t)=&-\frac{a^2H^*K}{2}\left(1-\cos\left(2\omega t\right)\right)\hat{G}(t)-\frac{a^2H^*K}{2}\left(1-\cos\left(2\omega t\right)\right)e(t)+\\&+\frac{3a^2\omega H^*}{8}\cos\left(3\omega t\right)-a^2\omega H^*\sin\left(2\omega t\right)\tilde{\theta}(t)-\left(a\omega Q^*+\frac{3a^2\omega H^*}{8}\right)\cos\left(\omega t\right)\,,\end{aligned} \tag{5.19}$$

$$\begin{aligned}\dot{\tilde{\theta}}(t)=&K\hat{G}(t_k)+K\hat{G}(t)-K\hat{G}(t)=K\hat{G}(t)+K\left[\hat{G}(t_k)-\hat{G}(t)\right]\\=&\frac{a^2H^*K}{2}\left(1-\cos\left(2\omega t\right)\right)\tilde{\theta}(t)+Ke(t)+\left(aQ^*K+\frac{3a^3H^*K}{8}\right)\sin\left(\omega t\right)+\\&-\frac{a^3H^*K}{8}\sin\left(3\omega t\right)\,.\end{aligned} \tag{5.20}$$

In a conventional sampled-data implementation, the transmission times are distributed equidistantly in time, meaning that $t_{k+1}=t_k+h$, for all k , and some interval $h>0$. In event-triggered control, however, these transmission are orchestrated by a monitoring mechanism that invokes transmissions when the difference between the current value of the output and its previously transmitted value becomes too large in an appropriate sense [69]. In the subsequent sections, the execution mechanism is analyzed.

5.1.4 Dynamic Event Triggering Condition

In Definition 5 our dynamic-triggering strategy is presented.

Definition 5 (Dynamic Triggering Condition)**.** *Consider the quadratic mapping*

$$\Xi(\hat{G},e)=a^2|H^*||K|\left[\sigma\hat{G}^2(t)+\hat{G}(t)e(t)\right]\,, \tag{5.21}$$

where $\sigma\in(0,1)$, H^* is the Hessian, K be control gain in (5.16) and $\upsilon(t)$ as the solution of the dynamics

$$\dot{\upsilon}(t)=-\mu\upsilon(t)+\Xi(\hat{G},e)\,,\mu>0\,,\upsilon(0)\geq 0\,. \tag{5.22}$$

The event-triggered controller with dynamic-triggering condition consists of two components:

1. *A set of increasing sequence of time $I=\{t_0\,,t_1\,,t_2\,,\ldots\}$ with $t_0=0$ generated*

under the following rule:

- *If* $\left\{t\in\mathbb{R}^+ : t > t_k \wedge \upsilon(t)+\gamma\Xi(\hat{G},e)<0 = \emptyset\right\}$, *then the set of the times of the events is* $I = \{t_0\,, t_1\,, \ldots, t_k\}$.
- *If* $\left\{t\in\mathbb{R}^+ : t > t_k \wedge \upsilon(t)+\gamma\Xi(\hat{G},e)<0 \neq \emptyset\right\}$, *next event time is given by*

$$t_{k+1} = \inf\left\{t\in\mathbb{R}^+ : t > t_k \wedge \upsilon(t)+\gamma\Xi(\hat{G},e)<0\right\}, \tag{5.23}$$

which is the dynamic event-trigger mechanism.

2. *A feedback control action updated at the generated triggering instants given by*

$$u_k = K\hat{G}(t_k)\,, \tag{5.24}$$

for all $t \in [t_k\,, t_{k+1})$, $k \in \mathbb{N}$.

5.2 Closed-Loop System

5.2.1 Time-scaling System

By using the transformation $\bar{t} = \omega t$ where

$$\omega := \frac{2\pi}{T}\,, \tag{5.25}$$

it is possible to rewrite the dynamics (5.18)–(5.20) in a different time-scale such that

$$\frac{d\hat{G}(\bar{t})}{d\bar{t}} = \frac{1}{\omega}\hat{\mathcal{G}}\left(\bar{t}, \hat{G}, \tilde{\theta}, \upsilon, \frac{1}{\omega}\right)\,, \tag{5.26}$$

$$\frac{d\tilde{\theta}(\bar{t})}{d\bar{t}} = \frac{1}{\omega}\tilde{\Theta}\left(\bar{t}, \hat{G}, \tilde{\theta}, \upsilon, \frac{1}{\omega}\right)\,, \tag{5.27}$$

$$\frac{d\upsilon(\bar{t})}{d\bar{t}} = \frac{1}{\omega}\Upsilon\left(\bar{t}, \hat{G}, \tilde{\theta}, \upsilon, \frac{1}{\omega}\right)\,, \tag{5.28}$$

with

$$\hat{\mathcal{G}}\left(\bar{t},\hat{G},\tilde{\theta},\upsilon,\frac{1}{\omega}\right)=\frac{a^2H^*K}{2}\left(1-\cos\left(2\omega t\right)\right)\hat{G}(t) + \frac{a^2H^*K}{2}\left(1-\cos\left(2\omega t\right)\right)e(t)-\frac{3a^2\omega H^*}{8}\cos\left(3\omega t\right) + a^2\omega H^*\sin\left(2\omega t\right)\tilde{\theta}(t)+\left(a\omega Q^*+\frac{3a^2\omega H^*}{8}\right)\cos\left(\omega t\right)\,, \quad (5.29)$$

$$\tilde{\Theta}\left(\bar{t},\hat{G},\tilde{\theta},\upsilon,\frac{1}{\omega}\right)=\frac{a^2H^*K}{2}\left(1-\cos\left(2\omega t\right)\right)\tilde{\theta}(t)+Ke(t) + \left(aQ^*K+\frac{3a^3H^*K}{8}\right)\sin\left(\omega t\right)-\frac{a^3H^*K}{8}\sin\left(3\omega t\right)\,, \quad (5.30)$$

$$\Upsilon\left(\bar{t},\hat{G},\tilde{\theta},\upsilon,\frac{1}{\omega}\right)=-\mu\upsilon(t)+\Xi(\hat{G},e)\,. \quad (5.31)$$

An appropriate average system in the time-scale $\bar{t}$ can be derived in the next Section.

5.2.2 Average System

Now, by defining the augmented state

$$X^T(\bar{t}):=\left[\hat{G}(\bar{t})\,,\tilde{\theta}(\bar{t})\,,\upsilon(\bar{t})\right]\,, \quad (5.32)$$

one arrives at the dynamics

$$\frac{dX(\bar{t})}{d\bar{t}}=\frac{1}{\omega}\mathcal{F}\left(\bar{t},X,\frac{1}{\omega}\right)\,, \quad (5.33)$$

$$\mathcal{F}^T=\left[\hat{\mathcal{G}}\,,\tilde{\Theta}\,,\Upsilon\right]\,. \quad (5.34)$$

Due to the discontinuous nature of the proposed control strategy, throughout the article the averaging theory for discontinuous systems is used, as presented by [103].

The augmented system (5.33) has a small parameter $1/\omega$ as well as a T-periodic function $\mathcal{F}\left(\bar{t},X,\frac{1}{\omega}\right)$ in $\bar{t}$, hence it admits the averaging method for stability analysis

by averaging $\mathcal{F}\left(\bar{t}, X, \frac{1}{\omega}\right)$ at $\lim_{\omega\to\infty}\frac{1}{\omega}=0$, as shown in [103], *i.e.*,

$$\frac{dX_{\rm av}(\bar{t})}{d\bar{t}} = \frac{1}{\omega}\mathcal{F}_{\rm av}\left(X_{\rm av}\right)\,, \tag{5.35}$$

$$\mathcal{F}_{\rm av}\left(X_{\rm av}\right) = \frac{1}{T}\int_0^T \mathcal{F}\left(\delta, X_{\rm av}, 0\right) d\delta\,. \tag{5.36}$$

Basically, the problem in the averaging method is to determine in what sense the behavior of the autonomous system (5.35) approximates the behavior of the nonautonomous system (5.33) such that (5.33) can be represented as a perturbation of system (5.35).

Therefore, treating the states $\hat{G}(\bar{t})$, $e(\bar{t})$ and $\tilde{\theta}(\bar{t})$ as constants in (5.18), and using the averaging values, one gets

$$\frac{d\hat{G}_{\rm av}(\bar{t})}{d\bar{t}} = \frac{a^2H^*K}{2\omega}\hat{G}_{\rm av}(\bar{t}) + \frac{a^2H^*K}{2\omega}e_{\rm av}(\bar{t})\,, \tag{5.37}$$

$$e_{\rm av}(\bar{t}) = \hat{G}_{\rm av}(\bar{t}_k) - \hat{G}_{\rm av}(\bar{t})\,. \tag{5.38}$$

Hence, from (5.37) it is easy to verify the ISS relations of $\hat{G}_{\rm av}(\bar{t})$ with respect to the averaged measurement error $e_{\rm av}(\bar{t})$.

Moreover, from (5.10), one has

$$\hat{G}_{\rm av}(\bar{t}) = \frac{a^2H^*}{2}\tilde{\theta}_{\rm av}(\bar{t})\,, \tag{5.39}$$

and, consequently,

$$\tilde{\theta}_{\rm av}(\bar{t}) = \frac{2}{a^2H^*}\hat{G}_{\rm av}(\bar{t})\,, \tag{5.40}$$

with time-derivative

$$\frac{d\tilde{\theta}_{\rm av}(\bar{t})}{d\bar{t}} = \frac{a^2H^*K}{2\omega}\tilde{\theta}_{\rm av}(\bar{t}) + \frac{1}{\omega}Ke_{\rm av}(\bar{t})\,. \tag{5.41}$$

Therefore, the following average event-triggered detection laws can be introduced for the average system.

Definition 6 (Average Dynamic Triggering Condition)**.** *Consider the quadratic matrix (5.21), where $\sigma\in(0,1)$, and K be the control gain in (5.16), $\gamma>0$ a positive constant and $\upsilon(t)$ the solution of the dynamics*

$$\frac{d\upsilon_{\rm av}(\bar{t})}{d\bar{t}} = -\frac{\mu}{\omega}\upsilon_{\rm av}(\bar{t}) + \frac{1}{\omega}\Xi(\hat{G}_{\rm av}, e_{\rm av})\,, \mu>0\,, \upsilon_{\rm av}(0)\geq 0\,, \tag{5.42}$$

where $\Xi(\hat{G}_{\text{av}}, e_{\text{av}}) = a^2|H^*||K|\left[\sigma\hat{G}^2_{\text{av}}(\bar{t}) + \hat{G}_{\text{av}}(\bar{t})e_{\text{av}}(\bar{t})\right]$. *The event-triggered controller with dynamic-triggering condition consists of two components:*

1. *A set of increasing sequence of time* $I = \{\bar{t}_0\,, \bar{t}_1\,, \bar{t}_2\,, \ldots\}$ *with* $\bar{t}_0 = 0$ *generated under the following rule:*

   - *If* $\left\{\bar{t} \in \mathbb{R}^+ : \bar{t} > \bar{t}_k \wedge \upsilon_{\text{av}}(\bar{t}) + \gamma\Xi(\hat{G}_{\text{av}}, e_{\text{av}}) < 0 = \emptyset\right\}$, *then the set of the times of the events is* $I = \{\bar{t}_0\,, \bar{t}_1\,, \ldots, \bar{t}_k\}$.
   - *If* $\left\{\bar{t} \in \mathbb{R}^+ : \bar{t} > \bar{t}_k \wedge \upsilon_{\text{av}}(\bar{t}) + \gamma\Xi(\hat{G}_{\text{av}}, e_{\text{av}}) < 0 \neq \emptyset\right\}$, *next event time is given as*

   $$\bar{t}_{k+1} = \inf\left\{\bar{t} \in \mathbb{R}^+ : \bar{t} > \bar{t}_k \wedge \upsilon_{\text{av}}(\bar{t}) + \gamma\Xi(\hat{G}_{\text{av}}, e_{\text{av}}) < 0\right\}, \tag{5.43}$$

   that is the average dynamic event-trigger mechanism.

2. *A feedback control action updated at the the generated triggering instants given as*

   $$u_k = K\hat{G}(\bar{t}_k)\,, \tag{5.44}$$

   for all $\bar{t} \in [\bar{t}_k\,, \bar{t}_{k+1})$, $k \in \mathbb{N}$.

5.3 Stability Analysis

Theorem 4. *Consider the closed-loop average dynamics of the gradient estimate (5.37) and the average event-triggered mechanism given by Definition 6. Suppose that Assumptions (A1)–(A5) hold. If the quadratic mapping* $\Xi(\hat{G}_{\text{av}}, e_{\text{av}})$ *is given by (5.21) and* ω *in (5.25) is a constant sufficiently large, the average gradient estimate system (5.37) with state* $\hat{G}_{av}(t)$ *is locally exponentially stable. Consequently,* $\tilde{\theta}_{av}(t)$ *converges exponentially to zero. Therefore, there exist constants* $m\,, M_\theta\,, M_y > 0$ *such that*

$$|\theta(t) - \theta^*| \leq M_\theta \exp(-mt) + \mathcal{O}\left(a + \frac{1}{\omega}\right)\,, \tag{5.45}$$

$$|y(t) - Q^*| \leq M_y \exp(-mt) + \mathcal{O}\left(a^2 + \frac{1}{\omega^2}\right)\,, \tag{5.46}$$

where $a > 0$, *and the constants* M_θ *and* M_y *depend on the initial condition* $\theta(0)$. *Moreover, there exists a lower bound* τ^* *for the inter-execution interval* $t_{k+1} - t_k$ *for all* $k \in \mathbb{N}$ *precluding the Zeno behavior.*

Proof. First, notice that the dynamic execution mechanism in (5.23) ensures, for all

$t \in [t_k\,, t_{k+1}[$,

$$\upsilon_{\rm av}(\bar{t}) + \gamma \Xi(\hat{G}_{\rm av}, e_{\rm av}) \geq 0\,, \tag{5.47}$$

therefore,

$$\Xi(\hat{G}_{\rm av}, e_{\rm av}) \geq -\frac{1}{\gamma}\upsilon_{\rm av}(\bar{t})\,. \tag{5.48}$$

Now, by using the inequality (5.48), the equation (5.42) can be lower bounded with

$$\begin{aligned}\frac{d\upsilon_{\rm av}(\bar{t})}{d\bar{t}} &= -\frac{\mu}{\omega}\upsilon_{\rm av}(\bar{t}) + \frac{1}{\omega}\Xi(\hat{G}_{\rm av}, e_{\rm av}) \\ &\geq -\frac{\mu}{\omega}\upsilon_{\rm av}(\bar{t}) - \frac{1}{\omega\gamma}\upsilon_{\rm av}(\bar{t}) = -\frac{1}{\omega}\left(\mu + \frac{1}{\gamma}\right)\upsilon_{\rm av}(\bar{t})\,.\end{aligned} \tag{5.49}$$

Invoking [94, Comparison Lemma, pp. 102], the solution $\hat{\upsilon}_{\rm av}(\bar{t})$ of the following first-order dynamics

$$\frac{d\hat{\upsilon}_{\rm av}(\bar{t})}{d\bar{t}} = -\frac{1}{\omega}\left(\mu + \frac{1}{\gamma}\right)\hat{\upsilon}_{\rm av}(\bar{t})\,, \quad \hat{\upsilon}_{\rm av}(0) = \upsilon_{\rm av}(0) > 0\,, \tag{5.50}$$

precisely,

$$\hat{\upsilon}_{\rm av}(\bar{t}) = \exp\left(-\frac{1}{\omega}\left(\mu + \frac{1}{\gamma}\right)\bar{t}\right)\hat{\upsilon}_{\rm av}(0) > 0\,, \quad \forall \bar{t} \geq 0\,, \tag{5.51}$$

is a lower bound for $\upsilon_{\rm av}(\bar{t})$. To verify this fact, notice that, from (5.49) and (5.50),

$$\frac{d(\upsilon_{\rm av}(\bar{t}) - \hat{\upsilon}_{\rm av}(\bar{t}))}{d\bar{t}} \geq -\frac{1}{\omega}\left(\mu + \frac{1}{\gamma}\right)(\upsilon_{\rm av}(\bar{t}) - \hat{\upsilon}_{\rm av}(\bar{t}))\,. \tag{5.52}$$

Thus,

$$\upsilon_{\rm av}(\bar{t}) - \hat{\upsilon}_{\rm av}(\bar{t}) \geq \exp\left(-\frac{1}{\omega}\left(\mu + \frac{1}{\gamma}\right)\bar{t}\right)\underbrace{(\upsilon_{\rm av}(0) - \hat{\upsilon}_{\rm av}(0))}_{=0} \tag{5.53}$$

and

$$\upsilon_{\rm av}(\bar{t}) \geq \hat{\upsilon}_{\rm av}(\bar{t}) > 0\,, \quad \forall \bar{t} \geq 0\,. \tag{5.54}$$

Now, since $\upsilon_{\rm av}(\bar{t}) > 0$, for all $\upsilon_{\rm av}(\bar{t}) \neq 0$, consider the following candidate to average Lyapunov function

$$V_{\rm av}(\bar{t}) = \hat{G}^2_{\rm av}(\bar{t}) + \upsilon_{\rm av}(\bar{t})\,, \tag{5.55}$$

with time-derivative

$$\frac{dV_{\rm av}(\bar{t})}{d\bar{t}} = -\frac{a^2|H^*||K|}{\omega}\hat{G}^2_{\rm av}(\bar{t}) - \frac{a^2|H^*||K|}{\omega}\hat{G}_{\rm av}(\bar{t})e_{\rm av}(\bar{t}) - \frac{\mu}{\omega}v_{\rm av}(\bar{t}) + \frac{1}{\omega}\Xi(\hat{G}_{\rm av}, e_{\rm av})\,. \tag{5.56}$$

Now, adding and subtracting the term $\sigma\frac{a^2|H^*||K|}{\omega}\hat{G}^2_{\rm av}(\bar{t})$ in equation (5.56), it is possible to rewrite it as

$$\begin{aligned}\frac{dV_{\rm av}(\bar{t})}{d\bar{t}} &= -\frac{(1-\sigma)a^2|H^*||K|}{\omega}\hat{G}^2_{\rm av}(\bar{t}) - \frac{1}{\omega}\Xi(\hat{G}_{\rm av}, e_{\rm av}) - \frac{\mu}{\omega}v_{\rm av}(\bar{t}) + \frac{1}{\omega}\Xi(\hat{G}_{\rm av}, e_{\rm av}) \\ &= -\frac{(1-\sigma)a^2|H^*||K|}{\omega}\hat{G}^2_{\rm av}(\bar{t}) - \frac{\mu}{\omega}v_{\rm av}(\bar{t})\,. \end{aligned} \tag{5.57}$$

By using (5.55), an upper bound for (5.57) is

$$\frac{dV_{\rm av}(\bar{t})}{d\bar{t}} \leq -\frac{1}{\omega}\min\left\{(1-\sigma)a^2|H^*||K|, \mu\right\}V_{\rm av}(\bar{t})\,. \tag{5.58}$$

Then, invoking the Comparison Lemma [94] an upper bound $\bar{V}_{\rm av}(\bar{t})$ for $V_{\rm av}(\bar{t})$ is

$$V_{\rm av}(\bar{t}) \leq \bar{V}_{\rm av}(\bar{t})\,, \quad \forall \bar{t} \in [\bar{t}_k, \bar{t}_{k+1})\,. \tag{5.59}$$

given by the solution of the following dynamics

$$\frac{d\bar{V}_{\rm av}(\bar{t})}{d\bar{t}} = -\frac{1}{\omega}\min\left\{(1-\sigma)a^2|H^*||K|, \mu\right\}\bar{V}_{\rm av}(\bar{t}), \quad \bar{V}_{\rm av}(\bar{t}_k) = V_{\rm av}(\bar{t}_k)\,, \tag{5.60}$$

In other words, $\forall \bar{t} \in [\bar{t}_k, \bar{t}_{k+1})$,

$$\bar{V}_{\rm av}(\bar{t}) = \exp\left(-\frac{1}{\omega}\min\left\{(1-\sigma)a^2|H^*||K|, \mu\right\}(\bar{t}-\bar{t}_k)\right)V_{\rm av}(\bar{t}_k)\,, \tag{5.61}$$

and the inequality (5.59) is rewritten as

$$V_{\rm av}(\bar{t}) \leq \exp\left(-\frac{1}{\omega}\min\left\{(1-\sigma)a^2|H^*||K|, \mu\right\}(\bar{t}-\bar{t}_k)\right)V_{\rm av}(\bar{t}_k)\,. \tag{5.62}$$

By defining, $\bar{t}_k^+$ and $\bar{t}_k^-$ as the right and left limits of $\bar{t} = \bar{t}_k$, respectively, it easy to verify that $V_{\rm av}(\bar{t}_{k+1}^-) \leq \exp\left(-\frac{1}{\omega}\min\left\{(1-\sigma)a^2|H^*||K|, \mu\right\}(\bar{t}_{k+1}^- - \bar{t}_k^+)\right)V_{\rm av}(\bar{t}_k^+)$. Since $V_{\rm av}(\bar{t})$ is continuous, $V_{\rm av}(\bar{t}_{k+1}^-) = V_{\rm av}(\bar{t}_{k+1})$ and $V_{\rm av}(\bar{t}_k^+) = V_{\rm av}(\bar{t}_k)$, and therefore,

$$V_{\rm av}(\bar{t}_{k+1}) \leq \exp\left(-\frac{1}{\omega}\min\left\{(1-\sigma)a^2|H^*||K|, \mu\right\}(\bar{t}_{k+1}-\bar{t}_k)\right)V_{\rm av}(\bar{t}_k)\,. \tag{5.63}$$

Hence, for any $\bar{t} \geq 0$ in $\bar{t} \in [\bar{t}_k, \bar{t}_{k+1})$, $k \in \mathbb{N}$, one has

$$\begin{aligned}
V_{\mathrm{av}}(\bar{t}) &\leq \exp\left(-\frac{1}{\omega}\min\left\{(1-\sigma)a^2|H^*||K|,\mu\right\}(\bar{t}-\bar{t}_k)\right)V_{\mathrm{av}}(\bar{t}_k) \\
&\leq \exp\left(-\frac{1}{\omega}\min\left\{(1-\sigma)a^2|H^*||K|,\mu\right\}(\bar{t}-\bar{t}_k)\right)\times \\
&\quad\times\exp\left(-\frac{1}{\omega}\min\left\{(1-\sigma)a^2|H^*||K|,\mu\right\}(\bar{t}_k-\bar{t}_{k-1})\right)V_{\mathrm{av}}(\bar{t}_{k-1}) \\
&\leq \ldots \leq \\
&\leq \exp\left(-\frac{1}{\omega}\min\left\{(1-\sigma)a^2|H^*||K|,\mu\right\}(\bar{t}-\bar{t}_k)\right)\times \\
&\quad\times\prod_{i=1}^{i=k}\exp\left(-\frac{1}{\omega}\min\left\{(1-\sigma)a^2|H^*||K|,\mu\right\}\right)V_{\mathrm{av}}(\bar{t}_{i-1}) \\
&= \exp\left(-\frac{1}{\omega}\min\left\{(1-\sigma)a^2|H^*||K|,\mu\right\}\bar{t}\right)V_{\mathrm{av}}(0)\,. \qquad (5.64)
\end{aligned}$$

Now, one obtains

$$\hat{G}^2_{\mathrm{av}}(\bar{t}) \leq V_{\mathrm{av}}(\bar{t}) = \hat{G}^2_{\mathrm{av}}(\bar{t}) + \upsilon_{\mathrm{av}}(\bar{t}) \qquad (5.65)$$

$$\leq \bar{V}_{\mathrm{av}}(\bar{t}) = \exp\left(-\frac{\min\left\{(1-\sigma)a^2|H^*||K|,\mu\right\}}{\omega}\bar{t}\right)\left(\hat{G}^2_{\mathrm{av}}(0)+\upsilon_{\mathrm{av}}(0)\right)\,. \qquad (5.66)$$

Since there exists a positive scalar κ such that

$$\upsilon_{\mathrm{av}}(0) \leq \kappa\hat{G}^2_{\mathrm{av}}(0)\,, \qquad (5.67)$$

it is possible to write

$$\hat{G}^2_{\mathrm{av}}(\bar{t}) \leq \exp\left(-\frac{\min\left\{(1-\sigma)a^2|H^*||K|,\mu\right\}}{\omega}\bar{t}\right)(1+\kappa)\,\hat{G}^2_{\mathrm{av}}(0)\,. \qquad (5.68)$$

Hence,

$$|\hat{G}_{\mathrm{av}}(\bar{t})| \leq \exp\left(-\frac{\min\left\{(1-\sigma)a^2|H^*||K|,\mu\right\}}{2\omega}\bar{t}\right)\sqrt{(1+\kappa)}|\hat{G}_{\mathrm{av}}(0)|\,. \qquad (5.69)$$

Since (5.18) is T-periodic in t, $1/\omega$ is a small positive parameter, and, from inequality (5.69) the origin $\hat{G}_{\mathrm{av}} = 0$ is at least an exponentially stable equilibrium point of the closed-loop event-triggered system, then, by invoking [103, Theorem 2], there exists

an upper bound for (5.10) such that

$$\begin{aligned}|\hat{G}(t)| &\leq |\hat{G}_{\text{av}}(t)| + \mathcal{O}\left(\frac{1}{\omega}\right) \\ &\leq \exp\left(-\frac{\min\left\{(1-\sigma)a^2|H^*||K|,\mu\right\}}{2}t\right)\sqrt{(1+\kappa)}|\hat{G}_{\text{av}}(0)| + \mathcal{O}\left(\frac{1}{\omega}\right). \end{aligned} \tag{5.70}$$

Although the analysis has been focused on the convergence of $\hat{G}_{\text{av}}(\bar{t})$ and, consequently $\hat{G}(t)$, the obtained results through (5.70) can be easily extended to the variable $\tilde{\theta}_{\text{av}}(\bar{t})$ and $\tilde{\theta}(t)$. Notice that, by using (5.39) and the inequality (5.69), one has

$$|\tilde{\theta}_{\text{av}}(\bar{t})| \leq \exp\left(-\frac{\min\left\{(1-\sigma)a^2|H^*||K|,\mu\right\}}{2\omega}\bar{t}\right)\sqrt{(1+\kappa)}|\tilde{\theta}_{\text{av}}(0)|\,, \tag{5.71}$$

and by invoking [103, Theorem 2], one has

$$|\tilde{\theta}(t)| \leq \exp\left(-\frac{\min\left\{(1-\sigma)a^2|H^*||K|,\mu\right\}}{2}t\right)\sqrt{(1+\kappa)}|\tilde{\theta}_{\text{av}}(0)| + \mathcal{O}\left(\frac{1}{\omega}\right). \tag{5.72}$$

Now, from (5.7), we have

$$\theta(t) - \theta^* = \tilde{\theta}(t) + a\sin(\omega t)\,, \tag{5.73}$$

whose its norm satisfies

$$\begin{aligned}|\theta(t) - \theta^*| &= |\tilde{\theta}(t) + S(t)| \\ &\leq |\tilde{\theta}(t)| + |a\sin(\omega t)| \\ &\leq \exp\left(-\frac{\min\left\{(1-\sigma)a^2|H^*||K|,\mu\right\}}{2}t\right)\sqrt{(1+\kappa)}|\theta(0) - \theta^*| + \mathcal{O}\left(a + \frac{1}{\omega}\right). \end{aligned} \tag{5.74}$$

Defining the error variable $\tilde{y}(t)$ as

$$\tilde{y}(t) := y(t) - Q^*\,, \tag{5.75}$$

and using (5.3) as well as the Cauchy-Schwarz Inequality [105], its absolute value satisfies

$$|\tilde{y}(t)| = |y(t) - Q^*| = |H^*||\theta(t) - \theta^*|^2\,, \tag{5.76}$$

and its upper bounded with (5.74)is given by

$$|y(t)-Q^*| \leq \exp\left(-\frac{\min\left\{(1-\sigma)a^2|H^*||K|,\mu\right\}}{2}t\right)|H^*|\times \\ \times\left[(1+\kappa)|\theta(0)-\theta^*|+2\left(a+\frac{1}{\omega}\right)\right]|\theta(0)-\theta^*|+\mathcal{O}\left(a^2+\frac{1}{\omega^2}\right). \quad (5.77)$$

Therefore, by defining the positive constants

$$m=\frac{\min\left\{(1-\sigma)a^2|H^*||K|,\mu\right\}}{2}, \quad (5.78)$$

$$M_\theta=|\theta(0)-\theta^*|, \quad (5.79)$$

$$M_y=\left[|\theta(0)-\theta^*|+2\left(a+\frac{1}{\omega}\right)\right]|\theta(0)-\theta^*|, \quad (5.80)$$

the inequalities (5.74) and (5.77) satisfy (5.45) and (5.46), respectively.

Notice that, from (5.43) and by using the Peter-Paul inequality [106], we can write $cd \leq \frac{c^2}{2\epsilon}+\frac{\epsilon d^2}{2}$, for all $c,d,\epsilon>0$, with $c=|e_{\rm av}(\bar{t})|$, $d=|\hat{G}_{\rm av}(\bar{t})|$ and $\epsilon=\sigma$, for all $\bar{t}\in[t_k\,,t_{k+1}[$, the following lower bound is verified

$$\begin{aligned}
&\upsilon_{\rm av}(\bar{t})+\gamma a^2|H^*||K|\left[\sigma\hat{G}^2_{\rm av}(\bar{t})+e_{\rm av}(\bar{t})\hat{G}_{\rm av}(\bar{t})\right]\\
&\geq \upsilon_{\rm av}(\bar{t})+\gamma a^2|H^*||K|\left[\sigma\hat{G}^2_{\rm av}(\bar{t})-|e_{\rm av}(\bar{t})||\hat{G}_{\rm av}(\bar{t})|\right]\\
&\geq \upsilon_{\rm av}(\bar{t})+\gamma a^2|H^*||K|\sigma\hat{G}^2_{\rm av}(\bar{t})+\\
&\quad-\frac{\gamma a^2|H^*||K|}{2}\left(\sigma\hat{G}^2_{\rm av}(\bar{t})+\frac{1}{\sigma}e^2_{\rm av}(\bar{t})\right)\\
&=\upsilon_{\rm av}(\bar{t})+\gamma\left(q\|\hat{G}_{\rm av}(\bar{t})\|^2-p\|e_{\rm av}(\bar{t})\|^2\right), \quad (5.81)
\end{aligned}$$

where

$$q=\frac{\gamma a^2|H^*||K|\sigma}{2} \quad \text{and} \quad p=\frac{\gamma a^2|H^*||K|}{2\sigma}. \quad (5.82)$$

In [107], it is shown that a lower bound for the inter-execution interval is given by the time duration it takes for the function

$$\phi(\bar{t})=\frac{\sqrt{\gamma p}|e_{\rm av}(\bar{t})|}{\sqrt{\upsilon_{\rm av}(\bar{t})+\gamma q|\hat{G}_{\rm av}(\bar{t})|^2}}, \quad (5.83)$$

to go from 0 to 1. The derivative of $\phi(\bar{t})$ in (5.83) is given by

$$\frac{d\phi(\bar{t})}{d\bar{t}} = \frac{\sqrt{\gamma p} e_{\rm av}(\bar{t}) \dfrac{de_{\rm av}(\bar{t})}{d\bar{t}}}{|e_{\rm av}(\bar{t})| \sqrt{\upsilon_{\rm av}(\bar{t}) + \gamma q |\hat{G}_{\rm av}(\bar{t})|^2}} + \\ - \frac{\sqrt{\gamma p} |e_{\rm av}(\bar{t})|}{2(\upsilon_{\rm av}(\bar{t}) + \gamma q |\hat{G}_{\rm av}(\bar{t})|^2)^{3/2}} \left(\frac{d\upsilon_{\rm av}(\bar{t})}{d\bar{t}} + \gamma q \hat{G}_{\rm av}(\bar{t}) \frac{d\hat{G}_{\rm av}(\bar{t})}{d\bar{t}} \right), \tag{5.84}$$

and satisfies the inequality

$$\frac{d\phi(\bar{t})}{d\bar{t}} \leq \frac{a^2|H^*||K|}{2\omega} \sqrt{\frac{p}{q}} + \frac{a^2|H^*||K|}{2\omega} \phi(\bar{t}) + \frac{1}{2\omega\gamma} \phi^3(\bar{t}) + \frac{a^2|H^*||K|}{2\omega} \sqrt{\frac{q}{p}} \phi^2(\bar{t}) + \\ + \frac{\mu}{2\omega} \phi(\bar{t}) + \frac{\gamma q |\hat{G}_{\rm av}(\bar{t})|^2}{2\omega(\upsilon_{\rm av}(\bar{t}) + \gamma q |\hat{G}_{\rm av}(\bar{t})|^2)} \left(-\mu - \frac{1}{\gamma} + 2 \frac{a^2|H^*||K|}{2} \right) \phi(\bar{t}) \,. \tag{5.85}$$

Hence, if $a^2|H^*||K| \leq \mu$, one has

$$\omega \frac{d\phi(\bar{t})}{d\bar{t}} \leq \frac{a^2|H^*||K|}{2} \left(\sqrt{\frac{p}{q}} + 2\phi(\bar{t}) + \sqrt{\frac{q}{p}} \phi^2(\bar{t}) \right). \tag{5.86}$$

By using the transformation $t = \frac{\bar{t}}{\omega}$, inequality (5.86) and invoking the Comparison Lemma [94], a lower bound for the inter-execution time is found as

$$\tau^* = \int_0^1 \frac{1}{b_0 + b_1\xi + b_2\xi^2 + b_3\xi^3} \, d\xi \,, \tag{5.87}$$

with $b_0 = \dfrac{a^2|H^*||K|}{2\sigma}$, $b_1 = a^2|H^*||K|$, $b_2 = \dfrac{a^2|H^*||K|\sigma}{2}$ and $b_3 = 0$.

If $a^2|H^*||K| > \mu$ and $\gamma \leq 1/(a^2|H^*||K| - \mu)$, inequality (5.85) is upper bounded by

$$\omega \frac{d\phi(\bar{t})}{d\bar{t}} \leq \frac{a^2|H^*||K|}{2} \sqrt{\frac{p}{q}} + \left(\frac{\mu}{2} + \frac{a^2|H^*||K|}{2} \right) \phi(\bar{t}) + \\ + \frac{a^2|H^*||K|}{2} \sqrt{\frac{q}{p}} \phi^2(\bar{t}) + \left(\frac{a^2|H^*||K|}{2} - \frac{\mu}{2} \right) \phi^3(\bar{t}) \,, \tag{5.88}$$

and the lower bound τ^* satisfies equation (5.87) with constants $b_0 = \dfrac{a^2|H^*||K|}{2\sigma}$, $b_1 = \dfrac{\mu + a^2|H^*||K|}{2}$, $b_2 = \dfrac{a^2|H^*||K|\sigma}{2}$ and $b_3 = \dfrac{a^2|H^*||K| - \mu}{2}$.

Finally, if $a^2|H^*||K| > \mu$ and $\gamma > 1/(a^2|H^*||K| - \mu)$, we obtain

$$\omega \frac{d\phi(\bar{t})}{d\bar{t}} \leq \frac{a^2|H^*||K|}{2} \sqrt{\frac{p}{q}} + \left(a^2|H^*||K| - \frac{1}{2\gamma} \right) \phi(\bar{t}) + \frac{a^2|H^*||K|}{2} \sqrt{\frac{q}{p}} \phi^2(\bar{t}) + \frac{1}{2\gamma} \phi^3(\bar{t}) \,, \tag{5.89}$$

and the lower bound τ^* satisfies the equation (5.87) with constants $b_0 = \dfrac{a^2|H^*||K|}{2\sigma}$, $b_1 = a^2|H^*||K| - \dfrac{1}{2\gamma}$, $b_2 = \dfrac{a^2|H^*||K|\sigma}{2}$ and $b_3 = \dfrac{1}{2\gamma}$.

Therefore, the Zeno behavior [107] is avoided which completes the proof. □

5.4 Simulation results

In order to highlight the main ideas of the proposed event-triggered extremum seeking strategy the nonlinear map (5.1) has input $\theta(t) \in \mathbb{R}$, output $y(t) \in \mathbb{R}$, Hessian $H = -1$ and unknown parameters $Q^* = 7$ and $\theta^* = 5$. The dither signals have parameters $a = 0.1$, $\omega = 3$ [rad/sec], and we have selected the event-triggered parameter $\sigma = 0.1$. The control gain matrix is $K = 30$ and the initial condition is $\hat{\theta}(0) = 10$.

In Figures 5.2(a), 5.2(b) and 5.2(c), the Gradient estimate, its sample and hold version and the error $e(t)$ are presented, respectively. The dynamic event-triggered mechanism ensures their convergence to zero. The Gradient stabilization implies reaching the optimizer θ^*, see Figures 5.2(g) and 5.2(h). Figures 5.2(e) and 5.2(f) show the aperiodic behavior of how often the control signal $U(t)$ is updated, see also Figure 5.2(d) for the control signal. During 300 seconds of simulation, there were 98 updates of the control signal, consequently, the average inter-execution interval was equal to 3.0612 seconds. Comparing the proposed strategy with the classic sample-hold implementation, assuming the same initial condition and a constant sampling period of $h = 0.01$ seconds, we would have 30,000 updates of the control signal during the simulation time. That is, a number more than 300 times higher than the strategy proposed in this chapter.

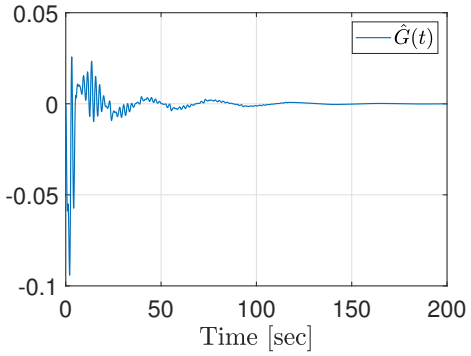

(a) Gradient estimate, $\hat{G}(t)$.

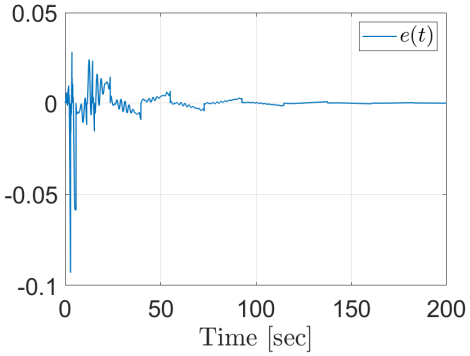

(b) Measurement error, $e(t)$.

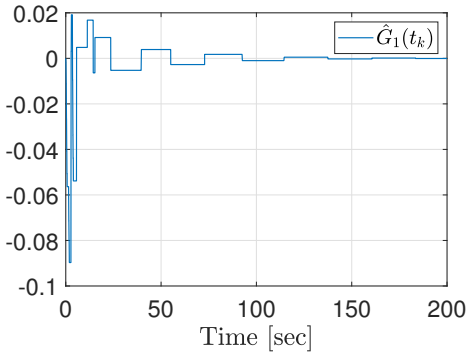

(c) Sample-and-Hold Gradient estimate, $\hat{G}(t_k)$.

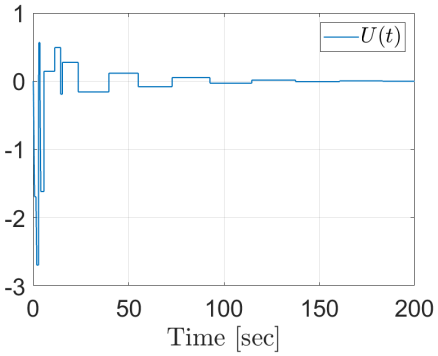

(d) Control input, $U(t)$.

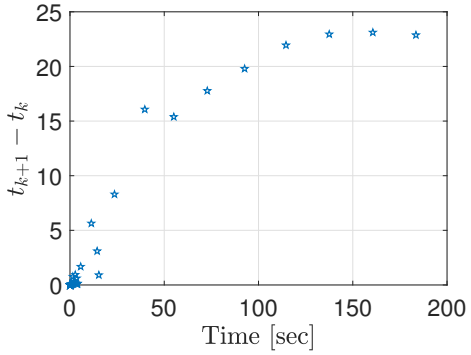

(e) Inter-execution intervals, $t_{k+1} - t_k$.

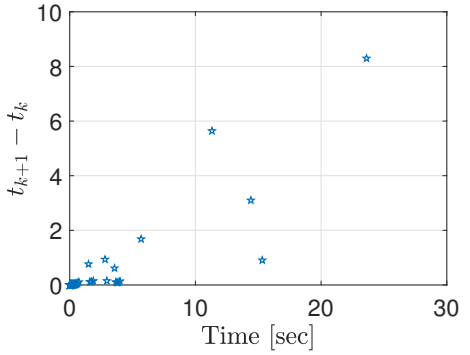

(f) Zoomed inter-execution intervals, $t_{k+1} - t_k$.

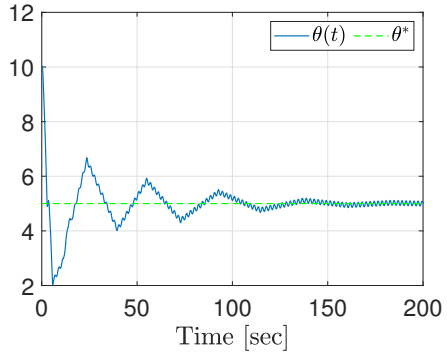

(g) Input of the nonlinear map, $\theta(t)$.

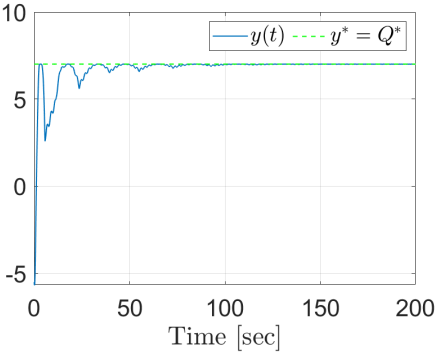

(h) Output of the nonlinear map, $y(t)$.

Figure 5.2: Event-triggered Extremum Seeking Control System.

Chapter 6

Multivariable Event-Triggered Extremum Seeking

Based on static maps, this chapter proposes an event-triggered scheme for multivariable extremum seeking control. Both static and dynamic triggering condition are developed. While the extremum seeking allows the output of a nonlinear map to be held within a vicinity of its extremum, the event-triggered strategy is responsible to execute the control task aperiodically by using a monitoring mechanism. The event-triggered strategy ensures asymptotic stability properties to the closed-loop system and reduces control effort since the control update and data communication only occur when a designed triggered-condition is satisfied. Integrating Lyapunov and averaging theories for discontinuous systems, a systematic design procedure and stability analysis are developed. Both event-based methods enable one to achieve an asymptotic stability result. Ultimately, the resulting closed-loop dynamics demonstrate the advantages of combining both approaches, namely, event-triggered and extremum seeking control. An illustration of the benefits of the new control method is presented using consistent simulation results, which compare the static and the dynamic triggering approaches.

6.1 Problem formulation

We define the following nonlinear static map

$$Q(\theta(t)) = Q^* + \frac{1}{2}(\theta(t) - \theta^*)^T H^* (\theta(t) - \theta^*)\,, \tag{6.1}$$

where $H^* = H^{*T} \in \mathbb{R}^{n\times n}$ is the Hessian matrix, $\theta^* \in \mathbb{R}^n$ is the unknown optimizer, $\theta(t) \in \mathbb{R}^n$ is the input map, designed as the real-time estimate $\hat{\theta}(t) \in \mathbb{R}^n$ of θ^*

additively perturbed by the vector $S(t)$ of sinusoids, *i.e.*,

$$\theta(t) = \hat{\theta}(t) + S(t)\,. \tag{6.2}$$

The output of the nonlinear map (6.1) can be written as $y(t) = Q(\theta(t))$. Fig. 6.1 shows the closed-loop structure of the event-triggered-based extremum seeking control system to be designed.

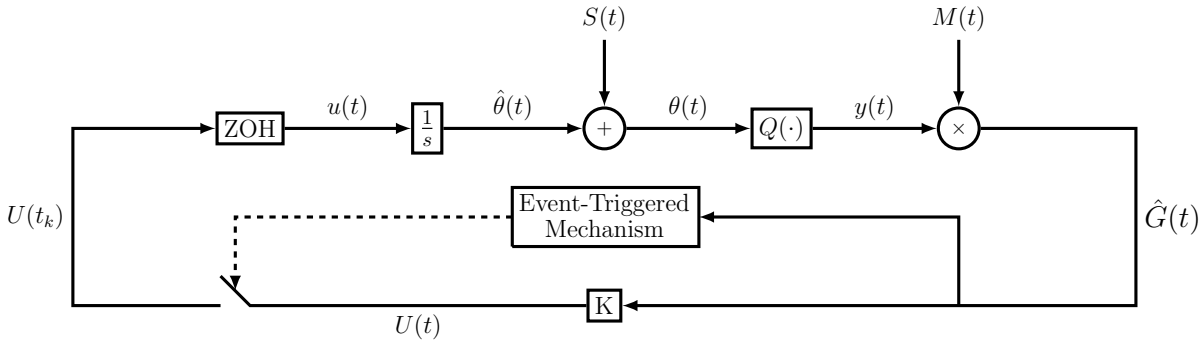

Figure 6.1: Event-triggered based on extremum seeking scheme.

The following assumptions are considered throughout the thesis.

Assumption 1. *The unique optimizer vector $\theta^* \in \mathbb{R}^n$, the Hessian matrix H^* and the scalar $Q^* \in \mathbb{R}$ are unknown parameters of the nonlinear map (6.1). Moreover, H^* is symmetric and has known definite sign, thus, being full rank.*

Assumption 2. *The matrix product H^*K is Hurwitz such that for any given $Q = Q^T > 0$ there exists a $P = P^T > 0$ that satisfies the Lyapunov equation*

$$K^T H^{*T} P + P H^* K = -Q\,. \tag{6.3}$$

Furthermore, the sum of the induced norms of the matrices $K^T H^{*T} P$ and $P H^* K$ is upper bounded by a known positive constant β,

$$\|K^T H^{*T} P\| + \|P H^* K\| \leq \beta\,, \tag{6.4}$$

and the least eigenvalue of the matrix Q is lower bounded by a known positive constant α,

$$\alpha \leq \lambda_{\min}(Q)\,. \tag{6.5}$$

6.1.1 Continuous-time Extremum Seeking

Let us define the estimation error

$$\tilde{\theta}(t) = \hat{\theta}(t) - \theta^* \,, \tag{6.6}$$

and the Gradient estimate by the demodulation

$$\hat{G}(t) = M(t)y(t) \,, \tag{6.7}$$

with dither vectors (see [51, 101])

$$S(t) = \left[a_1 \sin\left(\omega_1 t\right), \ldots, a_n \sin\left(\omega_n t\right)\right]^T \,, \tag{6.8}$$

$$M(t) = \left[\frac{2}{a_1}\sin\left(\omega_1 t\right), \ldots, \frac{2}{a_n}\sin\left(\omega_n t\right)\right]^T \,, \tag{6.9}$$

of nonzero amplitudes a_i. Moreover, the probing frequencies ω_i's can be selected as

$$\omega_i = \omega_i' \omega \,, \quad i \in \{1, \ldots, n\} \,, \tag{6.10}$$

where ω is a positive constant and ω_i' is a rational number.

Assumption 3. *The probing frequencies satisfy*

$$\omega_i' \notin \left\{\omega_j' \,,\ \frac{1}{2}(\omega_j' + \omega_k') \,,\ \omega_j' + 2\omega_k' \,,\ \omega_k' \pm \omega_l'\right\} \,, \tag{6.11}$$

for all i, j, k and l.

From (6.2) and (6.6), one has

$$\theta(t) = \tilde{\theta}(t) + S(t) + \theta^* \,, \tag{6.12}$$

and, therefore, by plugging (6.12) into (6.1), $y(t)$ can be written as

$$\begin{aligned} y(t) &= Q^* + \frac{1}{2}(\tilde{\theta}(t) + S(t))^T H^* (\tilde{\theta}(t) + S(t)) \\ &= Q^* + \frac{1}{2}\tilde{\theta}^T(t) H^* \tilde{\theta}(t) + S^T(t) H^* \tilde{\theta}(t) + \frac{1}{2} S^T(t) H^* S(t) \,. \end{aligned} \tag{6.13}$$

Thus, from (6.7), (6.13) and following [55], the gradient estimate in the average sense, is given by

$$\hat{G}(t) = M(t)Q^* + \frac{1}{2}M(t)\tilde{\theta}^T(t)H^*\tilde{\theta}(t) + M(t)S^T(t)H^*\tilde{\theta}(t) + \frac{1}{2}M(t)S^T(t)H^*S(t) \,. \tag{6.14}$$

Now, defining

$$\begin{aligned} H\left(t\right) &:= M(t)S^T(t)H^* \\ &= H^* + \Delta(t)H^*\,, \end{aligned} \tag{6.15}$$

where the elements of the $\Delta(t) \in \mathbb{R}^{n\times n}$ are given by

$$\Delta_{ii}(t) = -\cos(2\omega_i t)\,, \tag{6.16}$$

$$\begin{aligned} \Delta_{ij}(t) &= 2\frac{a_j}{a_i}\sin(\omega_i t)\sin(\omega_j t) \\ &= \frac{a_j}{a_i}\cos((\omega_i-\omega_j)t) - \frac{a_j}{a_i}\cos((\omega_i+\omega_j)t)\,, \end{aligned} \tag{6.17}$$

for all $i \neq j$, and using (6.15), one can rewrite (6.14) as follows

$$\hat{G}(t) = H(t)\tilde{\theta}(t) + M(t)Q^* + \frac{1}{2}H(t)S(t) + \vartheta(t)\,, \tag{6.18}$$

$$\vartheta(t) := \frac{1}{2}M(t)\tilde{\theta}^T(t)H^*\tilde{\theta}(t)\,. \tag{6.19}$$

The term $\vartheta(t)$ given above is quadratic in $\tilde{\theta}(t)$ and, therefore, may be neglected in a local analysis [102]. Thus, hereafter the gradient estimate is given by

$$\hat{G}(t) = H(t)\tilde{\theta}(t) + M(t)Q^* + \frac{1}{2}H(t)S(t)\,. \tag{6.20}$$

On the other hand, from the time-derivative of (6.6) and the ESC scheme depicted in Fig. 6.1, the dynamics that governs $\hat{\theta}(t)$, as well as $\tilde{\theta}(t)$, is given by

$$\dot{\tilde{\theta}}(t) = \dot{\hat{\theta}}(t) = u(t)\,, \tag{6.21}$$

where u is an ESC law to be designed.

By taking the time-derivative of (6.20), with the help of (6.15) and (6.21), one gets the following differential equation

$$\begin{aligned} \dot{\hat{G}}(t) &= f(t,\tilde{\theta}(t),u(t)) \\ &= H(t)u(t) + w(t,\tilde{\theta}(t))\,, \end{aligned} \tag{6.22}$$

where

$$w(t,\tilde{\theta}(t)) = \dot{\Delta}(t)H^*\tilde{\theta}(t) + \dot{M}(t)Q^* + \frac{1}{2}\dot{\Delta}(t)H^*S(t) + \frac{1}{2}H^*\dot{S}(t) + \frac{1}{2}\Delta(t)H^*\dot{S}(t)\,. \tag{6.23}$$

For all $t \geq 0$, the proposed continuous-time controller

$$u(t) = K\hat{G}(t)\,, \quad \forall t \geq 0 \tag{6.24}$$

where the controller gain K is such that H^*K is Hurwitz.

Our goal is to design a stabilizing controller for the closed-loop system (6.22) and (6.23) in a sampled and hold fashion by emulating the continuous-time control law (6.24). In the emulation approach the feedback control law (6.24) is first synthesized to stabilize the plant in the absence of network. Afterwards, the effect of network is considered and the sampling rule is constructed [108].

The control law is only updated for a given sequence of time instants $(t_k)_{k\in\mathbb{N}}$ defined by an event-generator that is constructed later on. More precisely, the execution of the control task is orchestrated by a monitoring mechanism that invokes control updates when the difference between the current value of the output and its previously computed value at time t_k becomes too large with respect to a constructed triggering condition that needs to be satisfied [69]. Note that in a conventional sampled-data implementation, the execution times are distributed equidistantly in time, meaning that $t_{k+1} = t_k + h$, where $h > 0$ is a known constant, for all $k \in \mathbb{N}$, while in event-triggered scheme aperiodic sampling may occur.

6.1.2 Emulation of the Continuous-Time Extremum Seeking Design

Defining the control input for all $t \in [t_k, t_{k+1}), k \in \mathbb{N}$ as

$$u_k = K\hat{G}(t_k)\,, \tag{6.25}$$

we introduce the error vector, that is to say the deviation of the output signal as

$$e(t) := \hat{G}(t_k) - \hat{G}(t)\,, \quad \forall t \in [t_k\,, t_{k+1})\,, \quad k \in \mathbb{N}\,. \tag{6.26}$$

Now, using the event-triggered control law (6.25), adding and subtracting the term $H(t)K\hat{G}(t)$ and $K\hat{G}(t)$ to (6.22) and (6.21), respectively, one arrives at the Input-to-State Stable (ISS) representation of (6.21) and (6.22) with respect to the error vector (6.26) and the time-varying disturbance $w(t, \tilde{\theta}(t))$. The resulting dynamics are given below:

$$\dot{\hat{G}}(t) = H(t)K\hat{G}(t) + H(t)Ke(t) + w(t, \tilde{\theta}(t))\,, \tag{6.27}$$

$$\dot{\tilde{\theta}}(t) = KH(t)\tilde{\theta}(t) + Ke(t) + KM(t)Q^* + \frac{1}{2}KH(t)S(t)\,. \tag{6.28}$$

In the subsequent developments, the static and dynamic triggering mechanisms, presented in Definitions 7 and 8, respectively.

6.1.3 Event-Triggered Control Mechanism

Definitions 7 and 8 show how the nonlinear mapping $\Xi : \mathbb{R}^n \times \mathbb{R}^n \mapsto \mathbb{R}$, given by

$$\Xi(\hat{G}, e) = \sigma\alpha\|\hat{G}(t)\|^2 - \beta\|e(t)\|\|\hat{G}(t)\|\,, \tag{6.29}$$

where, $\sigma \in (0, 1)$ is a given parameter, can be employed in the design of the static and dynamic execution mechanisms. The mapping $\Xi(\hat{G}, e)$ is designed to appropriately re-compute the control law (6.25) and update the ZOH actuator depicted in Fig. 6.1 such that the asymptotic stability of the closed-loop system is achieved [69].

Definition 7 (Multivariable Static Triggering Condition)**.** *Let $\Xi(\hat{G}, e)$ in (6.29) be the nonlinear mapping and K the control gain in (6.25). The event-triggered controller with static-triggering condition consists of two components:*

1. *A set of increasing sequence of time $I = \{t_0\,, t_1\,, t_2\,, \ldots\}$ with $t_0 = 0$ generated under the following rules:*
   - *If $\left\{t \in \mathbb{R}^+ : t > t_k \ \wedge\ \Xi(\hat{G}, e) < 0 = \emptyset\right\}$, then the set of the times of the events is $I = \{t_0\,, t_1\,, \ldots, t_k\}$.*
   - *If $\left\{t \in \mathbb{R}^+ : t > t_k \ \wedge\ \Xi(\hat{G}, e) < 0 \neq \emptyset\right\}$, next event time is given by*

$$t_{k+1} = \inf\left\{t \in \mathbb{R}^+ : t > t_k \ \wedge\ \Xi(\hat{G}, e) < 0\right\}\,, \tag{6.30}$$

   consisting of the static event-trigger mechanism.

2. *A feedback control action updated at the triggering instants (6.25).*

Although the aperiodicity of the control update is guaranteed by the static event generation mechanism (6.30), it is often convenient to use its filtered version to increase the inter-execution times. In this case, inspired by [107], we also construct a dynamic event-triggering mechanism described in the following definition.

Definition 8 (Multivariable Dynamic Triggering Condition)**.** *Let $\Xi(\hat{G}, e)$ in (6.29) be the nonlinear mapping and K the control gain in (6.25), $\gamma > 0$ a positive constant and $\upsilon(t)$ the solution of the dynamics*

$$\dot{\upsilon}(t) = -\mu\upsilon(t) + \Xi(\hat{G}, e)\,, \quad \mu > 0\,, \quad \upsilon(0) \geq 0\,. \tag{6.31}$$

The event-triggered controller with dynamic triggering condition consists of two components:

1. *A set of increasing sequence of time* $I = \{t_0\,, t_1\,, t_2\,, \ldots\}$ *with* $t_0 = 0$ *generated under the following rules:*

   - *If* $\left\{t \in \mathbb{R}^+ : t > t_k \ \wedge \ \upsilon(t) + \gamma\Xi(\hat{G}, e) < 0 = \emptyset\right\}$, *then the set of the times of the events is* $I = \{t_0\,, t_1\,, \ldots, t_k\}$.
   - *If* $\left\{t \in \mathbb{R}^+ : t > t_k \ \wedge \ \upsilon(t) + \gamma\Xi(\hat{G}, e) < 0 \neq \emptyset\right\}$, *next event time is given by*

$$t_{k+1} = \inf\left\{t \in \mathbb{R}^+ : t > t_k \ \wedge \ \upsilon(t) + \gamma\Xi(\hat{G}, e) < 0\right\}, \tag{6.32}$$

   which is the dynamic event-trigger mechanism.

2. *A feedback control action updated at the triggering instants (6.25).*

for all $t \in (t_j, t_{j+1})$, $\upsilon(t_0) = \upsilon(0) \geq 0$ *and* $\upsilon(t_j^-) = \upsilon(t_j) = \upsilon(t_j^+)$.

6.2 Closed-loop system

6.2.1 Time-scaling System

Now, we introduce a suitable time scale to carry out the stability analysis of the closed-loop system. From (6.10), one can notice that the dither frequencies (6.8) and (6.9), as well as their combinations (6.16) and (6.17), are both rational. Furthermore, there exists a time period T such that

$$T = 2\pi \times \mathrm{LCM}\left\{\frac{1}{\omega_i}\right\}\,, \quad \forall i\,\{1\,, 2\,, \ldots\,, n\}\,, \tag{6.33}$$

where LCM denotes the least common multiple such that it is possible to define the time-scale for the dynamics (6.27)–(6.28) with the transformation $\bar{t} = \omega t$, where

$$\omega := \frac{2\pi}{T}\,. \tag{6.34}$$

Hence, the system (6.27), (6.28) and (6.31) can be rewritten as

$$\frac{d\hat{G}(\bar{t})}{d\bar{t}} = \frac{1}{\omega}\hat{\mathcal{G}}\left(\bar{t}, \hat{G}, \tilde{\theta}, \upsilon, \frac{1}{\omega}\right)\,, \tag{6.35}$$

$$\frac{d\tilde{\theta}(\bar{t})}{d\bar{t}} = \frac{1}{\omega}\tilde{\Theta}\left(\bar{t}, \hat{G}, \tilde{\theta}, \upsilon, \frac{1}{\omega}\right)\,, \tag{6.36}$$

$$\frac{d\upsilon(\bar{t})}{d\bar{t}} = \frac{1}{\omega}\Upsilon\left(\bar{t}, \hat{G}, \tilde{\theta}, \upsilon, \frac{1}{\omega}\right)\,, \tag{6.37}$$

where

$$\hat{\mathcal{G}}\left(\bar{t},\hat{G},\tilde{\theta},\upsilon,\frac{1}{\omega}\right)=H(\bar{t})K\hat{G}(\bar{t})+H(\bar{t})Ke(\bar{t})+w(\bar{t},\tilde{\theta}(\bar{t}))\,, \tag{6.38}$$

$$\tilde{\Theta}\left(\bar{t},\hat{G},\tilde{\theta},\upsilon,\frac{1}{\omega}\right)=KH(\bar{t})\tilde{\theta}(\bar{t})+Ke(\bar{t})+KM(\bar{t})Q^{*}+\frac{1}{2}KH(\bar{t})S(\bar{t})\,, \tag{6.39}$$

and (6.31) as

$$\Upsilon\left(\bar{t},\hat{G},\tilde{\theta},\upsilon,\frac{1}{\omega}\right)=-\mu\upsilon(\bar{t})+\Xi(\hat{G},e)\,. \tag{6.40}$$

From the above dynamics, an appropriate averaging system in the new time-scale $\bar{t}$ can be introduced.

6.2.2 Average System

Defining the augmented state as follows

$$X^{T}(\bar{t}):=\left[\hat{G}^{T}(\bar{t})\,,\tilde{\theta}^{T}(\bar{t})\,,\upsilon(\bar{t})\right]\,, \tag{6.41}$$

the system (6.35)–(6.40) reduces to

$$\frac{dX(\bar{t})}{d\bar{t}}=\frac{1}{\omega}\mathcal{F}\left(\bar{t},X,\frac{1}{\omega}\right)\,, \tag{6.42}$$

where $\mathcal{F}^{T}=\left[\hat{\mathcal{G}}^{T}\,,\tilde{\Theta}^{T}\,,\Upsilon\right]$. Note that (6.42) is characterized by a small parameter $1/\omega$ as well as a T-periodic function $\mathcal{F}\left(\bar{t},X,\frac{1}{\omega}\right)$ in $\bar{t}$ and, thereby, the averaging method can be performed on $\mathcal{F}\left(\bar{t},X,\frac{1}{\omega}\right)$ at $\lim\limits_{\omega\to\infty}\frac{1}{\omega}=0$, as shown in references [94, 103]. The averaging method allows for determining in what sense the behavior of a constructed average autonomous system approximates the behavior of the non-autonomous system (6.42). By employing the averaging technique to (6.42), we derive the following average system

$$\frac{dX_{\mathrm{av}}(\bar{t})}{d\bar{t}}=\frac{1}{\omega}\mathcal{F}_{\mathrm{av}}\left(X_{\mathrm{av}}\right)\,, \tag{6.43}$$

$$\mathcal{F}_{\mathrm{av}}\left(X_{\mathrm{av}}\right)=\frac{1}{T}\int_{0}^{T}\mathcal{F}\left(\delta,X_{\mathrm{av}},0\right)d\delta\,, \tag{6.44}$$

where the averaging terms are given below

$$S_{\rm av}(\bar{t})=\frac{1}{T}\int_0^T S(\delta)d\delta=0\,,\dot{S}_{\rm av}(\bar{t})=\frac{1}{T}\int_0^T \dot{S}(\delta)d\delta=0\,, \tag{6.45}$$

$$M_{\rm av}(\bar{t})=\frac{1}{T}\int_0^T M(\delta)d\delta=0\,,\dot{M}_{\rm av}(\bar{t})=\frac{1}{T}\int_0^T \dot{M}(\delta)d\delta=0\,, \tag{6.46}$$

$$\Delta_{\rm av}(\bar{t})=\frac{1}{T}\int_0^T \Delta(\delta)d\delta=0\,,\dot{\Delta}_{\rm av}(\bar{t})=\frac{1}{T}\int_0^T \dot{\Delta}(\delta)d\delta=0\,, \tag{6.47}$$

and, consequently,

$$H_{\rm av}(\bar{t})=\frac{1}{T}\int_0^T H(\delta)d\delta=H^*\,,\dot{H}_{\rm av}(\bar{t})=\frac{1}{T}\int_0^T \dot{H}(\delta)d\delta=0\,. \tag{6.48}$$

Therefore, treating the states $\hat{G}(\bar{t})$, $e(\bar{t})$ and $\tilde{\theta}(\bar{t})$ as constants in (6.27) and (6.23), and by using the averaging values (6.45)–(6.48), one gets for all $\bar{t}\in[\bar{t}_k,\bar{t}_{k+1})$

$$\frac{d\hat{G}_{\rm av}(\bar{t})}{d\bar{t}}=\frac{1}{\omega}H^*K\hat{G}_{\rm av}(\bar{t})+\frac{1}{\omega}H^*Ke_{\rm av}(\bar{t})\,, \tag{6.49}$$

$$e_{\rm av}(\bar{t})=\hat{G}_{\rm av}(\bar{t}_k)-\hat{G}_{\rm av}(\bar{t})\,, \tag{6.50}$$

since the average value of $w(t,\tilde{\theta}(t))$ in (6.23) is

$$\begin{aligned} w_{\rm av}(\bar{t},\tilde{\theta}_{\rm av}(\bar{t}))&=\dot{\Delta}_{\rm av}(\bar{t})H^*\tilde{\theta}_{\rm av}(\bar{t})+\dot{M}_{\rm av}(\bar{t})Q^*+\frac{1}{2}\dot{\Delta}_{\rm av}(\bar{t})H^*S_{\rm av}(\bar{t})\\ &\quad+\frac{1}{2}H^*\dot{S}_{\rm av}(\bar{t})+\frac{1}{2}\Delta_{\rm av}(\bar{t})H^*\dot{S}_{\rm av}(\bar{t})\\ &=0\,. \end{aligned} \tag{6.51}$$

Hence, from (6.49) it is easy to verify the ISS relationship of $\hat{G}_{\rm av}(\bar{t})$ with respect to the averaged measurement error $e_{\rm av}(\bar{t})$ in (6.50).

Moreover, from (6.20), one has

$$\hat{G}_{\rm av}(\bar{t})=H^*\tilde{\theta}_{\rm av}(\bar{t})\,, \tag{6.52}$$

and, consequently,

$$\tilde{\theta}_{\rm av}(\bar{t})=H^{*-1}\hat{G}_{\rm av}(\bar{t})\,. \tag{6.53}$$

Taking the time-derivative of (6.53), we get

$$\frac{d\tilde{\theta}_{\rm av}(\bar{t})}{d\bar{t}}=\frac{1}{\omega}KH^*\tilde{\theta}_{\rm av}(\bar{t})+\frac{1}{\omega}Ke_{\rm av}(\bar{t})\,. \tag{6.54}$$

Therefore, the following average event-triggered detection laws can be introduced

for the average system.

Defining the average version of $\Xi(\hat{G}, e)$, *i.e.* as

$$\Xi(\hat{G}_{\rm av}, e_{\rm av}) = \sigma\alpha\|\hat{G}_{\rm av}(\bar{t})\|^2 - \beta\|e_{\rm av}(\bar{t})\|\|\hat{G}_{\rm av}(\bar{t})\|\,, \tag{6.55}$$

we construct the average event-triggered mechanisms.

Definition 9 (Multivariable Average Static Triggering Condition)**.** *Let $\Xi(\hat{G}_{\rm av}, e_{\rm av})$ in (6.55) be the nonlinear mapping and K the control gain in (6.25). The event-triggered controller with average static-triggering condition in the new time-scale consists of two components:*

1. *A set of increasing sequence of time $I = \{\bar{t}_0\,, \bar{t}_1\,, \bar{t}_2\,, \ldots\}$ with $\bar{t}_0 = 0$ generated under the following rule:*

   - *If $\left\{\bar{t} \in \mathbb{R}^+ : \bar{t} > \bar{t}_k \ \wedge\ \Xi(\hat{G}_{\rm av}, e_{\rm av}) < 0 = \emptyset\right\}$, then the set of the times of the events is $I = \{\bar{t}_0\,, \bar{t}_1\,, \ldots, \bar{t}_k\}$.*
   - *If $\left\{\bar{t} \in \mathbb{R}^+ : \bar{t} > \bar{t}_k \ \wedge\ \Xi(\hat{G}_{\rm av}, e_{\rm av}) < 0 \neq \emptyset\right\}$, next event time is given by*

   $$\bar{t}_{k+1} = \inf\left\{\bar{t} \in \mathbb{R}^+ : \bar{t} > \bar{t}_k \ \wedge\ \Xi(\hat{G}_{\rm av}, e_{\rm av}) < 0\right\}\,, \tag{6.56}$$

   which is the average static event-trigger mechanism.

2. *A feedback control action updated at the triggering instants:*

   $$u_k = K\hat{G}_{\rm av}(\bar{t}_k)\,, \tag{6.57}$$

   for all $\bar{t} \in [\bar{t}_k\,, \bar{t}_{k+1})$, $k \in \mathbb{N}$.

Definition 10 (Multivariable Average Dynamic Triggering Condition)**.** *Let $\Xi(\hat{G}_{\rm av}, e_{\rm av})$ in (6.55) be the nonlinear mapping and K the control gain in (6.25), $\mu > 0$ be a positive constant and $\upsilon_{\rm av}$ be the solution of the dynamics*

$$\frac{d\upsilon_{\rm av}(\bar{t})}{d\bar{t}} = -\frac{\mu}{\omega}\upsilon_{\rm av}(\bar{t}) + \frac{1}{\omega}\Xi(\hat{G}_{\rm av}, e_{\rm av})\,, \quad \mu > 0\,, \quad \upsilon(0) \geq 0\,. \tag{6.58}$$

Consequently, the event-triggered controller with dynamic-triggering condition consists of two components:

1. *A set of increasing sequence of time $I = \{\bar{t}_0\,, \bar{t}_1\,, \bar{t}_2\,, \ldots\}$ with $\bar{t}_0 = 0$ generated under the following rule:*

   - *If $\left\{\bar{t} \in \mathbb{R}^+ : \bar{t} > \bar{t}_k \ \wedge\ \upsilon_{\rm av}(\bar{t}) + \gamma\Xi(\hat{G}_{\rm av}, e_{\rm av}) < 0 = \emptyset\right\}$, then the set of the times of the events is $I = \{\bar{t}_0\,, \bar{t}_1\,, \ldots, \bar{t}_k\}$.*

- *If* $\left\{\bar{t} \in \mathbb{R}^+ : \bar{t} > \bar{t}_k \ \wedge \ \upsilon_{\text{av}}(\bar{t}) + \gamma\Xi(\hat{G}_{\text{av}}, e_{\text{av}}) < 0 \neq \emptyset\right\}$, *next event time is given by*

$$\bar{t}_{k+1} = \inf\left\{\bar{t} \in \mathbb{R}^+ : \bar{t} > \bar{t}_k \wedge \upsilon_{\text{av}}(\bar{t}) + \gamma\Xi(\hat{G}_{\text{av}}, e_{\text{av}}) < 0\right\}, \tag{6.59}$$

which is the average dynamic event-trigger mechanism.

2. A feedback control action updated at the triggering instants given by (6.57).

For all $\bar{t} \in (\bar{t}_j, \bar{t}_{j+1})$, $\upsilon_{\text{av}}(\bar{t}_0) = \upsilon_{\text{av}}(0)$ *and* $\upsilon_{\text{av}}(\bar{t}_j^-) = \upsilon_{\text{av}}(\bar{t}_j) = \upsilon_{\text{av}}(\bar{t}_j^+)$.

We claim that the two event-triggering mechanisms discussed above guarantee the asymptotic stabilization of $\hat{G}_{\text{av}}(\bar{t})$ and, consequently, that of $\tilde{\theta}_{\text{av}}(\bar{t})$. Since H^* is invertible, both $\hat{G}_{\text{av}}(\bar{t})$ and $\tilde{\theta}_{\text{av}}(\bar{t})$ converge to the origin according to the averaging theory [94].

Remark 1. *From the time-scaling relation* $\bar{t} = \omega t$, *where* ω *is a constant, the static and dynamic triggering mechanisms of the averaging and the original system are equivalent and only differ in the average sense.*

Next, the stability analysis will be carried out considering the static and dynamic event-triggering mechanisms. Note that, in both strategies it is considered the total lack of knowledge of the nonlinear map (6.1), *i.e.*, the Hessian H^*, the optimizer θ^* and the extremum Q^* are unknown parameters.

6.3 Static Event-Triggering in Extremum Seeking

6.3.1 Stability Analysis

Theorem 5 states the local asymptotic stability of the extremum seeking based on dynamic event-triggered execution mechanism shown in Fig. 6.2 is ensured.

Theorem 5. *Consider the closed-loop average dynamics of the gradient estimate (6.49) and (6.50) as well as the average static event-triggered mechanism given by Definition 9. Under Assumptions 1–3, and with the quadratic mapping* $\Xi(z_{\text{av}})$ *given by (6.55) and* $\omega > 0$ *defined in (6.34) is a sufficiently large, the average gradient estimate system (6.49) and (6.50) with state* $\hat{G}_{av}(t)$ *is locally exponentially stable. Consequently, the dynamics of* $\tilde{\theta}_{av}(t)$ *converges exponentially to zero. Therefore,*

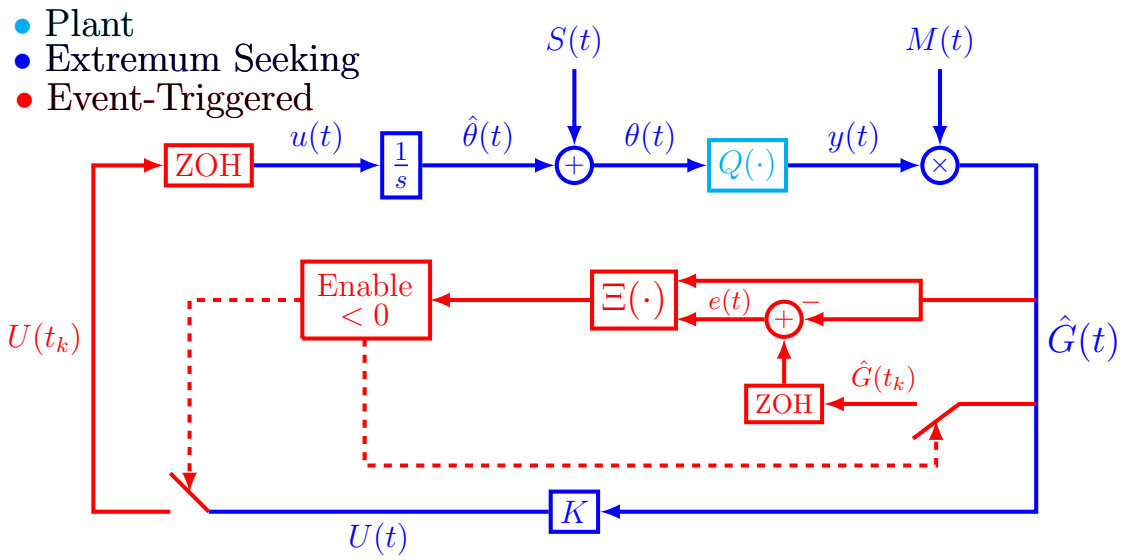

Figure 6.2: Event-triggered based on extremum seeking scheme.

there exist constants $m\,, M_\theta\,, M_y > 0$ *such that*

$$\|\theta(t) - \theta^*\| \leq M_\theta \exp(-mt) + \mathcal{O}\left(a + \frac{1}{\omega}\right)\,, \tag{6.60}$$

$$|y(t) - Q^*| \leq M_y \exp(-mt) + \mathcal{O}\left(a^2 + \frac{1}{\omega^2}\right)\,, \tag{6.61}$$

where $a = \sqrt{\sum_{i=1}^{n} a_i^2}$*, with* a_i *defined in (6.8) and the constants* M_θ*, and* M_y *depending on the initial condition* $\theta(0)$*. Moreover, there exists a lower bound* τ^* *for the inter-execution interval* $t_{k+1} - t_k$ *for all* $k \in \mathbb{N}$ *precluding the Zeno behavior.*

Proof. Now, consider the following candidate Lyapunov function for the average system (6.49)

$$V_{\text{av}}(\bar{t}) = \hat{G}_{\text{av}}^T(\bar{t}) P \hat{G}_{\text{av}}(\bar{t})\,,\; P = P^T > 0, \tag{6.62}$$

with time-derivative

$$\begin{aligned}\frac{dV_{\text{av}}(\bar{t})}{d\bar{t}} = &-\frac{1}{\omega}\hat{G}_{\text{av}}^T(\bar{t}) Q \hat{G}_{\text{av}}(\bar{t}) + \frac{1}{\omega} e_{\text{av}}^T(\bar{t}) K^T H^{*T} P \hat{G}_{\text{av}}(\bar{t}) \\ &+ \frac{1}{\omega}\hat{G}_{\text{av}}^T(\bar{t}) P H^* K e_{\text{av}}(\bar{t})\,,\end{aligned} \tag{6.63}$$

whose upper bound satisfies

$$\frac{dV_{\text{av}}(\bar{t})}{d\bar{t}} \leq -\frac{\lambda_{\min}(Q)}{\omega}\|\hat{G}_{\text{av}}(\bar{t})\|^2 + \frac{2\|PH^*K\|}{\omega}\|e_{\text{av}}(\bar{t})\|\|\hat{G}_{\text{av}}(\bar{t})\|. \tag{6.64}$$

Using Assumptions 2 and 3, we arrive at

$$\frac{dV_{\text{av}}(\bar{t})}{d\bar{t}} \leq -\frac{\alpha}{\omega}\|\hat{G}_{\text{av}}(\bar{t})\|^2 + \frac{\beta}{\omega}\|e_{\text{av}}(\bar{t})\|\|\hat{G}_{\text{av}}(\bar{t})\|\,. \tag{6.65}$$

In the proposed event-triggered mechanism, the update law is (6.56) and $\Xi(\hat{G}_{\text{av}}, e_{\text{av}})$ is given by (6.55). The signal $u_{\text{av}}(t)$ is held constant between two consecutive events, *i.e.*, while $\Xi(\hat{G}_{\text{av}}, e_{\text{av}}) \geq 0$, one has

$$\begin{aligned}\Xi(z_{\text{av}}) &= \sigma\alpha\|\hat{G}_{\text{av}}(\bar{t})\|^2 - \beta\|e_{\text{av}}(\bar{t})\|\|\hat{G}_{\text{av}}(\bar{t})\| \\ &= \beta\|\hat{G}_{\text{av}}(\bar{t})\|\left(\frac{\sigma\alpha}{\beta}\|\hat{G}_{\text{av}}(\bar{t})\| - \|e_{\text{av}}(\bar{t})\|\right) \geq 0\,.\end{aligned} \tag{6.66}$$

Therefore, considering the event-triggered approach, the average measurement error $e_{\text{av}}(\bar{t})$ is upper bounded by

$$\|e_{\text{av}}(\bar{t})\| \leq \frac{\sigma\alpha}{\beta}\|\hat{G}_{\text{av}}(\bar{t})\|\,. \tag{6.67}$$

Now, plugging (6.67) into (6.65),

$$\frac{dV_{\text{av}}(\bar{t})}{d\bar{t}} \leq -\frac{\alpha(1-\sigma)}{\omega}\|\hat{G}_{\text{av}}(\bar{t})\|^2\,. \tag{6.68}$$

By using the Rayleigh-Ritz Inequality [94],

$$\lambda_{\min}(P)\|\hat{G}_{\text{av}}(\bar{t})\|^2 \leq V_{\text{av}}(\bar{t}) \leq \lambda_{\max}(P)\|\hat{G}_{\text{av}}(\bar{t})\|^2\,, \tag{6.69}$$

and the following upper bound for (6.68)

$$\frac{dV_{\text{av}}(\bar{t})}{d\bar{t}} \leq -\frac{\alpha(1-\sigma)}{\omega}\|\hat{G}_{\text{av}}(\bar{t})\|^2 \leq -\frac{\alpha(1-\sigma)}{\omega\lambda_{\max}(P)}V_{\text{av}}(\bar{t})\,. \tag{6.70}$$

Then, invoking the Comparison Lemma [94] an upper bound $\bar{V}_{\text{av}}(\bar{t})$ for $V_{\text{av}}(\bar{t})$ is

$$V_{\text{av}}(\bar{t}) \leq \bar{V}_{\text{av}}(\bar{t})\,, \quad \forall \bar{t} \in [\bar{t}_k, \bar{t}_{k+1})\,. \tag{6.71}$$

given by the solution of the following dynamics

$$\frac{d\bar{V}_{\text{av}}(\bar{t})}{d\bar{t}} = -\frac{\alpha(1-\sigma)}{\omega\lambda_{\max}(P)}\bar{V}_{\text{av}}(\bar{t}), \quad \bar{V}_{\text{av}}(\bar{t}_k) = V_{\text{av}}(\bar{t}_k)\,, \tag{6.72}$$

In other words, $\forall \bar{t} \in [\bar{t}_k, \bar{t}_{k+1})$,

$$\bar{V}_{\text{av}}(\bar{t}) = \exp\left(-\frac{\alpha(1-\sigma)}{\omega\lambda_{\max}(P)}(\bar{t} - \bar{t}_k)\right)V_{\text{av}}(\bar{t}_k)\,, \tag{6.73}$$

and the inequality (6.71) is rewritten as

$$V_{\text{av}}(\bar{t}) \leq \exp\left(-\frac{\alpha(1-\sigma)}{\omega\lambda_{\max}(P)}(\bar{t}-\bar{t}_k)\right) V_{\text{av}}(\bar{t}_k)\,. \tag{6.74}$$

By defining, $\bar{t}_k^+$ and $\bar{t}_k^-$ as the right and left limits of $\bar{t}=\bar{t}_k$, respectively, it easy to verify that $V_{\text{av}}(\bar{t}_{k+1}^-) \leq \exp\left(-\frac{\alpha(1-\sigma)}{\omega\lambda_{\max}(P)}(\bar{t}_{k+1}^- - \bar{t}_k^+)\right) V_{\text{av}}(\bar{t}_k^+)$. Since $V_{\text{av}}(\bar{t})$ is continuous, $V_{\text{av}}(\bar{t}_{k+1}^-) = V_{\text{av}}(\bar{t}_{k+1})$ and $V_{\text{av}}(\bar{t}_k^+) = V_{\text{av}}(\bar{t}_k)$, and therefore,

$$V_{\text{av}}(\bar{t}_{k+1}) \leq \exp\left(-\frac{\alpha(1-\sigma)}{\omega\lambda_{\max}(P)}(\bar{t}_{k+1}-\bar{t}_k)\right) V_{\text{av}}(\bar{t}_k)\,. \tag{6.75}$$

Hence, for any $\bar{t} \geq 0$ in $\bar{t} \in [\bar{t}_k, \bar{t}_{k+1})$, $k \in \mathbb{N}$, one has

$$\begin{aligned}
V_{\text{av}}(\bar{t}) &\leq \exp\left(-\frac{\alpha(1-\sigma)}{\omega\lambda_{\max}(P)}(\bar{t}-\bar{t}_k)\right) V_{\text{av}}(\bar{t}_k) \\
&\leq \exp\left(-\frac{\alpha(1-\sigma)}{\omega\lambda_{\max}(P)}(\bar{t}-\bar{t}_k)\right) \exp\left(-\frac{\alpha(1-\sigma)}{\omega\lambda_{\max}(P)}(\bar{t}_k-\bar{t}_{k-1})\right) V_{\text{av}}(\bar{t}_{k-1}) \\
&\leq \ldots \leq \\
&\leq \exp\left(-\frac{\alpha(1-\sigma)}{\omega\lambda_{\max}(P)}(\bar{t}-\bar{t}_k)\right) \prod_{i=1}^{i=k} \exp\left(-\frac{\alpha(1-\sigma)}{\omega\lambda_{\max}(P)}(\bar{t}_i-\bar{t}_{i-1})\right) V_{\text{av}}(\bar{t}_{i-1}) \\
&= \exp\left(-\frac{\alpha(1-\sigma)}{\omega\lambda_{\max}(P)}\bar{t}\right) V_{\text{av}}(0)\,.
\end{aligned} \tag{6.76}$$

Now, lower bounding the left-hand side and upper bounding the right hand size of (6.76) with the corresponding sides of (6.69), one gets

$$\lambda_{\min}(P)\|\hat{G}_{\text{av}}(\bar{t})\|^2 \leq \exp\left(-\frac{\alpha(1-\sigma)}{\omega\lambda_{\max}(P)}\bar{t}\right) \lambda_{\max}(P)\|\hat{G}_{\text{av}}(0)\|^2\,. \tag{6.77}$$

Then,

$$\begin{aligned}
\|\hat{G}_{\text{av}}(\bar{t})\|^2 &\leq \exp\left(-\frac{\alpha(1-\sigma)}{\omega\lambda_{\max}(P)}\bar{t}\right) \frac{\lambda_{\max}(P)}{\lambda_{\min}(P)}\|\hat{G}_{\text{av}}(0)\|^2 \\
&= \left[\exp\left(-\frac{\alpha(1-\sigma)}{2\omega\lambda_{\max}(P)}\bar{t}\right) \sqrt{\frac{\lambda_{\max}(P)}{\lambda_{\min}(P)}}\|\hat{G}_{\text{av}}(0)\|\right]^2\,,
\end{aligned} \tag{6.78}$$

and

$$\|\hat{G}_{\text{av}}(\bar{t})\| \leq \exp\left(-\frac{\alpha(1-\sigma)}{2\omega\lambda_{\max}(P)}\bar{t}\right) \sqrt{\frac{\lambda_{\max}(P)}{\lambda_{\min}(P)}}\|\hat{G}_{\text{av}}(0)\|\,. \tag{6.79}$$

Although the analysis has been focused on the convergence of $\hat{G}_{\text{av}}(\bar{t})$ and, consequently, of $\hat{G}(t)$, the obtained results through (6.79) can be easily extended to the

variables $\tilde{\theta}_{\text{av}}(\bar{t})$ and $\tilde{\theta}(t)$. Using relation (6.52), (6.62) and (6.64) are rewritten as

$$V_{\text{av}}(\bar{t}) = \tilde{\theta}_{\text{av}}^{T}(\bar{t}) H^{*T} P H^{*} \tilde{\theta}_{\text{av}}(\bar{t}) \,, \tag{6.80}$$

$$\frac{dV_{\text{av}}(\bar{t})}{d\bar{t}} \leq -\frac{\alpha(1-\sigma)}{\omega \lambda_{\max}(P)} V_{\text{av}}(\bar{t}) \,. \tag{6.81}$$

From Assumption 1, the quadratic matrix H^{*} has linearly independent rows and columns. Furthermore, from Assumption 2, P is a symmetric and positive definite matrix. Thus, there exists a matrix R with independent columns such that $P = R^{T}R$ and, consequently, $\bar{P} = H^{*T} P H^{*}$ is a symmetric and positive definite matrix [109, Section 6.5] leading to

$$V_{\text{av}} = \tilde{\theta}_{\text{av}}^{T}(\bar{t}) \bar{P} \tilde{\theta}_{\text{av}}(\bar{t}) \,, \tag{6.82}$$

satisfying the Rayleigh-Ritz inequality

$$\lambda_{\min}(\bar{P}) \|\tilde{\theta}_{\text{av}}(\bar{t})\|^{2} \leq V_{\text{av}} \leq \lambda_{\max}(\bar{P}) \|\tilde{\theta}_{\text{av}}(\bar{t})\|^{2} \,. \tag{6.83}$$

Then, by using (6.76), (6.82) and (6.83), one has

$$\lambda_{\min}(\bar{P}) \|\tilde{\theta}_{\text{av}}(\bar{t})\|^{2} \leq \exp\left(-\frac{(1-\sigma)\lambda_{\min}(Q)}{\omega \lambda_{\max}(P)} \bar{t} \right) \lambda_{\max}(\bar{P}) \|\tilde{\theta}_{\text{av}}(0)\|^{2} \,, \tag{6.84}$$

and

$$\|\tilde{\theta}_{\text{av}}(\bar{t})\| \leq \exp\left(-\frac{\alpha(1-\sigma)}{2\omega \lambda_{\max}(P)} \bar{t} \right) \sqrt{\frac{\lambda_{\max}(\bar{P})}{\lambda_{\min}(\bar{P})}} \|\tilde{\theta}_{\text{av}}(0)\| \,. \tag{6.85}$$

Since (6.36) has discontinuous right-hand side and the mapping $\tilde{\Theta}(\bar{t}, \tilde{\theta}(\bar{t}), e(\bar{t}))$ in (6.39) is T-periodic in t. From (6.85), $\tilde{\theta}_{\text{av}}(\bar{t})$ is asymptotically stable, by invoking [103, Theorem 2], such that

$$\|\tilde{\theta}(t) - \tilde{\theta}_{\text{av}}(t)\| \leq \mathcal{O}\left(\frac{1}{\omega} \right) \,. \tag{6.86}$$

By using the Triangle inequality [110], one has

$$\begin{aligned} \|\tilde{\theta}(t)\| &\leq \|\tilde{\theta}_{\text{av}}(t)\| + \mathcal{O}\left(\frac{1}{\omega} \right) \\ &\leq \exp\left(-\frac{\alpha(1-\sigma)}{2\lambda_{\max}(P)} t \right) \sqrt{\frac{\lambda_{\max}(\bar{P})}{\lambda_{\min}(\bar{P})}} \|\tilde{\theta}_{\text{av}}(0)\| + \mathcal{O}\left(\frac{1}{\omega} \right). \end{aligned} \tag{6.87}$$

Furthermore,

$$\|\hat{G}(t) - \hat{G}_{\text{av}}(t)\| \leq \mathcal{O}\left(\frac{1}{\omega}\right), \tag{6.88}$$

and by using again the Triangle inequaliy [110], such that

$$\begin{aligned}\|\hat{G}(t)\| &\leq \|\hat{G}_{\text{av}}(t)\| + \mathcal{O}\left(\frac{1}{\omega}\right) \\ &\leq \exp\left(-\frac{\alpha(1-\sigma)}{2\lambda_{\max}(P)}t\right)\sqrt{\frac{\lambda_{\max}(P)}{\lambda_{\min}(P)}}\|\hat{G}_{\text{av}}(0)\| + \mathcal{O}\left(\frac{1}{\omega}\right).\end{aligned} \tag{6.89}$$

Now, from (6.12), we can write

$$\theta(t) - \theta^* = \tilde{\theta}(t) + S(t)\,, \tag{6.90}$$

whose norm satisfies

$$\begin{aligned}\|\theta(t) - \theta^*\| &= \|\tilde{\theta}(t) + S(t)\| \\ &\leq \|\tilde{\theta}(t)\| + \|S(t)\| \\ &\leq \exp\left(-\frac{\alpha(1-\sigma)}{2\lambda_{\max}(P)}t\right)\sqrt{\frac{\lambda_{\max}(\bar{P})}{\lambda_{\min}(\bar{P})}}\|\theta(0) - \theta^*\| + \mathcal{O}\left(a + \frac{1}{\omega}\right).\end{aligned} \tag{6.91}$$

Defining the error variable $\tilde{y}(t)$ as

$$\tilde{y}(t) := y(t) - Q^*\,, \tag{6.92}$$

using the fact that $y(t) = Q(\theta(t))$ where $Q(\theta(t))$ is defined in (6.1) and the Cauchy-Schwarz inequality [105], we get

$$\begin{aligned}|\tilde{y}(t)| &= |y(t) - Q^*| \\ &= |(\theta(t) - \theta^*)^T H^*(\theta(t) - \theta^*)| \\ &\leq \|H^*\|\|\theta(t) - \theta^*\|^2\,,\end{aligned} \tag{6.93}$$

and substituting (6.91) in (6.93), the following holds:

$$
\begin{aligned}
|\tilde{y}(t)| \leq & \|H^*\| \left[\exp\left(-\frac{\alpha(1-\sigma)}{2\lambda_{\max}(P)} t \right) \sqrt{\frac{\lambda_{\max}(\bar{P})}{\lambda_{\min}(\bar{P})}} \|\theta(0) - \theta^*\| + \mathcal{O}\left(a + \frac{1}{\omega} \right) \right]^2 \\
= & \|H^*\| \left[\exp\left(-\frac{\alpha(1-\sigma)}{\lambda_{\max}(P)} t \right) \frac{\lambda_{\max}(\bar{P})}{\lambda_{\min}(\bar{P})} \|\theta(0) - \theta^*\|^2 + \mathcal{O}\left(a + \frac{1}{\omega} \right)^2 \right. \\
& \left. + 2 \exp\left(-\frac{\alpha(1-\sigma)}{2\lambda_{\max}(P)} t \right) \sqrt{\frac{\lambda_{\max}(\bar{P})}{\lambda_{\min}(\bar{P})}} \|\theta(0) - \theta^*\| \mathcal{O}\left(a + \frac{1}{\omega} \right) \right] . \qquad (6.94)
\end{aligned}
$$

Since $\exp\left(-\frac{\alpha(1-\sigma)}{\lambda_{\max}(P)} t\right) \leq \exp\left(-\frac{\alpha(1-\sigma)}{2\lambda_{\max}(P)} t\right)$ and, according to [94, Definition 10.1], $\|H^*\| \mathcal{O}\left(a + \frac{1}{\omega}\right)^2$ is of order of magnitude $\mathcal{O}\left(a + \frac{1}{\omega}\right)^2$, (6.93) is upper bounded by

$$
\begin{aligned}
& |y(t) - Q^*| \leq \exp\left(-\frac{\alpha(1-\sigma)}{2\lambda_{\max}(P)} t \right) \|H^*\| \times \\
& \times \left[\frac{\lambda_{\max}(\bar{P})}{\lambda_{\min}(\bar{P})} \|\theta(0) - \theta^*\| + 2 \sqrt{\frac{\lambda_{\max}(\bar{P})}{\lambda_{\min}(\bar{P})}} \mathcal{O}\left(a + \frac{1}{\omega} \right) \right] \times \\
& \times \|\theta(0) - \theta^*\| + \mathcal{O}\left(a^2 + 2\frac{a}{\omega} + \frac{1}{\omega^2} \right) . \qquad (6.95)
\end{aligned}
$$

Finally, once $a\,, \omega > 0$, by using the Young inequality [94], $\frac{a}{\omega} \leq \frac{a^2}{2} + \frac{1}{2\omega^2}$, and

$$
\begin{aligned}
& |y(t) - Q^*| \leq \exp\left(-\frac{\alpha(1-\sigma)}{2\lambda_{\max}(P)} t \right) \|H^*\| \times \\
& \times \left[\frac{\lambda_{\max}(\bar{P})}{\lambda_{\min}(\bar{P})} \|\theta(0) - \theta^*\| + 2 \sqrt{\frac{\lambda_{\max}(\bar{P})}{\lambda_{\min}(\bar{P})}} \mathcal{O}\left(a + \frac{1}{\omega} \right) \right] \times \\
& \quad \times \|\theta(0) - \theta^*\| + \mathcal{O}\left(a^2 + \frac{1}{\omega^2} \right) , \qquad (6.96)
\end{aligned}
$$

since $\mathcal{O}\left(2a^2 + 2/\omega\right) = 2\mathcal{O}\left(a^2 + 1/\omega^2\right)$ has an order of magnitude of $\mathcal{O}\left(a^2 + 1/\omega^2\right)$ [94, Definition 10.1].

Therefore, by defining the positive constants

$$
m = \frac{\alpha(1-\sigma)}{2\lambda_{\max}(P)} , \qquad (6.97)
$$

$$
M_\theta = \sqrt{\frac{\lambda_{\max}(\bar{P})}{\lambda_{\min}(\bar{P})}} \|\theta(0) - \theta^*\| , \qquad (6.98)
$$

$$
M_y = \|H^*\| \frac{\lambda_{\max}(\bar{P})}{\lambda_{\min}(\bar{P})} \|\theta(0) - \theta^*\|^2 + 2\|H^*\| \sqrt{\frac{\lambda_{\max}(\bar{P})}{\lambda_{\min}(\bar{P})}} \|\theta(0) - \theta^*\| \mathcal{O}\left(a + \frac{1}{\omega} \right) , \qquad (6.99)
$$

inequalities (6.91) and (6.96) satisfy (6.60) and (6.61), respectively. Since the average closed-loop system consists of (6.49), with the event-triggered mechanism (6.55), (6.56), and a control signal's update law (6.67) satisfying $\|e_{\text{av}}(\bar{t})\| > \frac{\sigma\alpha}{\beta}\|\hat{G}_{\text{av}}(\bar{t})\|$, we conclude that $dV_{\text{av}}(\bar{t})/d\bar{t} < 0$ from (6.65) and for all $\bar{t} \in [t_k\,, t_{k+1}[$. Thus, one can state that

$$\sigma\alpha\|\hat{G}_{\text{av}}(\bar{t})\|^2 - \beta\|e_{\text{av}}(\bar{t})\|\|\hat{G}_{\text{av}}(\bar{t})\| \geq 0\,, \tag{6.100}$$

and using the Peter-Paul inequality [106], $cd \leq \frac{c^2}{2\epsilon} + \frac{\epsilon d^2}{2}$ for all $c, d, \epsilon > 0$, with $c = \|e_{\text{av}}(\bar{t})\|$, $d = \|\hat{G}_{\text{av}}(\bar{t})\|$ and $\epsilon = \frac{\sigma\alpha}{\beta}$, the inequality (6.100) is lower bounded by

$$\begin{aligned}
&\sigma\alpha\|\hat{G}_{\text{av}}(\bar{t})\|^2 - \beta\|e_{\text{av}}(\bar{t})\|\|\hat{G}_{\text{av}}(\bar{t})\| \geq \\
&\sigma\alpha\|\hat{G}_{\text{av}}(\bar{t})\|^2 - \beta\left(\frac{\sigma\alpha}{2\beta}\|\hat{G}_{\text{av}}(\bar{t})\|^2 + \frac{\beta}{2\sigma\alpha}\|e_{\text{av}}(\bar{t})\|^2\right) \\
&= q\|\hat{G}_{\text{av}}(\bar{t})\|^2 - p\|e_{\text{av}}(\bar{t})\|^2\,,
\end{aligned} \tag{6.101}$$

where

$$q = \frac{\sigma\alpha}{2} \quad \text{and} \quad p = \frac{\beta^2}{2\sigma\alpha}\,. \tag{6.102}$$

In [107], it is shown that a lower bound for the inter-execution interval is given by the time duration it takes for the function

$$\phi(\bar{t}) = \sqrt{\frac{p}{q}}\frac{\|e_{\text{av}}(\bar{t})\|}{\|\hat{G}_{\text{av}}(\bar{t})\|} \tag{6.103}$$

to go from 0 to 1. The time-derivative of (6.103) is

$$\frac{d\phi(\bar{t})}{d\bar{t}} = \sqrt{\frac{p}{q}}\frac{1}{\|e_{\text{av}}(\bar{t})\|\|\hat{G}_{\text{av}}(\bar{t})\|}\left[e_{\text{av}}^T(\bar{t})\frac{de_{\text{av}}(\bar{t})}{d\bar{t}} - \hat{G}_{\text{av}}^T(\bar{t})\frac{d\hat{G}_{\text{av}}(\bar{t})}{d\bar{t}}\left(\frac{\|e_{\text{av}}(\bar{t})\|}{\|\hat{G}_{\text{av}}(\bar{t})\|}\right)^2\right]. \tag{6.104}$$

Now, plugging equations (6.49) and (6.50) into (6.104), one arrives to

$$\begin{aligned}
\frac{d\phi(\bar{t})}{d\bar{t}} = \frac{1}{\omega}\sqrt{\frac{p}{q}}\frac{1}{\|e_{\text{av}}(\bar{t})\|\|\hat{G}_{\text{av}}(\bar{t})\|}\Big\{&-e_{\text{av}}^T(\bar{t})H^*Ke_{\text{av}}(\bar{t}) - e_{\text{av}}^T(\bar{t})H^*K\hat{G}_{\text{av}}(\bar{t}) + \\
&- \left[\hat{G}_{\text{av}}^T(\bar{t})H^*K\hat{G}_{\text{av}}(\bar{t}) + \hat{G}_{\text{av}}^T(\bar{t})H^*Ke_{\text{av}}(\bar{t})\right]\left(\frac{\|e_{\text{av}}(\bar{t})\|}{\|\hat{G}_{\text{av}}(\bar{t})\|}\right)^2\Big\}\,.
\end{aligned} \tag{6.105}$$

Then, the following estimate holds:

$$\begin{aligned}\frac{d\phi(\bar{t})}{d\bar{t}} &\leq \frac{1}{\omega}\sqrt{\frac{p}{q}}\frac{\|H^*K\|}{\|e_{\mathrm{av}}(\bar{t})\|\|\hat{G}_{\mathrm{av}}(\bar{t})\|}\Big\{\|e_{\mathrm{av}}(\bar{t})\|^2+\|e_{\mathrm{av}}(\bar{t})\|\|\hat{G}_{\mathrm{av}}(\bar{t})\| \\ &\quad+\Big[\|\hat{G}_{\mathrm{av}}(\bar{t})\|^2+\|\hat{G}_{\mathrm{av}}(\bar{t})\|\|e_{\mathrm{av}}(\bar{t})\|\Big]\left(\frac{\|e_{\mathrm{av}}(\bar{t})\|}{\|\hat{G}_{\mathrm{av}}(\bar{t})\|}\right)^2\Big\} \\ &= \frac{\|H^*K\|}{\omega}\sqrt{\frac{p}{q}}\left\{1+2\frac{\|e_{\mathrm{av}}(\bar{t})\|}{\|\hat{G}_{\mathrm{av}}(\bar{t})\|}+\frac{\|e_{\mathrm{av}}(\bar{t})\|^2}{\|\hat{G}_{\mathrm{av}}(\bar{t})\|^2}\right\}. \end{aligned} \tag{6.106}$$

Hence, using (6.103), inequality (6.106) is rewritten as

$$\omega\frac{d\phi(\bar{t})}{d\bar{t}} \leq \|H^*K\|\sqrt{\frac{p}{q}}+2\|H^*K\|\phi(\bar{t})+\|H^*K\|\sqrt{\frac{q}{p}}\phi^2(\bar{t})\,. \tag{6.107}$$

From the time-scaling $t=\frac{\bar{t}}{\omega}$, inequality (6.106) and invoking the Comparison Lemma [94], a lower bound for the inter-execution time is found as

$$\tau^* = \int_0^1 \frac{1}{b_0+b_1\xi+b_2\xi^2}\,d\xi\,, \tag{6.108}$$

with $b_0=\dfrac{\beta\|H^*K\|}{\alpha\sigma}$, $b_1=2\|H^*K\|$ and $b_2=\dfrac{\alpha\|H^*K\|\sigma}{\beta}$. Therefore, the Zeno behavior is avoided. □

Corollary 1. *(Static Event-Tiggered Extremum Seeking with known Hessian): Consider the partial knowledge of the nonlinear map (6.1) such that the Hessian matrix H^* is a known parameter. Although this hypothesis appears to simplify the problem, one should note that the extremum seeking strategy is still justified once the optimizer vector θ^* and parameter Q^* are unknown. Then, $\Xi(\hat{G},e)$ defined in (6.29) is equivalent to*

$$\Xi(\hat{G},e)=\sigma\hat{G}^T(t)Q\hat{G}(t)-2\hat{G}^T(t)PH^*Ke(t)\,,$$

resulting in the static event-triggered mechanism

$$t_{k+1}=\inf\Big\{t\in\mathbb{R}^+ : t>t_k \ \wedge\ \Xi(\hat{G},e)<0\Big\}\,,$$

which ensures the local asymptotic stability of the closed-loop system from Theorem 5.

6.4 Dynamic Event-Triggering in Extremum Seeking

6.4.1 Stability Analysis

Theorem 6 demonstrates how local asymptotic stability of the extremum seeking based on a dynamic event-triggered mechanism shown in Figure 6.3 is ensured.

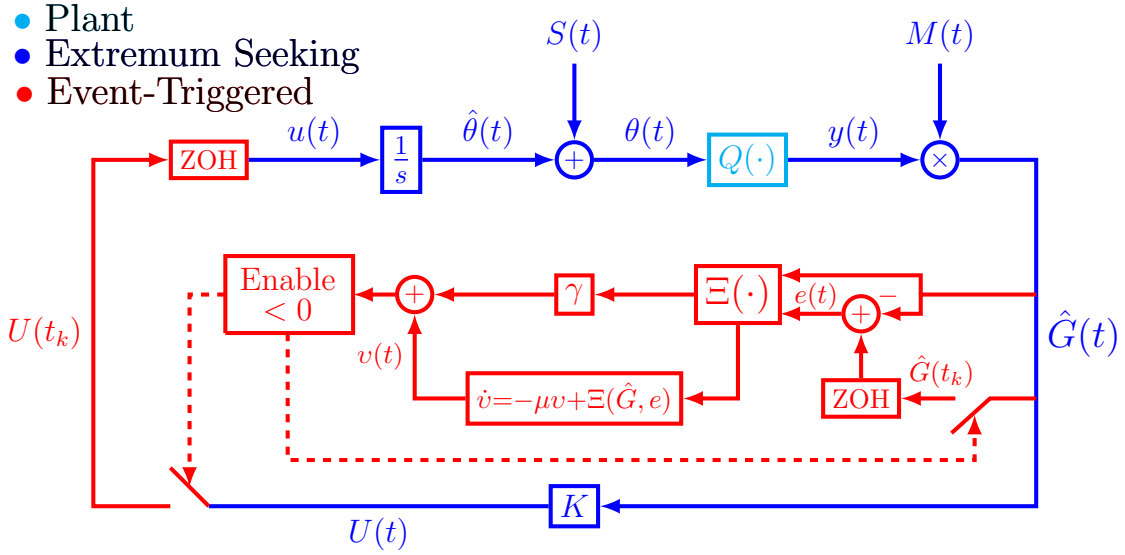

Figure 6.3: Block diagram of the extremum seeking based on dynamic event-triggered mechanism.

Theorem 6. *Consider the closed-loop average dynamics of the gradient estimate (6.49) and (6.50) as well as the average dynamic event-triggered mechanism given by Definition 10. Under Assumptions 1–3 with the quadratic mapping* $\Xi(\hat{G}_{\text{av}}, e_{\text{av}})$ *given by (6.55) and a sufficiently large* $\omega > 0$ *defined in (6.34), the average gradient estimate system (6.49) and (6.50) with state* $\hat{G}_{av}(t)$ *is locally exponentially stable. Consequently, the dynamics of* $\tilde{\theta}_{av}(t)$ *converges exponentially to zero. Therefore, there exist constants* $m\,, M_\theta\,, M_y > 0$ *such that*

$$\|\theta(t) - \theta^*\| \leq M_\theta \exp(-mt) + \mathcal{O}\left(a + \frac{1}{\omega}\right), \tag{6.109}$$

$$|y(t) - Q^*| \leq M_y \exp(-mt) + \mathcal{O}\left(a^2 + \frac{1}{\omega^2}\right), \tag{6.110}$$

where $a = \sqrt{\sum_{i=1}^{n} a_i^2}$*, with* a_i *defined in (6.8) and the constants* M_θ *and* M_y *depending on the initial condition* $\theta(0)$*. Moreover, there exists a lower bound* τ^* *for the inter-execution interval* $t_{k+1} - t_k$ *for all* $k \in \mathbb{N}$ *precluding the Zeno behavior.*

Proof. First, notice that the dynamic triggering mechanism (6.32) ensures, for all

$t \in [t_k\,, t_{k+1}[$,

$$\upsilon_{\rm av}(\bar{t}) + \gamma \Xi(\hat{G}_{\rm av}, e_{\rm av}) \geq 0\,, \tag{6.111}$$

and,

$$\Xi(\hat{G}_{\rm av}, e_{\rm av}) \geq -\frac{1}{\gamma}\upsilon_{\rm av}(\bar{t})\,. \tag{6.112}$$

Now, with the help of (6.112), the following estimate of (6.58) holds

$$\begin{aligned}\frac{d\upsilon_{\rm av}(\bar{t})}{d\bar{t}} &= -\frac{\mu}{\omega}\upsilon_{\rm av}(\bar{t}) + \frac{1}{\omega}\Xi(\hat{G}_{\rm av}, e_{\rm av}) \\ &\geq -\frac{\mu}{\omega}\upsilon_{\rm av}(\bar{t}) - \frac{1}{\omega\gamma}\upsilon_{\rm av}(\bar{t}) = -\frac{1}{\omega}\left(\mu + \frac{1}{\gamma}\right)\upsilon_{\rm av}(\bar{t})\,.\end{aligned} \tag{6.113}$$

Invoking [94, Comparison Lemma, pp. 102], the solution $\hat{\upsilon}_{\rm av}(\bar{t})$ of the following first-order dynamics

$$\frac{d\hat{\upsilon}_{\rm av}(\bar{t})}{d\bar{t}} = -\frac{1}{\omega}\left(\mu + \frac{1}{\gamma}\right)\hat{\upsilon}_{\rm av}(\bar{t})\,, \quad \hat{\upsilon}_{\rm av}(0) = \upsilon_{\rm av}(0) > 0\,, \tag{6.114}$$

precisely,

$$\hat{\upsilon}_{\rm av}(\bar{t}) = \exp\left(-\frac{1}{\omega}\left(\mu + \frac{1}{\gamma}\right)\bar{t}\right)\hat{\upsilon}_{\rm av}(0) > 0\,, \quad \forall \bar{t} \geq 0\,, \tag{6.115}$$

is a lower bound for $\upsilon_{\rm av}(\bar{t})$. To verify this fact, notice that, from (6.113) and (6.114),

$$\frac{d(\upsilon_{\rm av}(\bar{t}) - \hat{\upsilon}_{\rm av}(\bar{t}))}{d\bar{t}} \geq -\frac{1}{\omega}\left(\mu + \frac{1}{\gamma}\right)(\upsilon_{\rm av}(\bar{t}) - \hat{\upsilon}_{\rm av}(\bar{t}))\,. \tag{6.116}$$

Thus,

$$\upsilon_{\rm av}(\bar{t}) - \hat{\upsilon}_{\rm av}(\bar{t}) \geq \exp\left(-\frac{1}{\omega}\left(\mu + \frac{1}{\gamma}\right)\bar{t}\right)\underbrace{(\upsilon_{\rm av}(0) - \hat{\upsilon}_{\rm av}(0))}_{=0} \tag{6.117}$$

and

$$\upsilon_{\rm av}(\bar{t}) \geq \hat{\upsilon}_{\rm av}(\bar{t}) > 0\,, \quad \forall \bar{t} \geq 0\,. \tag{6.118}$$

Now, since $\upsilon_{\rm av}(\bar{t}) > 0$, for all $\upsilon_{\rm av}(\bar{t}) \neq 0$, consider the following Lyapunov candidate for the average system:

$$V_{\rm av}(\bar{t}) = \hat{G}_{\rm av}^T(\bar{t}) P \hat{G}_{\rm av}(\bar{t}) + \upsilon_{\rm av}(\bar{t})\,,\ P^T = P > 0 \tag{6.119}$$

The Rayleigh-Ritz inequality writes:

$$\lambda_{\min}(P)\|\hat{G}_{\text{av}}(\bar{t})\|^2 \leq \hat{G}_{\text{av}}^T(\bar{t})P\hat{G}_{\text{av}}(\bar{t}) \leq \lambda_{\max}(P)\|\hat{G}_{\text{av}}(\bar{t})\|^2 . \tag{6.120}$$

The time-derivative of (6.119) is given by

$$\frac{dV_{\text{av}}(\bar{t})}{d\bar{t}} = \frac{d\hat{G}_{\text{av}}^T(\bar{t})}{d\bar{t}}P\hat{G}_{\text{av}}(\bar{t}) + \hat{G}_{\text{av}}^T(\bar{t})P\frac{d\hat{G}_{\text{av}}(\bar{t})}{d\bar{t}} + \frac{d\upsilon_{\text{av}}(\bar{t})}{d\bar{t}} , \tag{6.121}$$

which, by using equations (6.49) and (6.58), can be rewritten as

$$\begin{aligned}\frac{dV_{\text{av}}(\bar{t})}{d\bar{t}} = &-\frac{1}{\omega}\hat{G}_{\text{av}}^T(\bar{t})Q\hat{G}_{\text{av}}(\bar{t}) + \frac{1}{\omega}e_{\text{av}}^T(\bar{t})K^TH^{*T}P\hat{G}_{\text{av}}(\bar{t}) + \\ &+ \frac{1}{\omega}\hat{G}_{\text{av}}^T(\bar{t})PH^*Ke_{\text{av}}(\bar{t}) - \frac{\mu}{\omega}\upsilon_{\text{av}}(\bar{t}) + \frac{1}{\omega}\Xi(\hat{G}_{\text{av}}, e_{\text{av}}) ,\end{aligned} \tag{6.122}$$

Under Assumption 2, the following inequality is derived

$$\frac{dV_{\text{av}}(\bar{t})}{d\bar{t}} \leq -\frac{\alpha}{\omega}\|\hat{G}_{\text{av}}(\bar{t})\|^2 + \frac{\beta}{\omega}\|e_{\text{av}}(\bar{t})\|\|\hat{G}_{\text{av}}(\bar{t})\| + \frac{1}{\omega}\Xi(\hat{G}_{\text{av}}, e_{\text{av}}) . \tag{6.123}$$

Plugging (6.55) into (6.123), one has

$$\frac{dV_{\text{av}}(\bar{t})}{d\bar{t}} \leq -\frac{(1-\sigma)\alpha}{\omega}\|\hat{G}_{\text{av}}(\bar{t})\|^2 - \frac{\mu}{\omega}\upsilon_{\text{av}}(\bar{t}) . \tag{6.124}$$

Now, using (6.120) and (6.119), inequality (6.124) can be upper bounded as follows

$$\frac{dV_{\text{av}}(\bar{t})}{d\bar{t}} \leq -\frac{(1-\sigma)\alpha}{\omega\lambda_{\max}(P)}\hat{G}_{\text{av}}^T(\bar{t})P\hat{G}_{\text{av}}(\bar{t}) - \frac{\mu}{\omega}\upsilon_{\text{av}}(\bar{t}) \tag{6.125}$$

$$\leq -\frac{1}{\omega}\min\left\{\frac{(1-\sigma)\alpha}{\lambda_{\max}(P)}, \mu\right\}(\hat{G}_{\text{av}}^T(\bar{t})P\hat{G}_{\text{av}}(\bar{t}) + \upsilon_{\text{av}}(\bar{t})) \tag{6.126}$$

$$\leq -\frac{1}{\omega}\min\left\{\frac{(1-\sigma)\alpha}{\lambda_{\max}(P)}, \mu\right\}V_{\text{av}}(\bar{t}) . \tag{6.127}$$

Then, invoking the Comparison Lemma [94] an upper bound $\bar{V}_{\text{av}}(\bar{t})$ for $V_{\text{av}}(\bar{t})$ is

$$V_{\text{av}}(\bar{t}) \leq \bar{V}_{\text{av}}(\bar{t}) , \quad \forall \bar{t} \in [\bar{t}_k, \bar{t}_{k+1}) . \tag{6.128}$$

given by the solution of the following dynamics

$$\frac{d\bar{V}_{\text{av}}(\bar{t})}{d\bar{t}} = -\frac{1}{\omega}\min\left\{\frac{(1-\sigma)\alpha}{\lambda_{\max}(P)}, \mu\right\}\bar{V}_{\text{av}}(\bar{t}), \quad \bar{V}_{\text{av}}(\bar{t}_k) = V_{\text{av}}(\bar{t}_k) , \tag{6.129}$$

In other words, $\forall \bar{t} \in [\bar{t}_k, \bar{t}_{k+1})$,

$$\bar{V}_{\text{av}}(\bar{t}) = \exp\left(-\frac{1}{\omega}\min\left\{\frac{(1-\sigma)\alpha}{\lambda_{\max}(P)}, \mu\right\}(\bar{t}-\bar{t}_k)\right) V_{\text{av}}(\bar{t}_k)\,, \tag{6.130}$$

and the inequality (6.128) is rewritten as

$$V_{\text{av}}(\bar{t}) \leq \exp\left(-\frac{1}{\omega}\min\left\{\frac{(1-\sigma)\alpha}{\lambda_{\max}(P)}, \mu\right\}(\bar{t}-\bar{t}_k)\right) V_{\text{av}}(\bar{t}_k)\,. \tag{6.131}$$

By defining, $\bar{t}_k^+$ and $\bar{t}_k^-$ as the right and left limits of $\bar{t} = \bar{t}_k$, respectively, it easy to verify that $V_{\text{av}}(\bar{t}_{k+1}^-) \leq \exp\left(-\frac{1}{\omega}\min\left\{\frac{(1-\sigma)\alpha}{\lambda_{\max}(P)}, \mu\right\}(\bar{t}_{k+1}^- - \bar{t}_k^+)\right) V_{\text{av}}(\bar{t}_k^+)$. Since $V_{\text{av}}(\bar{t})$ is continuous, $V_{\text{av}}(\bar{t}_{k+1}^-) = V_{\text{av}}(\bar{t}_{k+1})$ and $V_{\text{av}}(\bar{t}_k^+) = V_{\text{av}}(\bar{t}_k)$, and therefore,

$$V_{\text{av}}(\bar{t}_{k+1}) \leq \exp\left(-\frac{1}{\omega}\min\left\{\frac{(1-\sigma)\alpha}{\lambda_{\max}(P)}, \mu\right\}(\bar{t}_{k+1}-\bar{t}_k)\right) V_{\text{av}}(\bar{t}_k)\,. \tag{6.132}$$

Hence, for any $\bar{t} \geq 0$ in $\bar{t} \in [\bar{t}_k, \bar{t}_{k+1})$, $k \in \mathbb{N}$, one has

$$\begin{aligned}
V_{\text{av}}(\bar{t}) &\leq \exp\left(-\frac{1}{\omega}\min\left\{\frac{(1-\sigma)\alpha}{\lambda_{\max}(P)}, \mu\right\}(\bar{t}-\bar{t}_k)\right) V_{\text{av}}(\bar{t}_k) \\
&\leq \exp\left(-\frac{1}{\omega}\min\left\{\frac{(1-\sigma)\alpha}{\lambda_{\max}(P)}, \mu\right\}(\bar{t}-\bar{t}_k)\right) \times \\
&\quad \times \exp\left(-\frac{1}{\omega}\min\left\{\frac{(1-\sigma)\alpha}{\lambda_{\max}(P)}, \mu\right\}(\bar{t}_k-\bar{t}_{k-1})\right) V_{\text{av}}(\bar{t}_{k-1}) \\
&\leq \ldots \leq \\
&\leq \exp\left(-\frac{1}{\omega}\min\left\{\frac{(1-\sigma)\alpha}{\lambda_{\max}(P)}, \mu\right\}(\bar{t}-\bar{t}_k)\right) \times \\
&\quad \times \prod_{i=1}^{i=k} \exp\left(-\frac{1}{\omega}\min\left\{\frac{(1-\sigma)\alpha}{\lambda_{\max}(P)}, \mu\right\}(\bar{t}_i-\bar{t}_{i-1})\right) V_{\text{av}}(\bar{t}_{i-1}) \\
&= \exp\left(-\frac{1}{\omega}\min\left\{\frac{(1-\sigma)\alpha}{\lambda_{\max}(P)}, \mu\right\}\bar{t}\right) V_{\text{av}}(0)\,.
\end{aligned} \tag{6.133}$$

From (6.119), it follows

$$\hat{G}_{\text{av}}^T(\bar{t}) P \hat{G}_{\text{av}}(\bar{t}) \leq V_{\text{av}}(\bar{t})\,. \tag{6.134}$$

Consequently, combining (6.133) and (6.134), one gets

$$\begin{aligned}
\hat{G}_{\text{av}}^T(\bar{t}) P \hat{G}_{\text{av}}(\bar{t}) &\leq \exp\left(-\frac{1}{\omega}\min\left\{\frac{(1-\sigma)\alpha}{\lambda_{\max}(P)}, \mu\right\}\bar{t}\right) V_{\text{av}}(\bar{t}=0)\,, \\
&= \exp\left(-\frac{1}{\omega}\min\left\{\frac{(1-\sigma)\alpha}{\lambda_{\max}(P)}, \mu\right\}\bar{t}\right) \left(\hat{G}_{\text{av}}^T(0) P \hat{G}_{\text{av}}(0) + \upsilon_{\text{av}}(0)\right)\,.
\end{aligned} \tag{6.135}$$

Since there exists a positive scalar κ such that

$$\upsilon_{\rm av}(0) \leq \kappa \hat{G}_{\rm av}^T(0) P \hat{G}_{\rm av}(0)\,, \tag{6.136}$$

it is possible to write

$$\hat{G}_{\rm av}^T(\bar{t}) P \hat{G}_{\rm av}(\bar{t}) \leq \exp\left(-\frac{1}{\omega}\min\left\{\frac{(1-\sigma)\alpha}{\lambda_{\max}(P)}, \mu\right\}\bar{t}\right)(1+\kappa)\,\hat{G}_{\rm av}^T(0) P \hat{G}_{\rm av}(0)\,, \tag{6.137}$$

Therefore, from (6.120), one gets

$$\lambda_{\min}(P)\|\hat{G}_{\rm av}(\bar{t})\|^2 \leq \exp\left(-\frac{1}{\omega}\min\left\{\frac{(1-\sigma)\alpha}{\lambda_{\max}(P)}, \mu\right\}\bar{t}\right)(1+\kappa)\,\lambda_{\max}(P)\|\hat{G}_{\rm av}(0)\|^2\,. \tag{6.138}$$

Then,

$$\begin{aligned}\|\hat{G}_{\rm av}(\bar{t})\|^2 &\leq \exp\left(-\frac{1}{\omega}\min\left\{\frac{(1-\sigma)\alpha}{\lambda_{\max}(P)}, \mu\right\}\bar{t}\right)\frac{(1+\kappa)\,\lambda_{\max}(P)}{\lambda_{\min}(P)}\|\hat{G}_{\rm av}(0)\|^2 \\ &= \left[\exp\left(-\frac{1}{2\omega}\min\left\{\frac{(1-\sigma)\alpha}{\lambda_{\max}(P)}, \mu\right\}\bar{t}\right)\sqrt{\frac{(1+\kappa)\,\lambda_{\max}(P)}{\lambda_{\min}(P)}}\|\hat{G}_{\rm av}(0)\|\right]^2\,.\end{aligned} \tag{6.139}$$

equivalently,

$$\|\hat{G}_{\rm av}(\bar{t})\|^2 - \left[\exp\left(-\frac{1}{2\omega}\min\left\{\frac{(1-\sigma)\alpha}{\lambda_{\max}(P)}, \mu\right\}\bar{t}\right)\sqrt{\frac{(1+\kappa)\,\lambda_{\max}(P)}{\lambda_{\min}(P)}}\|\hat{G}_{\rm av}(0)\|\right]^2 \leq 0\,. \tag{6.140}$$

Hence,

$$\begin{aligned}&\left[\|\hat{G}_{\rm av}(\bar{t})\| + \exp\left(-\frac{1}{2\omega}\min\left\{\frac{(1-\sigma)\alpha}{\lambda_{\max}(P)}, \mu\right\}\bar{t}\right)\sqrt{\frac{(1+\kappa)\,\lambda_{\max}(P)}{\lambda_{\min}(P)}}\|\hat{G}_{\rm av}(0)\|\right] \\ &\times\left[\|\hat{G}_{\rm av}(\bar{t})\| - \exp\left(-\frac{1}{2\omega}\min\left\{\frac{(1-\sigma)\alpha}{\lambda_{\max}(P)}, \mu\right\}\bar{t}\right)\sqrt{\frac{(1+\kappa)\,\lambda_{\max}(P)}{\lambda_{\min}(P)}}\|\hat{G}_{\rm av}(0)\|\right] \leq 0\end{aligned} \tag{6.141}$$

and

$$\|\hat{G}_{\rm av}(\bar{t})\| \leq \exp\left(-\frac{1}{2\omega}\min\left\{\frac{(1-\sigma)\alpha}{\lambda_{\max}(P)}, \mu\right\}\bar{t}\right)\sqrt{\frac{(1+\kappa)\,\lambda_{\max}(P)}{\lambda_{\min}(P)}}\|\hat{G}_{\rm av}(0)\|\,. \tag{6.142}$$

Although the analysis has been focused on the convergence of $\hat{G}_{\rm av}(\bar{t})$ and, conse-

quently, $\hat{G}(t)$, the obtained results through (6.142) can be easily extended to the variables $\tilde{\theta}_{\text{av}}(\bar{t})$ and $\tilde{\theta}(t)$. From Assumption 1, the quadratic matrix H^* has linearly independent rows and columns. Furthermore, from Assumption 2, P is a symmetric and positive definite matrix. Thus, there exist a matrix R with independent columns such that $P = R^T R$ and, consequently, $\bar{P} = H^{*T} P H^*$ is a symmetric and positive definite matrix [109, Section 6.5]. Thus, by using (6.52), the quadratic term $\hat{G}_{\text{av}}^T(\bar{t}) P \hat{G}_{\text{av}}(\bar{t})$ in (6.119) is written as

$$\begin{aligned}\hat{G}_{\text{av}}^T(\bar{t}) P \hat{G}_{\text{av}}(\bar{t}) &= (H^* \tilde{\theta}_{\text{av}}(\bar{t}))^T P (H^* \tilde{\theta}_{\text{av}}(\bar{t})) \\ &= \tilde{\theta}_{\text{av}}^T(\bar{t}) H^{*T} P H^* \tilde{\theta}_{\text{av}}(\bar{t}) \\ &= \tilde{\theta}_{\text{av}}^T(\bar{t}) \bar{P} \tilde{\theta}_{\text{av}}(\bar{t}) \,, \end{aligned} \tag{6.143}$$

with the Rayleigh-Ritz inequality

$$\lambda_{\min}(\bar{P}) \|\tilde{\theta}_{\text{av}}(\bar{t})\|^2 \leq \tilde{\theta}_{\text{av}}^T(\bar{t}) \bar{P} \tilde{\theta}_{\text{av}}(\bar{t}) \leq \lambda_{\max}(\bar{P}) \|\tilde{\theta}_{\text{av}}(\bar{t})\|^2 \,. \tag{6.144}$$

Therefore, inequality (6.137) can be rewritten as

$$\tilde{\theta}_{\text{av}}^T(\bar{t}) \bar{P} \tilde{\theta}_{\text{av}}(\bar{t}) \leq \exp\left(-\frac{1}{\omega} \min\left\{ \frac{(1-\sigma)\alpha}{\lambda_{\max}(P)}, \mu \right\} \bar{t} \right) (1+\kappa)\, \tilde{\theta}_{\text{av}}^T(0) \bar{P} \tilde{\theta}_{\text{av}}(0) \,. \tag{6.145}$$

Now, by considering inequalities (6.145) and (6.144), and following the steps between (6.137) and (6.142), one obtains

$$\|\tilde{\theta}_{\text{av}}(\bar{t})\| \leq \exp\left(-\frac{1}{2\omega} \min\left\{ \frac{(1-\sigma)\alpha}{\lambda_{\max}(P)}, \mu \right\} \bar{t} \right) \sqrt{\frac{(1+\kappa)\, \lambda_{\max}(\bar{P})}{\lambda_{\min}(\bar{P})}} \|\tilde{\theta}_{\text{av}}(0)\| \,. \tag{6.146}$$

Since the differential equation (6.36) has discontinuous right hand size, $\tilde{\Theta}(\bar{t}, \tilde{\theta}(\bar{t}), e(\bar{t}))$ in (6.39) is T-periodic in t and satisfy the Lipschitz condition. From (6.146), by invoking [103, Theorem 2], the $\tilde{\theta}_{\text{av}}(\bar{t})$ is asymptotically stable. That is

$$\|\tilde{\theta}(t) - \tilde{\theta}_{\text{av}}(t)\| \leq \mathcal{O}\left(\frac{1}{\omega} \right) . \tag{6.147}$$

Using the triangle inequality [110], one has

$$\begin{aligned}\|\tilde{\theta}(t)\| &\leq \|\tilde{\theta}_{\text{av}}(t)\| + \mathcal{O}\left(\frac{1}{\omega} \right) \\ &\leq \exp\left(-\frac{1}{2\omega} \min\left\{ \frac{(1-\sigma)\alpha}{\lambda_{\max}(P)}, \mu \right\} \bar{t} \right) \sqrt{\frac{(1+\kappa)\, \lambda_{\max}(\bar{P})}{\lambda_{\min}(\bar{P})}} \|\tilde{\theta}_{\text{av}}(0)\| + \mathcal{O}\left(\frac{1}{\omega} \right). \end{aligned} \tag{6.148}$$

Furthermore,

$$\|\hat{G}(t) - \hat{G}_{\text{av}}(t)\| \leq \mathcal{O}\left(\frac{1}{\omega}\right), \tag{6.149}$$

and again using the triangle inequality [110], one obtains

$$\begin{aligned}\|\hat{G}(t)\| &\leq \|\hat{G}_{\text{av}}(t)\| + \mathcal{O}\left(\frac{1}{\omega}\right) \\ &\leq \exp\left(-\frac{1}{2\omega}\min\left\{\frac{(1-\sigma)\alpha}{\lambda_{\max}(P)}, \mu\right\}\bar{t}\right)\sqrt{\frac{(1+\kappa)\,\lambda_{\max}(\bar{P})}{\lambda_{\min}(\bar{P})}}\|\tilde{\theta}_{\text{av}}(0)\| + \mathcal{O}\left(\frac{1}{\omega}\right).\end{aligned} \tag{6.150}$$

Now, from (6.12), we have

$$\theta(t) - \theta^* = \tilde{\theta}(t) + S(t)\,, \tag{6.151}$$

whose norm satisfies

$$\begin{aligned}\|\theta(t) - \theta^*\| &= \|\tilde{\theta}(t) + S(t)\| \\ &\leq \|\tilde{\theta}(t)\| + \|S(t)\| \\ &\leq \exp\left(-\frac{1}{2\omega}\min\left\{\frac{(1-\sigma)\alpha}{\lambda_{\max}(P)}, \mu\right\}\bar{t}\right)\sqrt{\frac{(1+\kappa)\,\lambda_{\max}(\bar{P})}{\lambda_{\min}(\bar{P})}}\|\theta(0) - \theta^*\| + \\ &\quad + \mathcal{O}\left(a + \frac{1}{\omega}\right).\end{aligned} \tag{6.152}$$

Defining the error variable

$$\tilde{y}(t) := y(t) - Q^*\,, \quad y(t) = Q(\theta(t)), \tag{6.153}$$

and using Cauchy-Schwartz inequality [105], we get

$$\begin{aligned}|\tilde{y}(t)| = |y(t) - Q^*| &= |(\theta(t) - \theta^*)^T H^*(\theta(t) - \theta^*)| \\ &\leq \|H^*\|\|\theta(t) - \theta^*\|^2\,,\end{aligned} \tag{6.154}$$

and with the help of (6.152)

$$|\tilde{y}(t)| \leq \|H^*\| \left[\exp\left(-\frac{1}{\omega} \min\left\{ \frac{(1-\sigma)\alpha}{\lambda_{\max}(P)}, \mu \right\} \bar{t} \right) \frac{(1+\kappa)\,\lambda_{\max}(\bar{P})}{\lambda_{\min}(\bar{P})} \|\theta(0)-\theta^*\|^2 + \right.$$
$$+ 2\exp\left(-\frac{1}{2\omega} \min\left\{ \frac{(1-\sigma)\alpha}{\lambda_{\max}(P)}, \mu \right\} \bar{t} \right) \sqrt{\frac{(1+\kappa)\,\lambda_{\max}(\bar{P})}{\lambda_{\min}(\bar{P})}} \|\theta(0)-\theta^*\| \times$$
$$\left. \times \mathcal{O}\left(a + \frac{1}{\omega}\right) + \mathcal{O}\left(a + \frac{1}{\omega}\right)^2 \right]. \tag{6.155}$$

Since $\exp\left(-\min\left\{\frac{(1-\sigma)\alpha}{\lambda_{\max}(P)}, \mu\right\}\frac{\bar{t}}{\omega}\right) \leq \exp\left(-\min\left\{\frac{(1-\sigma)\alpha}{\lambda_{\max}(P)}, \mu\right\}\frac{\bar{t}}{2\omega}\right)$ and from [94, Definition 10.1], $\|H^*\|\mathcal{O}\left(a+\frac{1}{\omega}\right)^2$ is of order $\mathcal{O}\left(a+\frac{1}{\omega}\right)^2$. Hence, (6.154) leads to

$$|y(t)-Q^*| \leq \exp\left(-\frac{1}{2\omega} \min\left\{ \frac{(1-\sigma)\alpha}{\lambda_{\max}(P)}, \mu \right\} \bar{t} \right) \|H^*\| \left[\frac{(1+\kappa)\,\lambda_{\max}(\bar{P})}{\lambda_{\min}(\bar{P})} \|\theta(0)-\theta^*\| + \right.$$
$$\left. + 2\sqrt{\frac{(1+\kappa)\,\lambda_{\max}(\bar{P})}{\lambda_{\min}(\bar{P})}} \left(a + \frac{1}{\omega}\right) \right] \|\theta(0)-\theta^*\| + \mathcal{O}\left(a^2 + 2\frac{a}{\omega} + \frac{1}{\omega^2}\right). \tag{6.156}$$

Knowing that $a\,, \omega > 0$ and using Young's inequality $\frac{a}{\omega} \leq \frac{a^2}{2} + \frac{1}{2\omega^2}$, one gets

$$|y(t)-Q^*| \leq \exp\left(-\frac{1}{2\omega} \min\left\{ \frac{(1-\sigma)\alpha}{\lambda_{\max}(P)}, \mu \right\} \bar{t} \right) \|H^*\| \left[\frac{(1+\kappa)\,\lambda_{\max}(\bar{P})}{\lambda_{\min}(\bar{P})} \|\theta(0)-\theta^*\| + \right.$$
$$\left. + 2\sqrt{\frac{(1+\kappa)\,\lambda_{\max}(\bar{P})}{\lambda_{\min}(\bar{P})}} \left(a + \frac{1}{\omega}\right) \right] \|\theta(0)-\theta^*\| + \mathcal{O}\left(a^2 + \frac{1}{\omega^2}\right) \tag{6.157}$$

since $\mathcal{O}\left(2a^2 + 2/\omega\right) = 2\mathcal{O}\left(a^2 + 1/\omega^2\right)$ is of order $\mathcal{O}\left(a^2 + 1/\omega^2\right)$ [94, Definition 10.1].

Now, defining the positive constants:

$$m = \frac{1}{2} \min\left\{ \frac{(1-\sigma)\alpha}{\lambda_{\max}(P)}, \mu \right\}, \tag{6.158}$$

$$M_\theta = \sqrt{\frac{(1+\kappa)\lambda_{\max}(\bar{P})}{\lambda_{\min}(\bar{P})}} \|\theta(0)-\theta^*\|, \tag{6.159}$$

$$M_y = \|H^*\| \frac{(1+\kappa)\,\lambda_{\max}(\bar{P})}{\lambda_{\min}(\bar{P})} \|\theta(0)-\theta^*\|^2$$
$$+ 2\|H^*\| \sqrt{\frac{(1+\kappa)\,\lambda_{\max}(\bar{P})}{\lambda_{\min}(\bar{P})}} \left(a + \frac{1}{\omega}\right) \|\theta(0)-\theta^*\|, \tag{6.160}$$

inequalities (6.152) and (6.157) satisfy (6.109) and (6.110), respectively.

Notice that, from (6.55) and (6.59), and using the Peter-Paul inequality [106], we can write $cd \leq \frac{c^2}{2\epsilon} + \frac{\epsilon d^2}{2}$, for all $c, d, \epsilon > 0$, with $c = \|e_{\text{av}}(\bar{t})\|$, $d = \|\hat{G}_{\text{av}}(\bar{t})\|$,

$\epsilon = \frac{\sigma\lambda_{\min}(Q)}{2\|PH^*K\|}$ and $\bar{t} \in [t_k\,, t_{k+1})$. The following holds

$$\begin{aligned}
&\upsilon_{\rm av}(\bar{t})+\gamma\left[\sigma\alpha\|\hat{G}_{\rm av}(\bar{t})\|^2-\beta\|e_{\rm av}(\bar{t})\|\|\hat{G}_{\rm av}(\bar{t})\|\right] \geq \\
&\upsilon_{\rm av}(\bar{t})+\gamma\left[\sigma\alpha\|\hat{G}_{\rm av}(\bar{t})\|^2-\frac{\beta}{2}\left(\frac{\sigma\alpha}{\beta}\|\hat{G}_{\rm av}(\bar{t})\|^2+\frac{\beta}{\sigma\alpha}\|e_{\rm av}(\bar{t})\|^2\right)\right] \\
&= \upsilon_{\rm av}(\bar{t}) + \gamma\left(q\|\hat{G}_{\rm av}(\bar{t})\|^2 - p\|e_{\rm av}(\bar{t})\|^2\right)\,, \qquad (6.161)
\end{aligned}$$

where

$$q = \frac{\sigma\alpha}{2} \quad \text{and} \quad p = \frac{\beta^2}{2\sigma\alpha}\,. \qquad (6.162)$$

The minimum dwell-time of the event-triggered framework is given by the time it takes for the function

$$\phi(\bar{t}) = \frac{\sqrt{\gamma p}\|e_{\rm av}(\bar{t})\|}{\sqrt{\upsilon_{\rm av}(\bar{t}) + \gamma q\|\hat{G}_{\rm av}(\bar{t})\|^2}}\,, \qquad (6.163)$$

to go from 0 to 1. The derivative of $\phi(\bar{t})$ in (6.163) is given by

$$\begin{aligned}
\frac{d\phi(\bar{t})}{d\bar{t}} = &\frac{\sqrt{\gamma p}e_{\rm av}^T(\bar{t})\dfrac{de_{\rm av}(\bar{t})}{d\bar{t}}}{\|e_{\rm av}(\bar{t})\|\sqrt{\upsilon_{\rm av}(\bar{t}) + \gamma q\|\hat{G}_{\rm av}(\bar{t})\|^2}} + \\
&- \frac{\sqrt{\gamma p}\|e_{\rm av}(\bar{t})\|}{2(\upsilon_{\rm av}(\bar{t}) + \gamma q\|\hat{G}_{\rm av}(\bar{t})\|^2)^{3/2}}\left(\frac{d\upsilon_{\rm av}(\bar{t})}{d\bar{t}} + \gamma q\hat{G}_{\rm av}^T(\bar{t})\frac{d\hat{G}_{\rm av}(\bar{t})}{d\bar{t}}\right)\,. \qquad (6.164)
\end{aligned}$$

Now, from (6.31), (6.49), (6.50) and (6.161), one arrives at

$$\frac{de_{\rm av}(\bar{t})}{d\bar{t}} = -\frac{d\hat{G}_{\rm av}(\bar{t})}{d\bar{t}}\,, \qquad (6.165)$$

$$\left\|\frac{d\hat{G}_{\rm av}(\bar{t})}{d\bar{t}}\right\| \leq \frac{1}{\omega}\|H^*K\|\|\hat{G}_{\rm av}(\bar{t})\| + \frac{1}{\omega}\|H^*K\|\|e_{\rm av}(\bar{t})\|\,, \qquad (6.166)$$

$$\frac{d\upsilon_{\rm av}(\bar{t})}{d\bar{t}} \geq -\frac{\mu}{\omega}\upsilon_{\rm av}(\bar{t}) + \frac{q}{\omega}\|\hat{G}_{\rm av}(\bar{t})\|^2 - \frac{p}{\omega}\|e_{\rm av}(\bar{t})\|^2 \qquad (6.167)$$

and from (6.164) the following inequality holds

$$\begin{aligned}
\frac{d\phi(\bar{t})}{d\bar{t}} \leq &\frac{\|H^*K\|}{\omega}\sqrt{\frac{p}{q}} + \frac{\|H^*K\|}{\omega}\phi(\bar{t}) + \frac{1}{2\omega\gamma}\phi^3(\bar{t}) + \frac{\|H^*K\|}{\omega}\sqrt{\frac{q}{p}}\phi^2(\bar{t}) + \frac{\mu}{2\omega}\phi(\bar{t}) + \\
&+ \frac{\gamma q\|\hat{G}_{\rm av}(\bar{t})\|^2}{2\omega(\upsilon_{\rm av}(\bar{t}) + \gamma q\|\hat{G}_{\rm av}(\bar{t})\|^2)}\left(-\mu - \frac{1}{\gamma} + 2\|H^*K\|\right)\phi(\bar{t})\,. \qquad (6.168)
\end{aligned}$$

Hence, if $\|H^*K\| \leq \mu/2$, one has

$$\omega \frac{d\phi(\bar{t})}{d\bar{t}} \leq \|H^*K\| \sqrt{\frac{p}{q}} + 2\|H^*K\|\phi(\bar{t}) + \|H^*K\| \sqrt{\frac{q}{p}} \phi^2(\bar{t}) \,. \tag{6.169}$$

By using the transformation $t = \frac{\bar{t}}{\omega}$, inequality (6.169) and invoking the Comparison Lemma [94], a lower bound of the inter-execution time is found as

$$\tau^* = \int_0^1 \frac{1}{b_0 + b_1\xi + b_2\xi^2 + b_3\xi^3} d\xi \,, \tag{6.170}$$

with $b_0 = \dfrac{\beta\|H^*K\|}{\sigma\alpha}$, $b_1 = 2\|H^*K\|$, $b_2 = \dfrac{\sigma\alpha\|H^*K\|}{\beta}$ and $b_3 = 0$.

If $\|H^*K\| > \mu/2$ and $\gamma \leq 1/(2|H^*K\| - \mu)$, from (6.168) we get

$$\omega \frac{d\phi(\bar{t})}{d\bar{t}} \leq \|H^*K\| \sqrt{\frac{p}{q}} + \left(\frac{\mu}{2} + \|H^*K\|\right) \phi(\bar{t}) + \|H^*K\| \sqrt{\frac{q}{p}} \phi^2(\bar{t}) + \left(\|H^*K\| - \frac{\mu}{2}\right) \phi^3(\bar{t}) \tag{6.171}$$

and the minimum dwell-time τ^* satisfies (6.170) with $b_0 = \dfrac{\beta\|H^*K\|}{\sigma\alpha}$, $b_1 = \dfrac{\mu}{2} + \|H^*K\|$, $b_2 = \dfrac{\sigma\alpha\|H^*K\|}{\beta}$ and $b_3 = \|H^*K\| - \dfrac{\mu}{2}$.

Finally, if $\|H^*K\| > \mu/2$ and $\gamma > 1/(2\|H^*K\| - \mu)$, we obtain

$$\omega \frac{d\phi(\bar{t})}{d\bar{t}} \leq \|H^*K\| \sqrt{\frac{p}{q}} + \left(2\|H^*K\| - \frac{1}{2\gamma}\right) \phi(\bar{t}) + \|H^*K\| \sqrt{\frac{q}{p}} \phi^2(\bar{t}) + \frac{1}{2\gamma} \phi^3(\bar{t}) \,, \tag{6.172}$$

and the lower bound τ^* satisfies equation (6.170) with constants $b_0 = \dfrac{\beta\|H^*K\|}{\sigma\alpha}$, $b_1 = 2\|H^*K\| - \dfrac{1}{2\gamma}$, $b_2 = \dfrac{\sigma\alpha\|H^*K\|}{\beta}$ and $b_3 = \dfrac{1}{2\gamma}$.Therefore, Zeno behavior is avoided [107]. □

Corollary 2. *(Dynamic Event-Tiggered Extremum Seeking with known Hessian): Consider the partial knowledge of the nonlinear map (6.1) such that the Hessian matrix H^* is a known parameter. Although this hypothesis appears to simplify the problem, one should note that the extremum seeking strategy is still justified once the optimizer vector θ^* and parameter Q^* are unknown. Then, $\Xi(\hat{G}, e)$ defined in (6.29) is equivalent to*

$$\Xi(\hat{G}, e) = \sigma\hat{G}^T(t)Q\hat{G}(t) - 2\hat{G}^T(t)PH^*Ke(t)$$

and the dynamic event-triggered mechanism

$$t_{k+1} = \inf\left\{t \in \mathbb{R}^+ : t > t_k \ \wedge \ \upsilon(t) + \gamma\Xi(\hat{G}, e) < 0\right\},$$

where

$$\dot{\upsilon}(t) = -\mu\upsilon(t) + \Xi(\hat{G}, e)\,,$$

ensures the local asymptotically stability of the closed-loop from Theorem 6.

6.5 Simulation results

We consider the multivariable nonlinear map (6.1) with an input $\theta(t) \in \mathbb{R}^2$, an output $y(t) \in \mathbb{R}$, and unknown parameters

$$H = \begin{bmatrix} 100 & 30 \\ 30 & 20 \end{bmatrix} > 0\,, \tag{6.173}$$

$Q^* = 100$ and $\theta^* = \begin{bmatrix} 2 & 4 \end{bmatrix}^T$. The dither vectors (6.8) and (6.9) have parameters $a_1 = a_2 = 0.1$, $\omega_1 = 0.7$ [rad/sec], and $\omega_2 = 0.5$ [rad/sec], as in [51], and we select the event-triggered parameters $\sigma = 0.5$, $\alpha = 1$, $\beta = 3.1521$, $\mu = 0.4320$ and $\gamma = 0.0542$. The control gain matrix is $K = 10^{-2}\begin{bmatrix} -6 & 0 \\ 0 & -20 \end{bmatrix}$ and initial condition is $\upsilon(0) = 0$.

In Fig. 6.5, both strategies are simulated, static and dynamic event-triggered approaches with initial condition $\hat{\theta}(0) = \begin{bmatrix} 2.5, & 6 \end{bmatrix}^T$. Fig. 6.4(a) and Fig. 6.4(b) shows the convergence to zero of both the sampled-and-hold version of the gradient estimate when the control signals are given by Fig. 6.4(c) and Fig. 6.4(d), respectively. Of course, the gradient stabilization implies reaching the optimizer θ^*, as illustrated in Fig. 6.5(a) and Fig. 6.5(b), consequently, the variable $y(t)$ reaches its extremum value as shown in Fig. 6.5(c) and Fig. 6.5(d).

Hereafter, we have considered several simulations by using the set of initial conditions $\hat{\theta}(0) = \begin{bmatrix} 2 - 2\cos\left(\frac{2\pi}{100}i\right), & 4 - 2\sin\left(\frac{2\pi}{100}i\right) \end{bmatrix}^T$ for $i = 1, \ldots, 100$. Fig. 6.8 shows the time-evolution of the proposed dynamic event-triggered extremum seeking approaches. For all initial conditions, the input signal in Fig. 6.7(a) and Fig. 6.7(b) ensures convergence of the gradient estimate as well as the measurement error as presented in Fig. 6.7(c)–Fig. 6.8(d). Thus, $\theta_1(t)$ and $\theta_2(t)$ tend asymptotically to θ_1^* and θ_2^*, respectively, consequently, $y(t)$ to Q^* (see Fig. 6.6, Fig. 6.8(e) and Fig. 6.8(f).

Finally, Table 6.1 summarizes the statistical data obtained for a set of 5400 simulations of 300 seconds. For any value σ, it is possible to verify that the interval between executions as well as the dispersion measures (mean deviation, variance and standard deviation) are greater when the dynamic strategy is employed. For

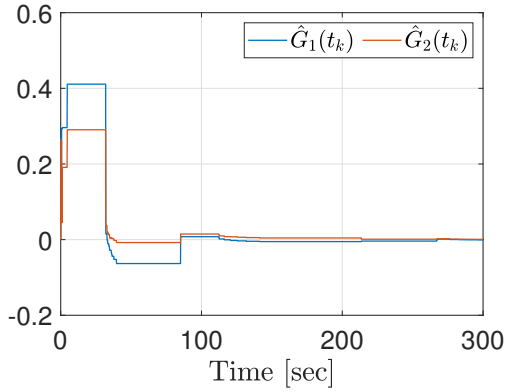

(a) **Static:** sample-and-hold gradient estimate, $\hat{G}(t_k)$.

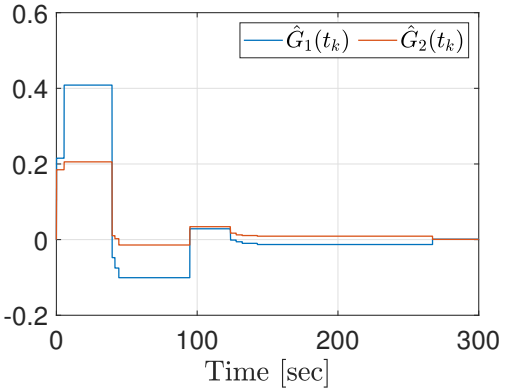

(b) **Dynamic:** sample-and-hold gradient estimate, $\hat{G}(t_k)$.

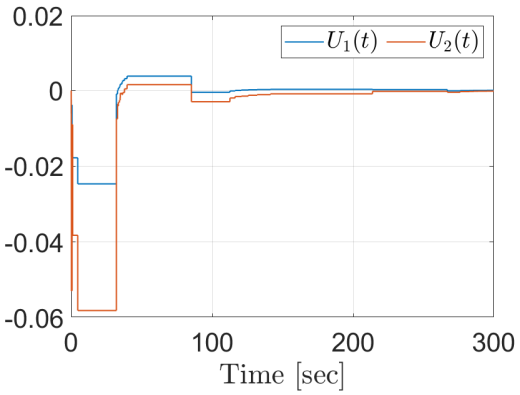

(c) **Static:** control input, $U(t)$.

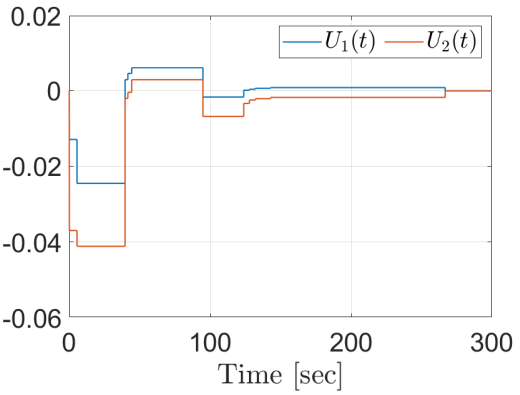

(d) **Dynamic:** control input, $U(t)$.

Figure 6.4: Static and Dynamic Event-triggered Extremum Seeking Systems.

instance, on average, with $\sigma = 0.001$, the static strategy performs 1021 updates while the dynamic one needs 755 updates. When, $\sigma = 0.9$, the static case requires 46 updates versus 15 for the dynamic case. Although the control objective is achieved with both strategies, it is worth noting that the dynamic strategy achieves the extremum employing less control effort and requiring a small number of control updates when compared with the static approach (see Table 6.1).

Table 6.1: Statistics of the inter-execution intervals, $t_{k+1} - t_k$.

	Mean		Mean Deviation		Variance		Standard Deviation	
σ	Static	Dynamic	Static	Dynamic	Static	Dynamic	Static	Dynamic
0.001	0.2939	0.3974	0.5088	0.7330	13.9295	22.3420	3.7322	4.7268
0.002	0.3099	0.4381	0.5337	0.8048	14.3554	23.8753	3.7888	4.8862
0.003	0.3301	0.7370	0.5670	1.3255	15.5122	39.9080	3.9386	6.3173
0.004	0.3496	0.7096	0.5983	1.2811	16.2814	38.8355	4.0350	6.2318
0.005	0.3818	0.8633	0.6512	1.5367	17.6344	48.3978	4.1993	6.9569
0.006	0.4150	0.8587	0.7029	1.5310	18.5522	48.7397	4.3072	6.9814
0.007	0.4365	1.0187	0.7369	1.7873	19.3296	56.6231	4.3965	7.5248
0.008	0.4260	0.7903	0.7179	1.4177	18.8293	43.4613	4.3393	6.5925
0.009	0.4284	0.8496	0.7209	1.5189	19.0454	48.5479	4.3641	6.9676
0.010	0.4686	0.9245	0.7843	1.6425	20.8145	53.0984	4.5623	7.2869
0.020	0.6191	1.3454	1.0229	2.3079	28.7969	73.6432	5.3663	8.5816
0.030	0.7958	1.4215	1.2801	2.4192	37.2480	78.3938	6.1031	8.8540
0.040	0.8192	1.5215	1.3319	2.5772	40.4228	85.4836	6.3579	9.2457
0.050	0.9848	1.9907	1.5642	3.2645	48.6906	109.4917	6.9779	10.4638
0.060	1.1553	2.4570	1.8035	3.9291	55.7665	133.7192	7.4677	11.5637
0.070	1.2836	2.3071	1.9779	3.7365	65.7437	127.1205	8.1082	11.2748
0.080	1.1995	2.8969	1.8986	4.5692	61.9130	160.1954	7.8685	12.6568
0.090	1.4664	2.9279	2.2550	4.5974	74.3021	163.4882	8.6199	12.7862
0.100	1.2588	2.5863	1.9952	4.1467	64.1229	147.5280	8.0077	12.1461
0.200	1.9571	5.1650	3.1000	7.7201	102.7835	286.3306	10.1382	16.9213
0.300	2.0788	7.0843	3.3859	10.2374	113.2025	391.6320	10.6397	19.7897
0.400	3.4475	9.3378	5.3195	12.8145	180.9892	479.3062	13.4532	21.8931
0.500	3.9839	10.5757	6.1247	14.4068	218.1339	566.1838	14.7694	23.7946
0.600	3.4004	12.8756	5.5095	16.9665	191.6231	608.7021	13.8428	24.6719
0.700	5.0007	14.7065	7.6219	18.9248	259.6896	677.2911	16.1149	26.0248
0.800	5.6172	16.5772	8.4851	21.8088	297.7478	807.1438	17.2554	28.4103
0.900	6.6610	20.2129	10.1423	25.3364	445.3767	876.5687	21.1039	29.6069

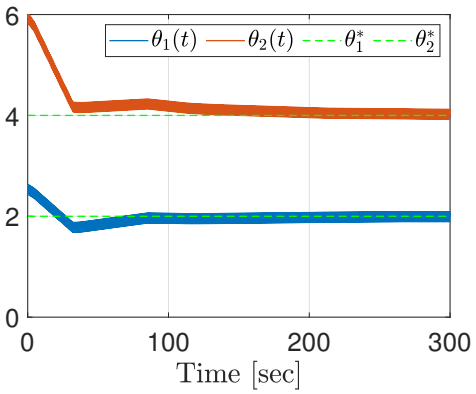

(a) **Static:** input of the nonlinear map, $\theta(t)$.

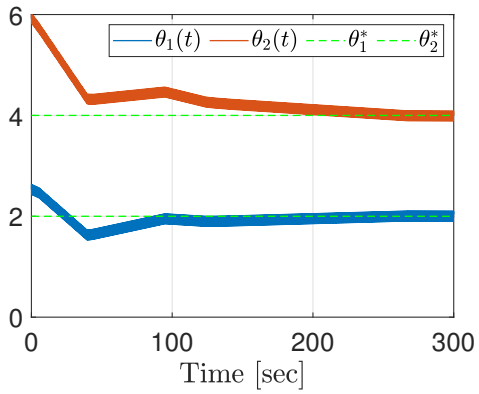

(b) **Dynamic:** input of the nonlinear map, $\theta(t)$.

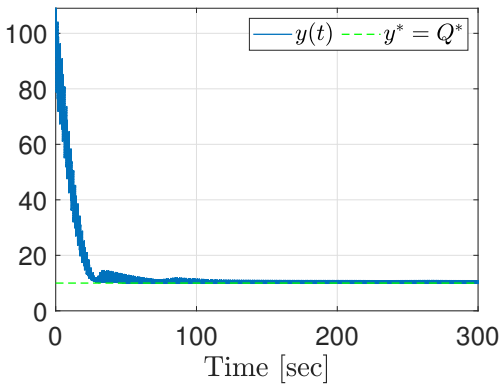

(c) **Static:** output of the nonlinear map, $y(t)$.

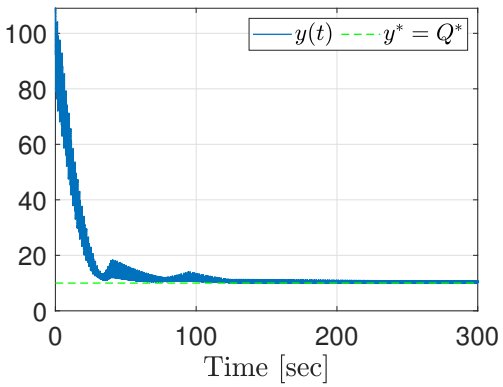

(d) **Dynamic:** output of the nonlinear map, $y(t)$.

Figure 6.5: Static and Dynamic Event-triggered Extremum Seeking Systems.

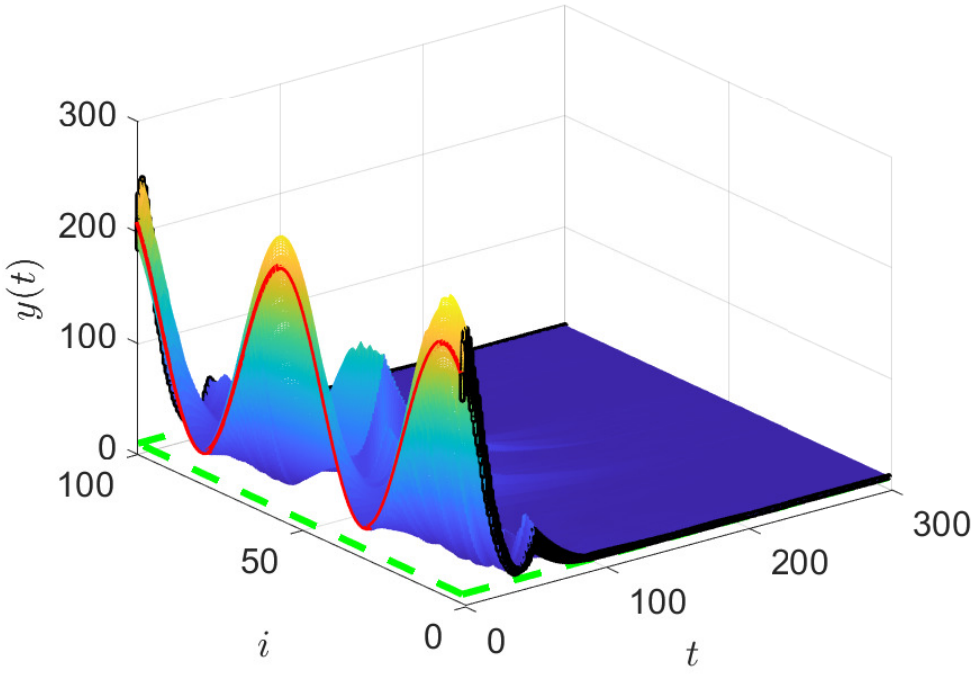

Figure 6.6: Output of the nonlinear map, $y(t)$.

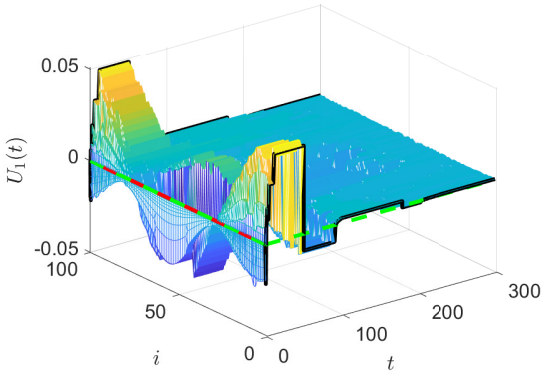

(a) Component of the control signal, $U_1(t)$.

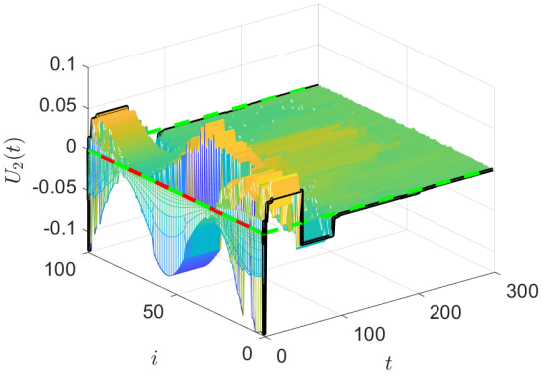

(b) Component of the control signal, $U_2(t)$.

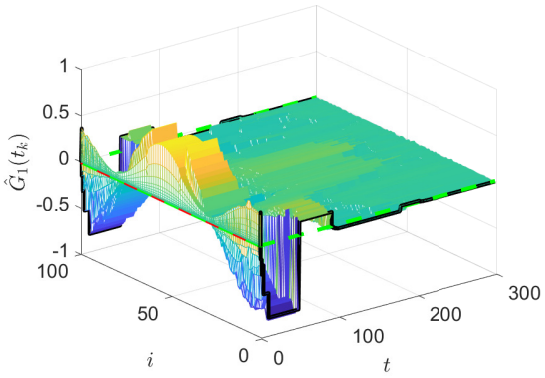

(c) Sample-and-hold of the gradient estimate component, $\hat{G}_1(t_k)$.

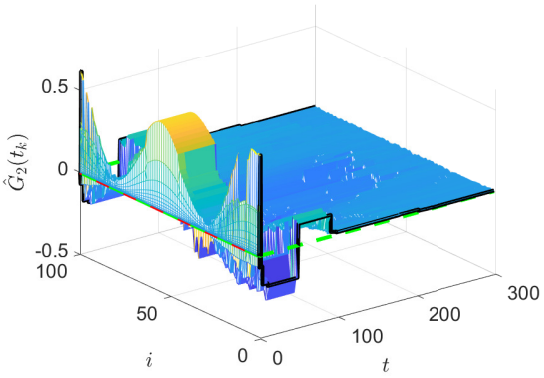

(d) Sample-and-hold of the gradient estimate component, $\hat{G}_2(t_k)$.

Figure 6.7: Dynamic Event-triggered Extremum Seeking Feedback System.

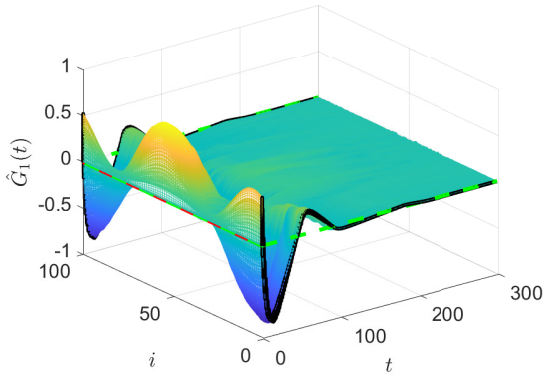

(a) Component of the gradient estimate, $\hat{G}_1(t)$.

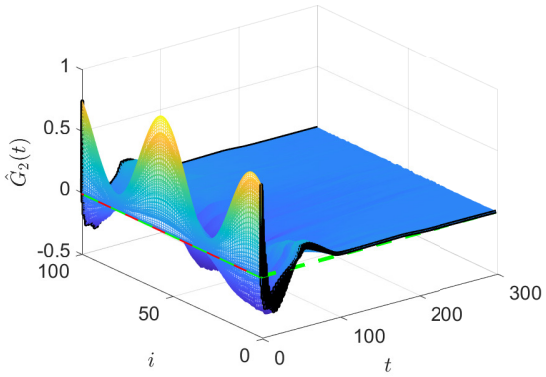

(b) Component of the gradient estimate, $\hat{G}_2(t)$.

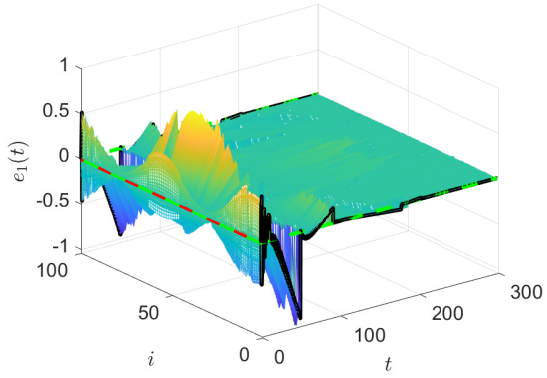

(c) Component of the measurement error, $e_1(t)$.

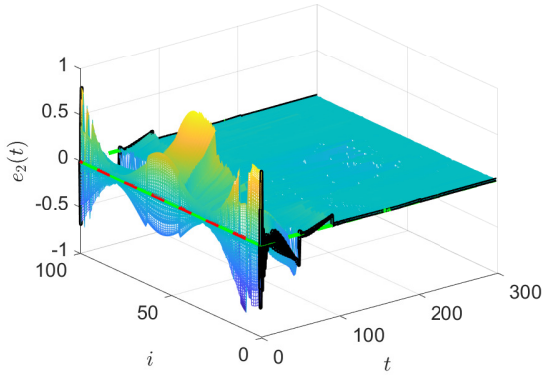

(d) Component of the measurement error, $e_2(t)$.

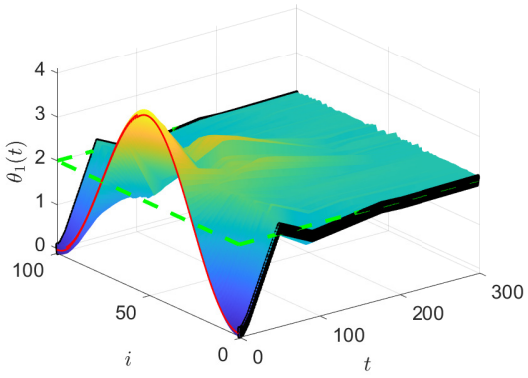

(e) Component of the nonlinear map input, $\theta_1(t)$.

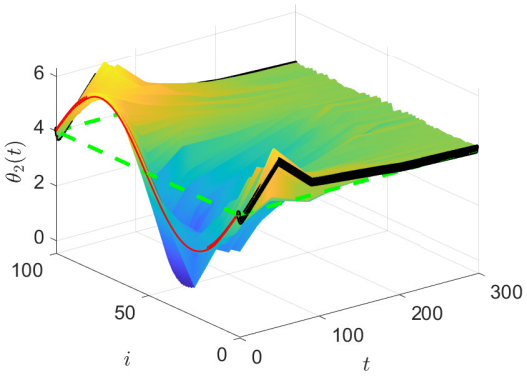

(f) Component of the nonlinear map input, $\theta_2(t)$.

Figure 6.8: Dynamic Event-triggered Extremum Seeking Feedback System.

Chapter 7

Conclusion, Publication List and Future Works

7.1 Conclusion

New output-feedback adaptive sliding mode (scalar) and unit vector (multivariable) controllers were proposed, respectively, in Chapters 2 and 3, for plants under parametric uncertainties and (un)matched disturbances with unknown upper bounds. By combining monitoring and barrier functions, the MBF controllers were shown to exhibit the advantages of each of the individual adaptive approaches. Namely, it allows a specified transient behavior to be achieved and ultimate finite-time convergence to a desired arbitrarily small invariant residual set of the tracking error, whilst avoiding overestimation of the control signal. In addition, the monitoring function can be adjusted in order to preclude abrupt control changes in the transition from monitoring to the barrier function. Nevertheless, the case in which the unmodeled dynamics is present [111] is left as an interesting future work. The theoretical results are illustrated by means of numerical simulations for an academic example as well as for an anti-lock braking system application.

In Chapters 4–6 we proposed the static and dynamic for both scalar and multivariable event-triggered extremum seeking. The contribution of treating the specific hybrid learning dynamics [86] constituted by the sample-and-hold system is clear. The approach provides explicit functional forms for the exponential convergence characterizing the stability properties of the closed-loop system. The approach will be extended to PDE systems following [55, 56] and [84, 85].

7.2 Publication List

In this section, it is shown the publications of the results obtained through this doctoral thesis.

Articles in Scientific Journals

1. **RODRIGUES, V. H. P.**; HSU, L.; OLIVEIRA, T. R.; DIAGNE, M.. *Multivariable Event-Triggered Extremum Seeking.* IEEE Transactions on Automatic Control. (UNDER REVIEW)
2. **RODRIGUES, V. H. P.**; FANTINATTI, M.; HSU, L.; OLIVEIRA, T. R.. *Population Control of Giardia lamblia.* IEEE/CAA Journal of Automatica Sinica (UNDER REVIEW)
3. **RODRIGUES, V. H. P.**; HSU, L.; OLIVEIRA, T. R.; FRIDMAN, L. M.. *Adaptive Sliding Mode Control with Guaranteed Performance based on Monitoring and Barrier Functions.* International Journal of Adaptive Control and Signal Processing, v. 36, p. 1252-1271, 2022. `https://doi.org/10.1002/acs.3278`

Book Chapter Published

1. **RODRIGUES, V. H. P.**; HSU, L.; OLIVEIRA, T. R.; FRIDMAN, L. M.. *Unit Vector Control with Prescribed Performance via Monitoring and Barrier Functions*, In: Studies in Systems, Decision and Control, Sliding-Mode Control and Variable-Structure Systems, Tiago Roux Oliveira, Leonid Fridman and Liu Hsu (editors), Springer Nature. (ACCEPTED)

Complete works published in proceedings of conferences

1. **RODRIGUES, V. H. P.**; HSU, L.; OLIVEIRA, T. R.. *Binary Model Reference Adaptive Control under Disturbances.* In: 16th International Workshop on Variable Structure Systems and Sliding Mode Control (VSS 2022), 2022, Rio de Janeiro. (UNDER REVIEW)
2. **RODRIGUES, V. H. P.**; HSU, L.; OLIVEIRA, T. R.; DIAGNE, M.. *Dynamic Event-Triggered Extremum Seeking Feedback.* In: 61st IEEE Conference on Decision and Control (CDC 2022), 2022, Cancún. (UNDER REVIEW)
3. **RODRIGUES, V. H. P.**; HSU, L.; OLIVEIRA, T. R.; ANJOS, P. V. M.. *Busca Extremal baseada em Eventos com Acionamento Dinâmico.* In: 24th Congresso Brasileiro de Automática (CBA 2022), 2022, Fortaleza. (UNDER REVIEW)

4. **RODRIGUES, V. H. P.**; HSU, L.; OLIVEIRA, T. R.; DIAGNE, M.. *Event-Triggered Extremum Seeking Control.* In: 14th IFAC International Workshop on Adaptive and Learning Control Systems (ALCOS 2022), 2022, Casablanca. (ACCEPTED)

5. **RODRIGUES, V. H. P.**; HSU, L.; OLIVEIRA, T. R.. *Global Synchronization and Secure Communication via Cascade Norm Observers and Equivalent Control.* In: 6th IFAC Conference on Analysis and Control of Chaotic Systems (CHAOS'2021), 2021, Catania. `https://doi.org/10.1016/j.ifacol.2021.11.026`

6. **RODRIGUES, V. H. P.**; HSU, L.; OLIVEIRA, T. R.; FRIDMAN, L. M.. *Busca Extremal baseada em Eventos.* In: Anais do 15º Simpósio Brasileiro de Automação Inteligente (SBAI'2021), 2021, Rio Grande. `http://dx.doi.org/10.20906/sbai2021/216633`

7. **RODRIGUES, V. H. P.**; HSU, L.; OLIVEIRA, T. R.; FRIDMAN, L. M.. *Controle Vetorial Unitário Adaptativo via Funções de Barreira e Monitoração.* In: Congresso Brasileiro de Automática 2020. `http://dx.doi.org/10.48011/asba.v2i1.1124`

8. **RODRIGUES, V. H. P.**; FANTINATTI, M.; HSU, L.; OLIVEIRA, T. R.. *Controle Populacional de Giardia lamblia.* In: Anais do 14º Simpósio Brasileiro de Automação Inteligente, 2019. `http://dx.doi.org/10.17648/sbai-2019-111578`

7.3 Future Works

The techniques developed in this thesis allow progress in the following research field:

1. Adaptive SMC with Monitoring and Barrier Functions

   - Generalization to Twisting SMC (SISO and MIMO);
   - Generalization to Super-Twisting Algorithm (STA) (SISO and MIMO);
   - Generalization to High-Order Sliding Mode (HOSM) Differentiator (SISO and MIMO);

2. B-MRAC with disturbance

   - Generalization to relative degree greater than the unity;

3. Event-Triggered Extremum Seeking

   - To develop co-design strategies (static and dynamic). In the co-design strategy the control law and the event-triggered mechanism are designed simultaneously, possibly leading to better performance and larger inter-event times [112];
   - To consider the data-packet dropout [61];
   - To consider delays [60].

References

[1] INTECO. *The laboratory Anti-lock Braking System controlled from PC – User's Manual*. Relatório técnico, INTECO sp. z o.o., Poland, 2011.

[2] HUANG, Y.-J., KUO, T.-C., CHANG, S.-H. "Adaptive Sliding-mode Control for Nonlinear Systems with Uncertain Parameters", *IEEE Transactions on System, Man, and Cybernetics – Part B: Cybernetics*, v. 38, pp. 534–539, 2008.

[3] UTKIN, V. I., GULDNER, J., SHI, J. *Sliding Mode Control in Electro-Mechanical Systems*. CRC Press, 2009.

[4] ANGULO, M. T., FRIDMAN, L., MORENO, J. A. "Output-feedback finite-time stabilization of disturbed feedback linearizable nonlinear systems", *Automatica*, v. 49, n. 9, pp. 2767–2773, 2013.

[5] ANGULO, M. T., FRIDMAN, L., LEVANT, A. "Output-feedback finite-time stabilization of disturbed LTI systems", *Automatica*, v. 48, n. 4, pp. 606–611, 2012.

[6] PLESTAN, F., SHTESSEL, Y., BRÉGEAULT, V., et al. "New methodologies for adaptive sliding mode control", *International Journal of Control*, v. 83, n. 9, pp. 1907–1919, 2010.

[7] SHTESSEL, Y., TALEB, M., PLESTAN, F. "A novel adaptive-gain supertwisting sliding mode controller: methodology and application", *Automatica*, v. 48, n. 5, pp. 759–769, 2012.

[8] EDWARDS, C., FLOQUET, T., SPURGEON, S. In: *Modern Sliding Mode Control Theory*, cap. Circumventing the relative degree condition in sliding mode design, pp. 137–158, Springer-Verlag, 2008.

[9] POLYAKOV, A., EFIMOV, D., PERRUQUETTI, W. "Finite-time and fixed-time stabilization: Implicit Lyapunov function approach", *Automatica*, v. 51, n. 1, pp. 332–340, 2015.

[10] UTKIN, V. I. *Sliding Modes in Control and Optimization.* Germany, Springer Verlag, 1992.

[11] LEVANT, A. "Higher-order sliding modes, differentiation and output-feedback control", *International Journal of Control*, v. 76, n. 9, pp. 924–941, 2003.

[12] OBEID, H., FRIDMAN, L. M., LAGHROUCHE, S., et al. "Barrier function-based adaptive sliding mode control", *Automatica*, v. 93, pp. 540–544, 2016.

[13] INCREMONA, G. P., CUCUZZELLA, M., MOSCA, A., et al. "Adaptive sub-optimal second-order sliding mode control for microgrids", *International Journal of Control*, v. 89, pp. 1849–1867, 2016.

[14] NEGRETE-CHÁVEZ, D. Y., MORENO, J. "Second-order sliding mode output feedback controller with adaptation", *International Journal of Adaptive Control and Signal Processing*, v. 30, n. 8–10, pp. 1523–1543, 2016.

[15] HSU, L., OLIVEIRA, T. R., CUNHA, J. P. V. S., et al. "Adaptive unit vector control of multivariable systems using monitoring functions", *International Journal of Robust Nonlinear Control*, v. 29, pp. 583–600, 2019.

[16] SHTESSEL, Y. B., MORENO, J. A., PLESTAN, F., et al. "Super-twisting Adaptive Sliding Mode Control: a Lyapunov Design". In: *Proceedings of the 49th IEEE Conference on Decision and Control*, pp. 5109–5113, Atlanta, 2010. Proceedings of the 49th IEEE Conference on Decision and Control.

[17] UTKIN, V. I., POZNYAK, A. S. "Adaptive sliding mode control with application to super-twist algorithm: Equivalent control method", *Automatica*, v. 49, pp. 39–47, 2013.

[18] EDWARDS, C., SHTESSEL, Y. "Adaptive dual-layer super-twisting control and observation", *International Journal of Control*, v. 89, pp. 1759–1766, 2016.

[19] HSU, L., LIZARRALDE, F., ARAUJO, A. D. "New results on output-feedback variable structure model-reference adaptive control: Design and stability analysis", *IEEE Transactions on Automatic Control*, v. 42, pp. 386–393, 1997.

[20] OLIVEIRA, T. R., PEIXOTO, A. J., NUNES, E. V. L., et al. "Control of uncertain nonlinear systems with arbitrary relative degree and unknown

control direction using sliding modes", *International Journal of Adaptive Control and Signal Processing*, v. 21, pp. 692–707, 2007.

[21] YAN, L., HSU, L., COSTA, R. R., et al. "A variable structure model reference robust control without a prior knowledge of high frequency gain sign", *Automatica*, v. 44, pp. 1036–1044, 2008.

[22] OLIVEIRA, T. R., PEIXOTO, A. J., HSU, L. "Sliding mode control of uncertain multivariable nonlinear systems with unknown control direction via switching and monitoring function", *IEEE Transactions on Automatic Control*, v. 55, pp. 1028–1034, 2010.

[23] OLIVEIRA, T., PEIXOTO, A., NUNES, E. "Binary robust adaptive control with monitoring functions for systems under unknown high-frequency-gain sign, parametric uncertainties and unmodeled dynamics", *International Journal of Adaptive Control and Signal Processing*, v. 30, pp. 1184–1202, 2016.

[24] HSU, L., OLIVEIRA, T., CUNHA, J. "Extremum seeking control via monitoring function and time-scaling for plants of arbitrary relative degree". In: *Proceedings of the 13th International Workshop on Variable Structure Systems*, pp. 1–6, Nantes, France, 2014. Institute of Electrical and Electronics Engineers (IEEE).

[25] RODRIGUES, V. H. P., OLIVEIRA, T. R. "Global adaptive HOSM differentiators via monitoring functions and hybrid state-norm observers for output feedback", *International Journal of Control*, v. 91, pp. 2060–2072, 2018.

[26] OLIVEIRA, T. R., MELO, G. T., HSU, L., et al. "Monitoring Functions Applied to Adaptive Sliding Mode Control for Disturbance Rejection". In: *Proceedings of the 20th IFAC World Congress*, pp. 2684–2689, Toulouse, 2017. Proceedings of the 20th IFAC World Congress.

[27] OBEID, H., FRIDMAN, L., LAGHROUCHE, S., et al. "Barrier function-based adaptive integral sliding mode control". In: *Proceedings of the 57th IEEE Conference on Decision and Control*, pp. 5946–5950, Miami Beach, USA, 2018. Institute of Electrical and Electronics Engineers (IEEE).

[28] OBEID, H., FRIDMAN, L., LAGHROUCHE, S., et al. "Barrier function-based adaptive twisting controller". In: *Proceedings of the 15th International Workshop on Variable Structure Systems*, pp. 198–202, Graz, Austria, 2018. Institute of Electrical and Electronics Engineers (IEEE).

[29] OBEID, H., FRIDMAN, L., LAGHROUCHE, S., et al. "Barrier function-based variable gain super-twisting controller", *IEEE Transactions on Automatic Control*, v. 65, pp. 4928–4933, 2019.

[30] OBEID, H., FRIDMAN, L., LAGHROUCHE, S., et al. "Barrier adaptive first order sliding mode differentiator". In: *Proceedings of the 20th IFAC World Congress*, pp. 1722–1727, Toulouse, France, 2017. International Federation of Automatic Control (IFAC).

[31] OBEID, H., FRIDMAN, L., LAGHROUCHE, S., et al. "Adaptation of levant's differentiator based on barrier function", *International Journal of Control*, v. 91, pp. 2019–2027, 2018.

[32] LEE, H.-H. "Modeling and Control of a Three-Dimensional Overhead Crane", *Journal of Dynamic Systems, Measurement, and Control*, v. 120, pp. 471–476, 1998.

[33] DADASHNIALEHI, A., BAB-HADIASHAR, A., CAO, Z., et al. "Intelligent Sensorless Antilock Braking System for Brushless In-Wheel Electric Vehicles", *IEEE Transactions on Industrial Electronics*, v. 62, pp. 1629–1638, 2015.

[34] PAHLEVANI, M., JAIN, P. "Soft-Switching Power Electronics Technology for Electric Vehicles: A Technology Review", *IEEE Journal of Emerging and Selected Topics in Industrial Electronics*, v. 1, pp. 1–12, 2020.

[35] EMMEI, T., WAKUI, S., FUJIMOTO, H. "Acceleration Noise Suppression for Geared In-wheel-motor Vehicles using Double-Encoder", *IEEE Journal of Emerging and Selected Topics in Industrial Electronics*, v. 1, pp. 1–9, 2020.

[36] OLIVEIRA, T. R., FRIDMAN, L., ORTEGA, R. "From adaptive control to variable structure systems - seeking harmony", *International Journal of Adaptive Control and Signal Processing*, v. 30, pp. 1074–1079, 2016.

[37] SUN, J., KRSTIC, M., BEKIARIS-LIBERIS, N. "Robust adaptive control: legacies and horizons", *International Journal of Adaptive Control and Signal Processing*, v. 27, pp. 1–3, 2013.

[38] CASAVOLA, A., HESPANHA, J., IOANNOU, P. "Recent trends on the use of switching and mixing in adaptive control", *International Journal of Adaptive Control and Signal Processing*, v. 26, pp. 690–691, 2012.

[39] HE, W., GE, S. "Cooperative control of a nonuniform gantry crane with constrained tension", *Automatica*, v. 66, pp. 146–154, 2016.

[40] ALMUTAIRI, N., ZRIBI, M. "Sliding Mode Control of a Three-dimensional Overhead Crane", *Journal of Vibration and Control*, v. 15, pp. 1679–1730, 2009.

[41] LEVANT, A. "Robust exact differentiation via sliding mode technique", *Automatica*, v. 34, pp. 379–384, 1998.

[42] RAMLI, L., MOHAMED, Z., ABDULLAHI, A., et al. "Control strategies for crane systems: A comprehensive review", *Mechanical Systems and Signal Processing*, v. 95, pp. 1–23, 2017.

[43] FANG, Y., MA, B., WANG, P., et al. "A Motion Planning-Based Adaptive Control Method for an Underactuated Crane System", *IEEE Transactions on Control Systems Technology*, v. 20, pp. 241–248, 2012.

[44] ABDEL-RAHMAN, E., NAYFEH, A., MASOUD, Z. "Dynamics and Control of Cranes: A Review", *Journal of Vibration and Control*, v. 9, pp. 863–908, 2001.

[45] LEBLANC, M. "Sur l'électrification des chemins de fer au moyen de courants alternatifs de fréquence élevée", *Revue Générale de l'Electricité*, v. 12, pp. 275–277, 1922.

[46] KRSTIĆ, M., WANG, H.-H. "Stability of extremum seeking feedback for general nonlinear dynamic systems", *Automatica*, v. 36, pp. 595–601, 2000.

[47] STERNBY, J. "Extremum control systems–an area for adaptive control?" In: *Proceedings of the 1980 IEEE Joint Automatic Control Conference (JACC)*, pp. 3270–3285, San Francisco, United States of America, 1980. Institute of Electrical and Electronics Engineers (IEEE).

[48] CHOI, J.-Y., KRSTIĆ, M., ARIYUR, K. B., et al. "Extremum seeking control for discrete-time systems", *IEEE Transactions on Automatic Control*, v. 47, pp. 318–323, 2002.

[49] MANZIE, C., KRSTIĆ, M. "Extremum seeking with stochastic perturbations", *IEEE Transactions on Automatic Control*, v. 54, pp. 580–585, 2009.

[50] LIU, S.-J., KRSTIĆ, M. "Stochastic averaging in continuous time and its applications to extremum seeking", *IEEE Transactions on Automatic Control*, v. 55, pp. 2235–2250, 2010.

[51] GHAFFARI, A., KRSTIĆ, M., NEŠIC, D. "Multivariable newton-based extremum seeking", *Automatica*, v. 48, pp. 1759–1767, 2012.

[52] FRIHAUF, P., KRSTIĆ, M., BAŞAR, T. "Nash equilibrium seeking in noncooperative games", *IEEE Transactions on Automatic Control*, v. 57, pp. 1192–1207, 2018.

[53] OLIVEIRA, T. R., KRSTIĆ, M., TSUBAKINO, D. "Extremum seeking for static maps with delays", *IEEE Transactions on Automatic Control*, v. 62, pp. 1911–1926, 2017.

[54] RUSITI, D., EVANGELISTI, G., T. R. OLIVEIRA, M. G., et al. "Stochastic extremum seeking for dynamic maps with delays", *IEEE Control Systems Letters*, v. 3, pp. 61–66, 2019.

[55] FEILING, J., KOGA, S., KRSTIĆ, M., et al. "Extremum seeking for static maps with actuation dynamics governed by diffusion PDEs", *Automatica*, v. 95, pp. 197–206, 2018.

[56] OLIVEIRA, T. R., FEILING, J., KOGA, S., et al. "Multivariable extremum seeking for pde dynamic systems", *IEEE Transactions on Automatic Control*, v. 65, pp. 4949–4956, 2020.

[57] OLIVEIRA, T. R., KRSTIĆ, M. "Extremum seeking boundary control for pde-pde cascades", *Systems & Control Letters*, v. 115, pp. 105004–15, 2021.

[58] YU, H., KOGA, S., OLIVEIRA, T. R., et al. "Extremum seeking for traffic congestion control with a downstream bottleneck", *ASME Journal of Dynamic Systems, Measurement, and Control*, v. 143, pp. 031007, 2021.

[59] OLIVEIRA, T. R., FEILING, J., KOGA, S., et al. "Extremum seeking for unknown scalar maps in cascade with a class of parabolic PDEs", *International Journal of Adaptive Control and Signal Processing*, v. 35, pp. 1162–1187, 2021.

[60] ZHANG, X.-M., HAN, Q.-L., GE, X., et al. "Networked control systems: A survey of trends and techniques", *IEEE/CAA Journal of Automatica Sinica*, v. 7, pp. 1–17, 2020.

[61] HESPANHA, J. P., NAGHSHTABRIZI, P., XU, Y. "A survey of recent results in networked control systems", *Proceedings of the IEEE*, v. 95, pp. 138–162, 2007.

[62] TABUADA, P., WANG, X. "Preliminary results on state-triggered scheduling of stabilizing control tasks". In: *Proceedings of the 45th IEEE Conference on Decision and Control (CDC)*, pp. 282–287, San Diego, United States of America, 2006. Institute of Electrical and Electronics Engineers (IEEE).

[63] TABUADA, P. "Event-triggered real-time scheduling of stabilizing control tasks", *IEEE Transactions on Automatic Control*, v. 52, pp. 1680–1685, 2007.

[64] BORGERS, D. P., HEEMELS, W. P. M. H. "On minimum inter-event times in event-triggered control". In: *Proceedings of the 52nd IEEE Conference on Decision and Control*, pp. 7370–7375, Firenze, Italy, 2013. Institute of Electrical and Electronics Engineers (IEEE).

[65] MONACO, S., NORMAND-CYROT, D. "Discrete time models for robot arm control". In: *Proceedings of the 11th IFAC World Congress*, pp. 525–529, Oslo, Norway, 1985. International Federation of Automatic Control (IFAC).

[66] ÅARZÉN, K. E. "A simple event-based PID controller". In: *Proceedings of the 14th IFAC World Congress*, pp. 423–428, Beijing, China, 1999. International Federation of Automatic Control (IFAC).

[67] ÅSTRÖM, K. J., BERNHARDSSON, B. P. "Comparison of periodic and event based sampling for first-order stochastic systems". In: *Proceedings of the 14th IFAC World Congress*, pp. 5006–5011, Beijing, China, 1999. International Federation of Automatic Control (IFAC).

[68] YOOK, J. K., TILBURY, D. M., SOPARKAR, N. R. "Trading computation for bandwidth: Reducing communication in distributed control systems using state estimators", *IEEE transactions on Control Systems Technology*, v. 10, pp. 503–518, 2002.

[69] HEEMELS, W. P. M. H., JOHANSSON, K. H., TABUADA, P. "An introduction to event-triggered and self-triggered control". In: *Proceedings of the 51nd IEEE Conference on Decision and Control*, pp. 3270–3285, Maui, United States of America, 2012. Institute of Electrical and Electronics Engineers (IEEE).

[70] HEEMELS, W. H., DONKERS, M. C. F., TEEL, A. R. "Periodic Event-Triggered Control for Linear Systems", *IEEE Transactions on Automatic Control*, v. 58, pp. 847–861, 2012.

[71] SEURET, A., PRIEUR, C. "Event-triggered sampling algorithms based on a Lyapunov function". In: *50th IEEE Conference on Decision and 20th Control and European Control Conference*, pp. 6128–6133, Orlando, Florida, United States of America, 2011. Institute of Electrical and Electronics Engineers (IEEE).

[72] ABDELRAHIM, M., POSTOYAN, R., DAAFOUZ, J., et al. "Stabilization of Nonlinear Systems Using Event-Triggered Output Feedback Controllers", *IEEE Transactions on Automatic Control*, v. 61, pp. 2682–2687, 2016.

[73] HETEL, L., FITER, C., OMRAN, H., et al. "Recent developments on the stability of systems with aperiodic sampling: An overview", *Automatica*, v. 76, pp. 309–335, 2017.

[74] BORGERS, D. P., HEEMELS, W. P. M. H. "Event-separation properties of event-triggered control systems", *IEEE Transactions on Automatic Control*, v. 59, pp. 2644–2656, 2014.

[75] XING, L., WEN, C., LIU, Z., et al. "Event-Triggered Adaptive Control for a Class of Uncertain Nonlinear Systems", *IEEE Transactions on Automatic Control*, v. 62, pp. 2071–2076, 2017.

[76] ZHANG, P., LIU, T., JIANG, Z.-P. "Event-triggered stabilization of a class of nonlinear time-delay systems", *IEEE Transactions on Automatic Control*, v. 66, pp. 421–428, 2021.

[77] CHENG, B., LI, Z. "Fully distributed event-triggered protocols for linear multiagent networks", *IEEE Transactions on Automatic Control*, v. 64, pp. 1655–1662, 2019.

[78] ABDELRAHIM, M., POSTOYAN, R., DAAFOUZ, J., et al. "Stabilization of nonlinear systems using event-triggered output feedback controllers", *IEEE Transactions on Automatic Control*, v. 61, pp. 2682–2687, 2016.

[79] SELIVANOV, A., FRIDMAN, E. "Distributed event-triggered control of diffusion semilinear PDEs", *Automatica*, v. 68, pp. 344–351, 2016.

[80] ESPITIA, N., KARAFYLLIS, I., KRSTIC, M. "Event-triggered boundary control of constant-parameter reaction-diffusion PDEs: a small-gain approach", *Automatica*, v. 128, pp. 109562, 2021.

[81] BAUDOUIN, L., MARX, S., TARBOURIECH, S. "Event-triggered damping of a linear wave equation". In: *3rd IFAC/IEEE CSS Workshop on Control of Systems Governed by Partial Differential Equation,*, pp. 58–63, Oaxaca,

Mexico, 2019. International Federation of Automatic Control (IFAC) and Institute of Electrical and Electronics Engineers (IEEE).

[82] ESPITIA, N., GIRARD, A., MARCHAND, N., et al. "Event-based boundary control of a linear 2×2 hyperbolic system via backstepping approach", *IEEE Transactions on Automatic Control*, v. 63, pp. 2686–2693, 2018.

[83] DIAGNE, M., KARAFYLLIS, I. "Event-triggered boundary control of a continuum model of highly re-entrant manufacturing systems", *Automatica*, v. 134, pp. 109902, 2021.

[84] RATHNAYAKE, B., DIAGNE, M., ESPITIA, N., et al. "Observer-based event-triggered boundary control of a class of reaction-diffusion PDEs", *IEEE Transactions on Automatic Control*, 2021. doi: 10.1109/TAC.2021.3094648.

[85] RATHNAYAKE, B., DIAGNE, M., KARAFYLLIS, I. "Sampled-data and event-triggered boundary control of a class of reaction–diffusion PDEs with collocated sensing and actuation", *Automatica*, v. 137, pp. 110026, 2022.

[86] POVEDA, J. I., TEEL, A. R. "A framework for a class of hybrid extremum seeking controllers with dynamic inclusions", *Automatica*, v. 76, pp. 113–126, 2017.

[87] CUNHA, J. P. V. S., COSTA, R. R., HSU, L. "Design of first-order approximation filters for sliding-mode control of uncertain systems", *IEEE Transactions on Industrial Electronics*, v. 55, pp. 4037–4046, 2008.

[88] CUNHA, J. P. V. S., COSTA, R. R., HSU, L. "Cooperative Actuators for Fault Tolerant Model-Reference Sliding Mode Control". In: *Proceedings of the 12th IEEE International Symposium on Industrial Electronics*, pp. 690–695, Rio de Janeiro, 2003. Proceedings of the 12th IEEE International Symposium on Industrial Electronics.

[89] GOEBEL, R., SANFELICE, R. G., TEEL, A. R. *Hybrid dynamical systems – Modeling, stability, and robustness.* Princeton, NJ, Princeton University Press, 2012.

[90] INCREMONA, G. P., REGOLIN, E., MOSCA, A., et al. "Sliding Mode Control Algorithms for Wheel Slip Control of Road Vehicles". In: *Proceedings of the 2017 American Control Conference*, pp. 4297–4302, Seattle, 2017. Proceedings of the 2017 American Control Conference.

[91] ANTIĆ, D., NIKOLIĆ, V., MITIĆ, D., et al. "Sliding Mode Control of Anti-lock Braking System: an overview", *Automatic Control and Robotics*, v. 9, pp. 2060–2072, 2010.

[92] SCHINKEL, M., HUNT, K. "Anti-Lock Bracking Control using a Sliding Mode like Approach". In: *Proceedings of the 2002 American Control Conference*, pp. 2386–2391, Anchorage, 2002. Proceedings of the 2002 American Control Conference.

[93] UTKIN, V. I. *Sliding Modes and Their Applications in Variable Structure Systems*. Moscow, MIR Publisher, 1978.

[94] KHALIL, H. K. *Nonlinear Systems*. New Jersey, Wiley, 2002.

[95] RODRIGUES, V., OLIVEIRA, T. "Monitoring function for switching adaptation in control and estimation schemes with sliding modes". In: *Proceedings of the 1st IEEE Conference on Control Technology and Applications*, pp. 608–613, Island of Hawai'i, USA, 2017. Institute of Electrical and Electronics Engineers (IEEE).

[96] CUNHA, J. P. V. S., HSU, L., COSTA, R. R., et al. "Output-Feedback Model-Reference Sliding Mode Control of Uncertain Multivariable Systems", *IEEE Transactions on Automatic Control*, v. 48, pp. 2245–2250, 2003.

[97] INTECO. *The laboratory 3D Crane – User's Manual*. Relatório técnico, INTECO sp. z o.o., Poland, 2011.

[98] DZIENDZIEL, T., GRUK, M., PIOTROWSKI, R. "Optymalizacja nastaw regulatorów PID do sterowania suwnicą", *Pomiary Automatyka Robotyka*, v. 6, pp. 78–85, 2014.

[99] BARTOLINI, G., PISANO, A., USAI, E. "Second-order sliding-mode control of container cranes", *Automatica*, v. 38, pp. 1783–1790, 2002.

[100] VÁZQUEZ, C., COLLADO, J., FRIDMAN, L. "Variable Structure Control of Perturbed Crane: Parametric Resonance Case Study". In: Yu, X., Efe, M. (Eds.), *Recent Advances in Sliding Modes*, 1 ed., cap. 15, pp. 317–347, New York, USA, Springer International Publishing, 2015.

[101] KRSTIĆ, M. "Extremum seeking control". In: Baillieul, J., Samad, T. (Eds.), *Encyclopedia of Systems and Control*, 1 ed., pp. 413–416, London, England, Springer, 2014.

[102] ARIYUR, K. B., KRSTIĆ, M. *Real-Time Optimization by Extremum-Seeking Control*. New Jersey, Wiley, 2003.

[103] PLOTNIKOV, V. A. "Averaging of differential inclusions", *Ukrainian Mathematical Journal*, v. 31, pp. 454–457, 1980.

[104] PISKUNOV, N. *Differential and Integral Calculus*. Moscow, Union of Soviet Socialist Republics, MIR Publishers, 1969.

[105] STEELE, J. M. *The Cauchy-Schwartz Master Class: an introduction to the art of mathematical inequalities*. New York, United States of America, Cambridge University Press, 2008.

[106] WARNER, F. *Foundations of differentiate manifolds and Lie group*. Chicago, Illinois, United States of America, Scott Foresman and Company, 1971.

[107] GIRARD, A. "Dynamic triggering mechanism for event-triggered control", *IEEE Transactions on Automatic Control*, v. 60, pp. 1992–1997, 2014.

[108] ABDELRAHIM, M., POSTOYAN, R., DAAFOUZ, J., et al. "Co-design of output feedback laws and event-triggering conditions for the L2-stabilization of linear systems", *Automatica*, v. 87, pp. 337–344, 2018.

[109] STRANG, G. *Introduction to Linear Algebra*. Wellesley, United States of America, Wellesley-Cambridge Press, 2016.

[110] APOSTOL, T. *Mathematical Analisys - A Modern Approach to Advanced Calculus*. Massachusetts, Addison-Wesley Publishing Company, 1957.

[111] OLIVEIRA, T. R., PEIXOTO, A. J., NUNES, E. V. L., et al. "Control of uncertain nonlinear systems with arbitrary relative degree and unknown control direction using sliding modes", *International Journal of Adaptive Control and Signal Processing*, v. 21, pp. 692–707, 2007.

[112] COUTINHO, P. H. S., PALHARES, R. M. "Dynamic periodic event-triggered gain-scheduling control co-design for quasi-LPV systems", *Nonlinear Analysis: Hybrid Systems*, v. 41, pp. 101044, 2021.

Appendix A

Anti-Lock Braking System Model

The dynamics of the slip rate $\lambda(t)$ is given by (2.40) where

$$f(\eta,t) = \begin{cases} f^+(\eta,t)\,, & s=1 \\ f^-(\eta,t)\,, & s=-1 \end{cases}\,, \tag{A.1}$$

$$\begin{aligned} f^+(\eta,t) = \frac{1}{|\eta_2|}\Bigg\{ & -(M_g+M_{10})\frac{1}{L}\left[\frac{r_1^2}{r_2J_1}+\frac{r_2}{J_2}(1-\lambda)\right]\frac{\mu(\lambda)}{(\sin(\theta)-\mu(\lambda)\cos(\theta))}+ \\ & -\frac{M_{20}}{J_2}(1-\lambda)+\frac{r_1M_{10}}{r_2J_1}\Bigg\}+ \\ & -\frac{d_1}{L}\left[\frac{r_1}{J_1}+\frac{r_2^2}{r_1J_2}(1-\lambda)\right]\frac{(1-\lambda)\mu(\lambda)}{(\sin(\theta)-\mu(\lambda)\cos(\theta))}+\left(\frac{d_1}{J_1}-\frac{d_2}{J_2}\right)(1-\lambda)\,, \end{aligned} \tag{A.2}$$

$$\begin{aligned} f^-(\eta,t) = -\frac{1}{|\eta_1|}\Bigg\{ & -(M_g+M_{10})\frac{1}{L}\left[\frac{r_2^2}{r_1J_2}+\frac{r_1}{J_1}(1-\lambda)\right]\frac{\mu(\lambda)}{(\sin(\theta)+\mu(\lambda)\cos(\theta))}+ \\ & -\frac{M_{10}}{J_1}(1-\lambda)+\frac{r_2M_{20}}{r_1J_2}\Bigg\}+ \\ & -\frac{d_1}{L}\left[\frac{r_2^2}{r_1J_2}+\frac{r_1}{J_1}(1-\lambda)\right]\frac{\mu(\lambda)}{(\sin(\theta)+\mu(\lambda)\cos(\theta))}+\left(\frac{d_2}{J_2}-\frac{d_1}{J_1}\right)(1-\lambda)\,, \end{aligned} \tag{A.3}$$

$$g(\eta,t) = sG(\eta,t)\,, \quad G(\eta,t) = \begin{cases} g^+(\eta,t)\,, & s=1 \\ g^-(\eta,t)\,, & s=-1 \end{cases}\,, \tag{A.4}$$

$$g^+(\eta,t) = \frac{1}{|\eta_2|}\left\{\frac{r_1}{r_2J_1}-\frac{1}{L}\left[\frac{r_1^2}{r_2J_1}+\frac{r_2}{J_2}(1-\lambda)\right]\frac{\mu(\lambda)}{(\sin(\theta)-\mu(\lambda)\cos(\theta))}\right\} = \frac{g_\lambda^+(\lambda)}{|\eta_2|}\,, \tag{A.5}$$

$$g^-(\eta,t) = \frac{1}{|\eta_1|}\left\{\frac{1}{J_1}(1-\lambda)+\frac{1}{L}\left[\frac{r_2^2}{r_1J_2}+\frac{r_1}{J_1}(1-\lambda)\right]\frac{\mu(\lambda)}{(\sin(\theta)+\mu(\lambda)\cos(\theta))}\right\} = \frac{g_\lambda^-(\lambda)}{|\eta_1|}\,. \tag{A.6}$$

In order to analyze the sign of $g(\eta,t)$, Figure A.1 shows the curves of $g_\lambda^+(\lambda)$ and

$g_\lambda^-(\lambda)$ for the possible values of variable λ. Note that $g_\lambda^+(\lambda) > 0$ and $g_\lambda^-(\lambda) > 0$ for all $0 < \lambda(t) < 1$ regardless the sign of s. However, from (A.4)–(A.6), it can be

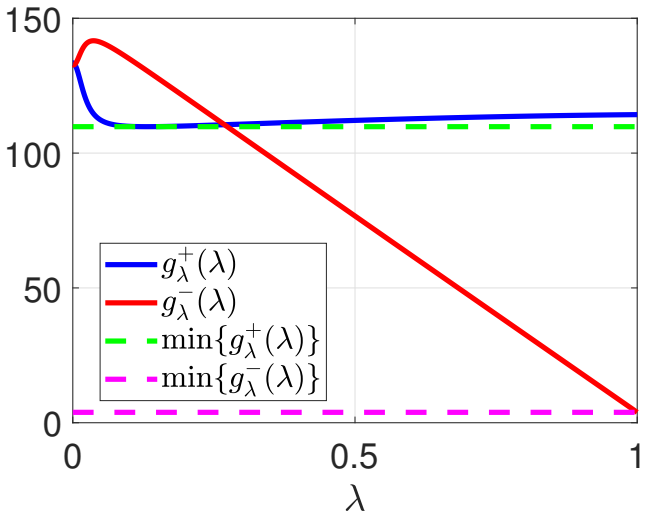

Figure A.1: Curves of $g_\lambda^+(\lambda)$ and $g_\lambda^-(\lambda)$, for $0 < \lambda < 1$ where $\min\{g_\lambda^+(\lambda)\} \approx 109.8$ and $\min\{g_\lambda^-(\lambda)\} \approx 3.9$, using the values of Tables 2.1 and 2.2.

observed that the sign of $g(\eta, t)$ only depends on the sign of s such that $g(\eta, t) > 0$ if $s = 1$ and $g(\eta, t) < 0$ if $s = -1$. Moreover, since the sign of $g_\lambda^+(\lambda) > 0$ and $g_\lambda^-(\lambda) > 0$ for all $\lambda \in [0\,, 1]$, $g(\eta, t)$ switches discontinuously without zero-crossing.

Although equation (2.32) seems to be simple, its use implies a severe restriction of the model. Note that for sufficiently low speeds, a mathematical indeterminacy may occur when calculating the slip coefficient. In practice, this problem is overcome by specifying lower speed limits $r_1\underline{\eta}_1$ and $r_2\underline{\eta}_2$, below which the ABS controller is deactivated.

Initially, since the vehicle is braking without skidding, $|\eta_1(t)| \leq |\eta_1(0)|$, $|\eta_2(t)| \leq |\eta_2(0)|$, $s_1 = s_2 = 1$ and $0 < \lambda(t) < 1$. Then, by defining $\overline{\mu} = \max\{\mu(\lambda)\}$, from (A.1)–(A.6),

$$
\begin{aligned}
|f^+(\eta,t)| \leq\ & \frac{1}{|\underline{\eta}_2|}\left\{(M_g + M_{10})\frac{1}{L}\left[\frac{r_1^2}{r_2 J_1} + \frac{r_2}{J_2}\right]\frac{\overline{\mu}}{(\sin(\theta) - \overline{\mu}\cos(\theta))} + \frac{M_{20}}{J_2} + \frac{r_1 M_{10}}{r_2 J_1}\right\} + \\
& + \frac{d_1}{L}\left[\frac{r_1}{J_1} + \frac{r_2^2}{r_1 J_2}\right]\frac{\overline{\mu}}{(\sin(\theta) - \overline{\mu}\cos(\theta))} + \left(\frac{d_1}{J_1} + \frac{d_2}{J_2}\right) \\
=\ & \overline{f}^{\,+}, \qquad \text{(A.7)} \\
|f^-(\eta,t)| \leq\ & \frac{1}{|\underline{\eta}_1|}\left\{(M_g + M_{10})\frac{1}{L}\left[\frac{r_2^2}{r_1 J_2} + \frac{r_1}{J_1}\right]\frac{\overline{\mu}}{\sin(\theta)} + \frac{M_{10}}{J_1} + \frac{r_2 M_{20}}{r_1 J_2}\right\} + \\
& + \frac{d_1}{L}\left[\frac{r_2^2}{r_1 J_2} + \frac{r_1}{J_1}\right]\frac{\overline{\mu}}{\sin(\theta)} + \left(\frac{d_2}{J_2} + \frac{d_1}{J_1}\right) \\
=\ & \overline{f}^{\,-}. \qquad \text{(A.8)}
\end{aligned}
$$

Hence, one has

$$|f(\eta,t)| \leq \overline{f}\,, \tag{A.9}$$

$$|g(\eta,t)| \geq \underline{g} \tag{A.10}$$

where $\overline{f}$ and $\underline{g}$ are constants described by

$$\overline{f} = \max\left\{\overline{f}^{\,+}, \overline{f}^{\,-}\right\}, \tag{A.11}$$

$$\underline{g} = \frac{\min\{g_\lambda^-(\lambda)\}}{\max\{|\eta_1(0)|, |\eta_2(0)|\}}\,. \tag{A.12}$$

Moreover, if the vehicle is skidding, from (2.32), $\lambda = 1$ and $\dot{\lambda} = 0$, therefore, it is not reasonable to talk about of $g(\eta,t)$ as well as $f(\eta,t)$.

In other words, during the time interval while the ABS is turned on, $f(\eta,t)$ is upper bounded by the unknown constant $\overline{f}$ whilst $|g(\eta,t)|$ is lower bounded by the constant $\underline{g}$.

Appendix B

Averaging Theory for Discontinuous Systems

From [103], let us consider the differential inclusion

$$\frac{dx}{dt} \in \varepsilon X(t,x)\,, \quad x(0) = x_0\,, \tag{B.1}$$

where x is an n-dimensional vector, t is time, ε is a small parameter, and $X(t,x)$ is a multivalued function that is T-periodic in t and puts in correspondence with with each point (t,x) of a certain domain of the $(n+1)$-dimensional space a compact set $X(t,x)$ of the n-dimensional space.

Let us put in correspondence with the inlusion (B.1) the average inclusion

$$\frac{d\xi}{dt} \in \varepsilon \bar{X}(\xi)\,, \quad \xi(0) = x_0\,, \tag{B.2}$$

where

$$\bar{X}(\xi) = \frac{1}{T}\int_0^T X(\tau,\xi)d\tau\,. \tag{B.3}$$

Theorem 7. *Let a multivalued mapping $X(t,x)$ be defined in the domain $Q\,\{t \geq 0\,, x \in D \subset \mathbb{R}^n\}$ and let in this domain the set $X(t,x)$ be a nonempty compactum for all admissible values of the arguments and the mapping $X(t,x)$ be continuous and uniformly bounded and satisfy the Lipschitz condition with respect to x with a constant λ, i.e., $X(t,x) \subset S_M(0)$, $\delta(X(t,x') - X(t,x'')) \leq \lambda\|x' - x''\|$, where $\delta(P,Q)$ is the Hausdorff distance between the sets P and Q, i.e., $\delta(P,Q) = \min\{d|P \subset S_d(Q), Q \subset S_d(P)\}$, $S_d(N)$ being the d-neighborhood of a set N in the space $\mathbb{R}^n$; the mapping $X(t,x)$ be T-periodic in t; for all $x_0 \in D' \subset D$ the solutions of inclusion (B.2) lie in the domain D together with a certain ρ-neighborhood. Them for each $L > 0$ there exist $\varepsilon^0(L) > 0$ and $c(L) > 0$ such that for $\varepsilon \in]0\,, \varepsilon^0]$ and*

$t \in [0, L\varepsilon^{-1}]$:

1. *for each solution $x(t)$ of the inclusion (B.1) there exists a solution $\xi(t)$ of the inclusion (B.2) such that*

$$\|x(t) - \xi(t)\| \leq c\varepsilon = \mathcal{O}(\varepsilon); \tag{B.4}$$

2. *for each solution $\xi(t)$ of the inclusion (B.2) there exists a solution $x(t)$ of the inclusion (B.1) such that the inequality (B.4) holds.*

Thus the following estimate is valid:

$$\delta(\bar{R}(t), R'(t)) \leq c\varepsilon = \mathcal{O}(\varepsilon)\,, \tag{B.5}$$

where $\bar{R}(t)$ is a section of the family of solutions of the inclusion (B.2) and $R'(t)$ is the closure of the section $R(t)$ of the family of solutions of the inclusion (B.1).

Theorem 8. *Let all the conditions of Theorem 7 and also the following condition be fulfilled: the R-solution $\bar{R}(t)$ of inclusion (B.2) is uniformly asymptotically stable. Then there exist $\varepsilon^0 > 0$ and $c > 0$ such that for $0 < \varepsilon \leq \varepsilon^0$*

$$\delta(\bar{R}(t), R'(t)) \leq c\varepsilon = \mathcal{O}(\varepsilon)\,, \tag{B.6}$$

for all $t \geq 0$.